CELL SHAPE TRANSITION DURING EPITHELIAL FUSION IN INNER EAR DEVELOPMENT

A THESIS TO BE SUBMITTED TO

THE UNIVERSITY OF TRANS-DISCIPLINARY HEALTH SCIENCES AND TECHNOLOGY

FOR THE AWARD OF THE DEGREE OF
DOCTOR OF PHILOSOPHY

BY

VARSHA.N.T

UNDER THE GUIDANCE OF

DR. RAJESH KUMAR LADHER

NATIONAL CENTRE FOR BIOLOGICAL SCIENCES, TATA INSTITUTE OF FUNDAMENTAL RESEARCH, BENGALURU-560065

NOVEMBER 2025

THE UNIVERSITY OF TRANS-DISCIPLINARY HEALTH SCIENCES AND TECHNOLOGY

Private University Established in Karnataka by ACT 35 of 2013
BENGALURU - 560064

DECLARATION BY THE CANDIDATE

I declare that this thesis entitled "**Cell shape transition during epithelial fusion in inner ear development**" submitted for the award of Doctor of Philosophy to THE UNIVERSITY OF TRANS-DISCIPLINARY HEALTH SCIENCES AND TECHNOLOGY, Bengaluru, is my original work, conducted under the supervision of my guide **Dr. Rajesh Kumar Ladher**. I also wish to inform that no part of the research has been submitted for a degree or examination at any university. References, help and material obtained from other sources have been duly acknowledged.

I hereby confirm the originality of the work and that there is no plagiarism in any part of the dissertation.

Place: Bengaluru **Signature of the Candidate**

Date: Nov 26 2025

Name of candidate: Varsha.N.T
Reg. No.: 2111720486
(January 2019)

THE UNIVERSITY OF TRANS-DISCIPLINARY HEALTH SCIENCES AND TECHNOLOGY

Private University Established in Karnataka by ACT 35 of 2013
BENGALURU - 560064

CERTIFICATE

This is to certify that the work incorporated in this thesis **"Cell shape transition during epithelial fusion in inner ear development"** submitted by **Varsha.N.T** was carried out under my supervision. No part of this thesis has been submitted for a degree or examination at any university. References, help and material obtained from other sources have been duly acknowledged. I hereby confirm the originality of the work and that there is no plagiarism in any part of the dissertation.

Research Supervisor
Date: Nov 26 2025
Dr. Rajesh Kumar Ladher
Professor
National Centre for Biological Sciences, Tata Institute of Fundamental Research, Bellary Road, Bengaluru-560065, Karnataka, India

ACKNOWLEDGMENTS

I have been fortunate so far to have a long list of people to be thankful to and for. The first humans who took me home with them, my parents and their parents; I have always had their support from my first step to my latest degree. My mother, Mrs. Shanthi Nila, a botanist by training was my first science teacher, who instilled in me a curiosity for the world around us, by patiently answering all of my questions, teaching me book chapters in advance, so I could answer the subject teacher's questions in class. My father, Mr.Tamilkumar, the best mathematician I have known, would carry my tiny notepad and crayon everywhere, so I could scribble my thoughts, since I learnt to hold a crayon. They always knew what I would need and get it even before I asked for it; my first aptitude book when I was just 6, a giant notebook for me to practice my lessons from school, paints and colour pencils for my art, dance classes, a taste for different cuisines and the best fruits and vegetables. Everything that I am, is from them. Their faith in me has given me the confidence and strength to venture into new territories and accept new challenges. They have always kept me protected in my bubble, even when I was miles away. They are the best parents any kid could wish for. My "younger" sister, Miss.Vyshaly, for being my personal cheer leader, ever since she took her first steps. She was my first baby sister, my first rival, my first villain who destroyed all of my well preserved toys, books and lego pieces and one of my inspirations. Over the course of my PhD studies, she has also bought me shoes and clothes like an elder sister. When I moved out of the house to pursue my dreams, she stayed with my parents and has taken care of them in her own way, and for that, I will forever be grateful to her. My family is my greatest support and every one of my achievements, small or big is all because of them.

My close family has always believed in me and in my dreams, even when I have failed to do so, on multiple occasions. Their belief on my capabilities and me has been the stability that I needed when exploring new territories. As their first grandchild, I was very special to my maternal grandparents (this was told to me by my sister and cousins). I have known unconditional love from all of my grandparents. My mom's siblings, her elder and younger brothers and younger sister have seen me as their first born and celebrated my success as their own. Her younger sister, Mrs.Amuthu, my chithi, has been

my first favourite person besides my parents. She has always supported me and shown me love and affection and was my first pen pal. Miss. Gowshiga, and Mrs.Anusha Devi, my other baby ducklings that followed me around every summer holiday at my grandparents, continue to inspire me. My mom's younger brother Mr.Prabhakar, has been instrumental in my academic achievements. He has always believed in my potential and was my spoken English tutor. My dad's elder sister and family, Mr. and Mrs. Gopala Krishnan, have always been a source of support and love to our family, and my cousin Dr.Brindha was my first source of scary stories and movies and the person who made me love chemistry.

I have again been lucky with the amazing, inspiring and supportive teachers who have taught me invaluable lessons throughout my life. From kindergarten until my PhD supervisor, I have had the best of teachers; constantly encouraging and pushing me beyond my comfort zone to realise my full potential in academics, extra-curricular, sports and other responsibilities. They have also been the source of my love for order, rules and discipline. All of these teachers were brilliant in their fields and also in imparting their knowledge to students. They have inspired me to be the best in what I do, and I have always considered that the goal of my life. All the teachers in my life, have often paid attention to my strengths and weaknesses and made me a better student by encouraging and motivating to go the extra mile.

A good mentor hopes you will move on. And a great mentor knows you will.

-Leslie Jr., *Ted Lasso*

Dr.Raj Ladher, my PhD mentor, has been more than a science advisor. His love for life, science, food, and laughter, is infectious. His perspective on life and his intellect would amaze anyone who has had the opportunity to know him. He has always cared for every one of his students, and made them feel better in his subtle ways. He has also admonished us in his diplomatic subtle ways. Mrs.Ayumi, his wife, is the other glowing presence in the lab, that has made me feel at home in the lab, always. I believe it is their positive aura, that binds the lab together, despite being composed of radically different individuals. He accepted me into his lab, and taught me every one of the techniques I

have used for my thesis. Whenever, I have had any questions, however juvenile or basic it had been, he always took the time and effort to teach me. Whenever I did not get the plasmid yield or PCR band, he has had a solution that worked every time. He is my senior in the lab, who has done it all and knows almost everything about everything in developmental biology. His intellect and memory would astonish anyone who has attended lab meetings or journal club with him. He always has the time and ears for his students. He has never said no to any of our new experiment related requests and encouraged us to “go for it” even when we were unsure. He has given us the space and freedom to pursue science in our own artistic way, letting us explore the world for ourselves. My love for embryology and MBL stems from him. He has always been with us and for us. He takes us out to places that he has been to and thought we might like. He has had house parties and pot lucks and played every parlour game. He has danced with us and cried with us. As a young adult, my PhD life was filled with ups and downs, and through that all, Raj was always there to cheer for us and motivate us, and not in a subtle way. I dedicate all of my scientific achievements to his excellent mentorship. And I could go on about him and his guidance for two more pages, but I will have to stop. I am grateful to Raj also for introducing me to Dr.Hiroshi Hamada, my post-doc mentor. Dr.Hamada looks out for my interests and helped me realise my long term dream of going to MBL, for which, I shall forever be indebted to him. He has been an excellent mentor, encouraging me to envision my long-term career goals. Dr. Rolf Ericsson, was my second senior in the lab. He was also my second source of MBL dreams and embryology. I have learnt techniques for my research, and have had fruitful scientific conversations on troubleshooting dissections, RNA-seq, insitu hybridisations, and cooking new recipes. Dr.Neerja, whom I met very recently, helped me with the publication of my first book review on a peer reviewed journal. Her lessons on writing and critique on my work has improved the way I communicate my ideas.

I have had an amazing set of colleagues who have taught me valuable lessons in science, and life, equally. Some of them played their role and stayed on the sidelines, and others persisted and forever became a part of my journey, my friends. Some of these friends also left me in India and went abroad- Dr.Shri Vidhya and Dr. Rohit; but the distance was just geographical. All of my intern-colleagues have been amazing with their

brilliance and charming personalities- Greeshma, Shivangi, Nidhi, Sukhada and Benson. I have been fortunate to see them learn new things and become amazing with what they do. They have made me a better scientist and good with communication.

Finally, my friends, my treasured possessions. I have felt love in their presence. Koushik, my 'best friend forever', has been with me through the bright and dark phases of life. He has always been the beacon of truth and honesty in my life, loving and caring for me, silently suffering through my emotional outbursts when I have felt lost and admonishing me when I was wrong. Shivangi, my sister away from home. She has been my younger and elder sister and sometimes even my mother, being there always, my tall source of wisdom and kindness. Sreesubha, Sreenath, Dr.Suraj, Raman ,Ray, and Vibhav have been my constant support system, illuminating darker alleys with their rays of sunshine, hope and laughter and the occasional science. The Yelahanka Spammers will always be my second family, protecting me from everything; even a pandemic! They will always be my people, the ones who are always up for cooking and eating and would "kill" for me! Harsha, who has come to become a major part of my life. From checking up on me regularly, training me in gym, helping me with experiments, taking me to amazing eateries throughout Bangalore, spending time with my guests, getting me home food and so many other things, has made invaluable contributions in the final phase of my doctoral studies. He has been my source of happiness on gloomy days when time stood still.

The importance of each one of these people is difficult to be described or justified by mere words with a space constraint. And there are other people, who have not been forgotten. In essence, thank you everyone for being there, and sometimes, not being there.

LIST OF TABLES

Chapter 2:

Chapter 4:

LIST OF FIGURES

CHAPTER 1

CHAPTER 2

CHAPTER 3

CHAPTER 4

TABLE OF CONTENTS

Appendix

ABSTRACT

Epithelial fusion is a recurrent morphogenetic event in embryogenesis. It is one contiguous sheet of epithelium giving rise to two sheets of epithelium. This involves the exchange of cellular neighbours through transient loss and gain of junction components and the formation of an intact basement membrane. Some examples are the formation of optic cup, otic vesicle, neural tube, and the body wall (Chan, Moosajee, & Rainger, 2021; Fernández-Santos et al., 2021; Lubarsky & Krasnow, 2003; Millard & Martin, 2008; Pyrgaki, Trainor, Hadjantonakis, & Niswander, 2010; Schöck & Perrimon, 2002). Failure of fusion leads to a variety of birth defects such as, cleft palate, spina bifida and omphalocele. Approximately 4 of 1000 live births in India have spina bifida, a neural tube closure defect (Allagh et al., 2015). While the process seems similar across embryonic development, studies have proved otherwise (Ray & Niswander, 2012

The inner ear is induced as a patch of thickened cells in the non-neural ectoderm by the adjacent neural tube and underlying mesenchyme to form the otic ectoderm. Upon induction, the otic ectoderm thickens to form the otic placode. This placode undergoes invagination to give rise to an otic pit and as development proceeds the edges of the otic vesicle are brought close to each other. Upon reaching close proximity, the cells in the edge recognise their counterparts in the apposed edge and fuse to form a closed otic vesicle that subsequently gets internalised in the mesenchyme of the head (Ladher, 2017).

The edge region (otic pore, OP) mediating fusion is the border of the non-neural ectoderm and the otic ectoderm. For the otic vesicle to get internalised after the fusion, the non-neural ectoderm and the otic ectoderm also have to segregate from each other. These edge cells mediating fusion, in neural tube, undergo partial epithelial to mesenchymal transition and migrate away as neural crest cells (Acloque, Adams, Fishwick, Bronner-Fraser, & Nieto, 2009; Amack, 2021; Duband, Monier, Delannet, & Newgreen, 1995; Park & Gumbiner, 2012; Scarpa et al., 2015). While the edge cells in otic vesicle closure do not migrate away, we hypothesised that these cells undergo a partial epithelial to mesenchymal transition to facilitate the fusion and subsequent segregation of the otic vesicle from the surface ectoderm. In this thesis, we have

characterised the edge cells and their role in epithelial fusion. We have also performed mosaic CRISPR-Cas9 mediated genetic knockdown of two genes, Grhl2 and SP8 to perturb epithelial fusion.

LIST OF ABBREVIATIONS

1.	ANOVA	Analysis of variance
2.	AP	Anterior- Posterior
3.	BM	Basement Membrane
4.	BMP	Bone Morphogenetic Protein
5.	BSA	Bovine Serum Albumin
6.	CNS	Central Nervous System
7.	CPD	Critical Point Drying
8.	CPM	Counts Per Million
9.	CV	Coefficient of Variation
10.	DAPI	4',6-diamidino-2-phenylindole
11.	DEPC	Diethyl pyro carbonate
12.	DV	Dorsal-Ventral
13.	ECM	Extra Cellular Matrix
14.	EMT	Epithelial to Mesenchymal Transition
15.	FGF	Fibroblast Growth Factor
16.	GPCR	G-Protein Coupled Receptor
17.	HH	Hamburger-Hamilton
18.	IHC	Immuno-Histo Chemistry
19.	INM	Interkinetic Nuclear Migration
20.	MET	Mesenchymal to Epithelial Transition
21.	NCC	Neural Crest Cells
22.	NE	Neural Ectoderm
23.	NF	Neural Folds
24.	NNE	Non-Neural Ectoderm
25.	NP	Neural Plate
26.	NPB	Neural Plate Border
27.	NT	Neural Tube
28.	NTD	Neural Tube Defect
29.	OE	Otic Edge

30. OEPD	Otic Epibranchial Progenitor Domain
31. OV	Otic Vesicle
32. PBS	Phosphate Buffered Saline
33. PBST	Phosphate Buffered Saline/Tween
34. PCP	Planar Cell Polarity
35. PFA	para-Formaldehyde
36. POM	Peri-Ocular Mesenchyme
37. PPR	Pre-Placodal Region
38. PS	Pseudo-Stratified
39. RPE	Retinal Pigment Epithelium
40. RT	Room Temperature
41. SE	Surface Ectoderm
42. SEM	Scanning Electron Microscopy
43. SMO	Spemann Mangold Organiser
44. SS	Somite Stage
45. TGF	Transforming Growth Factor
46. VEGF	Vascular-Endothelial Growth Factor
47. WhISH	Whole-mount In Situ Hybrisation

SYNOPSIS REPORT

BACKGROUND OF THE STUDY:

Epithelial fusion is a recurrent morphogenetic event in embryogenesis. It is a dynamic process with one contiguous sheet of epithelium giving rise to two sheets of epithelium. This involves the exchange of cellular neighbours through transient loss and gain of junction components and the formation of an intact basement membrane. This is seen at different instances throughout embryonic development, across species; including the formation of optic cup, otic vesicle, neural tube, and the body wall (Chan, Moosajee, & Rainger, 2021; Fernández-Santos et al., 2021; Lubarsky & Krasnow, 2003; Millard & Martin, 2008; Pyrgaki, Trainor, Hadjantonakis, & Niswander, 2010; Schöck & Perrimon, 2002). Failure of fusion leads to a variety of birth defects such as, cleft palate, spina bifida and omphalocele. Approximately 4 of 1000 live births in India have spina bifida, a neural tube closure defect (Allagh et al., 2015) . While epithelial fusion seems similar across embryonic development, studies of different systems, have proved otherwise (Ray & Niswander, 2012). Neural tube, the precursor of the brain and the spinal cord, is induced in the surface ectoderm. This flat sheet of cells undergoes multiple morphogenetic events including pseudo stratification, apical constriction, basal expansion, convergent extension, and epithelial fusion to give rise to an internalised hollow cylinder that spans the rostra-caudal axis of the embryo, overlaid by the surface ectoderm (Galea et al., 2017; Nikolopoulou, Galea, Rolo, Greene, & Copp, 2017) . Studies have shown that fusion is mediated by actin-based membrane protrusions-filopodia and lamellipodia sent out by the neural ectoderm (NE) and the non-neural or surface ectoderm (SE) (Rolo et al., 2016). Cells that mediate fusion in optic fissure closure also are shaped differently (Gestri, Bazin-Lopez, Scholes, & Wilson, 2018) .

Something similar happens in the formation of the otic vesicle (OV), the inner ear precursor. The inner ear is induced as a patch of thickened cells in the non-neural ectoderm by the adjacent neural tube and underlying mesenchyme to form the otic ectoderm. Upon induction, the otic ectoderm thickens to form the otic placode. This placode undergoes invagination to give rise to an otic pit and as development proceeds the edges of the otic vesicle are brought close to each other. Upon reaching close proximity, the cells in the edge recognise their counterparts in the apposed edge and fuse

to form a closed otic vesicle that subsequently gets internalised in the mesenchyme of the head (Ladher, 2017) .

The edge region (otic pore, OP) mediating fusion is the border of the non-neural ectoderm and the otic ectoderm. For the otic vesicle to get internalised after the fusion, the non-neural ectoderm and the otic ectoderm also have to segregate from each other. These edge cells mediating fusion, in neural tube, undergo partial epithelial to mesenchymal transition and migrate away as neural crest cells (Acloque, Adams, Fishwick, Bronner-Fraser, & Nieto, 2009; Amack, 2021; Duband, Monier, Delannet, & Newgreen, 1995; Park & Gumbiner, 2012; Scarpa et al., 2015) . While the edge cells in otic vesicle closure do not migrate away, we hypothesised that these cells undergo a partial epithelial to mesenchymal transition to facilitate the fusion and subsequent segregation of the otic vesicle from the surface ectoderm. In this thesis, we have characterised the edge cells and their role in epithelial fusion. Additionally, I have included some preliminary analysis on the use of metaphors in the field of epithelial to mesenchymal transition. The thesis is distributed as six chapters.

Chapter1: Introduction

This chapter is a review of literature on cell state transitions during development. It begins with a description of characteristic features of epithelial and mesenchymal cells and their transition to each other, during embryonic development across different species. This is followed by an account of embryonic epithelial fusion events, including Drosophila body wall closure, vertebrate neural tube closure and optic fissure closure. The chapter then is concluded with a detailed overview of avian otic vesicle development and pertinent questions in the field, that are yet to be answered, and thus form the basis of this thesis.

Chapter2: Materials and methods

The thesis has data obtained from experiments performed only on chick embryos. This chapter comprises of detailed protocols of all techniques that were used in the

experiments and the analysis of data relevant to the thesis. It also comprises of a list of reagents, antibodies and their manufacturer's details. The experimental protocols include collection and culture of embryos, cryo-sectioning and immuno-histochemistry, electroporation at different stages of development, making in-situ probes and whole mount in-situ hybridisation, microdissection and mosaic electroporation based genetic perturbation. Additionally, a detailed description of all the analysis and statistical tests that was performed in understanding the data is also included.

Chapter 3: Results Part I: Characterising epithelial fusion in otic vesicle

This chapter includes a thorough characterisation of otic vesicle closure using scanning electron microscopy and immunohistochemistry. Previous studies have shown filopodia being sent by cells on the edge of the otic vesicle during closure. Additionally, they also see some apoptosis at the edges that are fusing (Alvarez, Martín-Partido, Rodríguez-Gallardo, González-Ramos, & Navascués, 1989). SEM on a transversely bisected otic vesicle revealed the presence of a small population of round cells on the edge undergoing fusion. We confirmed the change in shape of these cells by staining thin frozen sections with phalloidin and 3D- reconstructing the confocal images. We observed three populations of cells based on their sphericity and location within the otic vesicle: the pseudostratified cells in the bulk of the otic vesicle, the squamous surface ectoderm cells and round cells in the edge of the closing otic vesicle. The round cells, hence are cells that populate the boundary between the surface ectoderm and the otic vesicle. Further, we looked at the expression profiles of cell-cell junctions and polarity proteins in the three populations using IHC. Quantitative analysis of protein localisation suggested that the round cells were not completely epithelial as compared to the pseudostratified cells or the surface ectoderm cells. The edge cells seemed to display a hybrid state that is neither epithelial nor mesenchymal, very similar to hybrid-EM phenotype as seen in cancer (Aiello et al., 2018; Goossens, Vandamme, Vlierberghe, & Berx, 2017; Gregory et al., 2011; Haensel et al., 2019; Hong et al., 2015; Nieto, Huang, Jackson, & Thiery, 2016) .

Chapter 4: Results Part II: Altered cell state of edge cells

This chapter delves into the investigation of the transcriptomic state of edge cells. The gene regulatory network required to maintain a hybrid-EM phenotype is well characterised in the context of cancer. To confirm if the round edge cells in otic vesicle closure also have a similar transcriptomic signature, we performed Whole-mount In-Situ Hybridisation for the genes- Grhl2, Grhl3, Zeb2 and Snail2. The four genes are components of the hybrid-EM regulatory network (Nieto et al., 2016). Grhl2 is upstream of Cadh1 and is responsible for the maintenance of epithelial nature of cells (Pyrgaki, Liu, & Niswander, 2011; Ray & Niswander, 2016; Senga, Mostov, Mitaka, Miyajima, & Tanimizu, 2012) .Grhl3 is essential for the proper fusion of neural tube and mouse mutants for the gene exhibit neural tube closure defects of varying severity (Castro et al., 2018; Chalmers et al., 2006; Gustavsson, Copp, & Greene, 2008; Yu et al., 2008) . Zeb2 and Snail2 are inducers of EMT (Goossens et al., 2017) . We saw there was an otic edge specific expression of Grhl2 and Zeb2. Grhl2 expression was seen from HH14 until HH17+ when closure was complete. Zeb2 expression was transient; it was only observed at the site of fusion of the otic edges. Thus, we proceeded to look at the transcriptomics signature of the cells on the edge and compare it with the cells of the otic vesicle and the surface ectoderm, by bulk mRNA sequencing. Differential gene expression analysis and subsequent reactome analysis of the enriched gene list revealed a similarity in the transcriptomic signature of the edge cells with other embryonic processes that involve EMT, including gastrulation, neural tube formation. We validated the enrichment analysis by WhISH and confirmed specific expression of the genes at the site of fusion in HH17 embryos. Two candidate genes: Grhl2 and SP8 were chosen for further gene perturbation studies. These genes were chosen for two major reasons: (i) Mutants for the genes exist in other model organisms, and show inner ear defects (Chung, Medina-Ruiz, & Harland, 2014; Han et al., 2011) and (ii) the WhISH data showed their expression domain extending from the adjacent surface ectoderm and ending at the edge of the otic vesicle. This would imply that the genes are not involved in the overall patterning of the inner ear itself, and may be implicated in the fusion of the vesicle. Genetic perturbation of either of the genes resulted in a similar phenotype; the cells at the site of fusion had not changed shape and Cadh1 was accumulating in the boundary of the cells mediating

fusion. This also perturbed the segregation of the otic vesicle from the surface ectoderm. This suggests that (i)both Grhl2 and SP8 are involved in the maintenance of a hybrid EM phenotype of the edge cells and (ii) cell shape change is essential for epithelial fusion to occur.

Chapter 5: Discussions, limitations and future directions of the study

The final chapter of the thesis condenses the results obtained in chapters 3 and 4 and discusses the broader perspective and implications of the study. It also includes possible hypotheses that can be tested in the future, while also pointing out the caveats of the current thesis.

References:

1. Acloque, H., Adams, M. S., Fishwick, K., Bronner-Fraser, M., & Nieto, M. A. (2009). Epithelial-mesenchymal transitions: the importance of changing cell state in development and disease. *The Journal of Clinical Investigation*, *119*(6), 1438–1449. https://doi.org/10.1172/jci38019
2. Aiello, N. M., Maddipati, R., Norgard, R. J., Balli, D., Li, J., Yuan, S., … Stanger, B. Z. (2018). EMT Subtype Influences Epithelial Plasticity and Mode of Cell Migration. *Developmental Cell*, *45*(6), 681-695.e4. https://doi.org/10.1016/j.devcel.2018.05.027
3. Allagh, K. P., Shamanna, B. R., Murthy, G. V. S., Ness, A. R., Doyle, P., Neogi, S. B., & Pant, H. B. (2015). Birth Prevalence of Neural Tube Defects and Orofacial Clefts in India: A Systematic Review and Meta-Analysis. *PLoS ONE*, *10*(3), e0118961. https://doi.org/10.1371/journal.pone.0118961
4. Alvarez, I. S., Martín-Partido, G., Rodríguez-Gallardo, L., González-Ramos, C., & Navascués, J. (1989). Cell proliferation during early development of the chick embryo otic anlage: Quantitative comparison of migratory and nonmigratory regions of the otic epithelium. *Journal of Comparative Neurology*, *290*(2), 278–288. https://doi.org/10.1002/cne.902900208
5. Amack, J. D. (2021). Cellular dynamics of EMT: lessons from live in vivo imaging of embryonic development. *Cell Communication and Signaling*, *19*(1), 79. https://doi.org/10.1186/s12964-021-00761-8
6. Castro, S. C. P. D., Hirst, C. S., Savery, D., Rolo, A., Lickert, H., Andersen, B., … Greene, N. D. E. (2018). Neural tube closure depends on expression of Grainyhead-like 3 in multiple tissues. *Developmental Biology*, *435*(2), 130–137. https://doi.org/10.1016/j.ydbio.2018.01.016

7. Chalmers, A. D., Lachani, K., Shin, Y., Sherwood, V., Cho, K. W. Y., & Papalopulu, N. (2006). Grainyhead-like 3, a transcription factor identified in a microarray screen, promotes the specification of the superficial layer of the embryonic epidermis. *Mechanisms of Development*, *123*(9), 702–718. https://doi.org/10.1016/j.mod.2006.04.006
8. Chan, B. H. C., Moosajee, M., & Rainger, J. (2021). Closing the Gap: Mechanisms of Epithelial Fusion During Optic Fissure Closure. *Frontiers in Cell and Developmental Biology*, *8*. https://doi.org/10.3389/fcell.2020.620774
9. Chung, H. A., Medina-Ruiz, S., & Harland, R. M. (2014). Sp8 regulates inner ear development. *Proceedings of the National Academy of Sciences*, *111*(17), 6329–6334. (world). https://doi.org/10.1073/pnas.1319301111
10. Duband, J. L., Monier, F., Delannet, M., & Newgreen, D. (1995). Epithelium-mesenchyme transition during neural crest development. *Acta Anatomica*, *154*(1), 63–78. https://doi.org/10.1159/000147752
11. Fernández-Santos, B., Caro-Vega, J. M., Sola-Idígora, N., Lazarini-Suárez, C., Mañas-García, L., Duarte, P., … Ybot-González, P. (2021). Molecular similarity between the mechanisms of epithelial fusion and fetal wound healing during the closure of the caudal neural tube in mouse embryos. *Developmental Dynamics*, *250*(7), 955–973. https://doi.org/10.1002/dvdy.306
12. Galea, G. L., Cho, Y.-J., Galea, G., Molè, M. A., Rolo, A., Savery, D., … Copp, A. J. (2017). Biomechanical coupling facilitates spinal neural tube closure in mouse embryos. *Proceedings of the National Academy of Sciences of the United States of America*, *114*(26), E5177–E5186. https://doi.org/10.1073/pnas.1700934114
13. Gestri, G., Bazin-Lopez, N., Scholes, C., & Wilson, S. W. (2018). Cell Behaviors during Closure of the Choroid Fissure in the Developing Eye. *Frontiers in Cellular Neuroscience*, *12*. https://doi.org/10.3389/fncel.2018.00042
14. Goossens, S., Vandamme, N., Vlierberghe, P. V., & Berx, G. (2017). EMT transcription factors in cancer development re-evaluated: Beyond EMT and MET. *Biochimica et Biophysica Acta (BBA) - Reviews on Cancer*, *1868*(2), 584–591. https://doi.org/10.1016/j.bbcan.2017.06.006
15. Gregory, P. A., Bracken, C. P., Smith, E., Bert, A. G., Wright, J. A., Roslan, S., … Goodall, G. J. (2011). An autocrine TGF-β/ZEB/miR-200 signaling network regulates establishment and maintenance of epithelial-mesenchymal transition. *Molecular Biology of the Cell*, *22*(10), 1686–1698. https://doi.org/10.1091/mbc.e11-02-0103
16. Gustavsson, P., Copp, A. J., & Greene, N. D. E. (2008). Grainyhead genes and mammalian neural tube closure. *Birth Defects Research Part A: Clinical and Molecular Teratology*, *82*(10), 728–735. https://doi.org/10.1002/bdra.20494
17. Haensel, D., Sun, P., MacLean, A. L., Ma, X., Zhou, Y., Stemmler, M. P., … Dai, X. (2019). An Ovol2-Zeb1 transcriptional circuit regulates epithelial directional migration and proliferation. *EMBO Reports*, *20*(1). https://doi.org/10.15252/embr.201846273
18. Han, Y., Mu, Y., Li, X., Xu, P., Tong, J., Liu, Z., … Meng, A. (2011). Grhl2 deficiency impairs otic development and hearing ability in a zebrafish model of

the progressive dominant hearing loss DFNA28. *Human Molecular Genetics*, *20*(16), 3213–3226. https://doi.org/10.1093/hmg/ddr234
19. Hong, T., Watanabe, K., Ta, C. H., Villarreal-Ponce, A., Nie, Q., & Dai, X. (2015). An Ovol2-Zeb1 Mutual Inhibitory Circuit Governs Bidirectional and Multi-step Transition between Epithelial and Mesenchymal States. *PLoS Computational Biology*, *11*(11), e1004569. https://doi.org/10.1371/journal.pcbi.1004569
20. Ladher, R. K. (2017). Changing shape and shaping change: Inducing the inner ear. *Seminars in Cell & Developmental Biology*, *65*, 39–46. https://doi.org/10.1016/j.semcdb.2016.10.006
21. Lubarsky, B., & Krasnow, M. A. (2003). Tube Morphogenesis Making and Shaping Biological Tubes. *Cell*, *112*(1), 19–28. https://doi.org/10.1016/s0092-8674(02)01283-7
22. Millard, T. H., & Martin, P. (2008). Dynamic analysis of filopodial interactions during the zippering phase of *Drosophila* dorsal closure. *Development*, *135*(4), 621–626. https://doi.org/10.1242/dev.014001
23. Nieto, M. A., Huang, R. Y.-J., Jackson, R. A., & Thiery, J. P. (2016). EMT: 2016. *Cell*, *166*(1), 21–45. https://doi.org/10.1016/j.cell.2016.06.028
24. Nikolopoulou, E., Galea, G. L., Rolo, A., Greene, N. D. E., & Copp, A. J. (2017). Neural tube closure: cellular, molecular and biomechanical mechanisms. *Development*, *144*(4), 552–566. https://doi.org/10.1242/dev.145904
25. Park, K.-S., & Gumbiner, B. M. (2012). Cadherin-6B stimulates an epithelial mesenchymal transition and the delamination of cells from the neural ectoderm via LIMK/cofilin mediated non-canonical BMP receptor signaling. *Developmental Biology*, *366*(2), 232–243. https://doi.org/10.1016/j.ydbio.2012.04.005
26. Pyrgaki, C., Liu, A., & Niswander, L. (2011). Grainyhead-like 2 regulates neural tube closure and adhesion molecule expression during neural fold fusion. *Developmental Biology*, *353*(1), 38–49. https://doi.org/10.1016/j.ydbio.2011.02.027
27. Pyrgaki, C., Trainor, P., Hadjantonakis, A.-K., & Niswander, L. (2010). Dynamic imaging of mammalian neural tube closure. *Developmental Biology*, *344*(2), 941–947. https://doi.org/10.1016/j.ydbio.2010.06.010
28. Ray, H. J., & Niswander, L. (2012). Mechanisms of tissue fusion during development. *Development*, *139*(10), 1701–1711. https://doi.org/10.1242/dev.068338
29. Ray, H. J., & Niswander, L. A. (2016). Grainyhead-like 2 downstream targets act to suppress epithelial-to-mesenchymal transition during neural tube closure. *Development*, *143*(7), 1192–1204. https://doi.org/10.1242/dev.129825
30. Rolo, A., Savery, D., Escuin, S., Castro, S. C. de, Armer, H. E., Munro, P. M., … Copp, A. J. (2016). Regulation of cell protrusions by small GTPases during fusion of the neural folds. *ELife*, *5*, e13273. https://doi.org/10.7554/elife.13273
31. Scarpa, E., Szabó, A., Bibonne, A., Theveneau, E., Parsons, M., & Mayor, R. (2015). Cadherin Switch during EMT in Neural Crest Cells Leads to Contact Inhibition of Locomotion via Repolarization of Forces. *Developmental Cell*, *34*(4), 421–434. https://doi.org/10.1016/j.devcel.2015.06.012

32. Schöck, F., & Perrimon, N. (2002). Molecular Mechanisms of Epithelial Morphogenesis. *Annual Review of Cell and Developmental Biology*, *18*(Volume 18, 2002), 463–493. https://doi.org/10.1146/annurev.cellbio.18.022602.131838
33. Senga, K., Mostov, K. E., Mitaka, T., Miyajima, A., & Tanimizu, N. (2012). Grainyhead-like 2 regulates epithelial morphogenesis by establishing functional tight junctions through the organization of a molecular network among claudin3, claudin4, and Rab25. *Molecular Biology of the Cell*, *23*(15), 2845–2855. https://doi.org/10.1091/mbc.e12-02-0097
34. Tamilkumar, V. N. (2023). Andrew S. Reynolds, The third lens: metaphor and the creation of modern cell biology, Chicago: the Chicago University Press, 2018. *History and Philosophy of the Life Sciences*, *45*(4), 38. https://doi.org/10.1007/s40656-023-00595-2
35. Yang, J., Antin, P., Berx, G., Blanpain, C., Brabletz, T., Bronner, M., … (TEMTIA), O. behalf of the E. I. A. (2020). Guidelines and definitions for research on epithelial–mesenchymal transition. *Nature Reviews Molecular Cell Biology*, *21*(6), 341–352. https://doi.org/10.1038/s41580-020-0237-9
36. Yu, Z., Bhandari, A., Mannik, J., Pham, T., Xu, X., & Andersen, B. (2008). Grainyhead-like factor Get1/Grhl3 regulates formation of the epidermal leading edge during eyelid closure. *Developmental Biology*, *319*(1), 56–67. https://doi.org/10.1016/j.ydbio.2008.04.001

LIST OF PUBLICATIONS

1. **Varsha N. Tamilkumar**, Harsha Purushothama, Raj K. Ladher; Epithelial fusion is mediated by a partial epithelial–mesenchymal transition. Biol Open 15 September 2025; 14 (9): bio062213. doi: https://doi.org/10.1242/bio.062213
2. **Tamilkumar, V.N**. Andrew S. Reynolds, The third lens: metaphor and the creation of modern cell biology, Chicago: the Chicago University Press, 2018. HPLS 45, 38 (2023). https://doi.org/10.1007/s40656-023-00595-2

Chapter 1: Introduction

1. Cells

Animals are composed of two cell types; epithelial and mesenchymal cells. Epithelial cells are characterised by the junctions they form with other epithelial cells, to form a contiguous sheet. This adhesion is mediated by a variety of inter-cellular protein complexes called adhesion complexes, including tight junctions, adherens junctions, desmosomes and gap junctions (Fig 1.1 and 1.2). Epithelial cells also exhibit an apico-basal polarity, apparent by the specific localisation of subsets of proteins to the apical and basal domains, and their anchorage to a basal Extracellular Matrix (ECM), known as the basal lamina. In contrast mesenchymal cells exist as individual cells and are capable of migrating through the extracellular matrix. They lack an apico-basal polarity and instead have a front-rear polarity that dictates their direction of migration. This categorization of the cells into two classes has been important for the understanding of morphogenetic events during embryonic development. As the authors of the review (Nakaya & Sheng, 2008) note, "Any morphogenetic process can be viewed conceptually as cell organizational changes either within the epithelial or mesenchymal state, or a transition between these two states (EMT for Epithelial to Mesenchymal Transition or MET for Mesenchymal to Epithelial Transition)."

1.1 The epithelium

The development of an organism starts from a single cell zygote, which eventually gives rise to all the cell types seen in an organism. These cell types fall into one of the two categories as described above; the epithelium, with a two-dimensional organisation attached to their neighbours and the mesenchyme in their three-dimensional space (Nakaya & Sheng, 2008). Epithelial cells are present throughout the body of metazoans. All three germ layers - the ectoderm, mesoderm and endoderm can form epithelia; for example, the lining of body cavities, the brain and sensory organs, the gut and so on.

A distinguishing feature of the epithelial cell is its polarity. They have three domains- apical, basal and lateral. These domains are established by localisation of junctions that play a barrier or fence like function that are involved in extracellular contacts between cells, linking the actin cytoskeletal network within the tissue and the regulation of gene transcription (Hartsock & Nelson, 2008). The tight or septate junctions also possess a gate function for a paracellular passage of solutes and ions. They are transmembrane proteins of two types, claudins and occludins that are the functional components of tight junctions and also associate with other cytosolic proteins for their downstream effects (Schneeberger & Lynch, 2004). Claudins are usually seen as paired protein strands that are constantly remodelled for their dynamic functions. Their gating function for ions is very similar to other ion channels (M. Furuse, Sasaki, Fujimoto, & Tsukita, 1998; Mikio Furuse, Fujita, Hiiragi, Fujimoto, & Tsukita, 1998).

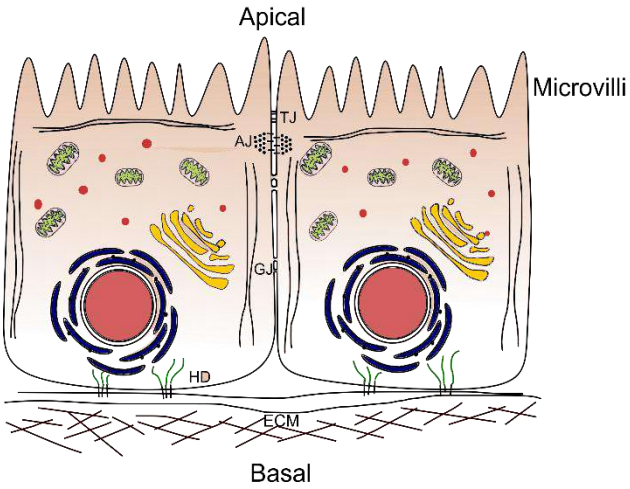

Fig. 1.1: Epithelial cells. These cells have apical, lateral and basal domains; demarcated by specific junctions that maintain the composition of the plasma membrane of that domain and their contact with the neighbouring cells. Additionally, they're tethered also, to the underlying basement membrane through specific junctions. The cells can also communicate with each other through the transmission of small molecules between two cells. TJ: Tight Junction, AJ: Adherens Junction, GJ: Gap Junction, HD: Hemi Desmosomes, ECM: Extra Cellular Matrix

The adherens junctions are involved in the initiation and stabilisation of cell contacts, formation of tight junctions, intracellular cytoskeletal regulation, and signalling leading to gene transcription (Gumbiner, 2005; Halbleib & Nelson, 2006). Cadherins are components of these junctions, that are transmembrane glycoproteins. They possess cytosolic domains that bind to other proteins including the catenin family to effect intracellular signalling upon sensing extracellular signal (Perez-Moreno & Fuchs, 2006). Their cytosolic domains also have an auto-regulatory function that mediates E-

cadherin endocytosis, recycling or degradation (Takeichi, 2014). Epithelial cells are connected to the basement membrane by integrins and hemidesmosomes. The basement membrane separates the epithelial cells from the underlying mesenchyme (Hartsock & Nelson, 2008).

The apical region of the epithelium often faces the lumen of an organ or the external environment. The cells consist of an externally protruding cytoskeletal structure such as a cilia or microvilli that aid in their interaction with the external environment. Cilia are made of microtubules. They are primarily involved in cell signalling, by acting as sensors of the cell. Microvilli are made of actin and usually are involved in secretion or absorption. Stereocilia are specialised actin projections organised in a staircase like pattern in the apex of the hair cells in the inner ear that sense sound waves.

Epithelial cells can be further subdivided in a variety of ways, but one of the simplest is based on their aspect, that is the ratio of the width to their length. Epithelial cells can be of the following forms:

a. Squamous: Have a flat sheet morphology
b. Cuboidal: The length and width of these cells are equal.
c. Columnar: The length of the cells is greater than their width.

Epithelia can also be categorised based on their organisation; they can be monolayered or stratified, that is consisting of two or more layers. Another type that is prominent during development, is pseudostratified epithelia; a monolayered sheet of epithelial cells with the nuclei localising at various levels along the apical-basal axis, imparting a stratified appearance to the tissue.

1.2 The mesenchyme

Mesenchymal cells usually do not possess characteristic features like their epithelial counterparts and are characterised by their differences (Trelstad, Hay, & Revel, 1967). They have an irregular shape, they are motile, and form very transient junctions with their neighbours; mostly gap junctions when they interact. They have a front-back polarity, with actin fibres localising in the front to create membrane protrusions, lamellipodia and filopodia, that help in active locomotion and a trailing pseudopodium (Fig 1.2). They secrete ECM components, and can also actively migrate through ECM with the help of invadopodia, actin rich structures, that have a proteolytic function.

Their active front is also enriched with the Golgi complex, which is a constant source of plasma membrane to the leading edge of the cell (Hay, 2005; Do Kim et al., 2017).

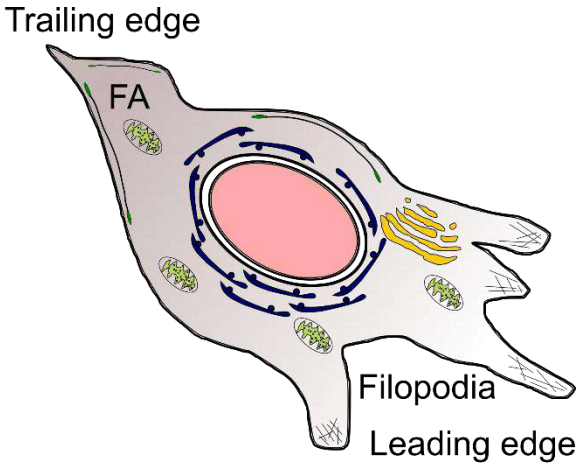

Fig. 1.2: Mesenchymal cells. These cells have a leading and trailing edge as identified by the localisation of actin stress fibers in the leading edge and more focal adhesions (FA) in the trailing edge. They usually have transient interactions with neighbours, if any, through junctions and repel away from each other. They migrate on a substrate such as ECM.

1.3 Epithelial to Mesenchymal Transition (EMT)

One of the striking features of most metazoans is their ability to give rise to non-epithelial cells, the mesenchyme, from epithelial cells and vice versa through a process called Epithelial to Mesenchymal Transition (EMT) and Mesenchymal to Epithelial Transition (MET), respectively. And as quoted above, the process is crucial during morphogenesis and organogenesis in the embryo. EMTs occur at multiple instances throughout embryonic development. EMT in a cell is characterised with the loss of cell junctional contact with their neighbours, loss of apical-basal polarity, reorganisation of their cytoskeletal structures to undergo shape change, acquisition of invasive migratory abilities and detachment from the underlying basement membrane. Besides the visible changes, significant changes in gene expression also takes place for effecting this process (J. Yang et al., 2020). The existence of two kinds of cell was known as early as the late 19th century, and the conversion of epithelial cells to mesenchymal cells was first described in 1908 by Frank Lillie (Lillie, 1908). The first detailed explanation of EMT was given by Elisabeth Hay, in 1968, during the formation of the chick primitive streak (Trelstad et al., 1967; Trelstad, Revel, & Hay, 1966). However, only in 1982, upon the conversion of epithelial cells into mesenchymal cells, in 3D collagen droplets

(Greenburg & Hay, 1982), was EMT acknowledged as a distinct process by itself (Thiery, 2002).

The process of EMT is reversible, and is also commonly seen during embryonic development, MET. This reversible nature of the cells is very crucial for normal organogenesis, and also plays a major role in pathogenesis. A plethora of signals are capable of inducing EMT in epithelial cells. For instance, cardiac muscle can induce EMT in endocardial cells (Runyan & Markwald, 1983), HGF transformed epithelial cells into migratory fibroblasts (Stoker & Perryman, 1985). While developmental studies on *Drosophila melanogaster* paved the way for the identification of transcription factors involved in EMT (M. Leptin, 1991) including Snail and Twist, the characterisation of related transcription factors in chordates established their significance and hence conservation during evolution (M. Angela Nieto, 2002). The discovery and study of their homologs in the embryonic development of other animal models, showed their regulation of EMT was partly through e-cadherin regulation (Batlle et al., 2000; Bolós et al., 2003; Cano et al., 2000; Hajra, Chen, & Fearon, 2002).

The link between EMT during development and in tumour progression was first suggested by the Weinberg lab. They demonstrated that the gene Twist, necessary for *Drosophila* gastrulation also promoted breast cancer metastasis (J. Yang et al., 2004). 80 to 90% of cancers reported are carcinomas (epithelial tissue origin), and the disease progression is marked by a loss of epithelial characteristics. Metastasis is initiated by tumour cells that have acquired migratory abilities, similar to the embryonic mesenchymal cells. EMT in development and tumour progression have similar cellular and molecular mechanisms, but the extent to which these programs are activated or repressed in either of the situations is not clear yet (Francou & Anderson, 2020).

During this transition, it is also possible for cells to exist in an intermediate/hybrid phenotype, exhibiting partial epithelial and mesenchymal traits (M. Angela Nieto, Huang, Jackson, & Thiery, 2016); this highly plastic phenotype is enriched in circulating tumour cells (Yu et al., 2013), and the existence of this hybrid state has a significant role during cancer metastasis and neural crest cell migration (Belacortu & Paricio, 2011; Cai et al., 2016; Heisenberg & Bellaïche, 2013; Martin & Wood, 2002; Pocha & Montell, 2014).

1.4 EMT during development

A major portion of the cells found in an adult organism emerge from multiple rounds of EMT and MET during embryonic development. This is crucial in the formation of complex internal organs that house multiple populations of differentiated cells. And these processes are categorised as primary, secondary and tertiary EMT, depending on the iteration of EMT the cell has undergone. Primary EMT is seen during mammalian implantation, gastrulation and neural crest cell formation. *Drosophila* gastrulation has been instrumental for developments in the field of EMT. *Twist* and *Snail* were discovered as essential in the formation of the mesoderm (M. Leptin, 1991). Secondary EMT is seen during differentiation of cells from somites, urogenital system, somatopleure and splanchnopleure, further restricting their fate choices. Tertiary EMT is seen during the development of the endo-cardiac jelly from the endothelial cells of the atrioventricular canal (Nakajima, Yamagishi, Hokari, & Nakamura, 2000; Thiery, Acloque, Huang, & Nieto, 2009).

EMT can be initiated by multiple transcription factors and signalling pathways. The FGF, TGF-β and Wnt signalling can activate EMT. The Snail 1,2 transcription factors repress Cdh1 and can also activate mesenchymal genes; both ways promote EMT in embryonic development and have been implicated in EMT seen in tumour progression. Twist, Zeb 1 and 2, also are transcription factors that promote EMT through a variety of targets in a context dependent manner (Shook & Keller, 2003; Thiery et al., 2009). All of these transcription factors and signalling pathways regulate the loss of epithelial properties and acquisition of mesenchymal properties.

1.4.1 Gastrulation

'It is not birth, marriage or death, but gastrulation which is truly the most important time in your life'

- Lewis Wolpert, in *Horizon,* 'Genesis' episode in BBC, January 1986(Hopwood, 2022) .

The relevance of the quote above is apparent in what happens during this process. Gastrulation, is the first step in the establishment of the body plan, whereby the germ layers are specified, spatially reorganised and finally laid down as organ rudiments to form the future organism. This process results in the formation of endoderm in diploblasts and both mesoderm and endoderm in triploblasts. Gastrulation can be

further divided into four distinct phases comprising of multiple morphogenetic events; it begins with emboly, when the prospective meso-endoderm tissue is internalised under the ectoderm. This is followed by epiboly, when the specified germs layers spread themselves thin, across the embryonic body plan. This is followed by convergence of the germ layers along the dorsal-ventral axis and finally the extension to elongate the germ layers along the anterior-posterior axis. These events themselves depend on various cellular processes including cell migration, both individual and collective, shape change, EMT, directed and random cell intercalations and division (R. Keller, Jr, & Griffin, 2012).

The first step, is emboly; during which the prospective mesoderm and endoderm are transported beneath the future ectoderm through an opening, the blastopore. This site of involution or ingression of cells is identified by specific names in different organisms; ventral furrow in fly, blastopore in amphibian, blastoderm margin in teleost, and primitive streak in avian and mammals (R. Keller, Davidson, & Shook, 2003). This transport starts from the surface of the embryo, where the precursors are a part of an intact epithelium as in the case of the worm, flies and amniotes or where the cells are part of an adherent and tightly packed mesenchymal tissue as seen in the case of amphibians and fishes. During gastrulation, we see EMT only during emboly and the accompanying cell migration (S.-Y. Wu, Ferkowicz, & McClay, 2007). As is the case elsewhere, EMT entails the disassembly of epithelial junctions with the down regulation of cell adhesion molecules and a cytoskeletal reorganisation involving the intermediate filaments and the microtubule network (Thiery et al., 2009).

Emboly can be further categorised based on the order of events; when EMT happens after the internalisation of cells, as seen in invagination and involution, and when EMT precedes internalisation of cells, as seen in ingression. Invagination is seen in *Drosophila melanogaster* gastrulation, when the epithelial cells in the ventral midline get constricted apically, and the cell shape transforms from a columnar to a wedge; nuclear translocation to the basal side and simultaneous shortening of the apical-basal dimensions leads to shape change. These changes aid in the formation of a furrow such that the future mesoderm is pushed deep within the embryo. Once within the embryo, the mesodermal epithelial tube establishes contact with the ventral aspect of the ectoderm (Sweeton, Parks, Costa, & Wieschaus, 1991) and the mesodermal precursors

undergo EMT (Maria Leptin, 2005), through junctional disassembly, as marked by loss of DE-cadherin and a cytoplasmic translocation of DN-cadherin and migrate along the basal side of the future ectoderm (Oda, Tsukita, & Takeichi, 1998). Subsequently, some of the endodermal precursors residing at the anterior side of the ventral furrow also get internalized into the furrow (McMahon, Supatto, Fraser, & Stathopoulos, 2008).

Involution is seen in amphibians. Here, the future mesoderm and endoderm arise from a cohesive tissue that is present just above the blastopore (R. E. Keller, 1981). The precursors of the ectoderm are located near the animal end and those of the endoderm more vegetally, and the mesoderm is seen as a band that connects the two (Dale & Slack, 1987; Lane & Sheets, 2002). "Bottle cells" of the nascent blastopore in the dorsal most region of the gastrula, undergo apical constriction (Hardin & Keller, 1988) . Here, β-catenin induces the formation of the Spemann-Mangold Organiser (SMO), leading to the induction of the mesodermal and endodermal cells through nodal signalling. This induction is also crucial for subsequent movements (Heasman, Kofron, & Wylie, 2000; Robertis, Larraín, Oelgeschläger, & Wessely, 2000). As gastrulation proceeds, the blastopore expands laterally and allowing the collective migration of the cohesive mesoderm. Similar to the flies, only after being pushed inside the gastrula stage embryo, the mesodermal cells undergo EMT and migrate along the basal side of the blastocoel roof (Winklbauer & Nagel, 1991). Vegetal rotation, a process by which the marginal zone is turned towards the blastocoel with the help of a distorted endodermal vegetal cell mass, is important in involution (Winklbauer & Schürfeld, 1999). The condensed packing of the mesodermal precursors requires proper timed movements for the completion of gastrulation. For instance, involution and epiboly are dependent on the convergent extension of the dorsal mesoderm (Shih & Keller, 1994).

Ingression, belonging to the second category of emboly, is seen in sea urchin and amniote gastrulation. Here, the precursors of mesoderm and endoderm reside at the primitive streak, which undergo EMT and migrate individually, deep into the embryo (Harrisson, Callebaut, & Vakaet, 1991; P. P. L. Tam & Behringer, 1997; P. P. Tam, Williams, & Chan, 1993). The chick blastula, despite being similar to frog and fish embryos with respect to the relative amounts of yolk in the egg, has a different gastrulation program (G. C. Schoenwolf & Sheard, 1990). The flat epiblast, a single cell thick epithelium, comprises of the area pellucida and the surrounding area opaca.

A small group of cells in the prospective posterior side of the epiblast become Koller's sickle and express SMO genes. Around the same time, cells delaminate from the area pellucida epithelium and form cellular islands below the epiblast. These cell groups fuse and become the hypoblast (Gary C. Schoenwolf, 1991). The Primitive Streak (PS) starts off as a slit in the posterior epiblast, extends in the anterior direction and shortens, during gastrulation. The anterior extension of the PS is due to the symmetrical convergence of cells from lateral epiblast to the posterior midpoint of the area pellucida. This entire process is described as a polonaise cell movement, owing to the cellular migratory patterns that resemble the dance form (Chuai & Weijer, 2009). The anterior aspect of the PS is known as the Hensen's node and as it extends, ingression begins; the precursors of mesoderm and endoderm undergo EMT and migrate into the region between the epiblast and hypoblast (X. Yang, Dormann, Münsterberg, & Weijer, 2002). The ingression is marked by apical constriction of cells that bend the PS in the centre along the AP axis. These cells exhibit robust apical junctions and delicate basement membrane. Rho A inhibition and microtubule instability lead to the breakdown of basement membrane. On acquiring an extreme form of wedge cell shape, the junctions dissolve, thus releasing the cells from the epithelium and allowing EMT for migration of the precursors (Nakaya & Sheng, 2008, 2009).

Cells undergo a variety of transformative processes during the course of development. The change in cell shape, cell migration and intercalation require a modulation in their adhesive properties and internal scaffolding of the cytoskeletal proteins. This modulation is brought about in two steps; a directed polarized membrane transport and endocytosis for further polarization of the cell (Nelson, 2009). Further characterisation of cellular properties in vitro has revealed a cyclic phenomenon in cytoskeletal regulation. The first cycle initiates a small change which is further reinforced by subsequent cycles as seen during actomyosin contractility and polymerization(Gorfinkiel & Blanchard, 2011). The microtubules play a crucial role in attributing polarity to the cell, either through polarized migration of cargo to or from distinct domains in epithelial cells. In mesenchymal cells, the microtubule dynamicity during rounds of growth or collapse aid with the motility and adhesion in the cell-substratum interaction (Kirschner & Mitchison, 1986). Cell intercalation is aided by a polarised distribution of the cytoskeleton and endocytosis of adhesion and other polarity proteins (Levayer, Pelissier-Monier, & Lecuit, 2011). The WNT/PCP pathway alters

Cdh1 adhesion, probably its distribution, through endocytosis (Ulrich & Heisenberg, 2008).

Differential adhesion of cells plays a very important role during gastrulation movements and cell sorting. Townes and Holtfreter (1955) showed embryonic cells when separated from each other could reaggregate and sort themselves into their corresponding germ layers (Townes & Holtfreter, 1955). There are two proposed explanations for this behaviour; Steinberg's (2007) differential adhesion hypothesis attributed the behaviour to "quantitative differences in surface adhesion" (Steinberg, 2007) and Kren and Heisenberg's (2011) differential surface contraction hypothesis attributed the behaviour to " a cell's stiffness or ability to contract its cortex" (Krens & Heisenberg, 2011). A reduction in the levels of Cadh1 adhesion by morpholino or hypo-morphic mutations, while not interfering with germ cell formation, affected radial cell intercalation, cellular attachment to the superficial enveloping layer and thus epiboly, in zebrafish embryos (Babb & Marrs, 2004; Kane, McFarland, & Warga, 2005; Shimizu et al., 2005; Winklbauer, 2009). In the anterior dorsal mesoderm, some cells also exhibited a rounded shape (Montero et al., 2005).

ECM, an assortment of secreted glycoproteins, supports and scaffolds cells and tissues from the outside, provides ligands to regulate signalling, and aids in cellular processes by modulating its composition and thus its interaction with the cell. They are crucial in cell migration during gastrulation in different species; PS formation in chick, for example. Meshwork of ECM move beneath the cells in the streak, providing a motile substratum, at earlier stages of PS formation and during the extension of the axis (Bénazéraf et al., 2010; Zamir, Rongish, & Little, 2008). During amphibian gastrulation, the migration of mesodermal precursors on the blastocoel roof is mediated by fibronectin, as is the case during their migration on the basal side of chick ectoderm (Boucaut et al., 1996; Lance A. Davidson, Keller, & DeSimone, 2004; Lance A. Davidson, Marsden, Keller, & DeSimone, 2006; Winklbauer, 2009). Gastrulation in teleost utilise the fibronectin-integrin interaction with a chemokine -GPCR pair to regulate polarised tissue morphogenesis of the endoderm random walk (Latimer & Jessen, 2010; Nair & Schilling, 2008; Pézeron et al., 2008). As the authors note in their review, "Striking parallels exist between the molecular mechanisms that regulate tumour growth and metastasis and those that govern gastrulation, especially the

processes of EMT, collective cell migration, chemotaxis and chemokinesis" (Solnica-Krezel & Sepich, 2012). These parallels, exist throughout development.

1.4.2 Neural crest cells

The neural tube is induced in the surface ectoderm, by signals from the underlying mesenchyme. The induced patch of cells, the neural plate, undergo thickening to give rise to the pseudostratified neural epithelium. The neural epithelium further undergoes morphogenetic processes, including invagination, convergent extension, dorsal hinge point bending, to bring the neural epithelium borders together. The neural epithelium borders are pushed closer together and juxtaposed for epithelial fusion, to obtain a closed neural tube.

The cells populating the border region between the neural epithelium and the non-neural epithelium are precursors of the neural crest cells. These epithelial cells undergo EMT to give rise to the neural crest cells that migrate to different parts of the organism. This migration of the neural crest cells is essential for proper embryonic development, as neural crest cells give rise to craniofacial cartilage, neurons and support cells of the peripheral nervous system and pigment cells, among others. Due to the multitude of cell lineages that arise from neural crest cells, they have been deemed as the fourth germ layer (B. K. Hall, 2000).

Neural crest cells have baffled biologists for decades by the complex mechanisms and numerous factors involved, from their genesis to their final destination in the embryo and beyond. As mentioned above, they arise from the presumptive Neural Plate Border (NPB) region of the embryo, which is specified by Pax3 expression in the early blastula stages of the embryo (Bang, Papalopulu, Kintner, & Goulding, 1997; Goulding, Chalepakis, Deutsch, Erselius, & Gruss, 1991). In the case of both *Xenopus laevis* and zebrafish, the expression of Slug/Snail starts around or soon after the specification of the NPB (Essex, Mayor, & Sargent, 1993; Hammerschmidt & Nüsslein-Volhard, 1993; Mayor, Morgan, & Sargent, 1995; Thisse, Thisse, & Postlethwait, 1995; Thisse, Thisse, Schilling, & Postlethwait, 1993), as opposed to the chick, where slug expression is only seen when the neural folds are closing (M. A. Nieto, Sargent, Wilkinson, & Cooke, 1994). Interestingly, in the case of the frog and chick embryos, not all slug positive cells are fated to migrate away as neural crest cells (LaBonne & Bronner-Fraser, 1999; Selleck & Bronner-Fraser, 1995).

Beginning with the NPB specification genes, there is a conservation seen across species; *Zic1*, *Msx1* and *Pax3* are essential in frogs (Maczkowiak et al., 2010; Monsoro-Burq, Wang, & Harland, 2005) as well as in fish (Garnett, Square, & Medeiros, 2012; Seo, Sætre, Håvik, Ellingsen, & Fjose, 1998). *Msx1* and *Pax7* specify the NPB in chick (Basch, Bronner-Fraser, & García-Castro, 2006; Streit & Stern, 1999). The NPB specifier genes in turn activate the transcription factors that specify the NCC; *Snail, FoxD* and *SoxE*, that have been shown to be conserved in both, their spatiotemporal and hierarchical expression pattern across vertebrate species. From their induction in the NPB until the initiation of EMT, the NCC are epithelial and remain adhered to their neural and non-neural epithelial neighbours. The NCC specification by these transcription factors initiates the EMT process, by changing the polarity and adhesion of NCC, thus permitting their delamination and collective exit from the neural tube in the chick. Snail2 inhibits the expression of Cdh6B leading to a loss of cell-cell adhesion and delamination from the NT. In frogs, however, Snail2 regulates the expression of Cdh1 (Roellig, Tan-Cabugao, Esaian, & Bronner, 2017; Seal & Monsoro-Burq, 2020; Stundl, Bertucci, Lauri, Arendt, & Bronner, 2021).

Slug/Snail transcription factors regulate the emigration of neural crest cells through their regulation of adhesion proteins. The physical effects following transcriptional changes include the reduction in levels of adhesion between cell-cell and cell-basement membrane, loss or modification of cellular polarity, and cytoskeletal rearrangement to facilitate cellular migration (Duband, Monier, Delannet, & Newgreen, 1995; Gouignard, Andrieu, & Theveneau, 2018; C.-Y. Wu & Taneyhill, 2019). These cytoskeletal rearrangements are often mediated by Rho-family GTPases that have been implicated in cell shape changes, in response to extracellular signals (Aelst & D'Souza-Schorey, 1997; A. Hall, 1998; J.-P. Liu & Jessell, 1998).

The NCC-EMT in chick embryos takes place in three phases- the delamination, collective migration and becoming mesenchymal cells. The pre-migratory NCCs that populate the NPB after the closure of the NFs, express Cdh6B during the closure of the NT and before their delamination (Coles, Taneyhill, & Bronner-Fraser, 2007; Taneyhill, Coles, & Bronner-Fraser, 2007). They express Cdh1 and Cdh11 as EMT is underway. These junction proteins are maintained as they delaminate, still maintaining contact with their neighbours. However, Cdh6B is downregulated and F-actin gets non-polarised (Manohar, Camacho-Magallanes, Echeverria, & Rogers, 2020; Rogers, Sorrells, & Bronner, 2018). As they proceed with their journey away from the neural

tube, still expressing Cdh11, they start expressing Cdh7, transiently, and the cytoskeleton is once again remodelled to impart a front- back polarity, aiding their migration (Manohar et al., 2020).

The migration of these cells from their site of specification involves cadherin switching and regulation; the pathways are different across species. For instance, Cdh1 and Cdh2 are present in the developing chick neural tube. Cdh2 is completely absent in the EMT stage of NCC, whereas Cdh1 is upregulated in the same stage (Dady, Blavet, & Duband, 2012; Rogers et al., 2018). In the case of *Xenopus laevis*, Cdh11 is upregulated in the pre-migratory NCCs and both Cdh11 and Cdh2 are required for their normal migration and survival (Bahm et al., 2017; Kotini et al., 2018; Scarpa et al., 2015). The regulation of Cdh1 in zebrafish, however, is inconclusive (C. Huang, Kratzer, Wedlich, & Kashef, 2016; Piloto & Schilling, 2010; Powell et al., 2015). As the neural crest cells are specified to undergo their migration, so must the facilitation for this starts; with the remodelling of the extracellular matrix/ the basement membrane (BM). The BM undergoes remodelling to become a channel for the NCCs to migrate through (Hutchins & Bronner, 2018).

Multiple signalling pathways are involved in NCC formation and EMT. Elevated levels of BMP signalling is necessary for NCC delamination and successful migration (Piacentino, Hutchins, & Bronner, 2021; Rekler & Kalcheim, 2022). On the other hand, a downregulation of FGF signalling is necessary for NCC specification and EMT (Martínez-Morales et al., 2011). In the frog, β-catenin, an effector of canonical WNT signalling expresses in pre-migratory NCC but not in migrating NCC thus implying a necessary WNT inhibition prior to their migration from NT (Maj et al., 2016).

In chick, Draxin, a WNT antagonist, is essential for laminin remodelling (Hutchins, Piacentino, & Bronner, 2021). Matrixmetalloproteinase9 (MMP9) has been shown to positively regulate NCC EMT possibly by the degradation of Cdh2 and Laminin (Monsonego-Ornan et al., 2012). In *Xenopus*, ADAM13, a metalloproteinase, has been shown to cleave Cdh11 and modulate WNT signalling, thus regulating the migration of cranial NCC (Abbruzzese, Becker, Kashef, & Alfandari, 2016; Leathers & Rogers, 2022; Li et al., 2018).

1.5 EMT in cancer

A host of transcription factors (Snail, Zeb, Twist) and miRNAs along with epigenetic and post-transcriptional regulators are able to initiate EMT during embryogenesis, wound healing, and cancer metastasis(Thiery et al., 2009) . The cell plasticity seen in carcinoma is reminiscent of the plasticity seen in embryogenesis; this similarity implicated EMT in tumour malignancies, specifically metastasis (Cano et al., 2000; Thiery, 2002). Multiple evidences from carcinomas have confirmed that dissociation of cells from the primary tumour is by EMT. These dissociated cells then migrate to other sites, and undergo MET and seed a new tumour.

The plasticity seen in EMT means also, the existence of cells in intermediary stages between epithelial and mesenchymal state and implies that the cells may undergo a partial EMT program. This has been observed in cell culture studies and confirmed in circulating tumour cells and during organ fibrosis. A partial EMT does not necessarily mean acquisition of mesenchymal traits; it can be a change in apico-basal polarity and/or remodelling of junctions in favour of cell-substrate adhesions (R. Y.-J. Huang, Guilford, & Thiery, 2012). Partial EMT in some cases, seems to be the final destination; as seen in dedifferentiated renal epithelial cells. They neither transition to a fully mesenchymal state nor do they revert back to their epithelial beginnings. These partial EM cells invade and stay integrated in the tubules (Grande et al., 2015). Thus, it is possible that these partial transitions might confer other characteristics or abilities, such as better survival or decreased proliferation (M. Angela Nieto et al., 2016).

Partial EMT can also be a transient state that aids in morphogenesis during development or a later programmed event in the lifetime of the organism, such as wound healing. Epithelial wound healing involves re-epithelialization wherein the cells on the edge of the wound move into the site of injury to rebuild. This coordinated movement of epithelial cells requires a behavioural change that is transient and allows also their reversal of identity upon repair of the wound. This repair involves partial EMT (Shaw & Martin, 2016). This is thought to depend on Snail2 (Arnoux, Nassour, L'Helgoualc'h, Hipskind, & Savagner, 2008). During *Drosophila* dorsal closure, the leading-edge cells undergo a partial EMT; they send out actin based protrusions, filopodia and lamellipodia that aid in cell migration through Rac/Cdc42 mediated activation of actomyosin contractility (Bahri et al., 2010).

Pancreatic ductal adenocarcinoma is common, aggressive and difficult to treat; numerous studies on cell lines, patient samples have been published to attribute a molecular signature for EMT in this disease. As mentioned above, several developmental genes have been identified; including, but not limited to the *Snail*, *Zeb* family, *Twist*, *VEGF*, *TGF-β* and *BMP4* (Burk et al., 2008; Ellenrieder et al., 2001; Hamada et al., 2007; Nishioka et al., 2010; A. D. Yang et al., 2006). These studies had differing results and were non-conclusive about the exact players involved. Lineage tracing in mouse model for the disease has revealed an alternate EMT program; instead of transcriptionally repressing epithelial genes, the proteins get sequestered and internalised from their usual localisation site. This is a partial EMT program, where in the cells still retain some of their epithelial properties and also are able to migrate and invade as clusters (Aiello et al., 2018). In this case, the genes imparting mesenchymal properties are not turned on, and the cells can still undergo partial EMT.

This is also seen in breast cancer cells that invade collectively as clusters. 3D culture assays have shown clusters of cells leaving the primary tumour expressing epithelial proteins such as cytokeratin 14, Cdh1, Cdh3 and not expressing classical EMT markers such as twist, snail2 and vimentin (Cheung, Gabrielson, Werb, & Ewald, 2013). Twist1 promoted dissemination of cells in a primary mammary epithelium organoid assay, where the downregulation of Cdh1 had no effect. The epithelial properties were retained even when dissemination was happening. Here, Twist1 was involved in ECM modification (Shamir et al., 2014).

Numerous studies in the field have made it clear that EMT is not mediated by standalone genes, rather involves complex gene regulatory networks. In addition to this, post translational mechanisms are often employed by cancer cells to alter their plasticity, thus challenging the interpretation of transcriptome-based studies as well (Francou & Anderson, 2020).

2. Epithelial Fusion

Epithelial fusion is a morphogenetic event where a pair of apposed epithelial tissues, are pushed together to form a continuous epithelial tissue, often to close an anatomical gap. Fusion here is the formation of junctions between cells in apposed epithelium, and can happen in two different contexts. In the case of wound healing and dorsal closure in flies, fusion repairs a rip in the epithelium. However, during neurulation and otic

vesicle closure, a pair of specified regions in a contiguous sheet of epithelium establish contact and fuse to form two separate sheets of epithelium.

Epithelial fusion is crucial during embryonic development in multiple contexts. For instance, during the formation of neural tube (Pai et al., 2012), optic fissure (Gestri, Bazin-Lopez, Scholes, & Wilson, 2018; Patel & Sowden, 2019), foregut (Kluth & Fiegel, 2003), palatal shelf (Greene & Pisano, 2010), presumptive genitalia of mammal (Wang & Baskin, 2008), and dorsal body wall closure in *Drosophila melanogaster* (Lu, Sokolow, Kiehart, & Edwards, 2015). Any error during this might lead to birth defects or embryonic lethality; exencephaly, spina bifida, omphalocele, cleft palate, coloboma, and hypospadias are some of the congenital malformations that arise due to improper epithelial fusion (Pai et al., 2012).

Zippering, is a process by which juxtaposed epithelial tissues are progressively united from a site of initiation and continues unidirectionally across developmental stages. The site of fusion is similar to a zip fastener, and thus requires considerable force for "zipping" the epithelial sheets into a unified structure (Molè et al., 2020). Dorsal closure in the fly and mammalian embryonic wound healing have provided valuable insights into the tissue and cellular level dynamics of fusion (Fernández-Santos et al., 2021; Hayes & Solon, 2017; Jacinto et al., 2000). Based on these studies, the prevailing, proposed mechanisms in the field are the purse string model and cell crawling model. The purse string model describes the presence of a tissue level actomyosin cable in the circumferential leading edge of the epithelial sheets that are closing in on the anatomical gap, and eventually sealing it. The cell crawling model describes the presence of membranous protrusions sent by the leading edge of the epithelial sheets that mediate closure of the anatomical gap (Begnaud, Chen, Delacour, Mège, & Ladoux, 2016).

However, in the case of neural tube closure, both of these mechanisms play a role in the fusion. In the case of mouse NT, actomyosin cables have been observed in the neural folds, transmitting forces to bio-mechanically couple the open NT. However, the anatomy of the embryonic NT does not permit the formation of a purse string until the final stages of posterior neuropore closure (Galea et al., 2017). Filopodia and lamellipodia protrusions have also been reported, emanating from the NNE and mediating the fusion process. However, unlike the wound healing model, these cells putting forth the membrane protrusions have no underlying substratum to crawl over; instead, the leading-edge cells in the neural tube have to extend into a fluid filled

anatomical gap, giving rise to a fluid filled lumen upon closure (Rolo et al., 2016). Thus, neither of the existing hypotheses in the field can fully account for this mode of fusion (Molè et al., 2020), which is also seen during otic vesicle closure.

2.1 Drosophila body wall closure

The embryonic development of drosophila starts before fertilisation with the specification of the body axes, rostral, caudal, dorsal and ventral by virtue of the positioning of the egg in the ovary due to its interaction with the neighbouring follicular cells. Upon fertilisation, the nucleus of the zygote undergoes eight rounds of mitotic division within the centre of the egg without undergoing cell division. The nuclei then migrate to the periphery of the egg and continue dividing to thirteen rounds. After this, the plasma membrane ingresses between the nuclei in the periphery and partitions them into single cells. The cells in the embryo continue dividing, although at a slower rate during the mid-blastula transition. This is followed by gastrulation that gives rise to the three germ layers.

The embryo eventually undergoes major morphogenetic events starting with the inward folding of the prospective mesoderm to form the ventral furrow. The invagination of the prospective endoderm gives rise to the cephalic furrow. Subsequently, the ectoderm and the mesoderm undergo convergent extension and give rise to the germ band. This is followed by the appearance of body segments, organogenesis and the segregation of imaginal discs. At the end of this is the dorsal closure, when the amnioserosa is covered by migrating epithelial sheets that ultimately fuse at the dorsal midline (Gilbert, 2000). The closure event can be divided into two phases, an initial mechanism to bring the two sheets together and a subsequent event that would knit these together to form one contiguous sheet.

During drosophila embryonic development, germ band retraction results in a dorsal epithelial hole exposing the underlying amnioserosa. The leading edge of the epithelial sheets is specified by a DV axis patterning as signalled by a member of the Transforming Growth Factor β (TGFβ) family and Decapentaplegic (DPP). The localised expression of DPP is regulated by the c-JNK pathway. Its upregulation in the leading-edge cells and down regulation in the amnioserosa ensure a localised expression of DPP, among others. Mutations of signalling components of this pathway exhibit an

open dorsal region and don't express DPP in the leading-edge cells (Martin & Wood, 2002).

The closure is mediated by integrins; they attach the amnioserosa to the yolk surface and help in the rearrangement of junctions between the leading epidermal cells and the peripheral amnioserosa cells underneath them. With the commencement of closure, the area of junctional contact between these two cells increases, by virtue of cell shape changes (Narasimha & Brown, 2004). This contact is essentially maintained until the end of the closure process. The leading-edge cells "migrate" over the underlying amnioserosa in such a way that their contact with the peripheral amnioserosa cells doesn't change at all. With the pushing of the leading epidermal cells, the bulk of the amnioserosa cells in the midline ingress (independently) and undergo apoptosis (Daniel P. Kiehart, Crawford, Aristotelous, Venakides, & Edwards, 2017; Lu et al., 2015; Rodriguez-Diaz et al., 2008; Wada, Kato, Uwo, Yonemura, & Hayashi, 2007).

The dorsal closure starts after the formation of canthi, at the anterior and posterior ends, and during this time, the leading edge gets populated with cellular projections similar to filopodia and lamellipodia (Eltsov et al., 2015; Jacinto, Woolner, & Martin, 2002). The two canthi have purse strings zipping into them, which shorten as closure proceeds. This shortening is accompanied by a shortening of the epidermal cells that get zipped at the canthus. The authors of the study hypothesised a possible alteration in the mechanical properties of the cells undergoing fusion at the canthus (Lu et al., 2015).

Mechanical forces play a major role in this morphogenetic event, and this is communicated through adherens junctions (Röper, 2015). It is of utmost importance that during the rapid remodelling of cells in the tissue, the junctions are localised accurately to be functional and still allow shape change. This is accomplished by a Rab-mediated trafficking of polarity and junction components during closure (Levayer & Lecuit, 2013; Roeth, Sawyer, Wilner, & Peifer, 2009). In the absence of these junctions, the continuity between cells is lost (Gorfinkiel & Arias, 2007).

Some studies have also implicated a potential role for ion channels in this process. For instance, K^+ ion channels have been implicated in the loss of amnioserosa cell volume (Saias et al., 2015). Clathrin mediated endocytosis removes Cdh1 from the wound margin, to facilitate actomyosin cable formation, and Ca^{2+} signalling is a regulator (Zulueta-Coarasa & Fernandez-Gonzalez, 2017). Their necessity has been

proven by inhibition experiments, where by following laser ablation, actomyosin cables fail leading to a closure defect.

The finer details of zipping, are as crucial as all the complex morphogenetic events leading up to it. The epidermal sheets that are pulled and pushed together from both sides, merge into one seamless sheet at the canthi in both the anterior and posterior ends as described earlier. And this is mediated by filopodial and lamellipodial extensions (Eltsov et al., 2015; Hutson et al., 2003; Jacinto et al., 2000; Millard & Martin, 2008; Peralta et al., 2007). This zipping event, at its core, entails the exchange of neighbours through disassembly of old junctions and formation of new ones. In this case, the epidermal cells of the leading edge have to lose their contacts with the underlying amnioserosa cells and form new ones with their epidermal counterparts from the apposed side (Lu et al., 2015; Wada et al., 2007). This process is facilitated by integrin-localised serine/threonine kinase Pak and the scribbled complex (Bahri et al., 2010) and marks the end of the dorsal closure in *drosophila melanogaster* (Daniel P. Kiehart et al., 2017).

2.2 Neural tube closure

Neural Tube (NT) is the precursor of the brain and the spinal cord. There are two different mechanisms involved in its formation; primary and secondary neurulation. In the case of primary neurulation, it starts off as a patch of differentiated cells on the surface ectoderm after gastrulation, the neural plate (NP). The induced NP undergoes a tissue level bending, giving rise to the neural folds (NF). The NF eventually is elevated towards the dorsal midline, and subsequently fuse to form a closed NT. This process is, however, not conserved across species; for instance, the closure in amphibians occurs almost simultaneously across the entire axial level of the neural tube. In the case of birds, the closure occurs at different levels in a sequential fashion and in mammals, a multi-site zippering happens. In the case of secondary neurulation, mammals, birds and amphibians have a similar mechanism; NT progenitor cells condense and form a solid cord, which then canalises to form a closed neural tube with a lumen (Copp et al., 2015). This process is similar to primary neurulation in teleost.

The formation of a proper neural tube is contingent on the NP, the adjacent Non-Neural Epithelium (NNE), and the underlying mesenchyme and the notochord. In addition to molecular signalling, mechanical signalling plays a major role also, in the

proper morphogenesis of the neural tube. Neural tube closure depends on the final fusion step whereby one contiguous sheet of epithelium becomes two intact sheets of epithelia; the internalised NT and the overlying NNE (Copp, Greene, & Murdoch, 2003). This fusion process is mediated by cellular protrusions sent out by the NFs that make the initial contact (Mak, 1978; Waterman, 1976). These protrusions originate from both the NE and the NNE, depending on the species and the axial level in the embryo; the first contact also, can be either between the NE or the NNE origin. There is no conservation in these aspects of fusion (L. A. Davidson & Keller, 1999; Gary C. Schoenwolf, 1979). The protrusions themselves are of different types, though predominantly actin based, they can either be the spike or finger like filopodia or sheet like ruffles (Geelen & Langman, 1977, 1979; Massarwa & Niswander, 2013; Pyrgaki, Trainor, Hadjantonakis, & Niswander, 2010a). These structures are produced under the control of small GTPases Cdc42 and Rac1(Rolo et al., 2016).

So far, in the case of neural tube closure, predominant attention has been given to the NP, both in a biochemical and biomechanical perspective. Recently, however, the NNE's contribution in the signalling and force generation is being studied. It is a source of BMP signalling that has been shown to regulate NF bending (Ybot-Gonzalez et al., 2007) in the spinal region. The initial contact during closure is mediated by the NNE in the closure of mid-hind brain and the spinal cord region (Ray & Niswander, 2012; Rolo et al., 2016). Two genes that play a crucial role in this belong to the grainyhead like family- Grhl2/3. They are required for the closure along the entire length of mammalian embryos, and embryos with genetic mutations exhibit severe cases of both cranial and spinal Neural Tube Defects (NTD) (Brouns et al., 2011; Castro et al., 2018; Rifat et al., 2010). Grhl2 is the upstream regulator of Cdh1 and is necessary for maintaining epithelial characteristics of cells in multiple contexts (Aue et al., 2015; Gao et al., 2013; Senga, Mostov, Mitaka, Miyajima, & Tanimizu, 2012; Werth et al., 2010a). Additionally, through Cdh1, Grhl2 has a role in altering the mechanical properties of the NNE, by the actomyosin network in mouse embryos(Nikolopoulou et al., 2019). The mis-regulation of Grhl2 has been implicated in cancers, and thus Grhl2 has a role in EMT as well (Cieply et al., 2012; Werner et al., 2013).

As mentioned earlier, the fusion here gives rise to two intact epithelia. This would require a considerable level of remodelling of the basement membrane; the timing and composition being pertinent, as the neural crest cells migrate away from the NT. For closure itself, integrin has been shown to provide the necessary anchorage for

the zippering to occur in mouse embryos. A fibronectin rich basement membrane is essential for the establishment of junctions between cells in apposed edges to establish an ITGβ1 mediated focal anchorage. This anchorage has also been shown to reduce the length of NNE junctions and the formation of semi-rosettes that aid in the zippering process (Molè et al., 2020; Zhou et al., 2020).

2.3 Optic fissure closure

The case of optic fissure closure is slightly different from the other systems described here. In other scenarios, the fusion initiates at the apical side of the tissue. Here, fusion starts when the two opposing tissues come into close apposition, basally (Fig 1.3) (Cote & Feldman, 2022) . The initial contact by the optic fissures is established basally. The basement membrane of the tissue breaks down, followed by cell rearrangement and reorientation to produce a continuous epithelium. The optic fissure comprises of the flat Retinal Pigment Epithelium (RPE) in continuation with the columnar neural retinal cells. Upon fusion of the optic fissure on the ventral side, contiguous and intact tube of retinal epithelium, overlaid by RPE is formed, both of which are polarised. The optic fissure is formed when the optic vesicle is invaginating. It is a transient opening on the ventral surface of the retina and optic stalk, through which hyaloid vasculature enters the eye and the retinal ganglion cell axons exit.

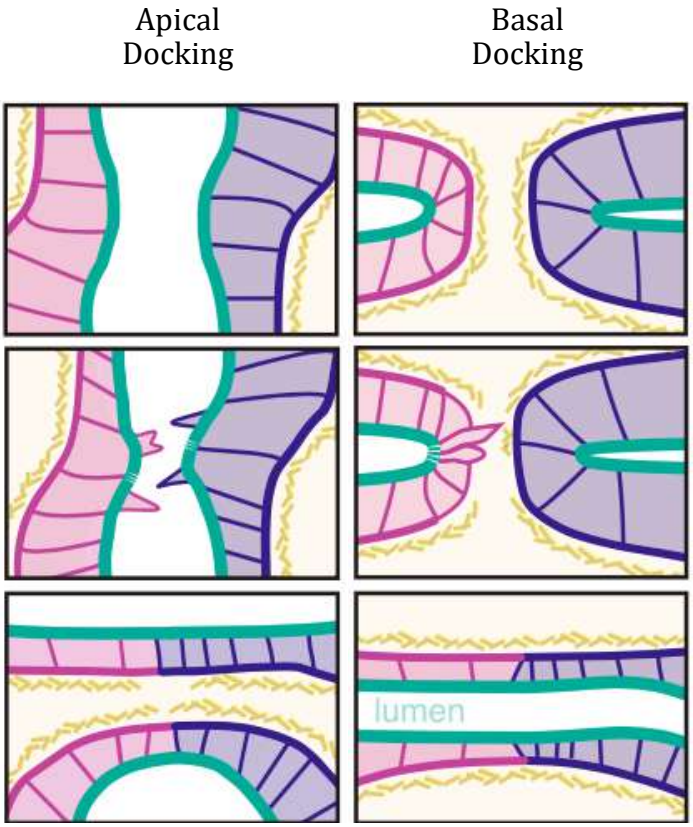

Fig 1.3: Initiating epithelial fusion: Epithelial fusion can get initiated apically (apical docking) or basally (basal docking). Here the two epithelial tissues are shown in pink and blue, the apical side marked in green and the basement membrane marked in yellow. In the case of apical docking, we see protrusions from the apical side, and in basal docking, there is a degradation of the basal lamina, followed by the initiation of cell protrusions.

And for the cells to truly establish contact, the intervening basal lamina is degraded first; this is followed by changes in the polarity of the cell, its adhesion and morphology (Bernstein et al., 2018). Cells of the optic fissure coordinate with the periocular mesenchymal (POM) cells for proper fusion, although the nature of this interaction remains to be understood (Bryan, Casey, Pfeiffer, Jones, & Kwan, 2020; Gage, Rhoades, Prucka, & Hjalt, 2005; Gestri et al., 2018; James et al., 2016). Studies have hinted at a potential role in the breakdown of the basal membrane that is required for initial contact of the fissures. EM studies in mouse optic fissure have revealed the presence of cells with phagocytic morphology (Hero, 1989). POM cells of neural crest origin migrate through the fissure transiently and do not establish any contact with regions that do not have basement membrane. A subpopulation of endothelial POM, on

the other hand, localise to regions of the fissure where laminin is absent (James et al., 2016). It is possible that these cells may aid in the breakdown of the ECM.

Matrix degrading enzymes including MMP2 and ADAMTS16 have been identified, although their source or function, is yet to be elucidated (Cao, Ouyang, Guo, Lin, & Chen, 2018; Weaver, Piedade, Meshram, & Famulski, 2020). Transcriptomics data from appropriately staged chick embryos has revealed a differential expression of a battery ECM genes in the fissure region as compared to the entire eye during closure (Hardy et al., 2019).

Cell polarity during fissure closure studies in zebrafish show disorganised and detached cell junctions, as marked by ZO1 and α-catenin, though after fusion, the polarity is re-established (Gestri et al., 2018). N-cadherin mediated cell-cell adhesion also plays a critical role in zebrafish; mutations in N-cadherin resulted in improper closure and eye defects (Masai et al., 2003).

Besides the basement membrane and polarity, morphological changes have also been observed. The fissure tissue comprises of RPE in continuation with neural retinal cells. The border of the optic fissure is the fusion plate. The cells in the fusion plate exhibit morphological changes. The cuboidal cells flatten to resemble the RPE (Eckert, Knickmeyer, Schütz, Wittbrodt, & Heermann, 2019). Elongations and protrusions have also been observed (Gestri et al., 2018). Despite their characterisation, the molecular mechanism underlying these morphogenetic changes and the molecular identity of the cells in the fusion plate is not well understood, and remains an open question in the field (Casey, Lusk, & Kwan, 2023).

Apoptosis has also been observed in the fusion plate in fissure closure in multiple animal models, including mouse, hamsters, and chick, although its relevance is not clear (Geeraets, 1976; Hardy et al., 2019; Hero, 1989). This attribute is not shared by the teleost (Gestri et al., 2018; James et al., 2016; Lusk & Kwan, 2022). TGF-β signalling has been implicated in tissue fusion, for instance, in palate fusion (Iwata, Parada, & Chai, 2011). Mutations in TGF- β2 fails to close the optic fissure in mouse. Although components of the signalling pathway are expressed in or near the fissure and POM, the exact role is yet to be deciphered (Knickmeyer et al., 2018). Mutation studies in other pathways including BMP (Dunn et al., 1997; Jena, Martín-Seisdedos, McCue, & Croce, 1997), Retinoic acid (See & Clagett-Dame, 2009) signalling also show eye malformation, but their roles in tissue morphogenesis is unclear.

3 The chick otic vesicle

All of the sensory organs and cranial nerves originate from the embryonic ectoderm. Except for the skin, the others start off as placodes in the embryonic head, or cranial placodes(Baker & Bronner-Fraser, 2001; Graham & Shimeld, 2013; Schlosser, 2006, 2014). Placodes are thickened ectodermal tissue, and all of them arise from a region that is competent to form the apropos placode on receiving the corresponding signals(Bailey & Streit, 2005; Groves & LaBonne, 2014; Saint-Jeannet & Moody, 2014). Around gastrulation, the ectoderm patterning is started off by signalling from all three germ layers separating the cranial ectoderm into the neural and non-neural epithelium (Ahrens & Schlosser, 2005; Bailey & Streit, 2005; Litsiou et al., 2005). Further signalling results in the formation of a pair of domains in the border of the neural and non-neural epithelium; the domain within the neural region becomes competent to give rise to the neural crest and the non-neural region, the sensory placodes. The latter is referred to as the pre-Pre Placodal Region (pre-PPR) (Pieper et al., 2012). The PPR is induced by Fgf4 and Fgf8 expressed by the mesoderm underlying the non-neural ectoderm and their inhibition led to the down regulation of some PPR markers in the chick. Additionally, inhibitors of Wnt and BMP expressed by mesoderm also contribute to the specification of the PPR (Ahrens & Schlosser, 2005; Litsiou et al., 2005).

In the embryonic head, along the AP axis of the embryo, the placodes are arranged thus: the olfactory placode that gives rise to the nasal epithelium and the first cranial nerve. This is followed by the lens placode, and the trigeminal placode, precursors to the lens and the ophthalmic, and maxilla mandibular found around the eye, respectively. The trigeminal placode is also neurogenic, and forms the sensory neurons of the fifth cranial nerve. The next placode in line is the otic placode that will form the inner ear and the eighth cranial nerve. The geniculate, petrosal and nodose are the final three epibranchial placodes, and are located lateral to the otic placode. The geniculate placode gives rise to the sensory components of the seventh cranial nerve that innervate the taste buds and convey touch information from the external ear. The petrosal placode gives rise to the ninth cranial nerve that innervates the tongue and carotid body and the nodose gives rise to the tenth cranial nerve(Baker & Bronner-Fraser, 2001; Ladher et al., 2010).

3.1 Otic placode induction

The inner ear is composed of numerous cell types; the mechano-receptor cells that perceive the signals through their actin based apical protrusions, the neurons of the VIII cranial nerve, the cochlear-vestibular nerve, and other support cells that help in the functioning of the inner ear (Highstein, 2004; Slepecky, 1996). All of these cell types are derived from the otic placode, a patch of epithelium in the non-neural region, caudal to and in continuation with the hindbrain and rostral to the first somite (Barald & Kelley, 2004; Groves & Fekete, 2012).

When the neural tube is closing, the expression of Pax2 or its homolog in the PPR marks the induction of the otic placode (Christophorou, Mende, Lleras-Forero, Grocott, & Streit, 2010; Freter et al., 2012). This Pax2 positive domain in the PPR is competent to give rise to the otic placode and the three epibranchial placodes, the Otic Epibranchial Progenitor Domain (OEPD)(Freter, Muta, Mak, Rinkwitz, & Ladher, 2008) . Pax2 expression in OEPD requires induction signals from both, the underlying mesoderm and the adjacent neural ectoderm (Ladher, O'Neill, & Begbie, 2010). Further signalling from the adjacent neural tube, the underlying mesoderm and the endoderm, segregate the OEPD into otic placode and the epibranchial placodes, as marked by their differential gene expression patterns, very specific to the placodes (Xiaorei Sai & Ladher, 2015a).

3.2 Otic vesicle formation

The surface induced otic placode undergoes several rounds of morphogenetic transformations to get internalised and become a part of the cephalic mesenchyme as a closed otic vesicle (Meier, 1978a, 1978b). After Pax2 induction, when the embryo has between 4-6ss, depending on the species, the otic placode undergoes thickening. This thickening has a distinctive appearance, separating the pseudostratified otic placode cells from their squamous neighbours, morphologically (Christophorou et al., 2010). Irrespective of their shape, both the cell types are epithelial in nature with tight apical junctions and intact basal lamina. The otic placode and its neighbour, form an intact contiguous epithelium.

The mechanism of thickening itself is unclear, although Rac1 has been implicated in the thickening of the lens placode, which is also pseudostratified

(Chauhan, Lou, Zheng, & Lang, 2011). There are speculations concerning the requirement for a thickened placode; so far higher cell packing density seems to be a plausible explanation. The cells of the otic placode divide by interkinetic nuclear migration (INM) (Sauer, 1936), and a higher cell packing density is necessary for this. The thickening and INM are akin to members of a feedforward loop; INM is thought to allow a tighter packing of epithelia (Fish, Dehay, Kennedy, & Huttner, 2008) and pseudo stratification is necessary for proper INM (Kosodo et al., 2011).

The next step in otic vesicle formation is the invagination of the placode. As the authors note in their review, "It is likely that thickened epithelial allow precise and separable control of both apical and basal domains of the placodal cells" (Xiaorei Sai & Ladher, 2015b). And this control is essential for invagination whereby changes in the basal side of the tissue leads to apical changes. The morphological changes have been well characterised by SEM and light microscopy of plastic sections (Alvarez & Navascués, 1990). The flat otic placode seen at 4-6ss, develops a slight depression at 8-10ss. This depression further deepens around 10-16ss through an initial expansion of the basal aspect of the otic placode, while the apical side remains the same. The otic placode at this stage has become the otic pit. As embryonic development proceeds, from 16-22ss, the otic pit is pushed deeper into the cranial mesenchyme through a significant reduction in the apical surface of the otic pit. The otic pit has now become the otic cup (Alvarez & Navascués, 1990; Xiaorei Sai, Yonemura, & Ladher, 2014).

Cytoskeletal elements play a major role in cell shape changes. Sai and Ladher, 2008 have characterised the role of F-actin and myosin light chain in basal expansion and apical constriction contributing to the invagination of the otic placode. F-actin localises in the apex and base of the placode at 10ss. This distribution changes as basal expansion starts in 13ss with F-actin accumulating on the apical side specifically and clearing from the basal side. This is mediated by extrinsic FGF signalling that clears F-actin basally and localizes phosphorylated myosin light chain instead. However, there is a shift in the localisation of the active myosin-II to the apical side, as apical constriction begins, while F-actin can still be seen localised apically (XiaoRei Sai & Ladher, 2008). This apical localisation of active myosin is mediated by a member the small GTPases, RhoA, as also seen in the case of neural tube closure (Nishimura, Honda, & Takeichi, 2012) and gastrulation in *Drosophila* (Mason, Tworoger, & Martin, 2013).

3.3 Otic vesicle closure, open questions:

As development proceeds, the otic cup is pushed deeper into the head mesenchyme, until only a small opening into the primordia is visible on the surface. At this stage, the otic cup has become otic vesicle. Throughout this process, the otic vesicle has been in contact with the surrounding non-neural epithelium. However, for further development of the inner ear, the otic vesicle has to close completely, by epithelial fusion and segregate from the non-neural epithelium to get internalised. This fusion mechanism has not been characterised completely. SEM descriptions have hinted at filopodia-membrane protrusions mediated fusion event. Similarities maybe seen in the mechanism of neural tube closure in amniotes (Colas & Schoenwolf, 2001) and wound healing (Martin & Parkhurst, 2004), amongst others.

As seen in fusion events described above, the epithelial cells that participate in the fusion event, do not behave completely epithelial and display some mesenchymal like properties; hinting at a possible partial EMT. This alteration in epithelial property is marked by cell shape changes, mis-localisation of junction and polarity proteins and ECM remodelling. Some of the open questions in the field are:

1. While the multiple model systems studied have been well characterised, the molecular identity of these less-epithelial cells remains to be elucidated.
2. If multiple transcription factors are implicated in the initiation or activation of partial EMT, will they all have similar effects when perturbed, hinting at a possible redundancy?
3. The temporal and spatial dynamicity of ECM is essential in the maintenance of the integrity of the tissue; but the factors responsible in the maintenance of ECM have not been elucidated, also.

The chick otic vesicle closure, is an ideal model system to answer all these questions. The epithelial fusion in otic vesicle is very similar to neural tube closure, but unlike the neural tube, it is not confounded by other cellular events. For instance, the curly tail mutant, is an example of open neural tube defect. The defect is not a result of improper epithelial fusion, but a case of neural folds that were not brought close to each other. The otic vesicle is a much smaller primordia, with less complicated morphogenesis, that is not extensively dependent on other tissues for its development. The fusion event does not extend beyond 12 hours. Any molecular or genetic perturbations to the otic vesicle will not affect the overall development of the embryo,

as might be the case in gastrulation, neural tube closure or body wall closure in *Drosophila*. The pair of otic vesicles are also well separated from each other, as opposed to the optic primordia, thus allowing for a contralateral control if need be.

Using the otic vesicle closure as a model, in this thesis we have answered some aspects of the open questions in the field.

Chapter 2: Materials and Methods

1. Materials

1.1 Chicken Eggs

Kaveri eggs were sourced from Central Poultry Development Organisation and Training Institute, Hessaraghatta. The eggs were stored at 25°C and incubated at 37°C in humidified incubators for development to proceed; the staging was done according to Hamburger Hamilton staging(Hamburger & Hamilton, 1951).Experiments were performed and carcasses discarded according to the Institutional Animal Ethics Committee guidelines.

1.2 List of Antibodies

Primary Antibodies	Catalogue No	Dilution used
Rac1 mouse	BD biosciences 610650	1:100
E cadherin mouse	BD biosciences 610182	1:100
ZO1 mouse	Thermo fisher 33-9100	1:100
ZO1 rabbit	Thermo fisher 40-2300	1:100
Connexin 43 rabbit	Sigma C6219	1:100
Ezrin mouse	Sigma E8897	1:100
Laminin rabbit	Sigma L9393	1:100
Pax2 rabbit	Thermo Fisher 71-6000	1:100
Anti GFP mouse	Roche 11814460001	1:100
Anti GFP rabbit	Abcam ab290	1:100
Cleaved Caspase 3 rabbit	Invitrogen 700182	1:100
Anti-Digoxigenin sheep	Roche 11093274910	1:2000
Secondary Antibody and Dyes		
Goat Anti-mouse IgG (H+L) Alexa Flour Plus 555	A32727 Invitrogen	1:1000
Alexa Fluor® 488 goat anti-rabbit IgG (H+L) *2 mg/mL*	A11008 Invitrogen	1:1000
Alexa Fluor® 647 goat anti-rabbit IgG (H+L) *highly cross-adsorbed* *2 mg/mL*	A21245 Invitrogen	1:1000
Goat anti-Mouse IgG (H+L) Cross-Adsorbed Secondary Antibody, Alexa Fluor™ 647	A-21235 Invitrogen	1:1000
Alexa Fluor 488 phalloidin	A12379 Invitrogen	1:500
Molecular Probes, Alexa Fluor 568 phalloidin	A12380 Invitrogen	1:500
DAPI	Sigma D9542	1:1000

Table. 2.1: List of antibodies

1.3 List of primers for in-situ hybridisation probes

Gene Name	Forward Primer	Reverse Primer	Cloned Vector	Anti-sense Probe	Linearize	Gene orientation confirmed with
Bambi	attgctgttcctata gctgg	acataggagcttgc atacag	pGEMT EASY	SP6	SPH1	M13_F
Dach1	cttcagacagaatc cctgtcca	ccacagaactccat ttgggtga	pGEMT EASY	SP6	SPH1	M13_F
DLX5	m13 forward	m13 reverse	pBS SK-	T7	CLA1	M13_F
EphA4	agcattgcttgatgt acaga	ggcaaattgaactg cttctt	pGEMT EASY	SP6	SPH1	M13_F
Grhl2	gcctggaagtcgta tttgga	gtcaaggaccctct gctttg	pGEMT EASY	T7	SPE1	M13_F
Grhl3	ggcatccctactcc tcacaa	tataggaattcagtc tctggcctca	pCR 2.1topo	T7	SPE1	M13_R
Itgb3	gtggagtgcaaga agtatga	tgtgtcctcaacac ataagg	pGEMT EASY	SP6	XHO1	M13_F
Msx1	gaagcagtacctgt ccatc	atagtacacagaga gagccc	pGEMT EASY	SP6	SPH1	M13_F
Rac3	gctgtagggaaga cctgctt	caggatggatgtct cagccc	pGEMT EASY	SP6	XHO1	M13_F
Snail2	agacagatccaatc tgaggg	ctctcttgcacttatt cccg	pCR 2.1topo	T7	SPE1	M13_R
Sp8	ggcgcatttggatc attccc	ggcaaaccgctaat gtggtg	pGEMT EASY	SP6	SPH1	M13_F
Wnt 3A	cgattctgtcggaa ctatgt	ggagccttgaaga agttgta	pGEMT EASY	SP6	XHO1	M13_F
Zeb2	ttcctggtcccattc cgttg	ggtcgcaacccag gaatact	pCR 2.1topo	T7	SPE1	M13_R

Table. 2.2: List of primers for in-situ hybridisation

1.4 List of gRNA

Name	sequence	grna sequence	position	forward /reverse	region of the gene
Sp8-grna	gacggctcagggccgcccttcccggggctgcg ggacgaggggcggcgtccgctccgtc ggggccccacgcggggcgaaccgctccggtc gcgggaccggaccgagtcgggccgaaccgaa ccgagccgcgccgagtcgaaccgggcagagc cgagccgggccgggccgtgctcgacggcgct gatgacctcacgcagtcacgtcggcgagcggc gcggcggggccggggattggctggcggcggc tcagcggcacttcaaagccggcgagggagcta caattgtggtggaatgggcggaactgagcattgt attgcacacctctaaaaaaacactgcctctgattt atcaatataaaaaagatcctctgagaggaggg	cacgcagtc acgtcggcg agcgg	211	fwd	exon 1
Grhl2-grna	aaattgcctcagttccacagaagctcagagtaat ttgagtgggggagagaaccgtgtgcaagtcttg aagacagtgcctgttaacctttccttgaaccaag acccattggagtcatccaagagggactacaaca caaatgtgtctggcagctccacgccaattacgg ggactgcagtgactgtgataaaagcagaagagt tcacccctgtttttatgaccccacaagcacactat acaagaggagaaaatgaggagcaccgagggg ttatctttgaaccgtatgaagtgtccagcattgctc cccacaccaattatctcaaagatgaccagcgca gtactcctgacagtacgtacagtgacaccttcaa ggacggaggaacagaa	tggcagctc cacgccaat tacgg	165	fwd	exon 4

Table. 2.3: List of gRNA

1.5 List of chemicals

Chemical	Catalogue no	Company name
100 bp DNA Ladder (Dye Plus)	3422A	Takara
1Kb DNA ladder	3426A	takara
Acetic Acid Glacial	11005	Fisher Scientific
Agar	PCT0901	himedia
Agarose	RM273	himedia
Agarose	N605-500G	Amresco
BCIP	11383221001	Roche
BM purple	11442074001	Roche
Bovine Serum Albumin	A9647	Sigma
Calcium Chloride	12135	Fisher Scientific
Carbenicilin disodium	C9231-10G	Sigma-Aldrich
Chaps hydrate	C3023-25G	Sigma-Aldrich
Citric acid	10339	spectrochem
di-Sodium hydrogen Orthophospate	15825	Fisher Scientific
DIETHYL PYROCARBONATE 97%	159220-25G	Sigma-Aldrich
DIG labeling kit	11277073910	Roche
EDTA	12635	Fisher Scientific
Ethanol	1009830511	EMD Millipore
Fast Green FCF	F7252	Sigma
Fluoroshield™	F6182-20ML	Sigma-Aldrich
Formamide deionized	S4117	Sigma
Gelatin from porcine skin,gel strength 300, Type a	G2500-1KG	Sigma-Aldrich
GelRedTM Nucleic Acid Gel Stain, 10,000X in water	41003	Biotium
Glutaraldehyde Grade I	G5882-10X1ML	Sigma-Aldrich

Glycerol Molecular Biology Reagent	G5516-1L	Sigma-Aldrich
Heparin sodium salt from porcine intestinal mucosa, Grade I-A, =180 USP units/mg, 500 KU	H3393-500KU	Sigma-Aldrich
Hydrochloric acid	H0090	genetix biotech asia
Invitrogen TOPO TA cloning kit for subcloning	K450040	Thermo Fisher Scientific
Insitu blocking kit	11585762001	Roche
Isopropyl Alcohol, 500mL	0918-500ML	Amresco
Lithium chloride	K445-100ML	Amresco
Luria broth	M575	himedia
Magnesium Chloride	15535	Fisher Scientific
Maleic acid	M0375-500G	Sigma-Aldrich
Methanol	1945162521	EMD Millipore
MN plasmid isolation kit	740588 50	Machery nagel
NBT	11383213001	Roche
Normal Goat serum	RM10701	Himedia Laboratories
Osmium Tetroxide	75632	Sigma
Paraformaldehyde	P6148-1KG	Sigma
pcU6_1sgRNA	92395	Addgene
pGEM T	A137A	Promega
Potassium chloride	P3911-500G	Sigma-Aldrich
Potassium Dihydrogen Orthophosphate	13405	Fisher Scientific
PrimeScript™ 1st strand cDNA Synthesis Kit	6110A	Takara
ProLong® Gold antifade reagent	P36930	Invitrogen
Qiaquick gel extraction kit	28704	Qiagen
Ribonucleic acid type vi from torula	R6625-25G	Sigma-Aldrich
RNaseZap	9780	Ambion

rTaq	R001A	Takara
Sodium dodecyl sulphate	RM205	himedia
Sodium acetate 3.0m sterile ph 5.2,100ml	E498-100ML	Amresco
Sodium Cacodylate Buffer, 0.2M	11652	Electron Microscopy Sciences
Sodium chloride	GRM853-500G	Himedia Laboratories
Sodium Hydroxide	15895	Fisher Scientific
Sodium phophate monobasic	0823-500G	Amresco
Sucrose	15925	Fisher Scientific
Tri-sodium citrate	14005	Fisher Scientific
Tris	15965	Fisher Scientific
TRI reagent	T9424	Sigma
Tween 20	P9416-100ML	Sigma

Table. 2.4: List of chemicals

2. Methods

2.1 Embryo Collection

After appropriate hours of incubation, the eggs were taken out of the incubator and flipped to ensure that the embryo floats to the upper surface of the yolk. The egg was cracked open on a clean petri plate and the embryo must be visible on the upper surface of the yolk. Thick albumin (usually present on embryos staged earlier than HH7) was removed with the help of Kimwipes tissue paper. Paper frames of an appropriate central aperture, roughly 1.5cm by 1.5cm, were made from Whatman Filter paper-1, using a paper punch and autoclaved prior to use. The paper frame was carefully placed on top of the embryo with fine forceps and the vitelline membrane was cut using spring bow scissors, around the paper frame. The paper window, along with the embryo was taken from the yolk and placed in a ringer's solution bath and gently rinsed to remove the yolk (Honda, Freeman, Sai, Ladher, & O'Neill, 2014). Ringer's solution was used for embryos that would be taken for live culture experiments, and PBS (pH 7.4) was used when the embryos were fixed for either IHC or WhISH.

2.2 Gelatine blocks for cryo-sectioning

Staged embryos were collected and washed in autoclaved PBS to remove yolk. The veins were cut to let the embryo bleed out quickly to reduce autofluorescence from blood. They were then fixed in a generous amount of 4% PFA, for 2 hours at RT. The embryos were then rinsed thrice in PBS to remove any residual fixative, and then washed in PBS thrice, every 20 minutes. The embryos were equilibrated in 15% sucrose/PBS. The embryos were then incubated at 37°C in a 7.5% gelatine/15% sucrose/PBS solution for an hour, and then embedded in a cryoblock with 7.5% gelatine/15% sucrose/PBS and left to solidify to gel consistency on ice for 5 minutes. This was followed by freezing the cryoblocks in a methanol bath placed on dry ice and frozen blocks were stored in -20°C. Cryosections of 25µm thickness were obtained using HMX125 (Thermo Scientific) cryostat and the sections were collected in positively charged super-frost glass slides. The slides were then stored at -20°C until further processing.

2.3 Scanning electron microscopy

Kaveri eggs were incubated at 37°C to produce embryonic stages varying from HH 12-HH17. The embryos were collected using paper windows and fixed in the primary fixative (2.5% Glutaraldehyde and 2% Paraformaldehyde in 0.1M Sodium Cacodylate buffer) at 4°C for 24 hours. The fixed embryos were then washed thrice in 0.1M Sodium Cacodylate buffer while still on ice and then subsequently fixed in chilled 1% OsO_4 on ice for 2 hours. The embryos were rinsed with filtered Milli-Q water thrice to remove residual paper fibre or yolk. The embryos were washed in a mixture of 50% Ethanol/Water twice for a duration of twenty minutes each. Subsequently, they were processed with a gradient series of 70%, 90%, 95%, 99.5% and 100% ethanol for fifteen minutes each. The embryos were rinsed in 100% absolute alcohol twice, 20 mins each and proceeded to critical point drying (CPD) in Critical Point Dryer Leica EM CPD300. The sludge worm protocol was used for CPD. The samples were coated with gold to a thickness of 10 nm using Sputter Coater K550X, Emitech and subsequently imaged using the Zeiss Merlin Compact VP system. For imaging the cells in the otic vesicle, the embryo was sliced through the otic vesicle using a scalpel prior to fixation with the primary fixative.

2.4 Immunohistochemistry (IHC)

The slides with sections were incubated at 37°C for 3 hours prior to the staining process. 0.1% tween/PBS(PBST) was used for washing the slides throughout the staining process. To remove gelatine from the sections, warm PBST was used twice, for fifteen minutes and RT PBST was used for the third wash. Borders were made on the glass slide using a hydrophobic pen in order to contain the reagents within the boundary of the glass slide. The sections were blocked for an hour at RT in PBST with 3% heat inactivated goat serum and 2mg/ml of BSA (blocking solution). Sections were incubated with primary antibodies diluted (see table for dilutions) appropriately in blocking solution for approximately 36 to 40 hours at 4°C. The sections were then washed thrice for 15 mins each in PBST and blocked once more with the blocking solution for an hour at RT. Secondary antibodies and fluorophore conjugated Phalloidin were also diluted appropriately in the blocking solution and sections were incubated at RT for 3 hours. The sections were then washed thrice in PBST, 15 minutes each and

finally counterstained with DAPI for 7-10 minutes. The sections were washed in PBS for ten minutes before mounting the coverslips with fluoroshield on the slides. Images were acquired using Olympus FV3000 confocal system in 10x and 63x objectives, with high sensitivity detectors, at a resolution of 2048 by 2048.

2.5 Whole Mount IHC

Embryos were collected and fixed as described above. After multiple washes in PBS, the allantois membrane was removed carefully. The embryo was cut just above and below the heart tube, which contains the otic vesicle, adjacent to the neural tube. The heart tube was removed. This tissue was then permeabilized at 4°C (in 0.1% tween/PBS) for 24 hours, and then blocked for 48 hours (Blocking solution: 3% heat inactivated goat serum and 2mg/ml of BSA in 0.1% PBST). The tissue was then incubated in primary antibody diluted in blocking solution at 4°C for 3-4 days. The tissue was then washed in 0.1% PBST for 24 hours in a roller at RT, and blocked once again for 24 hours at 4°C. The tissue was incubated with secondary antibody, phalloidin and DAPI diluted in the blocking solution at 4°C for 48 hours and then washed thoroughly in 0.1% PBST to remove non-specific staining. 35mm dishes were punctured to create a circular aperture of 10mm diameter and a cover slip was pasted on the bottom side of the plate, to create a groove. The tissue was bisected, starting from the neural roof plate towards the pharyngeal arches. 0.7% agarose/PBS was melted and a drop was placed in the groove of the punctured tissue culture plate. The tissue was then placed in the agarose droplet and quickly aligned so that the otic vesicle opening can be imaged using FV3000 upright confocal microscope. The embryo was then imaged using 20x and 60x water dipping objectives.

2.6 Electroporation for cell shape analysis

Kaveri eggs were incubated at 37°C to acquire HH12 embryos (Hamburger & Hamilton, 1951). The embryos were then carefully collected using paper windows and washed thoroughly with Ringer's solution to remove residual yolk. The allantois

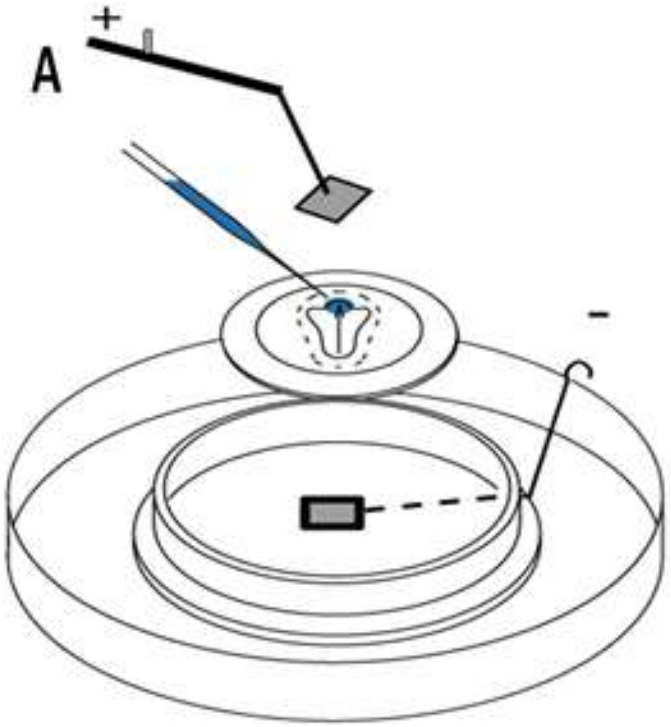

Fig 2.1: Scheme for ex-ovo embryo electroporation. A: HH12 Chick embryos were collected using a paper window and placed in an electroporation plate as indicated. A DNA solution containing a fluorescent protein, fast green and sucrose is layered on top of the embryo and the electrodes maneuvered in place. Electroporation is performed using a square-pulse generator, and thus electroporated embryos can be cultured on agar-albumin plates. Illustration by Dr.Raj Ladher.

membrane was removed using forceps and a mixture of the plasmid (final concentration always 2-3µg/µl) and 30% sucrose/PBS was dispensed on the region of interest and a voltage of 12V was applied across the electrodes in a CUY 721 system. The electroporated embryos were subsequently transferred to freshly prepared albumin agar plates (Chapman, Collignon, Schoenwolf, & Lumsden, 2001)and incubated at 37°C for the necessary duration. Embryos electroporated with constitutively active pCAG-eGFP were subsequently harvested and cryosectioned; the sections were subsequently stained with anti-GFP (Roche 11814460001) and imaged using Olympus FV3000 system. The Z-stacks were further analysed with Imaris for understanding the shape of cells mediating fusion. The surface module of Imaris was used for the purpose.

2.7 Cell shape analysis

2.7.1 Imaris-surface module

Sections of HH-16 and HH-17 chick embryos were stained with Phalloidin to mark cortical F-actin that roughly marks the boundary of the cell. Z stacks obtained from these sections were subsequently processed with the help of the surface tool in Imaris to manually mark the boundary of the cells of interest. The shape of the cells was marked across the z stacks of the sections to create an object. The surface of these objects was then processed by the software, and was also used to calculate various statistics pertaining to the object, including volume, surface area, average intensities, and sphericity, to name a few. Three different populations of cells were considered for the analysis, the pseudostratified cells in the otic vesicle, the rounded cells in the edge and the squamous cells of the surface ectoderm in continuity with the otic vesicle. The sphericity of the cells was considered to distinguish the three populations of cells. And the significance between the data was analysed using one-way ANOVA.

2.7.2 Protein localisation analysis

Sections of HH16 and HH17 chick embryos were probed for different proteins with antibodies using the IHC protocol described above and imaged using FV3000 Olympus confocal microscope, with a High Sensitivity Detector. The images were opened in imageJ. The proteins I was interested in localised to the cell boundary; the freehand line tool was used to mark the cell boundary in one optical section. The protein expression profile of the protein was quantified using the Plot profile tool and the intensity at different pixels were taken for further quantification. The coefficient of variation (CV) was measured for each circumference and taken as the data point for the final analysis. Here, the CV was a measure of how the intensity along the circumference of the cell, in one optical plane, varied from the mean of the intensity along the same circumference. For instance, if the protein localisation was more diffused, the CV would be lower and if the localisation was restricted to certain pockets along the circumference, the CV would be higher. This measure helped us to quantify the expression pattern of different proteins on the three cell types we were interested in.

2.8 RNA isolation

Samples were homogenised in TRI reagent (1ml per 50-100mg tissue). The volume of the tissue should not exceed 10% of the volume of the TRI reagent. The samples were let to stand for 5mins at RT for complete dissociation of nucleoprotein complexes. 0.1ml of 1-bromo-3-chloropropane per ml of TRI reagent was added to the samples and shaken vigorously for 15 seconds and allowed to stand for 2-15 mins at RT. The mixture was centrifuged at 12000g for 15mins at 2-8°C. Centrifugation separates the mixture into 3 parts- a red organic phase (containing protein), an interphase (containing DNA) and a colourless upper aqueous phase (containing RNA). The aqueous phase was transferred to a fresh tube and 1V of isopropanol was added and mixed by inverting the tube. The samples were allowed to stand for 5-10mins at RT and centrifuged at 12000g for 10mins at 2-8°C. The RNA precipitate will form a pellet on the side and bottom of the tube. The supernatant was removed and the RNA pellet was washed by adding a minimum of 1ml of 75% ethanol per ml of TRI Reagent used in sample preparation. The sample was vortexed and then centrifuged at 7500g for 5mins at 2-8°C. 100% ethanol was used to re-wash the pellet at 7500g for 5mins. This would help in the faster drying of the pellet in the next step. The residual ethanol was carefully removed with a filter tip, without disturbing the pellet. It is vital to remove as much ethanol as possible, when samples are to be used in enzymatic reactions, especially for small volume samples (5-20µl) which may contain a relatively high level of ethanol if not adequately dried. The pellet was resuspended in 20-30µl of DEPC treated water and stored at -80°C or used for synthesising cDNA immediately.

2.9 Reverse-transcriptase PCR

1st strand cDNA synthesis

a. Template RNA mix:

Random Hexamers	1µl
dNTP mix	1µl
Total RNA (<=5µg)	X µl
DEPC treated water	Make unto 10µl

Heat at 65°C for 5mins and cool immediately on ice.

b. cDNA synthesis

Template	10µl
5X buffer	4µ
Inhibitor (20U)	0.5µl
Enzyme (100U)	0.5µl
DEPC treated water	5µl

Incubate at 30°C for 10mins (for random hexameters) and then incubate at 42°C for 1 hour. Heat inactivate the mix at 70°C for 15mins and cool on ice.

c. PCR

10X buffer	2.5µl
dNTP 2.5mM	2µl
template	Xµl
Primers (F+R) 10µM	1µl
Enzyme	0.125µl
DEPC treated water	Make up to 25µl

Step	Temperature	Duration	No. Of Cycles
Step 1: Denaturation	94°C	5 mins	1
Step 2: a.Denaturation	94°C	30sec	35
b. Annealing	Annealing temp	30sec	
c. Extension	72°C	1min/kb	
Step 3: Final Extension	72°C	10mins	1

2.10 Cloning with TOPO TA cloning kit and rapid one-shot chemical transformation.

Fresh PCR product	4µl
Salt solution	1µl
Vector	1µl
Total Volume	6µl

The reaction mixture was gently mixed and incubated for 5 minutes at 22-23°C. The reaction was then placed on ice until transformation. The entire volume of cloning mixture was used for transformation and added into a vial of competent cells and mixed gently. This mixture was incubated on ice for 5 minutes and spread on pre-warmed LB agar plates containing 100µg of ampicillin/carbenicillin and incubated for not more than 16 hours at 37°C.

2.11 Cloning with pGEMT-easy vector

2X Rapid ligation buffer for T4 DNA Ligase	5µl
Vector (50ng)	1µl
PCR product (Gel extracted)	3µl
T4 DNA Ligase	1µl
Total Volume	10µl

The contents of the vector vial were short spun to ensure that the solution collects at the bottom of the tube. The ligation reaction was performed in a low DNA binding tube. The components were added and mixed by pipetting. The reaction was incubated for 1 hour at RT or overnight at 4°C.

2.12 Transformation

The plasmid to be transformed was added to 1.5ml tubes (50-100ng at least) and placed on ice. 50µl of freshly thawed competent cells was added to the tube and incubated on ice for 30 minutes. Mixing of the mixture is not necessary. After 30minutes, the competent cell-plasmid mixture was incubated in a 42°C water bath for 42seconds and immediately transferred to ice for 5 minutes. Antibiotic free, sterile, and pre-warmed 500µl LB media was added to the above mixture and incubated in a shaker at 37°C for 1 hour. 200µl of the mixture was spread in a pre-warmed LB agar plate containing the appropriate antibiotic (depends on the plasmid).

2.13 Competent cell preparation

DH5α cells were streaked on a LB agar plate with no antibiotic selection. Quadrant streaking was preferred to get isolated single colonies. The plates were incubated at 37°C for no more than 16hours. Autoclaved solutions of 100mM $CaCl_2$,100mM $MgCl_2$ and 15% glycerol (V/V) in 85mM $CaCl_2$ were stored at 4°C overnight. It is essential

that these solutions and all the equipment and plasticware be kept cold throughout the process. It is also very important that the culture only be opened under a sterile hood. A starter culture of a single colony was incubated at 37°C for overnight (1% volume of secondary culture) in a shaker. The next day, 1L of autoclaved LB media was inoculated with the starter culture at incubated in a shaker incubator at 37°C. The optical density at 600nm (OD_{600}) of the culture was measured every hour until the OD_{600} reached 0.2 and measured every 15-20 minutes until OD_{600} of 0.35-0.4. Un-inoculated LB media was used as a blank. When the necessary OD_{600} was reached, the culture was immediately transferred to ice and allowed to cool down to stop further growth of the bacterium. To ensure uniform cooling, the flasks were swirled frequently and returned to ice immediately. The centrifuge bottles were also left on ice to cool down. 1L culture was divided between 4 250ml bottles and centrifuged to pellet the cells at 3000g/4000rpm for 15 mins at 4°C in a Beckman ultracentrifuge- JA10 rotor. The supernatant was decanted and the pellet was gently resuspended in 100mL of ice-cold 100mM $MgCl_2$. At this point, cells from 2 centrifuge bottles can be combined and processed further. The resuspended cells were centrifuged further at 2000g/3000rpm for 15 mins at 4°C in the same rotor. The supernatant was decanted and 200ml of ice cold 100mM $CaCl_2$ was added to the pellets. The pellets were gently resuspended and this suspension was allowed to rest on ice for at least 20 minutes. At this point, the sterile Eppendorf tubes that will be used for aliquoting the competent cells were closed and placed on ice to chill them. The suspension was further centrifuged at 2000g/3000rpm for 15 mins at 4°C in the same rotor. The supernatant was decanted, and the pellet resuspended in 50ml of 15% glycerol (V/V) in 85mM $CaCl_2$ and transferred to 50ml conical tubes. The cells were harvested further by centrifugation at 1000g/2100rpm in Beckman GH 3.8 rotor for 15mins at 4°C. For the final time, the supernatant was decanted and the pellet resuspended in 20ml of 15% glycerol (V/V) in 85mM $CaCl_2$. The OD_{600} of the cells should be 200-250. 100µl of the cells were aliquoted into prechilled tubes and snap frozen in liquid nitrogen before transferring them to -80°C.

2.14 Plasmid digestion for probe synthesis

Plasmid	10µg
Restriction enzyme	5µl
Restriction enzyme buffer, 10x	5µl
Water	X µl
Total volume	50µl

The above components were mixed well in a 200µl PCR tube and incubated at the necessary temperature for 3-4 hours. 0.5µl of the digestion mixture was run in a 1% gel to confirm complete digestion of the plasmid. Undigested plasmids will have multiple confirmations and may not exist as a single band in the gel; completely digested plasmids would exist as a single band in the gel. If, the plasmid was not completely digested, 1µl of enzyme was added and incubated further for an hour. The digestion has to be confirmed by a 1% gel before proceeding further. The enzyme reaction can be stopped either by inactivation at the appropriate temperature (depending on the enzyme) or by proceeding to ethanol precipitation of the DNA.

2.15 Ethanol Precipitation of DNA

The DNA mixture was transferred to a container where it filled not more than one fourth the total volume (1.5mL tubes were used). 1/10 Volume of 3M sodium acetate (pH 5.2), ice cold, was added to the DNA mix to equalize ion concentration. 2 Volumes of ice cold 100% ethanol was added and left at -20°C, overnight. The samples were centrifuged at the highest speed for 15 mins at 4°C in a microcentrifuge. The supernatant was removed with a pipette, without disturbing the pellet. If necessary, the centrifugation was repeated and supernatant was removed further. 200µl of ice cold 70% ethanol was added to wash the pellet gently, and centrifuged in the same conditions for 5 minutes. The supernatant was removed carefully without disturbing the pellet. Rest of the supernatant was allowed to evaporate either at 37°C or room temperature. The pellet was resuspended in desired volume (10µl for probe synthesis) of DEPC water before the pellet dried completely.

2.16 Probe synthesis for in-situ hybridization

Digested plasmid concentrate 1µg	1µl
Inhibitor	0.25µl
Labelling mix	1µl
10x buffer	1µl
Polymerase	1µl
DEPC Water	5.75µl
Total Volume	10µl

The above components were mixed by pipetting, and subjected to a short spin to collect the solution to the tip of the tube. The reaction mixture was incubated at 37°C for 2 hours. 1µ**l** of RNase free DNase was added and the mixture was incubated further at 37°C for 15mins. The reaction was stopped by the addition of 1µ**l** of 0.2M EDTA (pH 8.0). The probes were next purified using RNA spin columns.

2.17 Probe purification using Roche RNA spin columns

The columns, stored at 4°C, had to be uniformly packed before their usage. The columns were gently tapped to remove any residual air bubbles and to ensure a uniform packing of the G50 sephadex, that may be stuck to the lid of the column. The lid and the snap tip in the bottom of the tube were removed carefully, without disturbing the column, and placed in a RNase free 1.5mL centrifuge tube and centrifuged at 1000g for 1 minute at 15-25°C. The eluent was discarded with the tube and the packed column was transferred to a fresh new tube and the probe mix was added carefully to the centre of the column. The column with the tube was centrifuged at 1000g for 4 minutes at 15-25°C. The eluent was taken for further precipitation.

2.18 Lithium chloride precipitation

Column purified probe	10µl
4M Lithium chloride	5µl
Ethanol, 100%	125µl
DEPC Water	40µl
Total Volume	170µl

The components were added in the same order as mentioned in the table, and incubated at -20°C overnight. The sample was then centrifuged in a microfuge for 10minutes at 4°C in the maximum speed possible. The supernatant was removed carefully and the pellet was washed twice with ice cold 75% ethanol without disturbing the pellet. The pellet was resuspended in 75µl of DEPC water. 1µl of the probe was tested in nanodrop for concentration and quality and 1µl was tested in a 1% gel for the size and integrity of the probe. The rest of the probe was diluted with the prehybridization solution at a concentration of 2µg/mL and stored in -20°C.

2.19 In-situ Hybridisation for HH15 and above

All solutions were 0.1% DEPC treated (DEPC added to a final concentration of 0.1% , and incubated at 37°C overnight) and autoclaved to prevent Rnase contamination. Solutions or components that cannot be DEPC treated and/or autoclaved, were made with DEPC treated water. Embryos were fixed in 4% PFA at RT for 2 hours and then washed with DEPC-PBS to rinse off the fixative. The allantois membrane was removed and the cavities were punctured. The embryos were then taken through a methanol-PBS gradient- 25% , 50% , 75% , 90% , 95% , 99% and then rinsed with 100% methanol twice before storing them in 100% methanol in -20°C. The embryos were rehydrated to PBST (0.1% tween20/PBS) on ice. Embryos were treated in 10µg/ml Proteinase K in DEPC water for a duration equivalent to their Hamburger-Hamilton stage (HH17 - 17 mins) on ice. The embryos were washed twice for 5 mins in PBST on ice and fixed in 4% PFA/0.2% Glutaraldehyde/ PBST for 20 minutes at RT. The embryos were rinsed

thoroughly with PBST thrice for 5 mins and transferred into Pre-hybridisation solution and allowed to sink. The embryos were then transferred to fresh Pre-hybridisation solution at 65°C for an hour, following which probe was added at a concentration of 1µg/ml and left to hybridise overnight at 65°C. The embryos were further subjected to a series of harsh washes (Solutions 1,2,3, and 4) at 65°C and then taken to aqueous washes with MABT. Roche blocking buffer kit was used for further washes. Heat inactivated goat serum was used with the Roche blocking solution at a concentration of 20% before adding anti-DIG antibody at a concentration of 1:2000, diluted in the same block and left at 4°C overnight. Washes with MABT were continued for an entire day at RT to remove non-specific binding. The colour reaction with NBT-BCIP was done in NTMT on the following day, at RT without shaking(Henrique et al., 1995).
The NBT/BCIP mix can also be replaced with BM-Purple. The embryos were equilibrated in 60% glycerol and imaged to make the embryo more transparent.

2.20 Microdissection

To understand the transcriptomic signature of the edge cells, in comparison to the otic vesicle cells and the surface ectoderm cells, microdissection of HH17 chicken embryo was performed. The dissection tools and petri dishes were RNAse treated by baking them at 200°C for 5 hours. The microscope and bench were thoroughly cleaned with RNAsezap. PBS was DEPC treated and autoclaves prior to use. Dispase solution was made at a concentration of 2.4U/ml, diluted with DEPC PBS and stored as aliquots in -20°C. The dispase solution was used for digesting the mesenchymal cells attached to the surface ectoderm and the otic vesicle, however, the otic edge was not treated with dispase, as the tissue was smaller in size, and dispase also digests cells that are damaged. The dissection was performed with electrolytically sharpened tungsten needles. The needles were sterilised often during dissection in an open flame. The embryos were pinned on the sylgard plate with the help of dissection pins. The otic edge was the first tissue to be removed; the tungsten needle was used to perforate the region around the otic pore from the top, followed by perforations in the perpendicular direction. This ensured a complete dissociation of the intact otic pore region, which was subsequently pipetted into a sterile 1.5ml tube containing 1 ml of trizol. The otic vesicle was next dissected by nudging the otic vesicle gently without damaging it or the surrounding

surface ectoderm. The otic vesicle without the edge was pipetted into a dispase droplet placed in a sterile 35mm dish. The dispase treatment was done for a period of 10 mins, followed by pipetting the tissue into a 1.5ml tube with 1 ml of trizol. This was then followed by surface ectoderm dissection. The tungsten needle was used to nudge off the surface ectoderm and two tungsten needles were used as scissors to get a small region of the surface ectoderm. The tissue was pipetted into a dispase droplet for a duration of 10 mins and transferred into a 1.5ml tube with TRI reagent in it. 8 pieces of tissue were collected per tube and stored at -20°C until RNA isolation. After RNA isolation, 1µl aliquot of the sample was allocated for bio-analyser and 1µl for qubit. Bio-analyser was the quality control for the integrity of total RNA from the sample and Qubit computed the concentration of total RNA in a sample. RNA resuspended in water was stored in -80°C until cDNA library preparation.

2.21 Bulk-mRNA sequencing and analysis of data in usegalaxy.org webserver.

A total of 12 samples (quadruplicates for three tissue type) with 100ng of total RNA, were used for the RNA library preparation. The quality of the samples was confirmed using a bioanalyzer and the concentration using qubit. The library was prepared by the Next-Gen Sequencing facility using the NEBNext® Ultra™ II Directional RNA Library Prep with Sample Purification Beads (Catalog no-E7765L) kit. The sequencing was performed on a Hiseq2500 platform using 1x50bp sequencing read length. The subsequent analyses of the reads were done accordingly. Online tutorial available on the usegalaxy.org webserver was followed for the Differential Gene Expression (DGE) Analysis of the data (Batut et al., 2018; Doyle, Phipson, Maksimovic, et al., 2018; Doyle, Phipson, & Dashnow, 2018; Hiltemann et al., 2023). The RNA seq reads were in a FASTQ format, which was uploaded to the server. The quality of the reads was analysed with the FASTQC tool (*Babraham Bioinformatics - FastQC A Quality Control Tool for High Throughput Sequence Data*, n.d.). After confirming that the reads were of good quality, the Illumina standard adaptor sequence added during the sequencing reaction was trimmed using the Trimmomatic tool (Bolger, Lohse, & Usadel, 2014).The following values were chosen for the tool:

a. Reads: Single end

b. Perform initial illuminaclip step: No
c. Trimmomatic operation to perform: Sliding window trimming
d. Number of bases to average across: 4
e. Average quality required: 20

The output of the tool is a fastq file with trimmed reads. The next step was to map the reads to a reference genome and the HISAT2 tool was used for this purpose (Daehwan Kim, Langmead, & Salzberg, 2015). The server has only older versions for the chick database (galGal4), hence we uploaded the grc6gca galGal6 (latest) reference genome to the server and used it instead of the built-in genome. Other information for the tool:

a. Library: Single-end
b. I/P file: Trimmomatic
c. Specify strand information: Unstranded

All other values remained as default. The output of this tool are BAM files which was used for counting the reads per gene. The featurecounts tool was used for this purpose (Liao, Smyth, & Shi, 2014). The output of this application will be used for the final DGE. Other information for the tool:

a. I/P file: BAM file from Hisat2
b. Strand information: Unstranded
c. Gene annotation file: From history, galGal6.refgene.gtf
d. O/P format: Gene-ID "\t" read-count (MultiQC/DESeq2/edgeR/limma-voom compatible).

The output is a table with the Gene-ID (gene name) and the counts per sample. These files was used for the next tool, the limma-voom (Law, Chen, Shi, & Smyth, 2014; R. Liu et al., 2015).

The information used for the tool:

a. Differential expression method: limma-voom
b. Apply voom with sample quality weights: no
c. Count files or Matrix: Separate count files
d. Factor: Tissue
    1. Group: Tissue_type
    2. I/P Count files: featurecounts of quadruplicates
e. Use gene annotations: No
f. Input contrast information from file: No
g. Contrast:

1. Otic_edge- otic_vesicle
2. Otic_edge-surface_ectoderm

h. Filter low counts:
    1. Filter lowly expressed genes: Yes
    2. Filter on CPM or count values: CPM
    3. Minimum CPM: 1
    4. Minimum Samples: 2

i. Output options:
    1. Glimma Interactive plots
    2. Box plots
    3. Heat Maps (top DE genes)
    4. Output Normalised counts table: Yes
    5. Everything else was deselected. (Default- No)

j. Advanced options:
    1. Minimum Log2 Fold Change: 0.58
    2. P-value adjusted threshold: 0.05
    3. P-value adjustment method: Benjamini and Hochberg (1995)
    4. Test significance relative to a fold change threshold: No
    5. Number of genes to highlight in plots: 30
    6. Normalisation method: TMM
    7. Use robust settings: Yes

The resulting plots and tables were used for further studies.

2.22 CRISPR- Cas9 Electroporation

Kaveri eggs were incubated for 50 hours to acquire HH15 embryos as shown in Fig 2.2. Micro-capillary needles were filled with the required amount of DNA mix (Plasmid (5µg/µl, fast green and 30% sucrose) using Eppendorf loading tips.

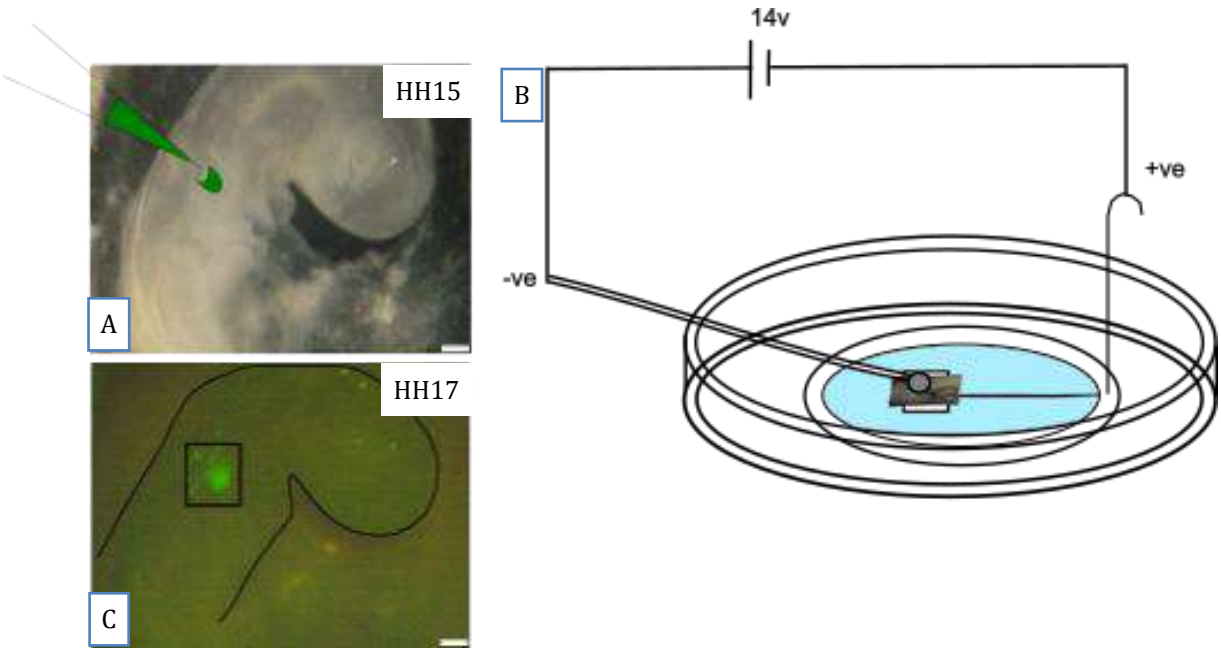

Fig 2.2: Electroporation of HH14 chick embryo. A: The embryo collected using a paper window is placed on the electrode plate (+ve electrode). The embryo is placed on ringer's solution. The otic vesicle is filled with DNA solution, using a capillary needle. **B:** The –ve platinum electrode is placed on top of the embryo and a potential difference is applied as a square pulse. The embryo is incubated for 8 hours. **C:** Embryo expressing GFP in the otic vesicle.

The vitelline membrane of the embryo was removed and the DNA mix was carefully injected into the open otic vesicle, without poking the embryo as shown in Fig 2.2A. Once the vesicle was filled, 5 square pulses of 14V for 50msec were applied on the embryo with an interval of 100msec. The embryos were then cultured in albumin agar plates for 8 hours and harvested for further processing.

Chapter 3: Characterising epithelial fusion in otic vesicle

3.1 Introduction

The inner ear primordia arise from bilaterally paired disks of thickened ectoderm known as the otic placode. This structure gives rise not only the auditory and the vestibular structures and sensory cells, but also the neurons that connect the inner ear to the CNS. Induction of the otic placode takes place during neurulation. Here, the surface ectoderm region, rostral to the first somite and adjacent to the neural tube, is acted upon by underlying mesoderm which secretes FGF (in chick this is Fgf3 and Fgf19, in mouse it is Fgf3 and Fgf10), to give rise to a multi-potent precursor domain known as the Otic-Epibranchial Progenitor Domain (OEPD). The OEPD is acted upon by Wnt8a from the adjacent neural ectoderm, steering the fate, segregating the fate of this tissue into otic placode (Wnt high) and epibranchial placode (Wnt low) (Xiaorei Sai & Ladher, 2015a).

As well as the change in gene expression, the induction of the otic placode, is accompanied by morphogenetic changes. The inductive events specialise a region of the contiguous surface ectoderm, otic placode cells thicken and exhibit a pseudostratified morphology, as compared to the squamous surrounding surface ectoderm. As thickening proceeds, the otic placode undergoes invagination. This is a biphasic process. There is a first phase, basal expansion of the otic placode at around HH10, which continues until HH12. This is subsequently followed by the apical constriction of the cells in the placode, which results in the deepening of the otic pit. Invagination also ensures that as the otic cells proliferate, the pit is pushed into the mesenchyme under the surface ectoderm. Concomitantly, the edges of the otic pit are brought close. The final step of the internalisation of the otic vesicle is closure. Closure accomplishes a complex tissue remodelling event: The edges of the otic cup are sealed, but also the contiguous epithelial sheet is transformed into two epithelia (Ladher, 2017). What are the mechanisms of otic closure?

The closure event starts around HH16 and continues till HH17+ (Ladher, 2017). The edges of the otic cup are pulled together by apical constriction of the pseudostratified cells within the otic vesicle and are also pushed by the surface

ectoderm as the embryo grows. The surface morphology of the cells has been thoroughly discussed by Bancroft and Bellairs earlier, using SEM (Bancroft & Bellairs, 1977)

The otic vesicle closure is a crucial event in inner ear development; complete segregation of the otic vesicle from the surface ectoderm is essential for proper positioning of the inner ear within the head of the fully developed organism. The site of epithelial fusion in the otic vesicle also gives rise to the future endolymphatic duct. Previous studies have shown epithelial fusion in the otic vesicle is mediated by actin-based finger-like projections, filopodia, as seen during neural tube closure in chick and mouse, and dorsal body wall closure in *Drosophila melanogaster*.

We started with characterising epithelial fusion during otic vesicle development using SEM and confocal microscopy to get a closer look at the surface morphology. This characterisation helped us understand the system better. We observed differently shaped cells on the otic edges; we explored the shape changes further by staining sections of otic vesicle. Additionally, the population of the differently shaped cells changed with phases of epithelial fusion. This observation led us to hypothesize that they may have a role in epithelial fusion, and thus further characterize them with respect to the localisation of junction proteins. Based on our preliminary data we hypothesized a reason and probable necessity for their change in shape, which we tested in Chapter 4.

3.2 Results

3.2.1 Otic vesicle closure in *Gallus gallus domesticus*.

The development of the otic vesicle from placode until its closure, internalisation, and disappearance from the surface of the embryonic head has been well characterised (Alvarez & Navascués, 1990; Bancroft & Bellairs, 1977).

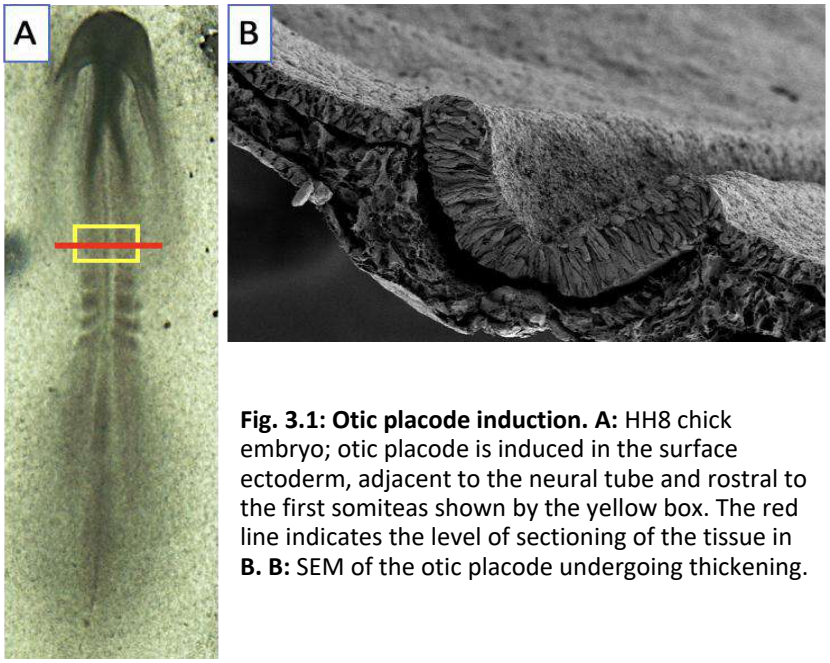

Fig. 3.1: Otic placode induction. A: HH8 chick embryo; otic placode is induced in the surface ectoderm, adjacent to the neural tube and rostral to the first somiteas shown by the yellow box. The red line indicates the level of sectioning of the tissue in **B. B:** SEM of the otic placode undergoing thickening.

The otic vesicle starts of as a thickened ectodermal placode as shown in Fig 3.1, a HH8 chick embryo, when the otic placode is induced in the surface ectoderm. This sheet of cells undergoes further development to give the closed otic vesicle in HH17 chick embryo, as shown in Fig.3.2. The otic vesicle is tear drop shaped; the red arrow points to the region of the otic vesicle undergoing epithelial fusion. This region marks the border between the surface ectoderm and the otic vesicle. We used SEM to image the otic primordia at different stages of development from HH12 to HH17+ (Fig 3.3).

At HH12, the major axis of the otic placode is dorsal- ventral and we see it opening to the ventral side. At HH13, we see the ventral side rear up, giving a cup-like morphology to the otic primordia. Eventually, the otic cup gets pushed into the mesenchyme of the head and only the opening of the otic vesicle is visible on the surface. The dorsal-ventral axis of the otic vesicle is maintained and continues to exist that way until the closure of the otic vesicle, after which the tear-drop shaped vesicle

undergoes further morphogenesis upon specification of different domains in the otic vesicle.

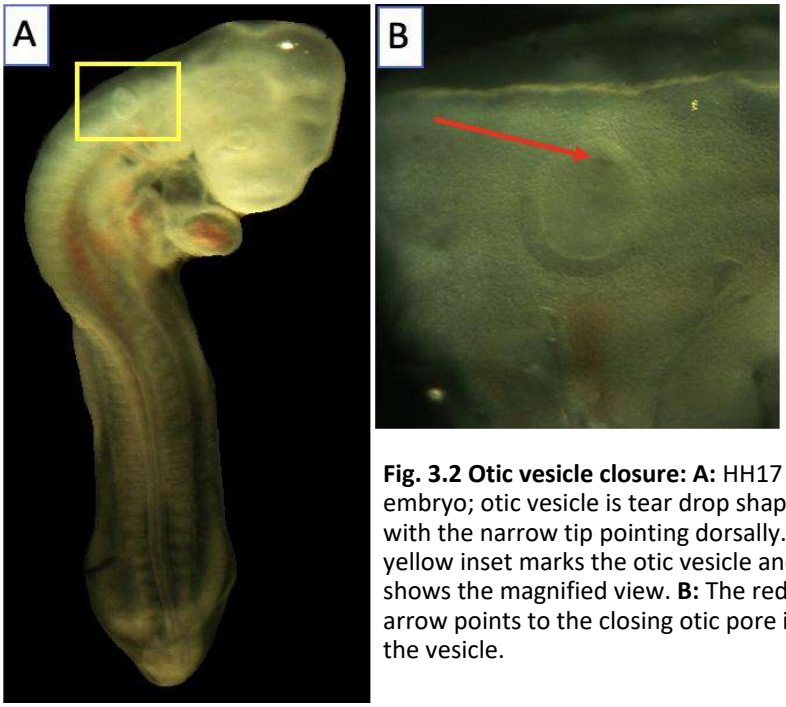

Fig. 3.2 Otic vesicle closure: A: HH17 chick embryo; otic vesicle is tear drop shaped with the narrow tip pointing dorsally. The yellow inset marks the otic vesicle and B shows the magnified view. **B:** The red arrow points to the closing otic pore in the vesicle.

The otic cup is buried within the head at HH15, and the size and shape of the otic pore had changed visibly; the width has considerably reduced in the rostral-caudal axis and the pore appears to be elongated in the dorsal ventral axis. We also saw the presence of elongated cells along the edge of the pore, these cells are involved in the overall tension experienced by the otic pore to bring the edges close to each other. Only upon reaching proximity, epithelial fusion starts. This is seen in the case of caudal neural tube closure in mice (Molè et al., 2020; Pyrgaki, Trainor, Hadjantonakis, & Niswander, 2010b), where the fusion is unidirectional, rostral to caudal. The width of the opening is the least before the edges fuse and progressively, the more caudal edges are brought together.

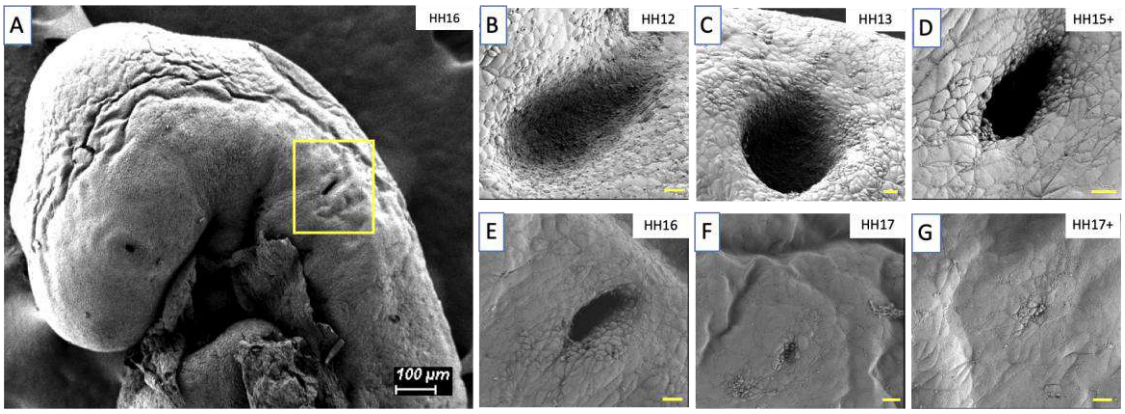

Fig. 3.3: Otic primordia at different stages of development. A: SEM of a HH16 chick embryo. The inset marks the opening of the otic vesicle, the otic pore. **B:** The otic pit stage of the primordium at HH12. **C:** The otic cup stage at HH13. **D:** The otic vesicle at HH15+ **E:** HH16 **F:** HH17 and **G:** HH17+. Scale bars for 10µm.

We also observed, the rostral-ventral side of the otic pore has cells with a rounded apical morphology unlike the flattened surface ectoderm cells; these cells are destined for an otic fate and will migrate into the otic vesicle. As the otic vesicle closure proceeds to completion, we see the number of these cells reducing and eventually stopping when the vesicle gets internalised (Alvarez & Navascués, 1990).

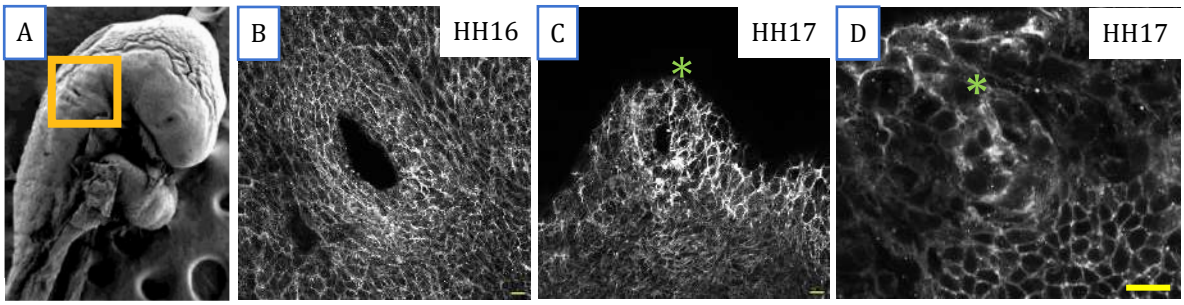

Fig. 3.4: Closure in the otic vesicle starts in the dorsal side of the pore. A: A HH16 chick embryo. The inset shows the approximate orientation of the otic pore in B,C, and D. **B:** A maximum intensity projection of F-actin staining of HH16 otic pore. We see uniform staining of F-actin in cells along the surface ectoderm edge of the pore. **C:** F-actin staining of HH17 otic pore. The * (green asterisk) shows an enrichment of F-actin as a cable showing the newly fused tissue. **D:** F-actin staining of a recently closed otic vesicle. The * (green asterisk) shows enrichment of f-actin as a cable. Scale bars are 10µm in B and C and 5µm in D.

Early on, the otic placode at HH8 to the otic cup at HH15 transition is mediated by a combination of apical constriction and basal expansion. After this, the otic vesicle closure takes place in two steps. At HH15, when only the otic pore is visible on the surface of the embryo, as explained above there is a significant reduction in the diameter of the pore. Based on SEM images, and whole mount staining of the otic vesicle closure,

this reduction can be attributed to a purse string model of closure. This mode of closure is aimed at bringing the edges closer together, before beginning epithelial fusion. The purse string model of closure has been well described in the case of wound healing (Bement, Mandato, & Kirsch, 1999; D. P. Kiehart, 1999) and drosophila body wall closure (Jacinto et al., 2002). At early stages, cells were elongated on the edge as shown above (Fig 3.3D). We see concentric cables of F-actin in the circumference of the otic pore (Fig 3.4 A, B). The second step in the process of closure can be attributed to the unidirectional zippering starting from the dorsal side and proceeding towards the ventral side. The opposing edges are close to each other in the dorsal side of the pore, indicating the direction of zippering in a dorsal-to-ventral direction as reported earlier. The newly fused neural tube in mouse embryos has a strong actin cable on the surface ectoderm, which we also saw in the otic vesicle, further confirming the direction of zippering (Fig 3.4 C, D,E) (Galea et al., 2017; Nikolopoulou et al., 2019) .

As development proceeds, in HH16, Fig 3.3 E, we see a reduction in the size of the otic pore, but the shape remains the same. At the site of fusion, in the caudomedial edge, apoptosis has been reported previously (Alvarez & Navascués, 1990). We also

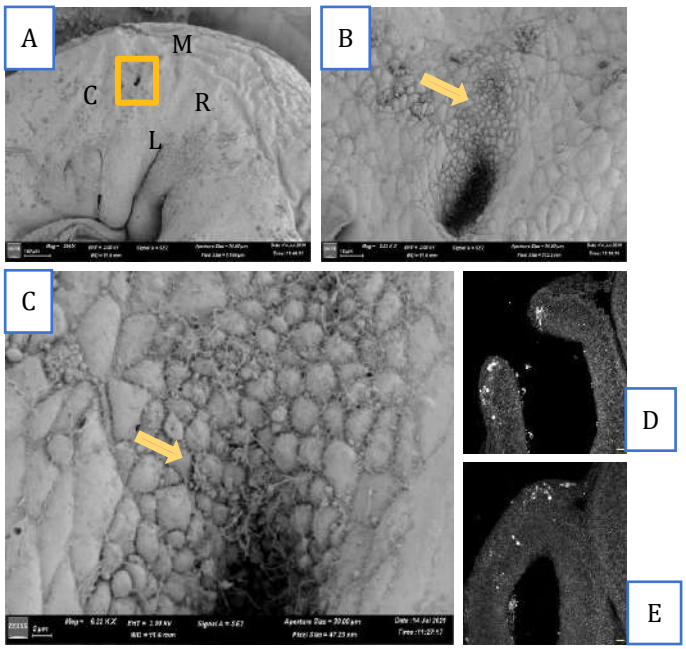

Fig. 3.5: Apoptosis at the caudo-medial edge of the closing otic vesicle. A: SEM of HH17- chick embryo showing the right otic vesicle. **B** and **C:** magnified views of the inset in **A**. The open arrows show where we see some apoptotic blebs on the surface ectoderm. **D:** HH15 otic vesicle section stained for cleaved caspase-3. We see apoptosis in the edges of the otic vesicle. **E:** HH17 otic vesicle section stained for cleaved caspase-3. We see some apoptotic cells in the surface ectoderm in the otic vesicle region that has already fused. M-medial, L-lateral, R-rostral, and C-caudal. Scale bars for 10µm.

see apoptosis in the caudo- medial edge region of the closing otic pore. SEM of HH17 embryo (Fig 3.5 A, B and C) shows cells undergoing apoptosis on the surface ectoderm adjacent to the otic vesicle. Apoptotic blebs can be seen between cells with the cobblestone appearance. Sections of otic vesicle at different stages of development, HH15 and HH17 were stained for cleaved caspase-3, one of the effector molecules in the programmed cell death pathway (Eckhart et al., 2008) . At HH15 (Fig 3.5D), we see apoptosis in both the edges of the otic pore. This could be cell death contributing to the bending of the tissue, as seen earlier in the case of neural tube formation and drosophila leg folding, among others. In the case of neural tube, apoptosis has also been implicated in generation of forces to pull the tissue together and aid in the formation of dorsal hinge points (Roellig et al., 2022). In the case of drosophila leg folding, the study showed the active role of an apoptotic nuclei in the bending of the leg epithelium (Ambrosini, Rayer, Monier, & Suzanne, 2019). In HH17, (Fig 3.5E), apoptosis is seen on the dorsal most region of the otic vesicle. It is not clear which lineage these apoptotic cells belong to, and if apoptosis itself is absolutely essential for the proper closure of the otic vesicle. Epithelial fusion is a common occurrence during embryonic development in different organ systems; however, the necessity of apoptosis for each of these processes is different (Ambrosini et al., 2019), hence parallels cannot be drawn with respect to the absolute requirement of apoptosis during otic vesicle closure. The apoptosis at the dorsal region in HH17 has previously been reported (Washausen & Knabe, 2019) and implicated in the spatial distinction of the otic, epibranchial and lateral line placodes in the embryo. So far, we have made cellular level observations on the apical surface of the surface ectoderm and the cells on the edge of the otic pore. We next wanted to look for cellular level changes inside the tissue.

3.2.2 Some cells in the otic vesicle edge have a different shape.

Throughout the development of the otic vesicle, the epithelium is continuous with the overlying surface ectoderm. The cells of the surface ectoderm are squamous; they are flat and have very large apical surfaces. After induction, the cells of the otic epithelium are pseudostratified, that is they are elongated and can have nuclei at varying levels along their apical-basal axis. The border of these two tissues, is the otic edge region, which is under tension owing to the bending of the tissue to internalise the vesicle. This edge region is usually populated by smaller pseudostratified cells. When we cut through

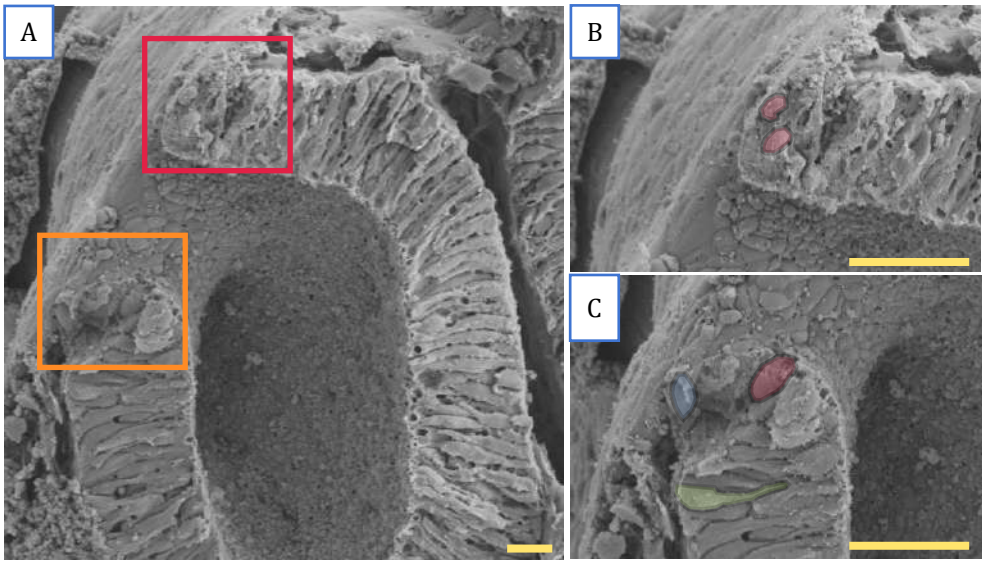

Fig 3.6: SEM of cross-section of HH16 otic vesicle. A: The left otic vesicle with the red and orange inset showing **B** and **C** respectively. The edge region marked by the insets show the presence of three different cell shapes which have been marked in three colours; the blue coloured cells represent the surface ectoderm cells, the green cells represent the pseudo-stratified otic vesicle cells and the red coloured cells represent a population of the cells that mediate epithelial fusion. Scale bars for 10µm.

a HH16 otic vesicle (Fig. 3.6 A), we saw some rounded cells in the edge region. These cells have been shaded with red in Fig. 3.6 B and C. The surface ectoderm cell is shaded in blue and the pseudostratified cell in green. The shape of the rounded cells can be attributed to the force they are experiencing from the otic vesicle as well as from the

surface ectoderm. To rule out the possibility of a SEM processing artefact, we used cryo-sections stained with F-actin, to look for cell shape changes.

Imaris is a software with multiple modules for automated and manual image processing. We used the 'surfaces' module to perform the analysis. The software allows the user to mark the shape of cells across different optical sections of the image and projects it as a 3-dimensional object as shown in Fig. 3.7 A and B. Multiple cells can be marked in a single section as shown. The software also gives quantitative values of multiple parameters based on the object, as created by the user. One such parameters is the sphericity index, which is a measure of how spherical a given object is. Fig 3.7 C shows the formula for this index. The more spherical the object is, the value tends towards 1 and elongated objects would tend towards a value of zero. In Fig 3.7 A-D, the cells are colour coded based on their sphericity as shown in the colour key.

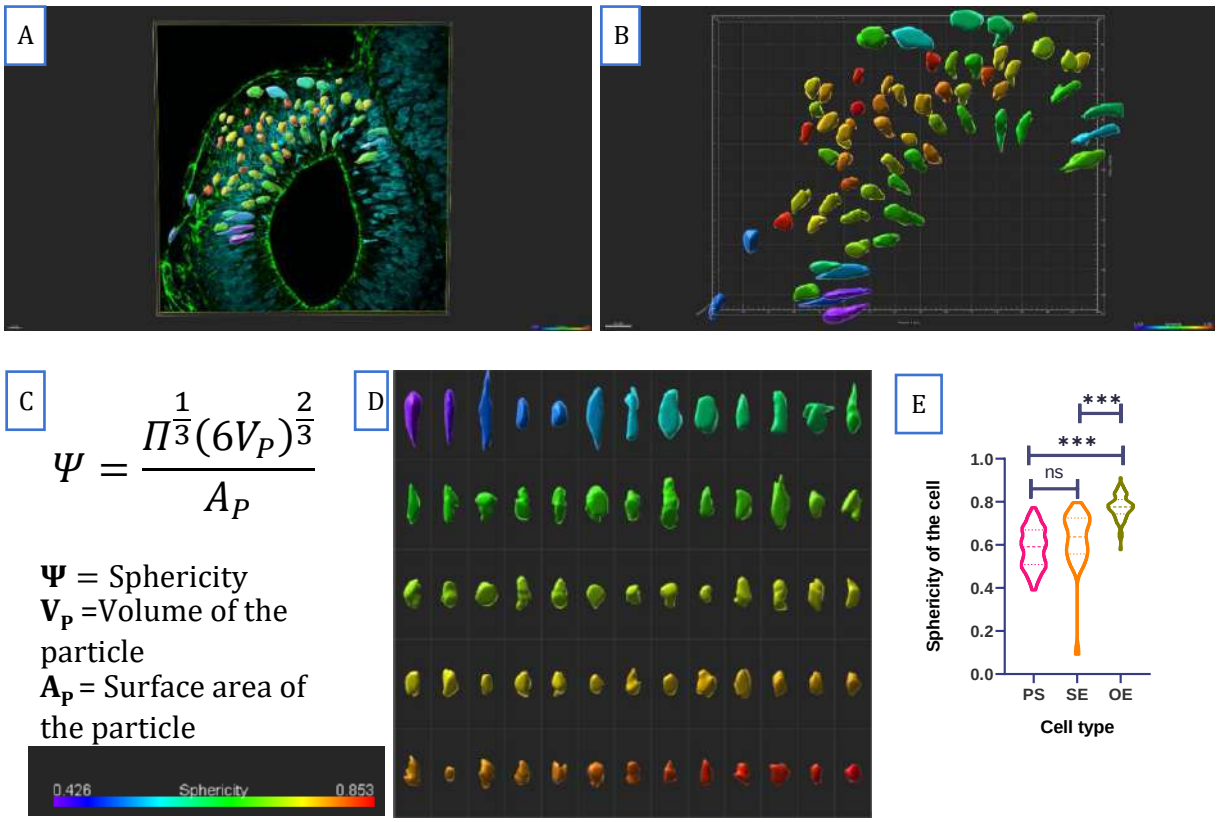

Fig. 3.7: Marking the shape of the cells. A: Cell boundaries of the three types of cells were manually marked with the help of Imaris using Z stacks of otic vesicle sections stained with F-actin. **B:** Individually marked cells depicted as 3D objects on a cartesian plane of the otic vesicle. **C:** The sphericity of the marked cells is calculated using the volume and surface area data. **D:** Marked cells arranged in the order of increasing sphericity. **E:** One-way ANOVA analysis of sphericity of the three cell types; PS-pseudostratified, SE-surface ectoderm and OE-otic edge. n=80 to 90 for each cell type.

Elongated cells have a lower sphericity index and are on the violet end of the VIBGYOR spectrum with a value of 0.426. The rounded cells in this image have a high

sphericity of .853 and are at the red end of the spectrum. The significance in sphericity change across cell types was tested using one way – ANOVA and plotted in Fig. 3.7E. We see a significant difference between the pseudostratified and the round cells in the otic edge (marked as OE in the graph). We also see a significant difference between the surface ectoderm cell and round cell in the edge. However, there is no significant difference between the pseudostratified and surface ectoderm cell.

To further confirm the shape of these rounded cells in the edge, we electroporated HH14 chick embryos with constitutively active eGFP plasmid under the pCAG promoter and incubated until HH17 on albumin agar plates. The embryos were processed further and imaged (Fig 3.8 A). Imaris analysis of the sections (Fig 3.8 B) confirmed the presence of rounded cells at the site of fusion. Further, we wanted to check if these rounded cells played a role in epithelial fusion and hence looked for their presence at different stages of fusion.

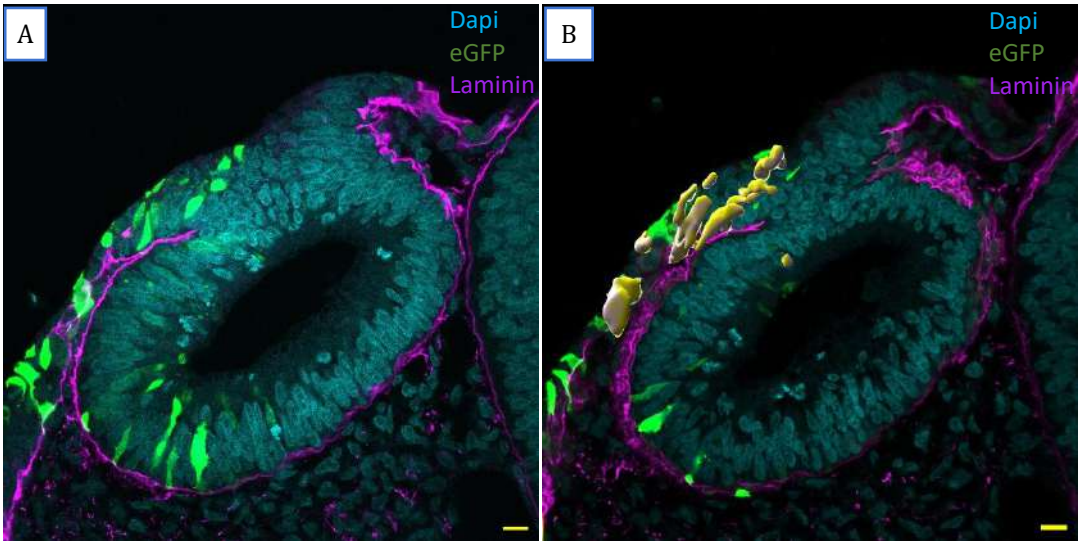

Fig. 3.8: Confirming the shape of cells through mosaic electroporation of eGFP. A: Section of HH17 chick embryo electroporated with constitutively active eGFP showing the presence of cells with altered cell shape (the edge cells) at the point of remodelling after fusion. **B:** Imaris was used to mark the shape of the cells using z-stacks obtained. Scale bars for 10µm.

The zipping in epithelial fusion is a continuum that occurs between HH16 and HH17+. This process consists of multiple steps. The otic edges are brought in close proximity. This is followed by, the cells from opposing sides sending out membrane-based protrusions to recognise their counterparts from the opposite side. After the initial recognition, the edges are pushed closer to each other, and fusion is initiated. This fusion is followed by the segregation of cells. Until now, the otic epithelium was in

continuation with the surface ectoderm, but for the otic vesicle to get completely internalised, the epithelium has to get segregated from each other, thus initiating the process of remodelling, when new junctions are established and new basement membrane is formed. And the final stage is when two intact epithelia are formed, the otic epithelium with a basement membrane and an overlying surface ectoderm with a basement membrane.

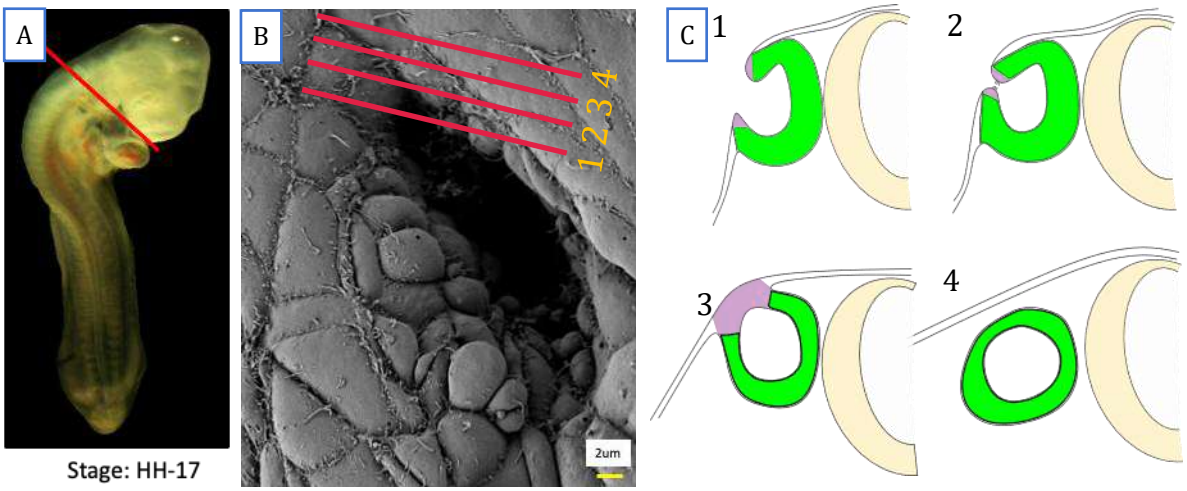

Fig. 3.9: Epithelial fusion is a continuum. A: A HH17 chick embryo. The red line shows the angle of cutting for all the subsequent sections in the figure. **B:** The level of sectioning of 1,2,3 and 4 in C. **C:** A schematic representation of the sections obtained. The yellow tissue is the neural tube, the purple tissue is the edge region and the green tissue is the otic epithelium.

We have observed that after the zipping starts in the otic vesicle, different levels of sections across the otic pore exists in different levels of epithelial fusion as depicted in Fig. 3.9 A-C. This was also seen in the case of optic fissure closure (Gestri et al., 2018). Stage 1 is when the otic edges are pushed together, stage 2 is when the edges are just beginning to fuse, stage 3 is when the site of fusion is getting remodelled and finally stage 4 is after the segregation. We looked at the cell composition in each of these four stages of epithelial fusion as shown in Fig. 3.10. We saw an increase in the number of the round cells in the edge in stages 2 and 3. These 4 stages would be used later in the chapter as landmarks for the characterisation of protein expression in the round edge cells.

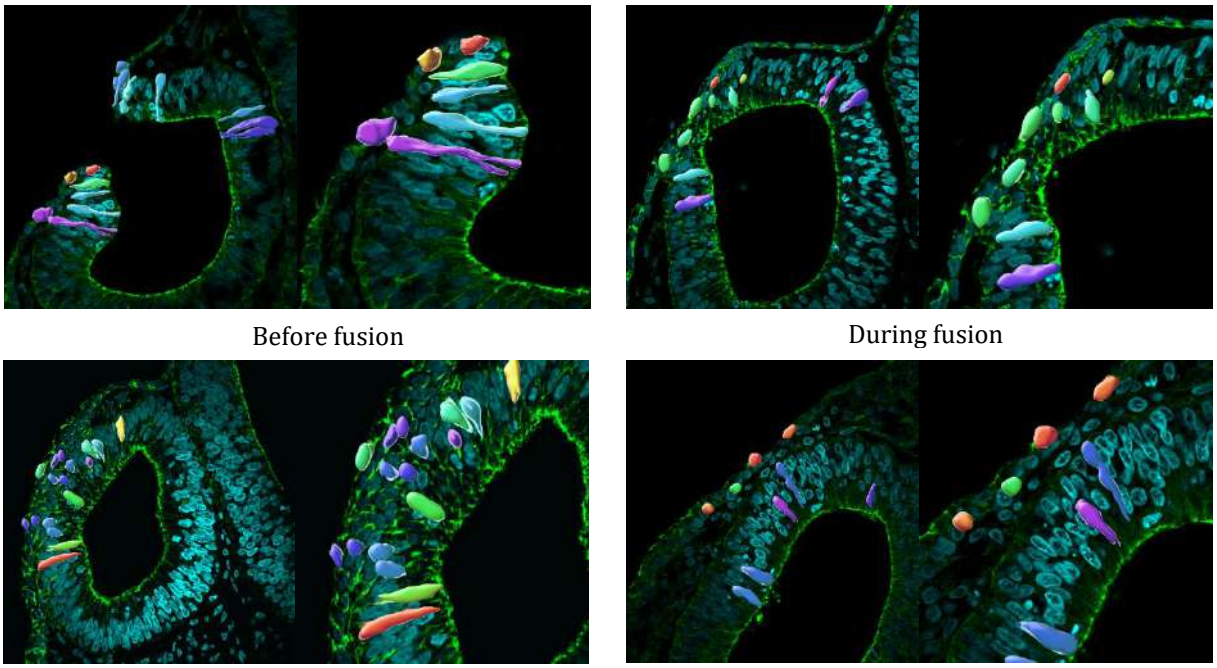

Fig. 3.10: Edge cell population across different stages of fusion. A: The edge cells are present before the fusion of the otic edges, **B:** during the fusion initiation of the otic edges, **C:** during the remodeling of the newly fused otic edges, **D:** but not after the segregation of the otic vesicle from the surface ectoderm.

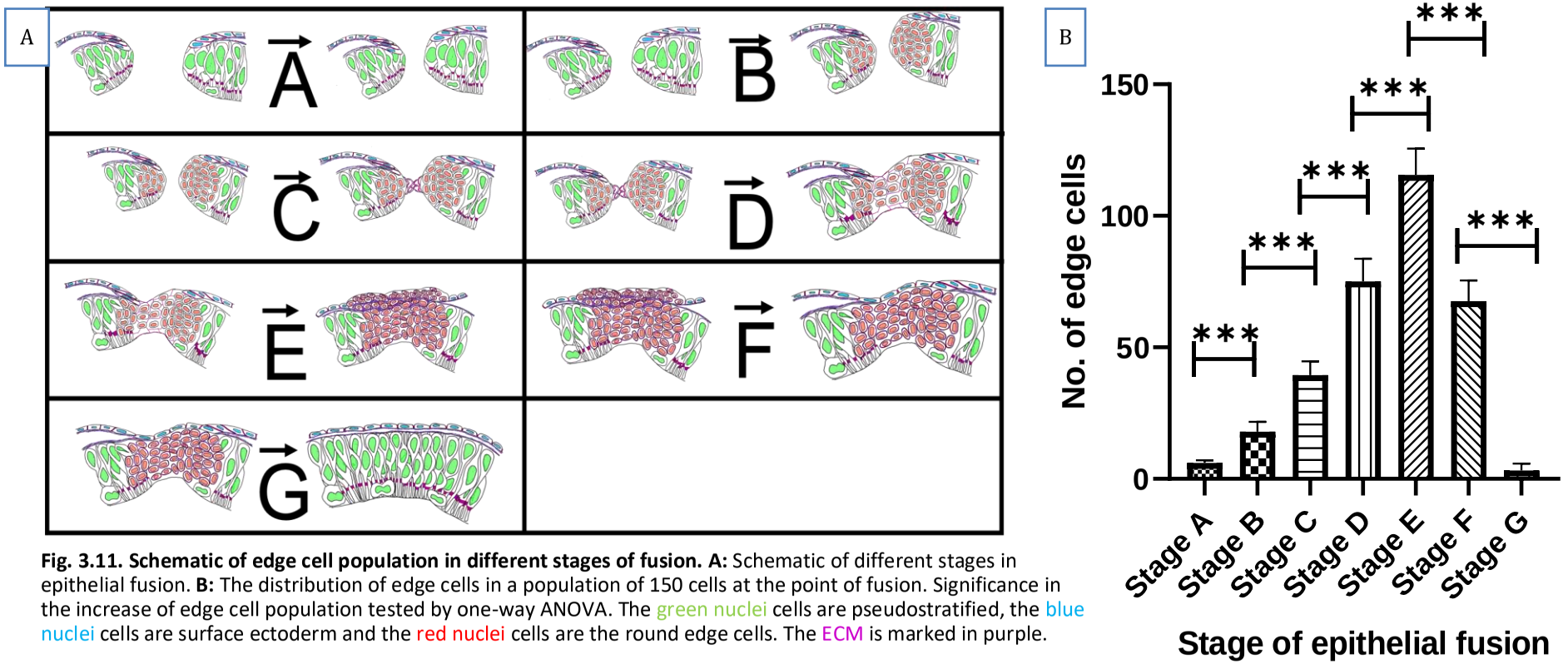

Fig. 3.11. Schematic of edge cell population in different stages of fusion. A: Schematic of different stages in epithelial fusion. **B:** The distribution of edge cells in a population of 150 cells at the point of fusion. Significance in the increase of edge cell population tested by one-way ANOVA. The green nuclei cells are pseudostratified, the blue nuclei cells are surface ectoderm and the red nuclei cells are the round edge cells. The ECM is marked in purple.

We divided the fusion process into shorter stages to acquire more information on the population of these round edge cells. As shown in Fig. 3.11 A, there are seven stages. Stage A is otic vesicle at HH15, when the edges are far apart. HH16+ embryos have otic vesicles that possess stages from B onwards. Stage B is when the edges are in close proximity. Stage C is when the edges send out membrane protrusions and meet their counterpart from the apposed side. Stage D is when the fusion has started, and we see nuclei at the site of fusion. Stage E is when the fusion is almost complete, and we see diffused extracellular matrix at the site of fusion; this could mark the beginning of the remodelling. Stage F is when the remodelling has finished and segregation has started. And finally, stage G is when segregation is complete.

Across these stages, we counted the number of rounded cells in a population of 150 cells, in the otic edges or the site of fusion depending on the stage. A steady increase of the round cell population in the edge was seen, until stage E when remodelling had just started and then we saw a steady decrease when the segregation started and ended. This change in population of these round cells in the edge across different stages of fusion was significant when a one-way ANOVA test was performed (Fig 3.11B).

The data indicated a possible role for these rounded cells in the edge during the fusion, remodelling and the segregation. Additionally, junction exchange among neighbours is a key aspect of epithelial fusion. We looked at the expression profile of major junctional complexes across the 4 major stages of epithelial fusion as described in Fig. 3.10.

3.2.3 Cell type specific localisation of adherens junctions

Epithelial cells are defined by multiple parameters; their strict domains that contribute to the polarity, their contact with the neighbours through junctions and adherence to the underlying basement membrane or the extra cellular matrix. During otic vesicle closure, the cells in the edge have to lose contacts with their existing surface ectoderm neighbours and form new ones with otic vesicle cells from the apposed side. And these new cells will also have to lose their adherence with the ECM underneath, so a new basement membrane can be formed under the cells that have established new neighbours and give rise to two intact epithelia.

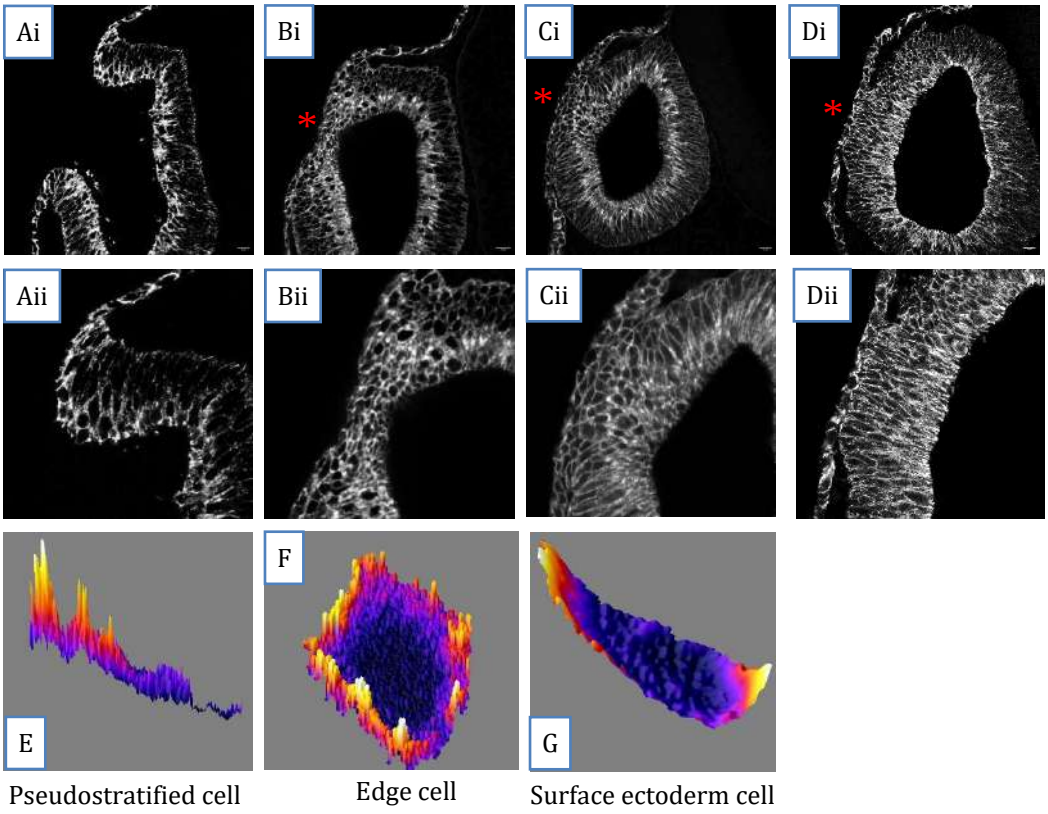

Fig. 3.12: Expression profile of Cdh1 during epithelial fusion. A(i,ii): Cdh1 expresses as a cortical belt in the otic epithelium before fusion. **B(i,ii):** At the site of fusion(*) the expression is diffused. **C(i,ii):** The diffused expression of the protein persists when the fused edges are remodelling to segregate from the surface ectoderm. **D(i,ii):** This diffused expression changes to cortical expression as the otic vesicle gets segregated and internalised. **E:** Expression of Cdh1 in a pseudostratified cell depicted in fire LUT. **F:** Expression of Cdh1 in a round cell depicted in fire LUT. **G:** Expression of Cdh1 in a surface ectoderm cell depicted in fire LUT. Scale bars are 10µm.

We started with the expression profile of Cdh1 in the otic vesicle. Cdh1 is an adherens junction component, usually seen in epithelial tissue. It is present below the tight junction, and plays two major roles; it acts as the blockage that stops the diffusion of apical plasma membrane proteins to the lateral domain of the cell and connects the cortical actin network of neighbouring cells thus maintaining tension across the tissue.

Cdh1 is very strongly expressed as a cortical belt in epithelial tissue. In Fig 3.12, we see Cdh1 expressed only in the otic vesicle and the surface ectoderm. The neural tube at this stage of embryonic development only expresses n-cadherin. In Fig 3.12, Ai and ii show the expression of Cdh1 in stage 1, when the edges are apart. We see a cortical belt of Cdh1 in the otic vesicle, with a strong expression near the apical side of the pseudostratified cell (Fig 3.12 E). We also see a lateral expression of Cdh1 on the surface ectoderm cells (Fig 3.12 G). When the edges are beginning to fuse, we see the round edge cells, and the expression profile of e-cadherin on these cells are not polarised like their counterparts. And this expression profile is seen when the remodelling has just begun (Fig 3.12 C). However, once the segregation is over, we did not see the rounded cells, as shown before. The expression of Cdh1 becomes uniform throughout the newly segregated otic vesicle and the overlaying surface ectoderm. We next looked at the expression profile of a tight junction component, ZO1. Tight junctions are important for maintaining the apical polarity of epithelial cells. At early stages of development, when the otic edges are apart (Fig 3.13 Ai,ii), the expression profile of ZO1 of cells on the edge was lower than the expression in the rest of the otic epithelium and the neural tube. We see a very apical localization of ZO1 in the pseudostratified cell (Fig 3.13 E and surface ectoderm cell (Fig 3.13 G). This localisation continues across the four stages of fusion. ZO1 expression on the membrane protrusions is higher (Fig 3.13 Bi,ii). It is possible that the localisation of tight junction components in these protrusions, aids in their recognition of counterparts. When the remodelling has initiated, we see the expression of ZO1 as tiny speckles only on one side of the cell. It is possible that the localisation of ZO1 in the round cells of the edge is dictating the polarity of the cell and by extension, its fate of becoming a part of either the otic vesicle or the surface ectoderm. After segregation we see a typical expression pattern of ZO1 in the intact surface ectoderm and the otic vesicle. A similar expression patter was seen during optic fissure closure as well (Gestri et al., 2018).

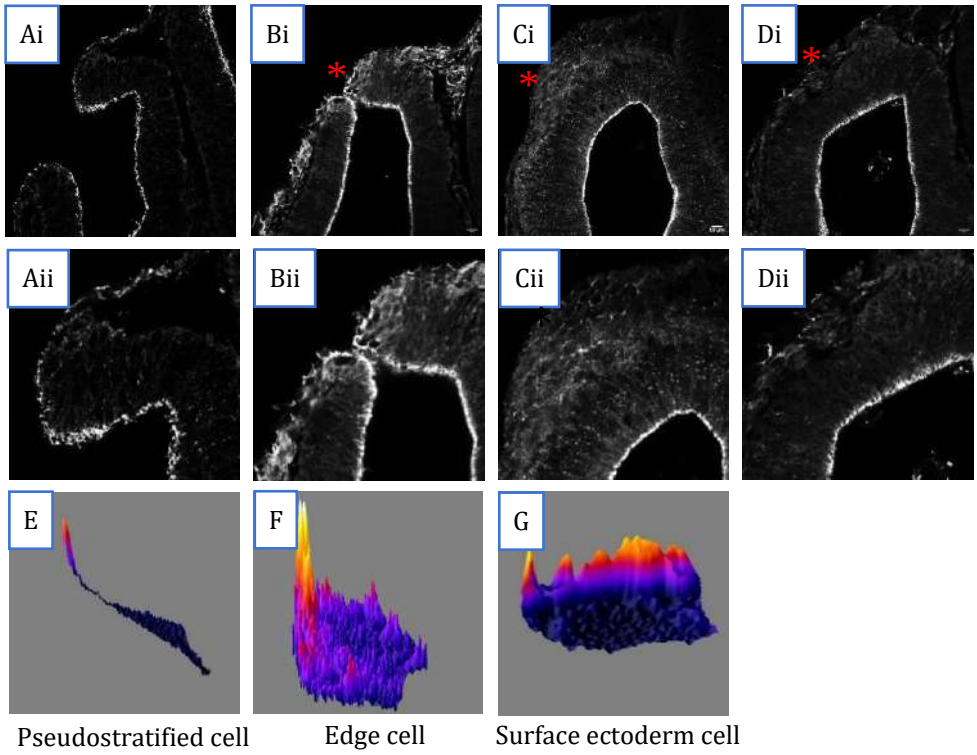

Fig 3.13: Expression of ZO1 during epithelial fusion. A(i,ii): ZO1 expresses apically marking the tight junctions between adjacent epithelial cells. Before fusion, the expression of ZO1 in the edge region of the otic vesicle is reduced as compared to the rest of the otic vesicle. **B(i,ii):** At the site of fusion(*) the expression of ZO1 in seen in the membrane ruffles mediating fusion. **C(i,ii):** A diffused expression seen at the site of fusion (*) during remodeling. **D(i,ii):** After segregation, expression of ZO1 becomes apical in the otic vesicle . **E:** Expression of ZO1 in a pseudostratified cell depicted in fire LUT. **F:** Expression of ZO1 in a round cell depicted in fire LUT. **G:** Expression of ZO1 in a surface ectoderm cell depicted in fire LUT. Scale bars are 10µm.

Next, we looked at the expression of gap junction component, Connexin43 (Cx43). Gap junctions help in the inter-cellular communication in tissue. The junctions have channel between two neighbouring cells that can transport small molecules and solutes. Mesenchymal cells are also known to make transient attachment with other mesenchymal cells they come in contact with, through gap junctions. Cx43 directly regulates the transcription of cadh2 thus aiding in the migration of mesenchymal cells in vivo (Kotini et al., 2018). Through all four stages of epithelial fusion, we saw a higher expression of Cx43 on the dorsal arm of the otic vesicle (Fig 3.14). This biased expression could be attributed to one of two reasons; the otic vesicle differentiation has begun, and the dorsal arm of the otic vesicle has already been committed to a particular fate and the other reason is the direct translation of the force experienced by the dorsal arm. As we saw earlier, the direction of zippering starts from the dorsal side of the otic

pore, hence it is possible that this force experienced by the dorsal arm increases the expression of Cx43. While there is almost a complete absence of Cx43 in the ventral arm in stage 1 (Fig 3.14 Ai,ii), we see expression when the edges have begun to fuse (Fig 3.14 Bi,ii). And this is only seen on the edge of the ventral arm. In stage 3, when

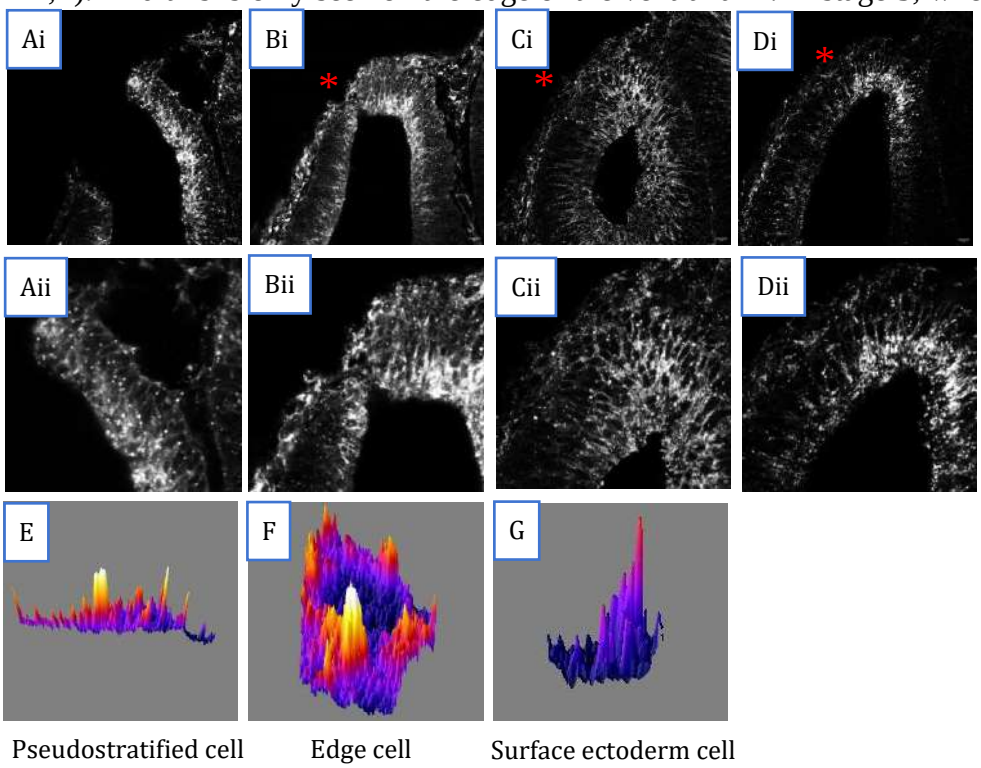

Fig 3.14: Expression of Cx43 during epithelial fusion. A(i,ii): Cx43, a gap junction marker, expresses only in the dorsal otic edge. And this pattern is seen before fusion. **B(i,ii):** At the site of fusion(*) the expression of Cx43 in seen in the membrane ruffles mediating fusion. And the expression of Cx43 is seen at the tip of the ventral otic edge. **C(i,ii):** The expression get restricted to the dorsal most region of the otic vesicle(*) during remodeling. **D(i,ii):** After segregation, expression of the protein continues to remain the same. **E:** Expression of Cx43 in a pseudostratified cell depicted in fire LUT. **F:** Expression of Cx43 in a round cell depicted in fire LUT. **G:** Expression of Cx43 in a surface ectoderm cell depicted in fire LUT. Scale bars are 10µm.

the remodelling has started (Fig 3.14 Ci,ii), we see expression at the site of fusion, on the round cells in the edge and in stage 4, the expression becomes biased to the dorsal region of the otic vesicle (Fig 3.14 Di,ii). On a cellular scale (Fig 3.14 E-G), Cx43 localisation is similar in all three cell types.

We next looked at the expression of polarity proteins; Rac1 and Ezrin. Rac1 is a small GTPase involved in actin regulation. The role of rac1 in epithelial fusion has been well studied in the case of neural tube closure (Rolo et al., 2016), body wall closure in D*rosophila* (Bahri et al., 2010) . Rac1 functions as a polarity marker in both epithelial and mesenchymal cells. It defines the apical domain in the epithelium and the front or

leading-edge polarity in mesenchymal cells. Rac1 localises apically in the surface ectoderm and the pseudostratified cells of the otic epithelium through all four stages of fusion (Fig 3.15). It localises in the membrane protrusions that establish the initial contact (Fig 3.15 Bi,ii). This could allude to its active role in their formation and stabilisation. The round cells also seem to have a diffused expression, however, due to the lack of a defined orientation of the cells, the localisation of rac1 seems to be random in the edge cells when remodelling is happening. This expression is also similar to the expression of rac1 transcripts in the pre-migratory neural crest cell population in chick neural tube as shown elsewhere. The pre-migratory neural crest cell population maybe considered analogous to the edge cells getting remodelled; although the neural crest

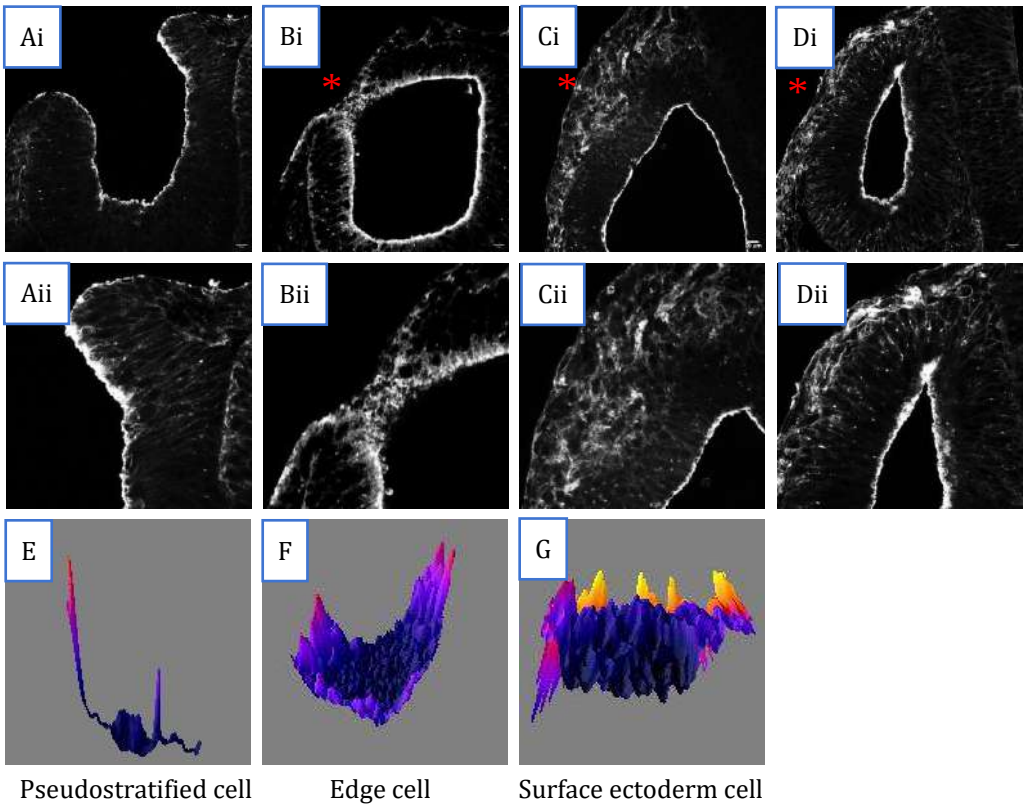

Fig 3.15: Expression of Rac1 during epithelial fusion. A(i,ii) Rac1, a small Rho GTPase involved in the regulation of membrane ruffles and an apical polarity marker has a reduced expression in the edge region before fusion **B(i,ii):** At the site of fusion(*) the expression Rac1 is seen in the membrane ruffles. **C(i,ii):** Rac1 also has a diffused expression in the edge cells when the edges are remodelling after fusion (*). **D(i,ii):** After segregation, the expression becomes apical in the otic vesicle. **E:** Expression of Rac1 in a pseudostratified cell depicted in fire LUT. **F:** Expression of Rac1 in a round cell depicted in fire LUT. **G:** Expression of Rac1 in a surface ectoderm cell depicted in fire LUT. Scale bars are 10µm.

cells undergo a partial epithelial to mesenchymal transition and then migrates away (Kee, Hwang, Sternberg, & Bronner-Fraser, 2007). They hypothesized a directional

function for rac1 in this case, where rac1 was implicated to orient the cells in the direction they are supposed to migrate away.

Ezrin(Ezr), belonging to a family of actin crosslinkers- the ERM, Ezrin, radixin, moesin, is involved in a myriad of functions- including the formation of microvilli, its dissociation in apoptotic cells, and in cell-cell and cell- substrate attachment (Gautreau, Poullet, Louvard, & Arpin, 1999). It has been shown to involved in connecting the plasma membrane to the actin cortex thereby regulating the mechanics and morphology of epithelial cells (Brückner, Pietuch, Nehls, Rother, & Janshoff, 2015).

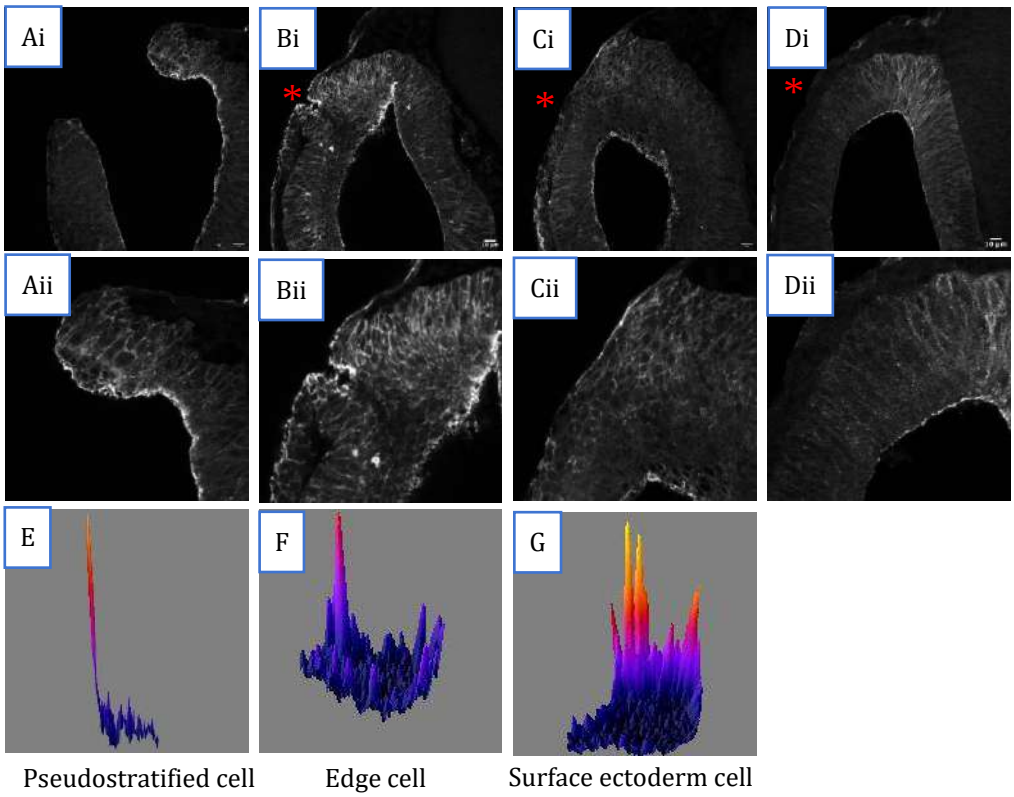

Fig 3.16: Expression of Ezr during epithelial fusion. A(i,ii) Ezr, an apical polarity marker, similar to Cx43 has a higher expression in the dorsal otic edge from before fusion **B(i,ii):** During the initiation of fusion (*) it is expressed in cells mediating fusion in both the otic edges. **C(i,ii):** The expression is diffused along the cells in the dorsal otic edge adjacent and not seen in the lateral edge during remodeling (*). **D(i,ii):** After segregation, the expression pattern continues to be the same. **E:** Expression of Ezr in a pseudostratified cell depicted in fire LUT. **F:** Expression of Ezr in a round cell depicted in fire LUT. **G:** Expression of Ezr in a surface ectoderm cell depicted in fire LUT. Scale bars are 10µm.

The expression profile of Ezr was similar to that Cx43. The expression was only seen on the edge of the dorsal arm and not the ventral arm or the rest of the otic vesicle (Fig 3.16). As hypothesised in the case of Cx43, even here, Ezr could play either a role in specification of the otic vesicle or be an effect of the difference in the force

experience by the dorsal side of the otic vesicle as compared to the ventral side. Ezr localised to the membrane protrusion emanating from both the dorsal and ventral edge of the otic vesicle in stage 2(Fig 3.16 Bi,ii). However, after the fusion, when the remodelling is initiated, we saw expression only on the dorsal side. This pattern continues even after the otic vesicle has segregated from the surface ectoderm. The localisation of Ezr a pseudostratified cell is limited to the apical domain of the cell (Fig 3.16 E), as is the case with a surface ectoderm cell (Fig 3.16 G). However, there is a more diffuse expression in the case of rounded cell (Fig 3.16 F).

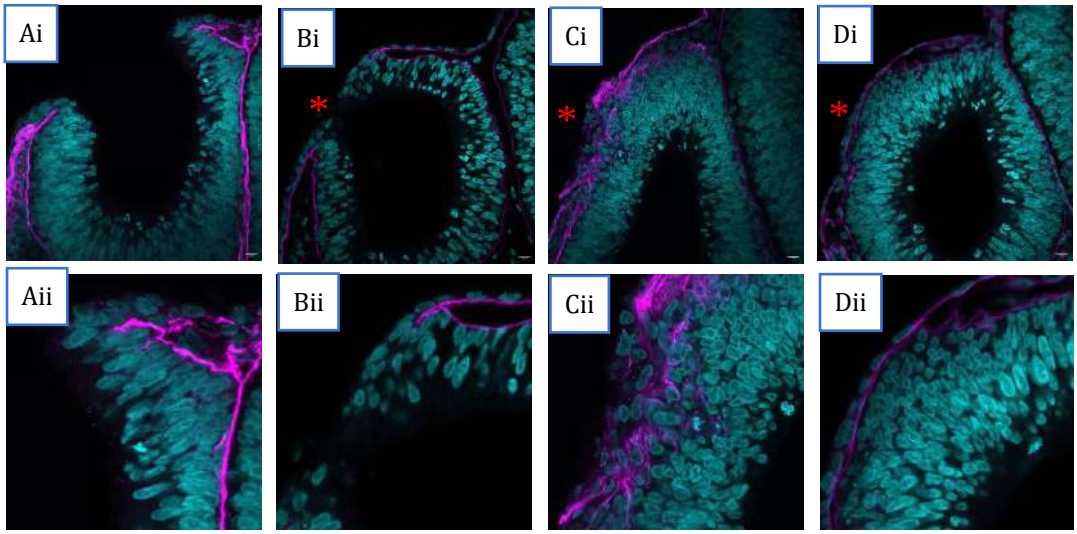

Fig 3.17: Expression of laminin during epithelial fusion. A(i,ii) Laminin, a component of extracellular matrix has a fibrillar contiguous expression before fusion **B(i,ii):** During the initiation of fusion (*) the expression pattern continues to be the same. **C(i,ii):** After the fusion of the otic edges, when the newly fused region is getting remodeled for the otic vesicle to segregate from the surface ectoderm, we see a diffused expression of laminin, with cells (identified with the presence of nucleus) between the surface ectoderm and the otic vesicle, waiting to be sorted into one of the two tissues (*). **D(i,ii):** Once the otic vesicle is segregated from the surface ectoderm and internalised, we see a fibrillar expression of laminin under the surface ectoderm and the otic vesicle. Scale bars are 10µm. Laminin DAPI

One of the key events in epithelial fusion is the reconfiguration of an intact epithelium to give rise to another intact epithelium. So far, we looked at junction components and polarity proteins. We next moved on to the Extra Cellular Matrix (ECM); the final step in achieving epithelial integrity. The ECM, marked by laminin expression here is intact until stage 2 when the edges are just beginning to fuse. The ECM degradation only begins when the remodelling starts. It is unclear if the round cells in the edge or adjacent mesenchyme secrete the ECM. It is possibly a combination of both the population, as both these cells are present in the interstitial space between the surface ectoderm and the otic vesicle (Fig 3.18). In stages 1 and 2 of epithelial fusion (Fig 3.17 A,B), laminin expression is fibrillar and continuous with the adjacent surface

ectoderm, on both the edges. In stage 3(Fig 3.17 C), we see a discontinuous and reduced expression of laminin. It is possible that the round cells in the edge are secreting ECM components and depending on their location, they either become a part of the otic vesicle or the surface ectoderm. After the remodelling and segregation, we see fibrillar expression of laminin in the basal side of the otic vesicle and the overlying surface ectoderm at stage 4 (Fig 3.17 D).

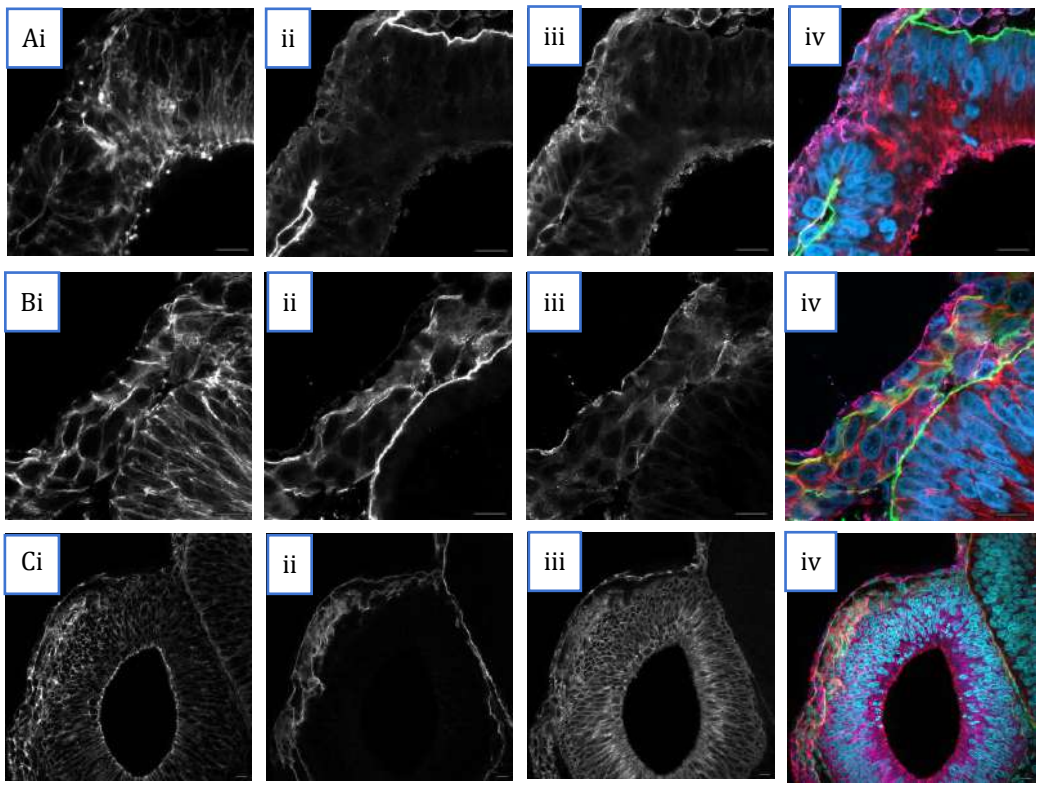

Fig 3.18: Cells in the interstitial space between the otic epithelium and the surface ectoderm. A: Super resolution image of HH17 chick embryo otic vesicle section showing fusion taking place. (i) F-actin (ii) Laminin (iii) Rac1 (iv) DAPI. **B:** Super resolution image of HH17 chick otic vesicle section at final stages of remodeling. (i) F-actin (ii) Laminin (iii) Rac1 (iv) DAPI. **C:** Confocal image of HH17 chick otic vesicle remodelling. (i) F-actin (ii) Laminin (iii) Cdh1 (iv) DAPI. Scale bars are 10µm.

Super resolution images of stage 2 stained for rac1 and laminin, show a clear localisation of rac1 in the membrane protrusions and absence of nuclei at the site of fusion, at this stage we see an intact ECM (Fig 3.18 Ai-iv). In Fig 3.18 Bi-iv, we see intact ECM in the basal side of the otic vesicle, and a discontinuous expression in the surface ectoderm cells. We also see some interstitial cells with non-polarized expression of rac1. And some of these cells seem to be secreting ECM components. The co-expression of rac1 with laminin, could help in the segregation of cells. We looked at the co-expression of Cdh1 with laminin at a similar stage of epithelial fusion

(Fig 3.18 Ci-iv). The otic vesicle is almost intact, and both Cdh1 and laminin are co-expressing at the interstitial space. It is possible that a combination of junction components, polarity proteins and ECM modellers are involved in the segregation of the otic vesicle from the surface ectoderm. The ECM remodelling components would include matrix degrading and secreting pathways.

We did SEM with HH17 chick embryos, by fracturing the surface ectoderm tissue close to the otic vesicle, to reveal the interstitial space (Fig 3.19). We saw the region that is being remodelled, in continuation with the surface ectoderm (Fig 3.19 Ai,ii) in the dorsal side of the otic pore. We also see the presence of mesenchymal cells adjacent to the otic vesicle under the surface ectoderm and around this region of remodelling (Fig 3.19 Bi,ii). It would be interesting to see the roles of the round cells and the mesenchymal cells in the remodel and segregation of the tissue. Optic fissure closure requires interaction with endothelial periocular mesenchymal cells for proper fusion to occur; and it was suggested that they had a role to play in the breakdown of ECM in the basal lamina (Bryan et al., 2020; Gage et al., 2005; Gestri et al., 2018; James et al., 2016).

In Fig.3.11B, we saw a steady increase in the round cells until remodelling and then a decrease. We wanted to know if the increase in number is due to an increase in mitosis in the region. We stained HH15 and HH17 otic vesicle sections for PH3 (Fig

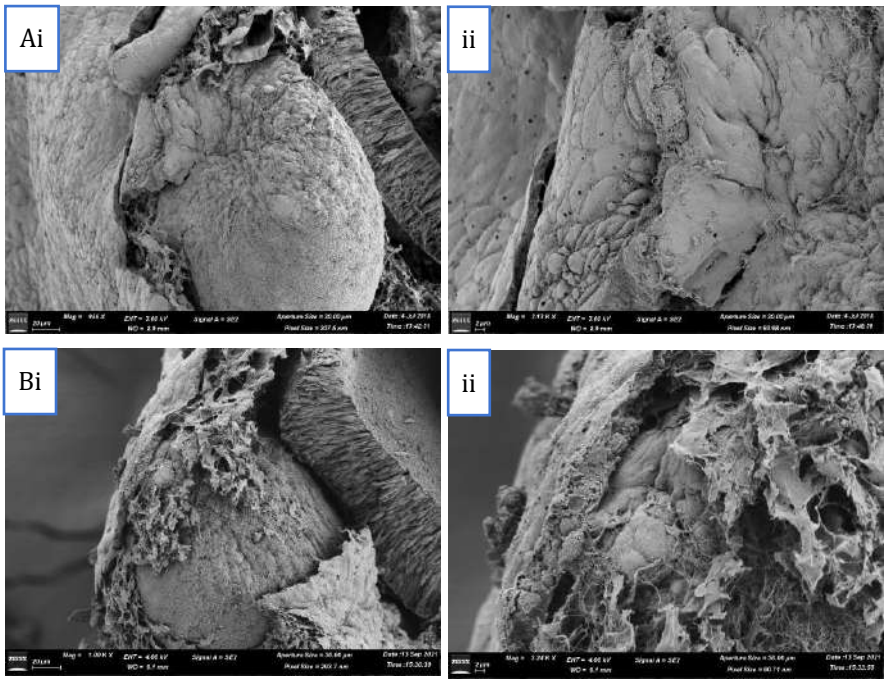

Fig 3.19: Cells that populate the border between the otic epithelium and the surface ectoderm. A, B: SEM of HH17 otic vesicle, cut and fractured very close to the otic pore.

3.20), a marker for dividing cells. We observed that the mitosis at the edge was not very different from the rest of the embryo section.

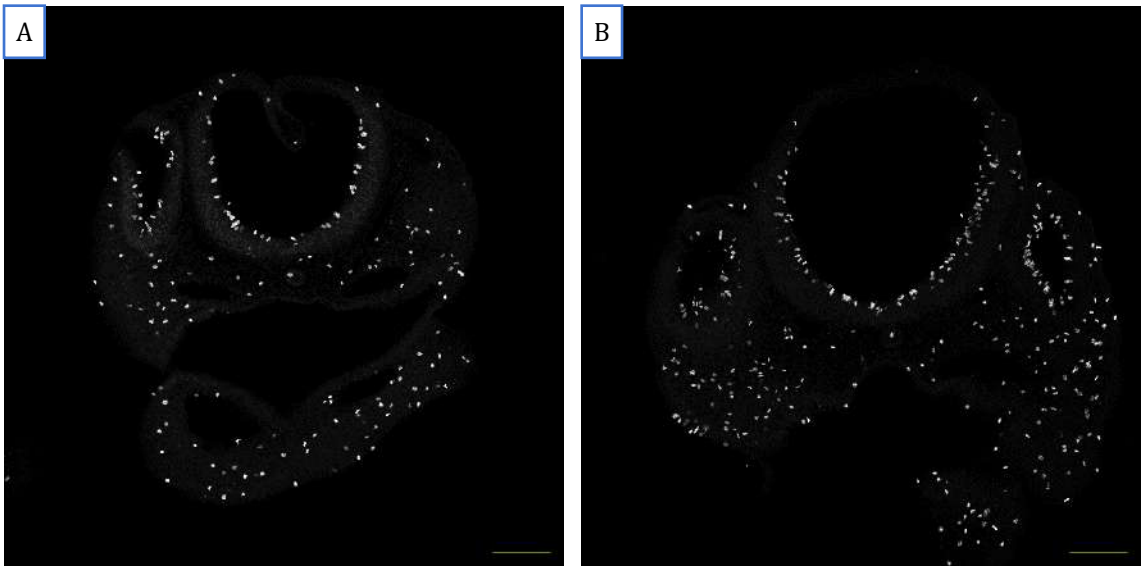

Fig 3.20: The edge cells are mitotic. A: A HH15 chick embryo section stained for PH3 to mark mitotic cells. **B:** A HH17 chick embryo section stained for PH3 to mark mitotic cells. Scale bars are 100µm.

So far, we saw the expression profile of multiple proteins across different stages of epithelial fusion in a tissue level and at a cellular level. We wanted to understand the localisation of Cdh1, ZO1, Cx43 and rac1 in round cells in the edge (OE) with respect to the pseudostratified and surface ectoderm cells. The statistic we chose for this was

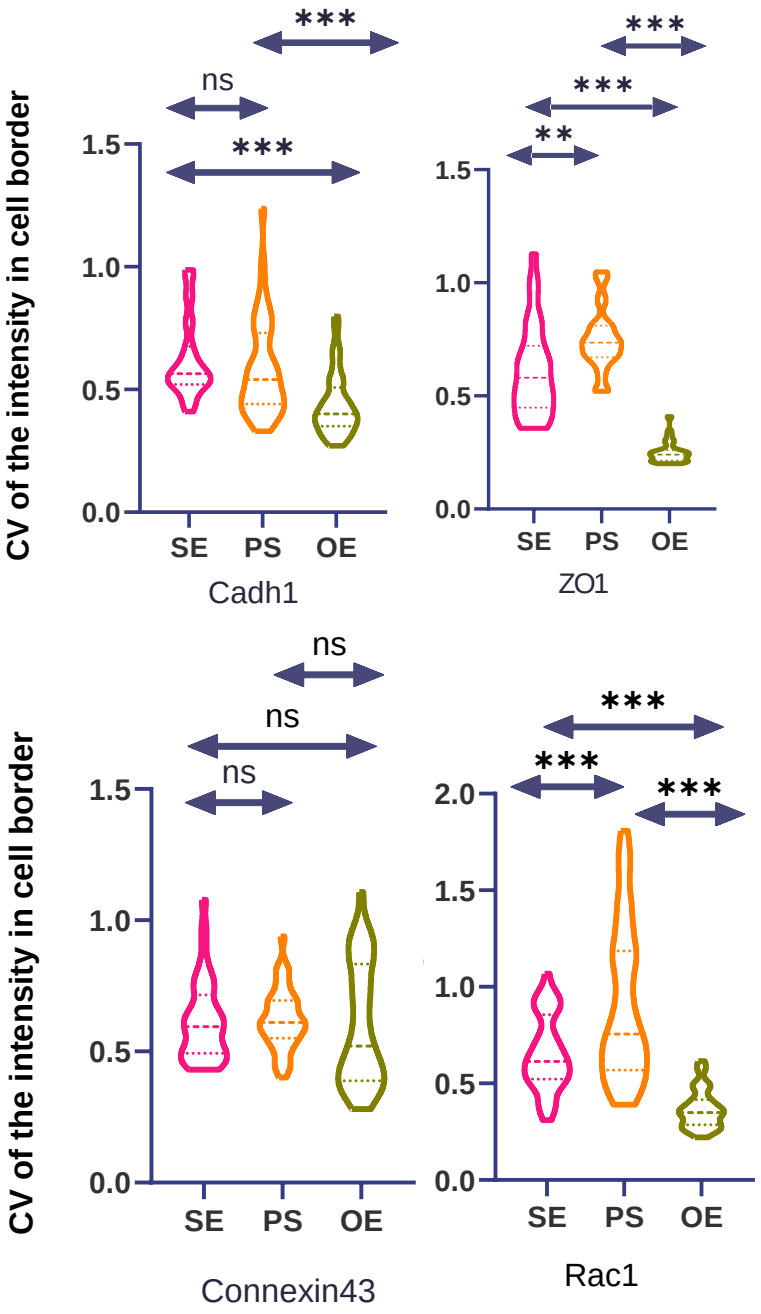

Fig 3.21 Cellular localisation of proteins. The covariance of intensity for any protein localised on 1um thick circumference of a cell translates to the deviation of each point from the mean. A higher covariance would mean a restricted localisation of the protein and a lower covariance would mean a diffused localisation along the cellular circumference. **A:** E-cadherin **B:** ZO1 **C:** Cx43 **D:**Rac1 SE- surface ectoderm, PS- Pseudostratified and OE- Otic edge

the Coefficient of Variation (CV) of intensity. Coefficient of variation is the ratio of mean to the standard deviation of a given data set. We measured the intensity of a given protein in the circumference of the cell, in a single plane. This was used as one data point, and the CV was calculated. CV is a measure of how restricted or diffused the

expression domain of the protein. Essentially, a cell with a polarized expression would have a very high CV and vice versa. We see the CV of Cdh1 localisation in round cell of the edge (Fig. 3.21 A) is significantly lower than pseudostratified cell or the surface ectoderm cell, as seen earlier in Fig 3.12F. There is no significant difference in the CV of Cdh1 between the SE and the PS. The profile for ZO1 was slightly different between SE and PS as well. We see a diffused expression of ZO1 in the round cells. Tight junctions localise to the apical surface of epithelial cells; the ratio of apical surface area to the total surface area of a pseudostratified cell is less than that of a surface ectoderm cell, hence the difference in their CV. Cx43 localisation in a cell, was similar in all three types and we did not see any significant differences. Rac1, an apical polarity protein, has a similar expression profile as that of ZO1 in the three cell types. The differences in the expression profile in cells imply an inherent difference in the phenotype of the cells.

3.3 Conclusions

In this chapter, we started with the characterisation of epithelial fusion in the otic vesicle. While multiple studies have done the morphological description using SEM micrographs and resin sections, a detailed molecular characterisation had not been performed. Previous studies on epithelial fusion in other systems, have alluded to a partial-EMT phenotype in cells undergoing fusion. Changes in cell shape, polarity, junctions and ECM remodelling have been some indicators for the phenotype. We closely looked for these in our system, the otic vesicle; we see similarities in cell behaviour. We looked at different aspects of fusion and how the cell behaviour changes. Based on our results, as described above, we think our system, is also exhibiting a partial EM phenotype. Thus, in the next chapter, we have looked at the transcriptomic state of these cells, as compared to their neighbours.

Chapter 4: Altered state of cells aid in epithelial fusion

4.1 Introduction

The otic vesicle closure happens in two phases; the first phase is mediated in a purse string model, where the otic pore size reduces from all sides as the otic vesicle is pushed within the mesenchyme of the head and the second phase involves a unidirectional epithelial fusion or zippering that is essential for the segregation of the otic vesicle from surface ectoderm and its complete internalisation. In chapter 3, we had defined the different stages of epithelial fusion. We had also characterised the three types of cells we see in the system; the pseudostratified cells of the otic vesicle, the squamous cells of the surface ectoderm and the round cells in the edge that seem to aid in the fusion.

Further characterisation of the localisation of junction components in round cells, suggested significant differences when compared to their epithelial neighbours. The pseudostratified cells and the squamous cells are epithelial in nature and have an apical expression of tight junction components and polarity proteins and lateral expression of adherens and gap junctions. However, the round cells in the edge had a different profile; the tight and adherens junction components and the polarity proteins were diffused, and these cells were not connected to their basement membrane. The round cells did not seem completely epithelial.

Partially epithelial cells have been described elsewhere: leading edge cells in *Drosophila* body wall closure (Bahri et al., 2010), collective migration during neural crest cell migration in *Xenopus* (Scarpa et al., 2015), collective epithelial cell migration in avian epiboly (Futterman, García, & Zamir, 2011), leading edge cells in wound healing (Arnoux et al., 2008; Shaw & Martin, 2016), and metastasis in cancers (Aiello et al., 2018; Cheung et al., 2013), all consist of cells that have a partial epithelial phenotype. A variety of cancer cells have been shown to exist in stable hybrid states, where they are neither completely epithelial nor completely mesenchymal. This hybrid state confers them the ability to metastasise without having to undergo complete epithelial to mesenchymal transition (EMT) at the site of the primary tumour and undergo mesenchymal to epithelial transition (MET) at the site of the secondary

tumour. It confers also, the ability to resist chemotherapeutic drugs (Grigore, Jolly, Jia, Farach-Carson, & Levine, 2016; Ocaña et al., 2012; W. L. Tam & Weinberg, 2013; Tsai, Donaher, Murphy, Chau, & Yang, 2012).

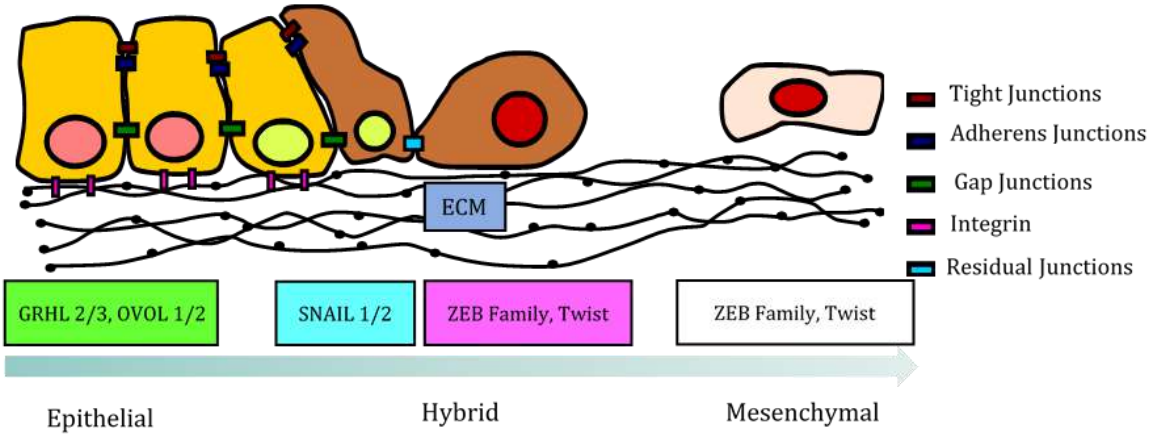

Fig 4.1: Intermediate cell states during Epithelial to Mesenchymal Transition (EMT). Adapted from Nieto.et al, 2016.

Bulk mRNA sequencing of these hybrid cell states in cancer cell lines have revealed the existence of a balanced transcript level of opposing transcription factors. These transcription factors include the grainy-head like, and OVO-like family that are involved in the differentiation and maintenance of epithelial nature of the cells and the Snail and ZEB family of transcription factors involved in the induction of EMT (Craene & Berx, 2013). The epithelial nature promoting factors have been shown to suppress tumour in cell lines and their expression was also reduced in transcriptomics of patient samples. On the contrary, the EMT inducers were found to have elevated levels in the transcriptomic signatures of patient samples and in cancer cell lines. Based on these data, one of the existing models for the partial EM phenotype is shown in Fig.4.1 (adapted from (M. Angela Nieto et al., 2016)). The model describes the transition of E to M as not a simple oscillation between a completely epithelial or mesenchymal state; rather a spectrum with intermediary phases. These intermediary phases imply that the cells could undergo a partial EMT program. In the Fig.4.1, EMT is considered a continuum, and cells can exist as epithelial (left end), mesenchymal (right end) or intermediate (in the middle). The transition from E to M is sequential; begins with loss of apical-basal polarity, cell-cell adhesive junctions, and starts acquiring a front-rear polarity and enhanced cell-matrix interaction. The transcription factors expressed in the cell, dictate the position of the cell in the EMT spectrum. The cells and nuclei are coloured accordingly, along the x-axis, to denote their position and differences on the

spectrum. The model suggests that, “Intermediate states probably reflect the delicate balance of transcriptional drivers and suppressors of EMT. This equilibrium is inevitably affected by epigenetic changes and by the main effectors in the cytoskeleton, the cellular machinery driving migration and invasion. This wider view of EMT offers a more dynamic interpretation of the fluidity and plasticity of this phenomenon” (M. Angela Nieto et al., 2016).

Studies have shown Grhl-2 and Grhl-3 to be involved in neural tube closure. Their mutants display neural tube defects of varying severity; depending on the kind of allelic mutation, the embryos display neural tube defects of varying causes. Grhl-2 mutants display epithelial fusion defects in other organs of the embryo, including the face, optic fissure, body wall closure and also have a perturbed heart and lung development at early embryonic stages. Microarray analysis of mutants confirmed a down regulation of genes involved in adhesion, two important proteins specifically, Cdh1 and claudin-4 (Pyrgaki, Liu, & Niswander, 2011).

4.2 Results

4.2.1 Partial Epithelial-Mesenchymal (E-M) phenotype in the otic edges.

Our experiments so far had hinted at the possibility of the round cells having a partial EM phenotype. To explore this avenue further, we performed Whole-mount In-Situ Hybridisation (WhISH) on HH17 embryos for the genes: *Grhl2, Grhl3, Snail2 and Zeb2*. As mentioned earlier, Grhl2 is an upstream regulator of Cdh1 and claudin4, Grhl3 deficiency was implicated in neural tube closure defects, and Snail2 and Zeb2 are known inducers of EMT and are markers of neural crest cells as well.

As shown in Fig.4.2, Grhl2 expression was restricted to the dorsal side of the otic vesicle and the surface ectoderm adjacent to the vesicle. The expression was also seen at the site of fusion. Unlike the neural tube, Grhl3 expression was not seen in the otic vesicle. Snail2 expression was not seen in the otic vesicle, although we saw the expression in the mesenchymal cells cushioning the otic vesicle. We saw a transient expression of Zeb2 only on the edges when they were fusing. The results of the WhISH also indicated an altered state of the edge cells. To obtain a broader picture of how the

edge cells are different from the adjacent surface ectoderm cells and the rest of the otic vesicle, we proceeded with bulk mRNA sequencing.

Fig. 4.3 shows the side view of HH17 chick embryo, showing the otic vesicle. We dissected out three tissue types, the otic edge marked in green, the rest of the otic vesicle marked in red and the adjacent surface ectoderm, marked in purple. Other details of the dissection are described in Chapter 2. We only chose HH17 staged embryos for this purpose, as we wanted to capture the transcriptomic signature of the round cells in the edge exclusively. As seen in chapter 3, the population of these round cells was the highest at the fusion and remodelling stages. We ensured proper embryonic stage before the dissection by counting the somites, approximately 32 somites and above, and also observing the size of the otic pore. Embryos that looked malformed or defective were not used to collect samples.

It is a standard protocol to check for the quality of the dissection, to ensure any level of contamination amongst the three types of samples. Due to the unavailability of enough concentration of total RNA from the samples for qPCR, we were unable to confirm the same. The RNA library preparation and sequencing were done by the NGS facility in NCBS and data obtained were taken for further processing in the usegalaxy.org webserver. We used their tutorials (Doyle, Phipson, Maksimovic, et al.,

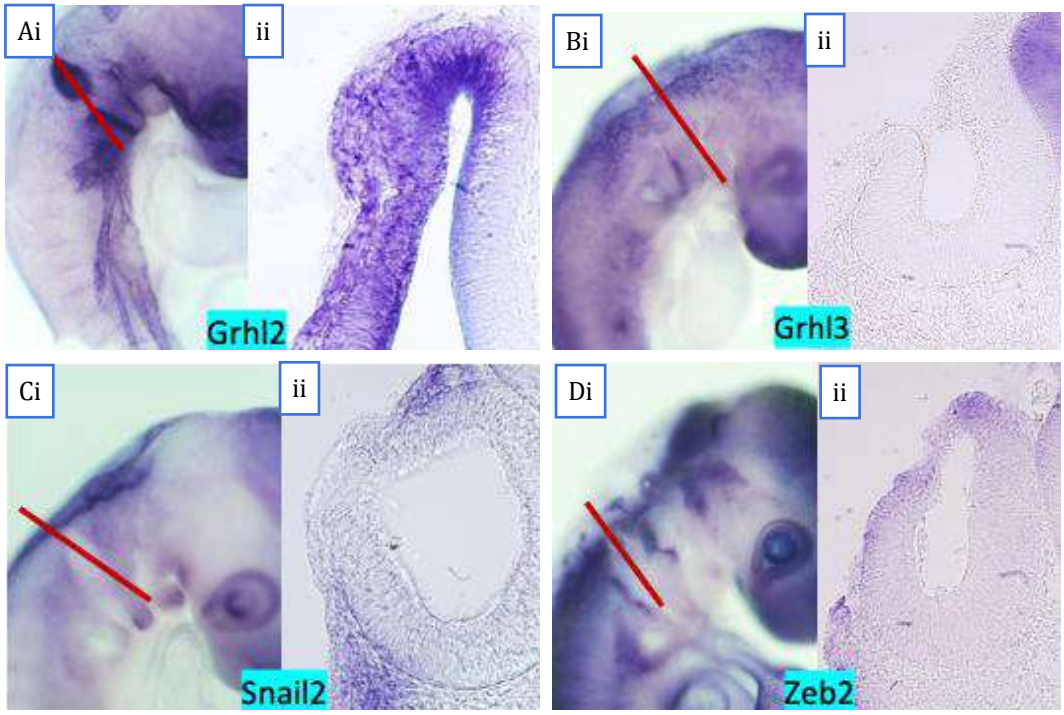

Fig 4.2: Whole mount in-situ hybridisation of genes involved in maintenance of hybrid EM. **A(i,ii):** Grhl-2 expresses at the site of fusion in a HH17 otic vesicle. **B(i,ii):** Grhl3 does not express in the HH17 otic vesicle. **C(i,ii):** Snail2 does not express in the HH17 otic vesicle, but expresses in the mesenchyme adjacent to the vesicle. **D(i,ii):** Zeb2 expresses only in the edge cells at the site of fusion in a HH17 otic vesicle.

2018; Doyle, Phipson, & Dashnow, 2018) to perform the Differential Gene Expression (DGE) analysis, as described in Chapter 2.

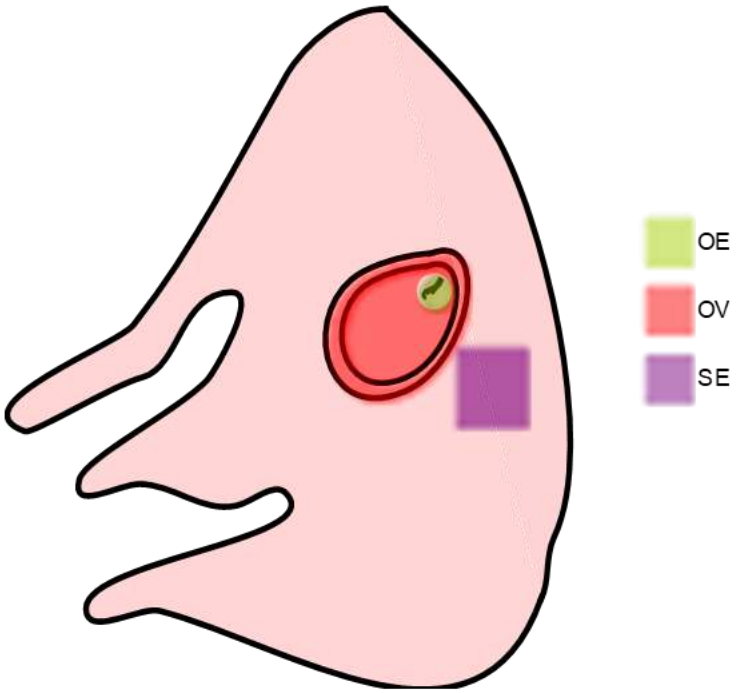

Fig. 4.3: Microdissection: Schematic of HH17 chick embryo, side view, marking the three kinds of tissue taken for bulk mRNA-sequencing. The green tissue marks the otic edge sample, the red tissue marks the otic vesicle without the edge region and the purple tissue marks the adjacent surface ectoderm.

4.2.2 Bulk mRNA sequencing and DGE analysis.

We started with assessing the quality of the reads and the sample. The reads were of very good quality. To test the level of possible cross-contamination in the samples, we performed a Multi-Dimensional Scaling (MDS) analysis. The distance

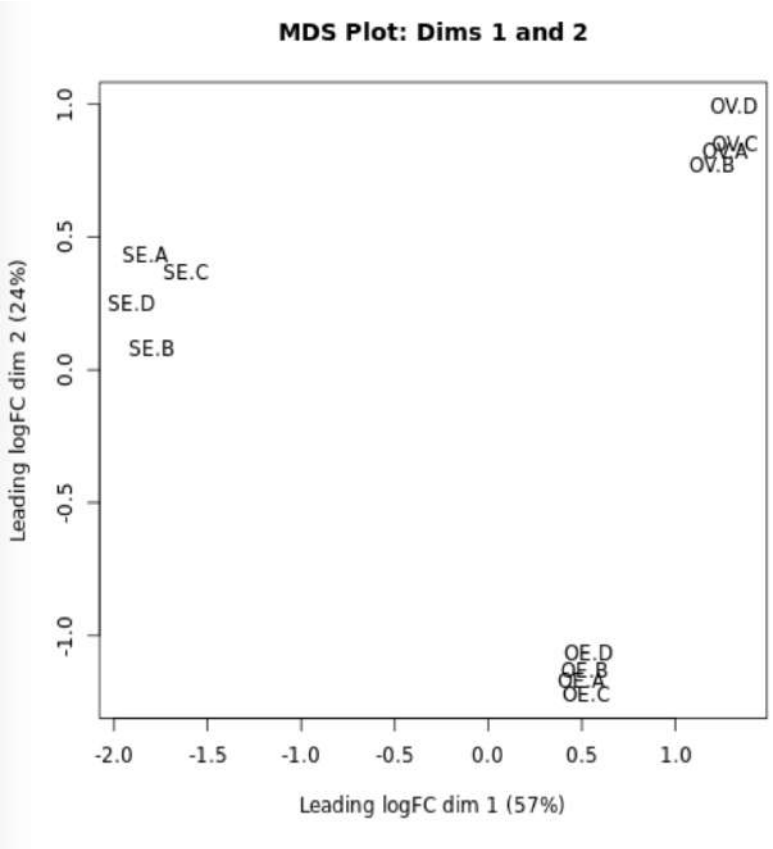

Fig. 4.4: MDS plot of samples used in RNA-seq analysis. We see quadruplicates of the three tissue types clustering together and the three tissue types well segregated from each other.

between data points in an MDS plot would indicate how dissimilar they are. As we see here in Fig 4.4, the three samples are very well segregated from each other, confirming the absence of any cross contamination during the dissection and processing of the samples. Between the samples, the quadruplicates clustered together, indicating confidence and robustness in the sampling of the tissue.

The DGE analysis was performed using the latest *Gallus gallus domesticus* reference (galGal6) genome available online. The server was only updated with galGal4, so we had uploaded the latest reference genome to the server and used it. The protocol we followed for the DGE is described in detail in Chapter 2, including the parameters we chose for the analysis. The chick reference genome, unfortunately is not as well annotated as the *Mus musculus* or *Homo sapiens*. For instance, the *Grhl* family or the *Zeb* family of genes were not annotated and hence we did not see them in the list

of genes present in the genome. Another major limitation was the unavailability of a chick database for further analysis (GoSeq) with the DGE data. Hence, we resorted to a reactome analysis and looked for plausible pathways from the DGE data. The reactome software, takes in the list of genes as provided by the user and maps the genes to existing pathways in the human database. The genes that do not possess the same human identifier is automatically converted to their equivalent and over-representation analysis is performed.

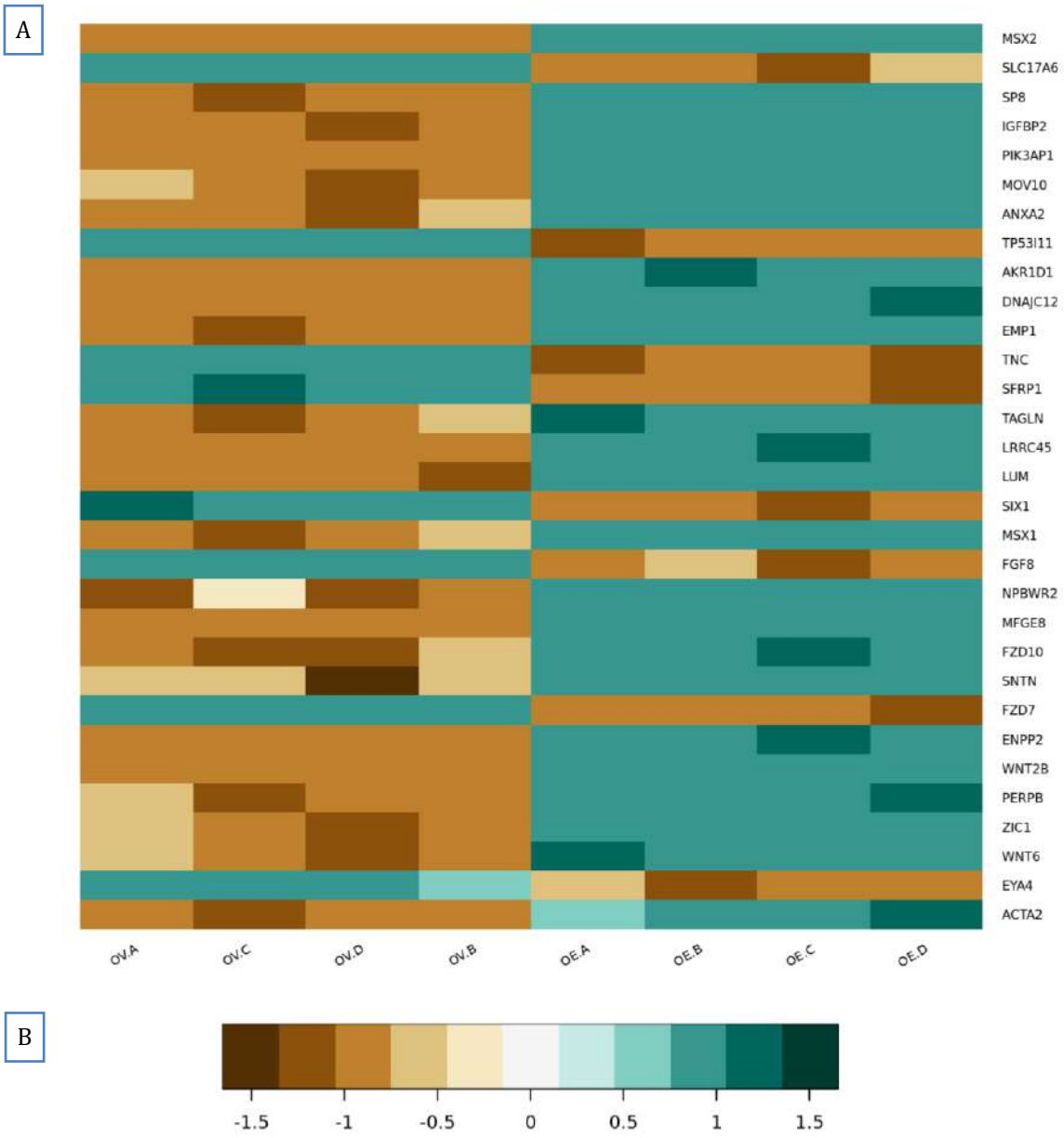

Fig. 4.5 Differential gene expression analysis OE vs OV.
A: A heat map showing the top-30 differentially expressed genes between the otic vesicle (OV) and the otic edge (OE). **B:** The key indicates the fold change in expression between the two tissue types.

For the DGE analysis, we performed two separate comparisons, otic edge versus otic vesicle and otic edge versus surface ectoderm. Fig 4.5 A, B shows the heat

map and key for fold change, for top 30 differentially expressed genes between otic vesicle and otic edge. Fig 4.6 shows parts of the reactome analysis; 417 out of 584 genes from the DGE list were found in the reactome, and 1246 pathways were hit by at least one of them. We saw an enrichment of certain pathways over others in the otic edge; gastrulation, neural plate border specification, anterior and posterior neural plate formation, kidney development, ECM formation and degradation, collagen

biosynthesis, modification and fibril assembly, integrin cell surface interaction and

Pathway name	Entities				Reactions	
	found	ratio	p-value	FDR*	found	ratio
Developmental Biology	140 / 1,732	0.111	5.07e-11	6.79e-08	375 / 910	0.061
Gastrulation	31 / 177	0.011	6.44e-10	4.31e-07	56 / 104	0.007
Specification of the neural plate border	11 / 24	0.002	2.70e-08	1.21e-05	13 / 15	0.001
Class B/2 (Secretin family receptors)	20 / 99	0.006	7.55e-08	2.53e-05	12 / 24	0.002
Kidney development	17 / 75	0.005	1.46e-07	3.93e-05	26 / 50	0.003
ECM proteoglycans	17 / 79	0.005	2.99e-07	6.67e-05	17 / 23	0.002
Formation of the posterior neural plate	8 / 14	8.96e-04	4.18e-07	7.02e-05	6 / 6	4.00e-04
Extracellular matrix organization	38 / 328	0.021	4.20e-07	7.02e-05	167 / 319	0.021
Formation of the ureteric bud	10 / 29	0.002	1.48e-06	2.20e-04	9 / 14	9.33e-04
Formation of the anterior neural plate	8 / 19	0.001	3.94e-06	5.27e-04	10 / 15	0.001
POU5F1 (OCT4), SOX2, NANOG activate genes related to proliferation	8 / 21	0.001	8.09e-06	9.55e-04	16 / 16	0.001
NCAM1 interactions	11 / 44	0.003	9.27e-06	9.55e-04	6 / 10	6.67e-04
Collagen chain trimerization	11 / 44	0.003	9.27e-06	9.55e-04	10 / 28	0.002
Transcriptional regulation of pluripotent stem cells	11 / 45	0.003	1.14e-05	0.001	31 / 35	0.002
Integrin cell surface interactions	15 / 86	0.006	1.73e-05	0.002	23 / 55	0.004
Signal Transduction	187 / 3,054	0.195	2.05e-05	0.002	842 / 2,572	0.171
Assembly of collagen fibrils and other multimeric structures	13 / 67	0.004	2.11e-05	0.002	19 / 26	0.002
Phospholipase C-mediated cascade; FGFR2	8 / 25	0.002	2.78e-05	0.002	3 / 3	2.00e-04
Degradation of the extracellular matrix	20 / 148	0.009	2.93e-05	0.002	43 / 105	0.007
Transcriptional regulation of granulopoiesis	13 / 70	0.004	3.30e-05	0.002	26 / 27	0.002
FGFR2 ligand binding and activation	8 / 26	0.002	3.65e-05	0.002	5 / 5	3.33e-04
Collagen formation	16 / 104	0.007	4.08e-05	0.002	52 / 77	0.005
FGFR2 mutant receptor activation	10 / 43	0.003	4.27e-05	0.002	18 / 18	0.001
Signaling by Receptor Tyrosine Kinases	52 / 634	0.041	6.78e-05	0.004	297 / 759	0.051

Table. 4.1: Pathway over-representation in OE vs OV using reactome: Top pathways over represented in the differential gene expression analysis.

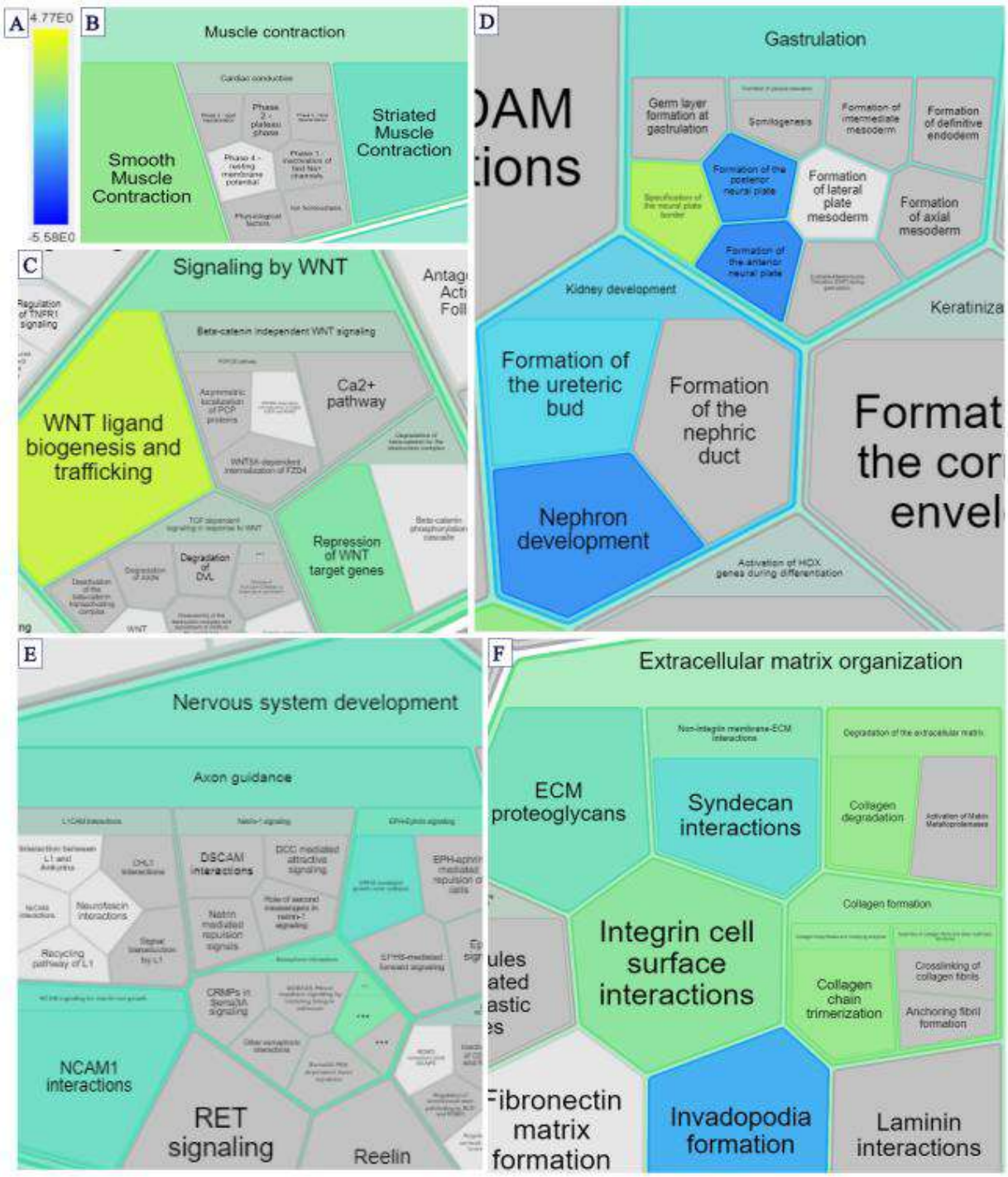

Fig. 4.6: Pathway over-representation in OE vs OV using reactome analysis: Top pathways over represented in the differential gene expression analysis. The list version of the figure is in Table 4.1. **A:** Colour key for the reactome. The yellow to blue colour indicates the pathways with high to low over representation. **B:** Muscle contraction pathway. **C:** Genes involved in WNT signalling **D:** Pathways active principally during embryogenesis. **E:** Genes involved in nervous system development and **F:** Genes involved in ECM organization.

FGFR2 and RTK signalling, among others. The over-represented pathways have been listed in Table 4.1.

Fig 4.7 A, B shows the heat map depicting fold change of top 30 differentially expressed genes between surface ectoderm and otic edge. Fig 4.8 shows parts of the reactome analysis, 418 out of 613 genes from the DGE list were mapped to reactome pathways, and 1242 pathways were hit by at least one of them. An enrichment of pathways in gastrulation, neural plate border specification, anterior and posterior neural plate formation, kidney development, WNT ligand biogenesis and trafficking, ECM

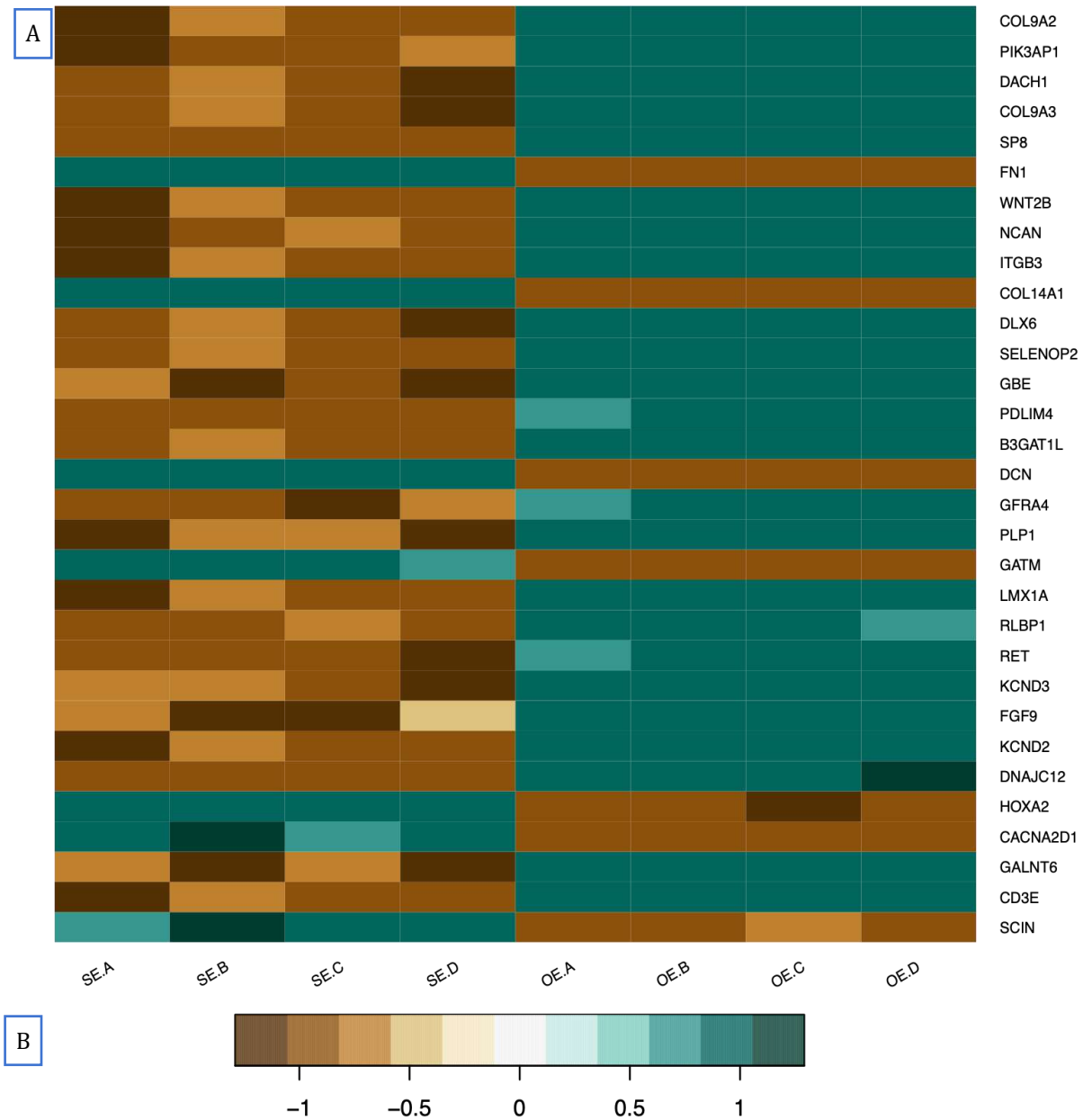

Fig. 4.7: Differential gene expression analysis OE vs SE.
A: A heat map showing the top-30 differentially expressed genes between the surface ectoderm (SE) and the otic edge (OE). **B:** The key indicates the fold change in expression between the two tissue types.

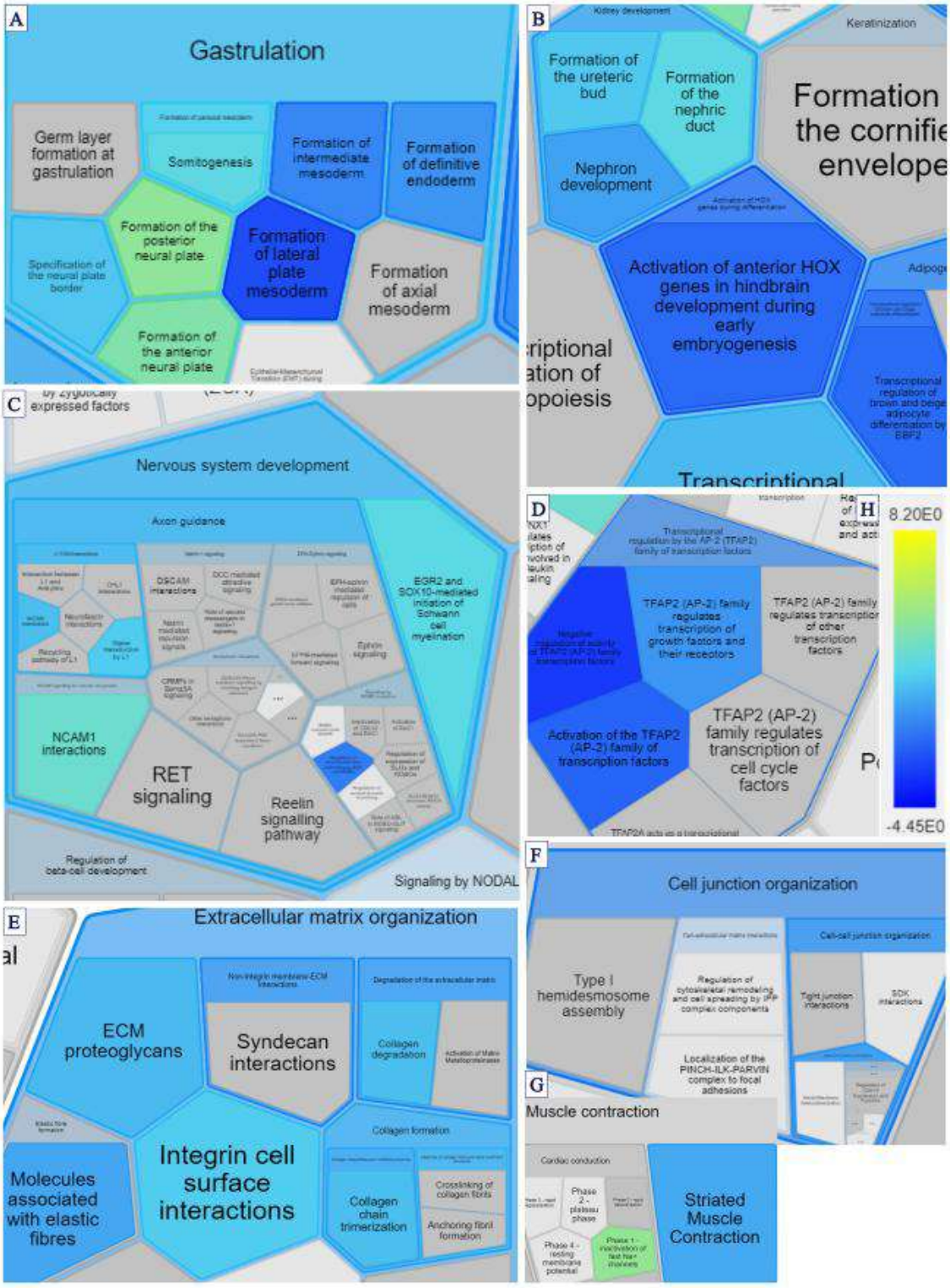

Fig. 4.8: Pathway over-representation in OE vs SE using reactome analysis: Top pathways over represented in the differential gene expression analysis. The list version of the figure is in Table 4.1. **A:** Genes expressed during gastrulation, B**:** Genes expressed during embryogenesis **C:** Genes involved in nervous system development **D:** Genes involved in active transcription E: Genes involved in ECM organization **F:** Genes involved in cell junction organization and **G:** Genes involved **H:** Colour key for the reactome. The yellow to blue colour indicates the pathways with high to low over representation.

organisation and degradation, collagen formation and fibril assembly, ERBB2 and

RUNX2 signalling, among others. The over-represented pathways have been listed in

Pathway name	Entities				Reactions	
	found	ratio	p-value	FDR*	found	ratio
Gastrulation	38 / 177	0.011	5.88e-14	7.73e-11	74 / 104	0.007
Developmental Biology	150 / 1,732	0.111	9.48e-13	6.22e-10	499 / 910	0.061
Specification of the neural plate border	12 / 24	0.002	3.72e-09	1.62e-06	15 / 15	0.001
Kidney development	18 / 75	0.005	4.82e-08	1.58e-05	33 / 50	0.003
Formation of the posterior neural plate	8 / 14	8.96e-04	5.55e-07	1.46e-04	6 / 6	4.00e-04
Class B/2 (Secretin family receptors)	17 / 99	0.006	9.70e-06	0.002	10 / 24	0.002
Transcriptional Regulation by MECP2	17 / 100	0.006	1.10e-05	0.002	22 / 77	0.005
WNT ligand biogenesis and trafficking	9 / 28	0.002	1.15e-05	0.002	8 / 12	8.00e-04
Extracellular matrix organization	35 / 328	0.021	1.55e-05	0.002	159 / 319	0.021
Degradation of the extracellular matrix	21 / 148	0.009	1.60e-05	0.002	37 / 105	0.007
Assembly of collagen fibrils and other multimeric structures	13 / 67	0.004	3.12e-05	0.004	11 / 26	0.002
ECM proteoglycans	14 / 79	0.005	4.14e-05	0.004	13 / 23	0.002
Formation of the anterior neural plate	7 / 19	0.001	4.64e-05	0.004	9 / 15	0.001
Formation of intermediate mesoderm	6 / 13	8.32e-04	4.77e-05	0.004	4 / 5	3.33e-04
Transcriptional regulation of testis differentiation	7 / 21	0.001	8.62e-05	0.007	13 / 18	0.001
Formation of the ureteric bud	8 / 29	0.002	1.01e-04	0.008	11 / 14	9.33e-04
Nephron development	7 / 23	0.001	1.50e-04	0.011	7 / 17	0.001
Formation of the nephric duct	8 / 31	0.002	1.58e-04	0.011	15 / 19	0.001
MECP2 regulates neuronal receptors and channels	8 / 32	0.002	1.95e-04	0.013	8 / 26	0.002
Collagen formation	15 / 104	0.007	2.11e-04	0.014	39 / 77	0.005
RUNX2 regulates genes involved in differentiation of myeloid cells	4 / 6	3.84e-04	2.27e-04	0.014	2 / 2	1.33e-04
ERBB2 Activates PTK6 Signaling	6 / 18	0.001	2.75e-04	0.016	2 / 2	1.33e-04
ERBB2 Regulates Cell Motility	6 / 19	0.001	3.65e-04	0.02	2 / 2	1.33e-04
TFAP2 (AP-2) family regulates transcription of growth factors and their receptors	6 / 21	0.001	6.14e-04	0.032	16 / 18	0.001

Table. 4.2: Pathway over-representation in OE vs SE: Top pathways over represented in the differential gene expression analysis.

Table 4.2.

We see a significant overlap in the pathways that were found enriched in the edge region, most of them corresponding to ECM remodelling, and early embryonic development. Besides this we saw an over-representation of particular signalling pathways that might have a role in cellular polarity, migration, differentiation and mechano-transduction. We performed WhISH to confirm the enrichment analysis.

4.2.3 Validating the sequencing data.

We chose a set of 10 genes from both the top 30 DGE data, based on the following criteria,

1. They were part of the reactome pathways.
2. Their count in the sequencing data (from feature counts) was at least 2000, and highest in the edge, as compared to the surface ectoderm and the otic vesicle.
3. They were found to be expressed in the pre-migratory neural crest cell population.
4. Their mutations in other models have shown inner ear defects.

Most of the genes were common to both the lists. We designed the primers for PCR of the cDNA library of the whole embryo, and made probes, as described in Chapter 2.

We imaged the chick embryos, as whole mounts and then processed them for cryo-sectioning. The sections are shown in Fig. 4.9 for nine genes. For each gene, there is a representative section for when the edges are apart, when the edges are remodelling and when the otic vesicle has segregated from the surface ectoderm.

BMP and activin membrane-bound inhibitor (BAMBI), has been shown to regulate a variety of processes, including cell proliferation, differentiation, metabolism and inflammatory responses (Chen et al., 2024). It has also been implicated in the maintenance of a feedback loop in BMP signalling (Grotewold, Plum, Dildrop, Peters, & Rüther, 2001). Here, we saw BAMBI expression only on the edges, and the site of remodelling. The expression was lost after segregation of the tissue layers.

DACH1, homolog of *Drosophila* Dachshund (Dach), has been shown to repress BMP mediated transcriptional control in chick limb development; regulating the formation of the apical ectodermal ridge (Kida, Maeda, Shiraishi, Suzuki, & Ogura, 2004). A recent study in *Xenopus* suggested a role for Dach1 in NC migration (Y.-K.

Kim, Lee, Ismail, Kim, & Lee, 2020). Here, we saw a biased expression of Dach1. When the edges were apart, we saw Dach1 expression only on the dorsal arm. During remodelling, we see an extended expression on the ventral side as well, and after segregation we see a dorsal expression.

DLX5, homolog of *Drosophila* Distal-less gene, has a role to play in the specification of limb territories of the lateral plate (Ferrari, Harrington, Dealy, & Kosher, 1999) in chick. DLX5 has also been shown to be involved in the specification of the neural plate border; it represses neural properties of cells, giving rise to border cells that express neural fold markers MSX1 and BMP4 along with PPR marker SIX4. However, it is not a sufficient factor to fully specify the neural plate border region (McLarren, Litsiou, & Streit, 2003). We see expression of DLX5 specifically in the edge region when they are apart, the expression is very high at the site of remodelling and continues after segregation also. DLX5 and 6 are important in the formation of the inner ear. The dorsal region of the otic vesicle gives rise to the semi-circular canals, utricles, saccule and the endolymphatic duct, through the restriction of Pax2 and activation of Gbx2 and BMP4 in the mammalian system. The extended expression of DLX5 could be attributed to the inner ear fate specification (Robledo & Lufkin, 2006).

EphA4 has been well characterised for its role in MET during somitogenesis, through cytoskeletal regulation. In a study in chick, EphA4 was expressed in the segmental plate where cells were undergoing cell shape changes, as part of their epithelialization. They also showed that in the absence of EphA4 expression, cells had an irregular morphology, and failed to form somites. The study identified the midline ectoderm and the ectoderm covering the somites as sources of EphA4 (Schmidt, Christ, Maden, Brand-Saberi, & Patel, 2001). Here, we saw a very transient expression of EphA4 at the site of remodelling, and not before or after fusion. It is possible that EphA4 has a similar role to play during otic vesicle closure as well.

ITGB3, Integrin-β3, belongs to a class of cell surface receptors that link cells to other cells through counter receptors or link cells to ECM through ligands. It has been studied extensively for its role in tumorigenesis in multiple ways, including the reprogramming of metabolism, maintenance of tumour stemness, promoting angiogenesis and facilitating EMT (Fuentes et al., 2020; Zhu et al., 2019). Here we saw expression of ITGB3 in both the edges when they were apart, and the expression

Fig 4.9: Validation of bulk mRNA sequencing by WhISH. Embryos probed for expression of different genes were cryo-sectioned and imaged. The three panels per gene represent (i) when the otic edges are apart (ii) when the otic edges are fusing (iii) otic closure is complete. Gene names are written next to the panel. At least 3 or 4 embryos were confirmed per gene. All the gene names are mentioned next to the panel.

continued at the site of fusion during remodelling and even after segregation. It is

possible that ITGB3 has a role to play in the specification of the inner ear.

MSX1 has been shown to play an active role in the formation of the neural crest cells through the induction of the other neural crest specifier genes; along with WNT and FGF signalling (Monsoro-Burq et al., 2005). It also induces apoptosis of prospective neural crest cells that do not express Slug, in *Xenopus* and this equilibrium the authors suggest is required for generating sharp boundaries (Tríbulo, Aybar, Sánchez, & Mayor, 2004). We saw a biased expression of MSX1 on the dorsal arm, and very high expression specifically at the site of fusion and remodelling. After the segregation, the expression level reduces. We also observed apoptosis at the site of fusion, it is possible, they have a pro-apoptotic role here as well.

Rac3 is a member of the Rho family of small GTPases that include Rac, Cdc42 and Rho. They are known regulators of cytoskeletal dynamics. In vitro culture studies have shown their role in the maintenance and stabilization of epithelial structures through cadherin mediated cell adhesion (Braga, 2002; Fukata & Kaibuchi, 2001; Schöck & Perrimon, 2002). Rac1 has also been shown to have an epithelializing role during somitogenesis. The levels of Rac1 during this process is also critical, as both the increased levels or inhibition of Rac1 in cells failed to get epithelialized (Nakaya, Kuroda, Katagiri, Kaibuchi, & Takahashi, 2004). We saw Rac3 expression in both the edges when they were just meeting, and at the site of fusion and remodelling we saw very high expression, and after segregation, there was no Rac3 expression in the otic vesicle, but seen in the overlying ectoderm.

SP8 is a transcription factor, expressed in limb ectoderm and AER during limb development. Mutations in the gene lead to severe limb truncations. Along with SP6, it has been shown crucial in mediating Wnt-βcatenin and BMP signalling in the development of the limb (Haro et al., 2014). Here, we saw expression of SP8 specifically in the edge and at the site fusion and remodelling. However, SP8 expression was only seen in the overlying ectoderm after the segregation.

Wnt 3A, expressed in the primitive streak, is suggested to have a chemotactic effect on the migration of certain population of cells. In-vitro chemotaxis assay for the effects of Wnt 3A, alluded to a similar observation; cardiac progenitors were repelled by Wnt3A, independent of FGF signalling, and without interfering with the migration of other mesodermal cells (Yue, Wagstaff, Yang, Weijer, & Münsterberg, 2008). It is involved in the formation of the chick AER through the β-catenin pathway (Narita, Nishimatsu, Wada, & Nohno, 2007). Here, we saw a biased expression of Wnt3A on

the dorsal arm edge, and at the site of fusion and remodelling. After the segregation, Wnt3A expression persisted in the otic vesicle, suggesting a possible role in the differentiation of the otic vesicle.

So far, all the candidate genes we had picked for the validation of dissection and analysis of our RNA seq results showed very specific spatial-temporal expression pattern. Though putative roles can be assigned for differentially expressed genes, their exact role in otic vesicle closure can only be studied upon perturbation. We performed a CRISPR/Cas9 mediated genetic perturbation of selected genes to study their role in otic vesicle closure.

4.2.4 Genetic perturbation of candid genes

We had shown the spatial and temporal expression of multiple genes involved in different pathways. Some of them belong to signalling pathways, including Wnt and BMP signalling, that have known chemical inhibitors and some of them are transcription factors, studied in other developmental pathways. We chose to perform genetic perturbation of transcription factors; specifically, the ones that were not actively transcribed in the otic vesicle. As we wanted to look for regulators of epithelial fusion, and not interfere with the development and specification of the inner ear. Thus, we chose transcription factors that were present in the surface ectoderm and the otic edges, but not the otic vesicle. We also looked for transcription factors that have mutant animal models with inner ear defects. Based on these criteria, we chose *grhl2* and *sp8* for our CRISPR-Cas9 mediated knock down studies.

Grhl2 is an upstream regulator of Cdh1 and has a zebrafish mutant that does not show any hair cell related defects, but exhibits enlarged otic vesicle, small or lack of otoliths, and malformed semi-circular canals. These mutants are insensitive to sound stimulation and display an imbalanced swimming motion. They showed an absence or reduced expression of *claudinb* and *epcam*. TEM studies showed an abnormal morphology of apical junctions in otic epithelium in mutant embryos, which could be rescued upon the injection of *cldnb* and *epcam* mRNA (Han et al., 2011).

SP8 is an EMT inducing transcription factor and has a *Xenopus laevis* mutant that showed otic dys-morphogenesis; including the absence of an endolymphatic duct, abnormal semi-circular canals, swelling of the membranous labyrinth, epithelial dilation and abnormal sensory organs. This phenotype, as they describe, was similar to

mouse mutants for *Fgf3, Mafb, Gbx2* (Choo et al., 2006; Hatch, Noyes, Wang, Wright, & Mansour, 2007; Lin, Cantos, Patente, & Wu, 2005). They attribute the phenotype to an enlarged otic vesicle due to the absence of the endolymphatic duct. Their study also showed that MSX1 was a downstream target of SP8. The *grhl2* zebrafish mutants also had a similar phenotype, as they mention in their discussions; but the authors think the mode of action of either of the genes are different and are likely to be mutually exclusive or independent of each other. While Grhl2 is involved in the regulation of epithelial integrity, SP8 might have a more severe mode of action and the epithelial defects described in the study are probably just a subset of the defects. They also observed an overlap of SP8 expression on the dorsal region where the Wnt/β catenin signalling is active. Perturbation of the signalling affected SP8 (Chung, Medina-Ruiz, & Harland, 2014).

Figs. 4.10- 4.13 show otic vesicle stained for Cdh1 and the nucleus (DAPI). Five stages of fusion have been shown here: A. when the edges are apart, B. when the edges are just meeting, C. when the edges have met and are fusing, D. when remodelling is happening and E. when segregation has happening. The bottom panel (ii) are the closing regions magnified from their corresponding top panel (i).

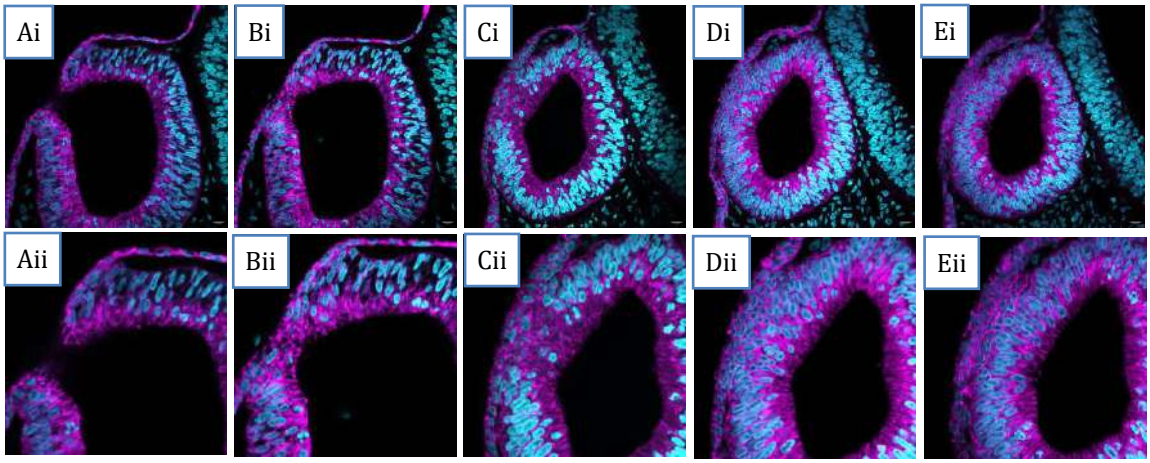

Fig 4.10: Expression of Cdh1 and DAPI in otic vesicle, un-electroporated embryos. A (i,ii): The otic edges are apart. (Aii) is a magnified view of (Ai). Cdh1 expression levels are uniform in the surface ectoderm and in the pseudostratified cells. **B(i,ii):** The otic edges are just meeting, as mediated by membrane protrusions expressing e-cadherin and a lack of DAPI staining. **C(i,ii):** The otic edges are fusing and we see some nuclei at the site of fusion. **D(i,ii):** The fusion has happened and the epithelial tissues have to segregate from each other. Cdh1 expression is seen throughout and is uniform. **E(i,ii):** The otic vesicle has segregated from the surface ectoderm. The expression of Cdh1 is uniform throughout the tissue. Cdh1, DAPI. Scale bars are 10µm.

In Fig. 4.10, we see Cdh1 expression in the otic edge, otic vesicle and the surface ectoderm. The expression pattern in the cells has been described in Chapter 3. Fig 4.11

(A-E) has sections from embryos that were electroporated with the control gRNA. There was some debris found within the lumen of the otic vesicle, which was observed in other electroporated embryos as well. But we notice that the expression pattern of Cdh1 was similar to the wild type embryos in the otic edge cells, the pseudostratified otic vesicle cells and the surface ectoderm cells. We also noticed that there were rounded edge cells at the site of fusion, and remodelling. We marked the shape of the cells in the sections, some of them were GFP positive, and measured their sphericity index (Fig 4.14), which was comparable to the wild types as described in Chapter 3.

Fig 4.12(A-E) has sections from embryos that were electroporated with the

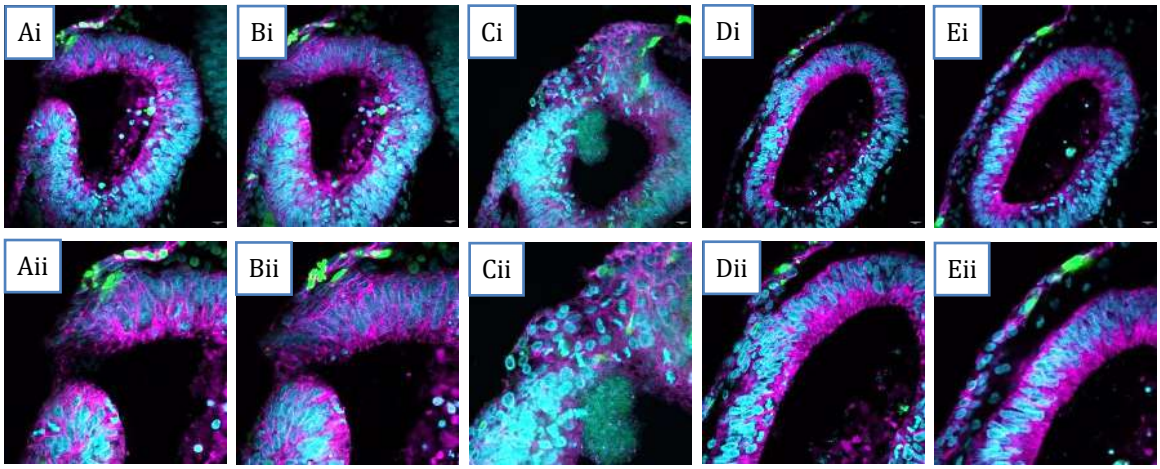

Fig 4.11: Expression of Cdh1 and DAPI in otic vesicle of control-gRNA electroporated embryos. A (i,ii): The otic edges are apart. (ii) is a magnified view of (i). Cdh1 expression levels are uniform in the surface ectoderm and in the pseudostratified cells. **B(i,ii):** The otic edges are just meeting, as mediated by membrane protrusions expressing Cdh1 and a lack of DAPI staining. **C(i,ii):** The otic edges are fusing and we see some nuclei at the site of fusion. **D(i,ii):** The fusion has happened and the epithelial tissues have to segregate from each other. Cdh1 expression is seen throughout and is uniform. **E(i,ii):** The otic vesicle has segregated from the surface ectoderm. The expression of Cdh1 is uniform throughout the tissue. Cdh1, DAPI, gRNA-GFP. Scale bars are 10µm.

grhl2 gRNA. Even here, we saw some cell debris found within the lumen of the otic vesicle. The expression of Cdh1 looked different in the edges, and at the site of fusion in all five stages of epithelial fusion. Accumulation of Cdh1 was observed (as indicated by the red asterisk in the figure) at the site of fusion. Although there was no dearth of Cdh1, the fusion did not occur completely as usually seen in the wild type embryos (Fig 4.10 D). We also observed that the surface ectoderm adjacent to the otic edge did not have Cdh1 expression (as indicated by the yellow asterisk). At the site of fusion and

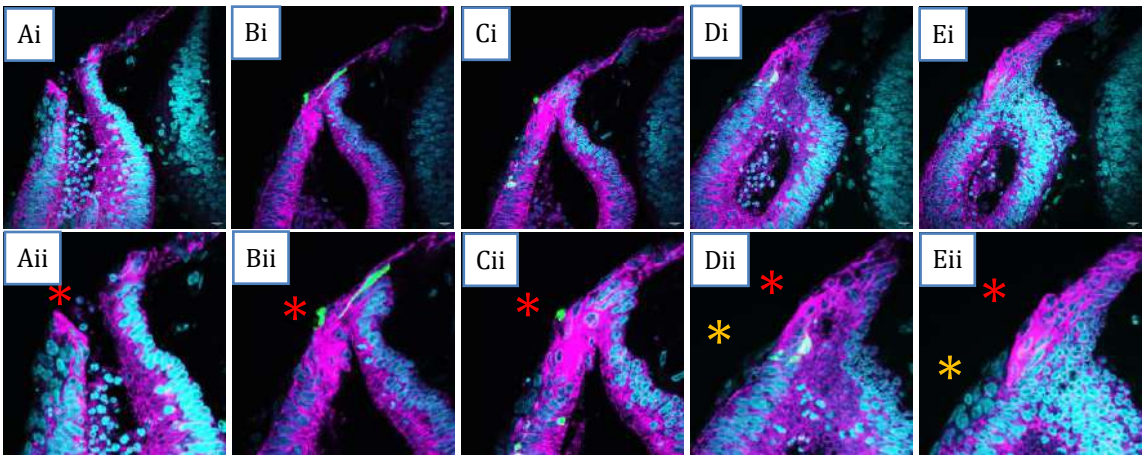

Fig 4.12: Expression of Cdh1 and DAPI in otic vesicle of Grhl2-gRNA electroporated embryos. A (i,ii): The otic edges are apart. (ii) is a magnified view of (i) Cdh1 expression is higher in some parts of the tissue, as indicated by the red asterisk. **B (i, ii):** The otic edges are just meeting, and Cdh1 expression is much higher in the ventral edge. Some of the dorsal edge cells are pseudostratified (the GFP filled cell). **C(i, ii):** The otic edges are fusing and the mis-expression of Cdh1 persists at the site of fusion. **D(i, ii):** The fusion has happened, and elevated levels of Cdh1 still persists. However, the surface ectoderm region, denoted by the yellow asterisk (*) shows no expression of Cdh1. **E(i,ii):** The otic vesicle has not segregated from the surface ectoderm. Both, the mis-expression of Cdh1 in the fusing region and the absence of Cdh1 in the surface ectoderm continues at this stage of fusion. Cdh1, DAPI, gRNA-GFP. The red asterisk * denotes the mis-expression of Cdh1 at the site of fusion and the yellow asterisk * denotes the absence of Cdh1 expression in the surface ectoderm. Scale bars are 10µm.

remodelling, we also saw pseudostratified cells, which are not usually present. And

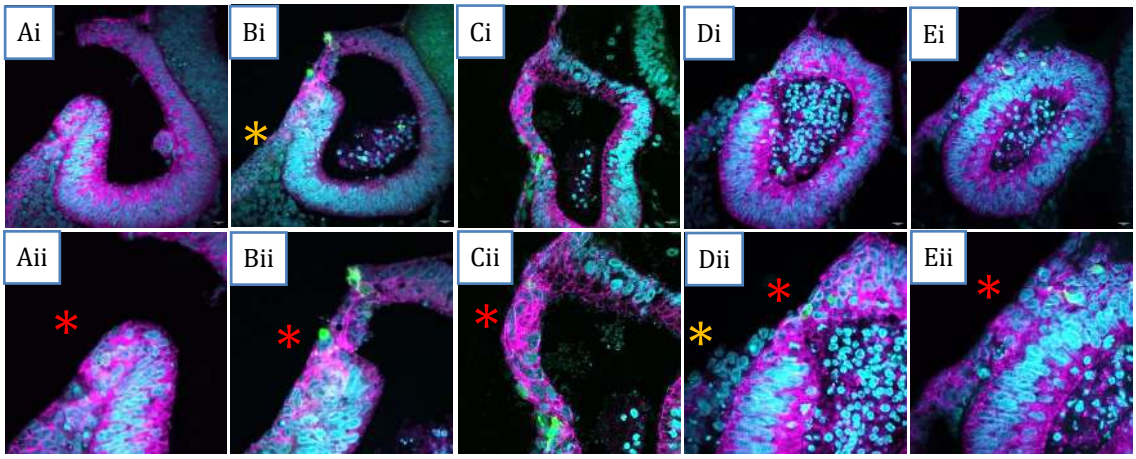

Fig 4.13: Expression of Cdh1 and DAPI in otic vesicle of SP8-gRNA electroporated embryos. A (i,ii): The otic edges are apart. (ii) is a magnified view of (i). Cdh1 expression is higher in some parts of the tissue, as indicated by the red asterisk. **B(i,ii):** The otic edges are just meeting, and Cdh1 expression is much higher in the ventral edge. **C(i,ii):** The otic edges are fusing and the mis-expression of Cdh1 persists at the site of fusion. **D(i,ii):** The fusion has happened, and elevated levels of Cdh1 still persists. However, the surface ectoderm region, denoted by the yellow asterisk (*) shows no expression of Cdh1. **E(i,ii):** The otic vesicle has not segregated completely from the surface ectoderm. The mis-expression of Cdh1 in the fusing region continues at this stage of fusion. Cdh1, DAPI, gRNA-GFP. The red asterisk * denotes the mis-expression of Cdh1 at the site of fusion and the yellow asterisk * denotes the absence of Cdh1 expression in the surface ectoderm. Scale bars are 10µm.

they also had an accumulation of Cdh1. As seen previously, most of the cells at the site of fusion are round edge cells. Here, we considered the bigger pseudostratified cells at the site of fusion, with abnormal Cdh1 expression as round edge cells that have been

perturbed by the mosaic electroporation of the *grhl2*-gRNA. We marked the shape of cells, some of them were GFP positive cells and measured their sphericity index (Fig 4.14). We notice that the pseudostratified cells were unperturbed, as we expected. However, we could see a significant difference in the shape of the otic edge cells and the surface ectoderm cells. Their sphericity index was lower than their control-gRNA counter parts.

Interestingly, we saw a similar phenotype of Cdh1 when *sp8* was perturbed by a mosaic electroporation of *sp8*-gRNA (Fig 4.13). We saw an accumulation of Cdh1 on cells without a round shape, at the site of fusion (as indicated by the red asterisk). There was no expression of Cdh1 on the surface ectoderm, adjacent to the ventral edge of the otic vesicle. Our shape analysis revealed, no perturbation of pseudostratified cells, however, the sphericity index of the round cells mediating fusion and the surface ectoderm cells had reduced as compared to their control-gRNA counterparts.

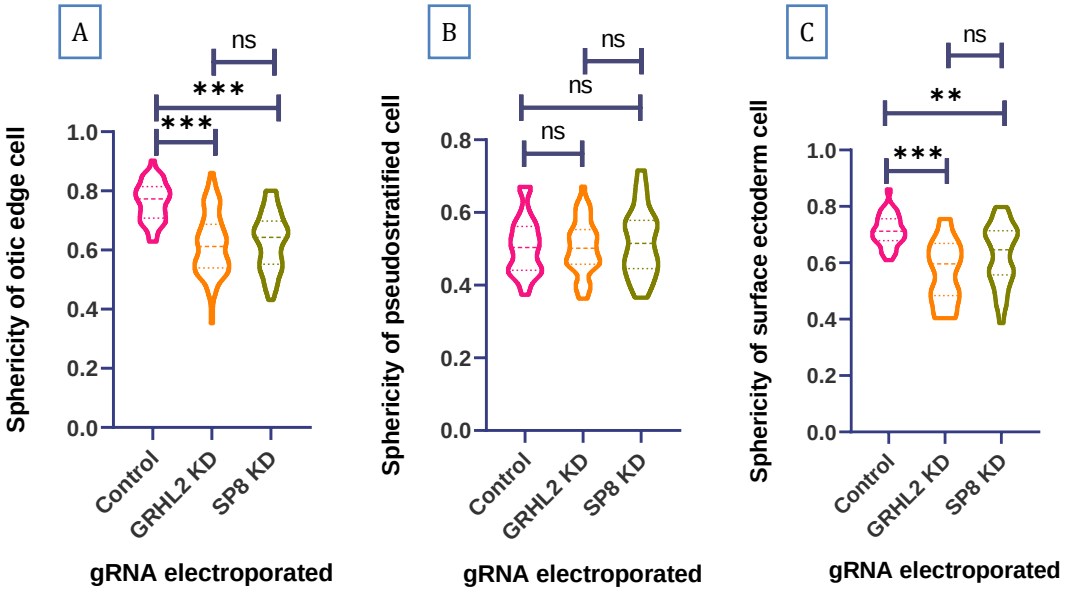

Fig 4.14: Cell shape change in electroporated embryos. One way ANOVA was performed on sphericity data of three cell types in embryos electroporated with different gRNA constructs at HH15 and fixed after 8 hours of incubation. **A:** The sphericity of the otic edge cells mediating fusion. **B:** The sphericity of pseudostratified cells in the otic vesicle. **C:** The sphericity of cells in the surface ectoderm adjacent to the otic vesicle.

4.3 Conclusion

In this chapter, we started with studying the expression of genes that have been implicated in partial-EM phenotype, in our system. We saw a clear expression of Grhl2

and Zeb2, two opposing transcription factors express at the site of fusion. This suggested the possibility of the otic edge cells having an altered transcriptomic state with respect to the otic vesicle cells and the surface ectoderm cells. Thus, we did a bulk mRNA sequencing of the three types of tissue dissected from HH17 embryo; the otic edge, rest of the otic vesicle and the adjacent surface ectoderm. Differential Gene Expression (DGE) analysis gave us putative targets that can play a role in epithelial fusion. We validated the specificity of the dissection by performing WhISH on appropriately staged embryos. We chose targets from the DGE list. Based on their expression pattern and literature review, we chose two genes for a CRISPR-Cas9 mediated mosaic knock down; *grhl2* and *sp8*. Mosaic knock-down of these two genes had a similar phenotype, when we looked at the expression of Cdh1 and analysed cell shape changes. Cdh1 seemed to accumulate on cells that mediate the fusion. In the wild type, the cells that mediate the fusion also undergo shape change and are more round shape, as we saw in Chapter 3. In the case of the mosaic knockdown of both genes, the cells did not change their shape and were close to pseudostratified. Interestingly, the mutants for these two genes in different animal models have similar phenotype, although *sp8* mutants had severe effects as compared to the *grhl2* mutant. The mosaic knockdown emphasized the necessity of spatial-temporal expression of putative transcription factors involved in the maintenance of the partial EM phenotype.

Chapter 5: Discussions and scope of the study

5.1 Discussions

The development of an organism begins with a single cell zygote. This single cell contains all the information necessary to form an entire organism. This information extends beyond chromosomal DNA alone. Maternal mRNA, polarity proteins, cell organelles, and cytoskeletal structures that localise within specific domains of the cell (spatially), as well as those that are initiated or activated in a temporal manner, are some intrinsic properties of cells that assist in development. The cell engages in various activities facilitated by these intrinsic factors, including cell proliferation, migration, transition, shape change, secretion, internalisation, and communication—receiving signals, transducing them, and conveying information internally. Additionally, the cell can also send out signals it receives from within and from its neighbours and undergoes programmed cell death.

As the cell divides further, the embryonic cells need to be patterned. Patterning at this stage would mean imparting identity on cells such that they would become anterior, posterior, dorsal, ventral, left and right. This information is either provided by maternal determinants or asymmetries develop when the egg is fertilised. The mass of cells is clumped together by sticky or adhesive proteins in different concentrations, types and combinations. Besides connecting the cells in different arrangements, they are also involved in linking the cytoskeletal scaffolding of cells with their neighbours' scaffolding. They also help the cell know if they are a part of a collective. They also help the cells attach to a substratum transiently during cell migration. Some of the properties also help in the characterisation of cells as belonging to either epithelial or mesenchymal type.

As a collective, the organised tissue can then undergo morphogenesis, including folding, tube formation, and stratification. These abilities help make the final body plan of a fully formed functional organism. Big scale morphogenetic events require minute coordinated cellular events to occur properly. Epithelial fusion is one such morphogenetic event, whereby two tissues that are apart, are pushed together across an anatomical gap and fuse to form a closed structure, sometimes with a central lumen (Ray & Niswander, 2012). Epithelial fusion is a recurrent process during normal

embryonic development, across species, both vertebrates and invertebrates alike as seen in neural tube closure (Pai et al., 2012), optic fissure closure(Hero, 1989), otic vesicle closure (Meier, 1978a, 1978b), palatal shelf fusion (Greene & Pisano, 2010; Iwata et al., 2011), *drosophila* body wall closure (Jacinto et al., 2000) and wound healing (Bement et al., 1999). Birth defects arise when one or more of these morphogenetic events fail to occur, due to a myriad of reasons, either genetic or environmental. In India, the prevalence of neural tube defects is around 4.5 per 1000 total births and orofacial clefts is around 1.3 per 1000 total births (Allagh et al., 2015). Omphalocele is when the abdominal body wall fails to fuse, which is another common birth defect, although this can be surgically rectified, if intervened at the right stage of pregnancy. As common as these fusion related birth defects are, epithelial fusion has not been completely understood during embryogenesis. Some aspects of fusion have been well characterised, including the morphology and polarity of cells, junction complex switching, basement membrane changes and remodelling and cytoskeletal regulations, and some upstream regulators of these processes. Some aspects remain to be explored further, the molecular identity of the cells that fuse, for instance. Studies have hinted at a possible partial EM phenotype for these cells in multiple contexts (Bahri et al., 2010; Futterman et al., 2011; Galea et al., 2017; Shaw & Martin, 2016); our study too, hypothesised something similar with respect to otic vesicle closure. To that end, in this thesis, we have worked towards a better understanding of epithelial fusion in the inner ear and to check if a partial EM phenotype is also seen in our system.

The otic placode is specified in the surface ectoderm adjacent to the neural tube. Throughout the development of the vesicle, it is in continuation with the surface ectoderm; until the closure, when they get segregated and become two separate and intact epithelia. The overall surface morphology of the otic vesicle and surface ectoderm have been well studied using SEM. These descriptions include the change in apical surface area of the open vesicle across multiple stages, changes in volume of the otic vesicle and changes in the pore size of the partially internalised otic vesicle (Alvarez & Navascués, 1990). The signalling pathways leading to the differentiation of the otic placode from the surface ectoderm have been well studied (Ladher et al., 2010; Xiaorei Sai & Ladher, 2015a). The signalling involved in the specification of different domains in the otic vesicle that would later give rise to different regions of the inner ear is also an active area of research in the field. Earlier studies on the subject have described the shape of the otic pore prior to fusion, the morphology of the cells in

different regions of the pore, and the presence of filopodia aiding in the fusion. Cell migration from the pharyngeal arches into the otic vesicle have also been described (Bancroft & Bellairs, 1977). However, there are very few studies that look at the closure of otic vesicles in the context of epithelial fusion. More importantly the molecular signature of the cells that aid in the fusion has not been looked at.

We started with the characterisation of our system using SEM in Fig 3.3. From early stages of development beginning at HH12, the inner ear primordium is just an otic pit, that looks like a slight depression on the otherwise seemingly flat embryo. And as embryonic development proceeds, the otic pit transforms to an otic cup that gets internalised into the cranial mesenchyme. This otic cup further gets internalised until the otic cup becomes an otic vesicle, by HH15, that is only visible as an opening on the surface of the embryo, adjacent to a closed neural tube. As seen in previous studies and here, there is a reduction in the size of the pore diameter. The elongated cells along the circumference of the pore are reminiscent of the cells on the leading edge (Fig 3.4) during wound healing and *drosophila* body wall closure. This phase is mediated by a purse string mode of closure, whereby the cytoskeletal structures in the elongated cells generate coordinated contractile force that reduces the size of the opening from along the circumference equally. Following this reduction is when the zipping phase starts. In flies, canthi are formed on the anterior and posterior side of the opening, where the fusion happens, such that a seamless body wall is formed. Something similar is also seen in the case of wound healing. However, in the case of mouse neural tube closure, a purse string is only seen in the final stages of posterior neuropore closure (Belacortu & Paricio, 2011; Galea et al., 2017; Daniel P. Kiehart et al., 2017; Millard & Martin, 2008).

In the second phase of fusion, when the zipping starts in the region where the tissues are in close proximity, the cells in the leading edge, that mediate the fusion, undergo some changes such that they are now able to initiate contact with the other tissue. Some of these studies have acknowledged the presence of differently shaped cells mediating the fusion, as shown in the live imaging of mouse neural tube closure (Pyrgaki et al., 2010b) or chick optic fissure closure (Gestri et al., 2018). Serial-block SEM of mouse neural tube closure has also shown the existence of the differently shaped cells (Rolo et al., 2016). In the case of wound healing, EGF mediated re-epithelialization leads to loosen cell-cell contact during migration of the keratinocytes. Overexpression of slug led to the remodelling of cytoskeleton, detachment of actin

cables from cell-cell junctions and spreading of keratinocytes (Arnoux et al., 2008). Irrespective of whether the leading-edge cells are pushed across an anatomical gap with or without a substratum, they acquire some invasive properties that include cell shape changes and membrane protrusions to make the initial contact. The zipping in otic vesicle pore starts from the dorsal side. The presence of a cable of F-actin, exclusively on the dorsal side of the otic pore confirmed the direction of closure (Fig 3.4). Such a cable was previously observed in mouse neural tube closure (Galea et al., 2017; Nikolopoulou, Galea, Rolo, Greene, & Copp, 2017). We also observed some blebbing at the site of fusion Fig 3.5, reminiscent of apoptotic bodies as observed in other systems when epithelial fusion occurs (Geeraets, 1976; Hardy et al., 2019). This was also confirmed with activated Casp-3 staining of otic vesicle sections. Apoptosis can have different roles during development, force generation to bend the tissue as seen during neurulation (Roellig et al., 2022) or *drosophila* leg epithelium folding, or to clear away cells that are not necessary (Washausen & Knabe, 2019). The presence of the apoptotic bodies in the edges where the otic vesicle bends can also allude to cell extrusion by the epithelium to fine tune the shape of the epithelium as seen in *drosophila* wing discs and pupal wings (Matamoro-Vidal, Cumming, Davidović, Levillayer, & Levayer, 2024; Monier et al., 2015; Rosenblatt, Raff, & Cramer, 2001; Villars & Levayer, 2022).

We saw differently shaped cells on the dorsal side of the closing pore Fig 3.6. These cells were more rounded than others. This shape changing phenomenon has been reported in other systems as well. During *drosophila* body wall closure, the epithelial cells at the canthus get shortened, before getting zipped. The authors hypothesized a possible alteration in the mechanical properties of the cells undergoing fusion at the canthus (Lu et al., 2015). Similar shape changes have been reported during zipping in mouse neural tube closure. An ITGB1 mediated focal anchorage to the fibronectin rich basement membrane, reduces the length of cell junctions. This results in the formation of semi-rosettes that aid in the zipping process (Molè et al., 2020; Zhou et al., 2020). In optic fissure closure, prior to and during fusion, some of the retinal cells have a cuboidal morphology, intermediary to the columnar neural retinal cells and the squamous retinal pigmented epithelial cells. These cells had changed their orientation towards the fissure opening and displayed protrusive activity (Gestri et al., 2018).

While we know that the cells change shape, and we also know how these shape changes are regulated, the question now is why a cell shape change necessary? Or is the cell shape change an effect of fluidic cytoskeleton and related adhesive

components? If it is a side effect, then how does the system not consider this a breach in the epithelial integrity and try to repair the system? This is a crucial question, as epithelial cells that pose a threat to the tissue integrity are often destined to undergo apoptosis and be extruded out of the tissue (Andrade & Rosenblatt, 2011). Before we ask why a cell shape change might be happening, we started with the question of what kind of cell shape change do we see in our system, and what other changes accompany the cell shape change?

In this study we used cryosections stained for F-actin (Fig 3.7). The cell shape was marked using Imaris, and sphericity index was used as the metric to define cell shapes. Our system comprises of three cell types, the pseudostratified cell of the otic vesicle lineage, the squamous surface ectoderm cells and the round cells in the otic edge. At stages HH16+ to HH17, the fusion process has already begun, transverse sections of the embryo at an angle parallel to the pharyngeal arches would capture all the stages involved in fusion (Fig 3.9); this approach was previously done in (Gestri et al., 2018). An elongated cell would have a sphericity index tending towards zero, whereas a round cell would have a value tending towards one. This was the trend we observed in our study as well. The pseudostratified cells and surface ectoderm cells had a value of approximately 0.6, and the otic edge cells had a value of 0.8. Based on the shape of the cells, we characterised their population across stages of fusion (Fig 3.10-3.11) and observed a gradual increase in their numbers as fusion progressed until remodelling, after which their numbers dropped. This implied a possible role of these round cells in fusion and remodelling.

After having confirmed that there is a subset of cells whole population increases and decreases during different stages of fusion, we decided to ask if these cells had altered properties. We characterised the localisation of junctions and polarity proteins of these round cells. Perturbed junctions, reoriented polarity proteins and cytoskeletal structures, and remodelled basement membranes are a common theme in epithelial fusion. Optic fissure studies in zebrafish showed disorganised polarity and detached cell junctions as seen with ZO1 and alpha catenin staining. However, after fusion, the polarity was re-established (Gestri et al., 2018). This remodelling is also seen in *drosophila* body wall closure; the caveat is that the remodelling of junctions should be accurate to be functional, while also allowing a shape change. In the absence of these junctions, the continuity between cells is lost, and by extension the integrity of the epithelium is lost (Gorfinkiel & Arias, 2007). In some cases, this remodelling is

accomplished through a Rab-mediated trafficking of polarity and junction components (Levayer & Lecuit, 2013; Roeth et al., 2009).

We studied the expression of Cdh1 in otic vesicle (Fig 3.12). We observed a diffused expression of the protein on the round cell throughout fusion and remodelling (Fig 3.21). It is possible that this diffused expression helps in the establishment of new contacts initially, and as the cells segregate to either become a part of the otic vesicle or the surface ectoderm, it might play a role in the segregation. Cadherins aiding in the segregation of cells has been an active area of research. There are two schools of thought on how the cadherins could mediate this, one is through the difference in surface adhesion as proposed by (Steinberg, 2007) and the other is the regulation of cell stiffness by the cadherin, as proposed by (Krens & Heisenberg, 2011). This segregation could probably be mediated by cell intercalation as seen during convergent extension movements in gastrulation (Nelson, 2009). ZO1, a component of tight junction, showed a similar expression pattern (Figs. 3.13 and 3.21). The polarity proteins Rac1 and Ezrin (Figs. 3.15, 3.16 and 3.21) also had a similar expression pattern in the cell types. Thus, it is possible that the altered expression of junction proteins and polarity proteins on the round cells can be aiding in the cell sorting for the proper segregation of the otic vesicle from the surface ectoderm. This cell sorting is the first step and has to be followed by the formation of a basement membrane to form two intact epithelia.

ECM remodelling is a crucial step in epithelial morphogenesis. Laminin is a component of ECM and in our system, we only see a breakdown of the intact basement membrane when the fusion and remodelling are happening (Fig 3.17). Super resolution image of one of the stages of epithelial fusion had hinted at a possible role for mesenchymal like cells in establishing a new ECM (Fig 3.18). SEM of the closing region (Fig 3.19) also suggested a similar idea; the basement membrane remodelling in optic fissure closure is mediated by endothelial periocular mesenchymal cells. These cells help in the initial breakdown of the basement membrane for the cells to establish contact (Gestri et al., 2018). Multiple signalling pathways have been studied with regard to ECM remodelling; TGF-beta signalling has been shown necessary in zebrafish optic fissure closure (Knickmeyer et al., 2018), mammalian palatal fusion (Iwata et al., 2011), heart formation (Nakajima et al., 2000) and wound healing (Fernández-Santos et al., 2021). Wnt inhibition by draxin is also implicated in ECM remodelling (Hutchins et al., 2021). In this study, we have not addressed the source of the ECM degrading components or ECM components.

Through these studies we have established that otic vesicle closure also has cell shape changes, reorganised cell polarity and junctions, cell sorting and intercalation, and remodelled ECM possibly mediated by mesenchymal interactions. This behaviour suggests that the cells mediating fusion might not be completely epithelial and may have less epithelial properties or a partial EMT phenotype. A partial EMT phenotype does not necessarily mean the acquisition of new mesenchymal traits, rather it could be a change in the apical-basal polarity, and/or remodelling of cell-cell junctions in favour of cell-matrix adhesion, and a cytoskeletal remodelling (R. Y.-J. Huang et al., 2012). A partial EMT has been implicated where cells have displayed a similar phenotype: in wound healing (Shaw & Martin, 2016), *drosophila* body wall closure where they see cells extending Rac/Cdc42 mediated actin protrusions, filopodia and lamellipodia (Bahri et al., 2010), in mammalian neural tube closure (Galea et al., 2017; Nikolopoulou et al., 2019; Rolo et al., 2016) and cancers (Aiello et al., 2018). This partial phenotype might confer other abilities to cells, including better survival or decreased proliferation and a quicker transition to its initial state (M. Angela Nieto et al., 2016).

We wanted to characterise the altered phenotype of round cells further and started by looking at the transcript level expression pattern of key players implicated in the maintenance of a partial EM phenotype, based on meta studies in cancer (Figs. 4.1 and 4.2). We saw expression of Grhl2 and Zeb2 at the site of fusion. Grhl2, is an upstream regulator of Cdh1 and Cldn4, and is necessary for maintaining epithelial characteristics of cells (Aue et al., 2015; Gao et al., 2013; Senga et al., 2012; Werth et al., 2010b). Grhl2, through Cdh1 can also alter the mechanical properties of the mammalian non-neural ectodermal cells by the actomyosin network (Nikolopoulou et al., 2019) and its mis-regulation has been implicated in cancers through EMT (Cieply et al., 2012; Werner et al., 2013). Zeb2 is a known inducer of EMT and has been well studied in cancers (M. Angela Nieto et al., 2016).

The in-situ hybridisation alluded to an altered state of the cells mediating fusion. Bulk mRNA sequencing and subsequent differential gene expression analysis of the otic edge cells revealed the over-representation of pathways that could be active at the site of fusion. Two comparisons were made: OE vs OV and OE vs SE (Figs. 4.5 and 4.7). Gastrulation was one of pathways that had higher hits, and as we saw gastrulation is one of the earliest morphogenetic events involving EMT, cell migration, intercalation and ECM remodelling at different phases (Nakaya & Sheng, 2008, 2009; S.-Y. Wu et al., 2007). We also saw an over-representation of ECM remodelling, which was also a

trend that was observed in a transcriptomics study of chick optic fissure closure (Hardy et al., 2019). Wnt signalling was found to be over-represented. Transcription machinery related pathways and muscle contraction was also seen. Most of the over represented pathways were enriched in both the comparisons, suggesting that the edge cells have a unique cell state essential for fusion. It would be interesting to compare transcriptome data of epithelial fusion in different systems, and look for partial EMT signatures in development. This might tell us if the partial EM phenotype is a conserved program. We have now established that the edge cells have an altered cell state. We wanted to check how this altered state is initiated and maintained. We chose two transcription factors based on some criteria as described in Chapter 4 and proceeded with electroporation of the CRISPR-cas9 system, targeted to the otic edge region by loading the plasmid into the vesicle. As the transcription factors Grhl2 and SP8 are not actively transcribed in the vesicle, this approach would only target the otic edge/pore and the surface ectoderm right next to it.

The mosaic knockdown of Grhl2 and SP8 revealed interesting phenotypes that was not so apparent in their knock out phenotypes previously published (Chung et al., 2014; Han et al., 2011). In our knockdown of both genes, we saw that the cells mediating fusion had not changed their shape and were similar to the surface ectoderm cells or the pseudostratified cells (Fig 4.14). We also saw an accumulation of Cdh1 at the site of fusion. It is possible that, here Cdh1 recycling was perturbed. In our RNA-seq we did not see an upregulation of Cdh1, implying that it is not being actively transcribed. Thus, it is possible that for proper fusion to occur, Cdh1 is being recycled through endocytosis as previously seen elsewhere (Ulrich & Heisenberg, 2008). We also saw that the segregation of the tissue has not happened, which can also be attributed to a very high localisation of Cdh1 at the site of fusion. Interestingly, the mosaic loss of Grhl2 or SP8 from the surface ectoderm, had the opposite effect; Cdh1 expression was completely absent from these cells. Mouse mutants for Grhl2 had a similar effect in the non-neural ectoderm or the surface ectoderm wherein the epithelial cells did not express Cdh1, instead expressed cadh2, exhibiting a neural fate (Nikolopoulou et al., 2019). However, we had not tested for the expression of any other cadherins in our mutants. In the same study, mutants over expressing Grhl2 also did not fuse, as an increased level of adherens junctions could make cells more rigid or stiff and disrupt the coupling of cell adhesion and actomyosin contractility required for fusion. The

authors then speculated that the cells mediating fusion probably require a less epithelial state for proper fusion and remodelling to occur (Nikolopoulou et al., 2019).

Our study has established that a partial EMT state is essential for the proper fusion and segregation of the epithelia. When pro-epithelial factor Grhl2 or pro-EMT factor SP8 were genetically knocked down, the partial EMT state was perturbed and resulted in improper epithelial fusion. This implied that a completely epithelial or mesenchymal state of cells mediating fusion might lead to improper epithelial fusion. There are other factors to be considered about the existence of the partial EMT state as well; the number of edge cells in partial EM state, the duration of their existence, the maintenance of this population and their eventual fate. The otic vesicle closure entails continuous, unidirectional zippering of the otic pore. When the epithelia fuse and remodelling is underway, a peak in the population of the otic edge cells is observed. This population at the site is essential for maintaining tissue integrity while the cells rearrange their junctions to make new neighbors. We observed that some of the edge cells were mitotic, and some were apoptotic. But neither of these processes seemed to significantly affect the population of the edge cells during fusion. Extended period of incubation after CRISPR-Cas9 based gene knockdown stopped tissue segregation. It is probable that the genetic manipulation also interfered with the regulatory network that maintained the duration of the partial EMT state. An interesting observation in our study was that a mosaic knockdown disturbed more than the cell with the CRISPR construct (GFP+ cells). The neighbouring cells also failed to change their shape, and showed a high localisation of Cdh1. Thus, it is possible that the cortical actin network that connects neighbouring cells through junctions play a major role in the maintenance of this partial EM state. Additionally, signalling pathways could also play a role in the maintenance of the partial EM state. Our bulk-mRNA seq analysis revealed multiple componnents of the WNT signalling pathway, differentially regulated at the otic edge. But this was not perturbed using chemical inhibitors. The fate of these edge cells after fusion is unclear. When embryos perturbed with CRISPR constructs were incubated for longer durations, we observed that the site of fusion extended as thin epithelial tissue, beyond the embryo. In this case, it is probable that the edge cells became epithelial as they could not become a part of the surface ectoderm or the otic vesicle. We have not performed cell mapping of the partial EM cells to observe their eventual destination. The cells that remain in the otic epithelium do become epithelial again. The fate of the interstitial, mesenchymal, cells is unclear. We did not observe a significant increase in

apoptosis in the interstitial region. Thus these cells may either become a part of the surface ectoderm or migrate away as mesenchymal cells. I checked the literature on lineage labelling of the otocyst. Quail-check transplants or DiI labelling do not provide any information. In mouse, the Six1enh21-cre is expressed in the otic placode. By crossing with Rosa26-LSL-EYFP all cells of the otic placode should be labelled. In these animals, some mesenchymal cells with EYFP are observed around the otic vesicle at E10.5 after the otic vesicle is completely closed and the two epithelia are segregated (Ono et al., 2014). At E9.5, some EYFP cells are seen on the surface ectoderm, which is still in continuation with the otic epithelium (Ono et al., 2014). While this is not definitive, it is possible that these cells could become a part of the otic or surface epithelium, or remain mesenchymal cell and migrate away.

As previously published, our mosaic knockdowns showing very similar phenotype is not surprising. The phenotypes of the published knockdowns had major defects in the vestibular region which arise from the dorsal region of the otic vesicle, where fusion occurs. Rather, this similar phenotype suggested that there is a balanced mechanism at play during otic vesicle closure. Grhl2 is an epithelial maintenance transcription factor and SP8 is an EMT inducing transcription factor. The similar phenotype we see upon their perturbation implies their role in the maintenance of an altered or a partial EM phenotype in the edge cells. After electroporation of the CRISPR constructs, we saw extrusion of the cells with the construct when allowed to grow for longer durations; despite that we also saw closure defects (data not shown). The knockdown of the genes in the pseudostratified cells did not have any effect on the expression of Cdh1 or cell shape change, as neither Grhl2 nor SP8 were actively transcribed in the otic vesicle region. Thus, we only saw the effects of the mosaic knockdown in regions that expressed both the gene transcripts, the otic edge and the surface ectoderm region. It is possible that cells with the gRNA (GFP+) get ejected out of the tissue; however, given their roles in maintaining the epithelial integrity through junctions, it is possible that the cells adjacent to these GFP+ cells might get affected as a result of the compromised adherens junctions on their neighbours. As the cytoskeletal structures are directly linked to these junctions, it is also possible that the necessary cell shape changes that occur are also perturbed. This genetic perturbation, suggests a requirement for an accurate localisation of junctions which can maintain the epithelial integrity while also allowing cell shape changes (Levayer & Lecuit, 2013).

Through these experiments we see that cells have to change their shape for proper fusion to occur. These shape changes are mediated by strictly regulated junctions that allow for cytoskeleton mediated shape change and a neighbour exchange. We also speculate that this tight regulation of junctions would be essential for probable cell intercalations that would allow successful cell sorting and epithelial segregation.

5.2 Limitations of the study

1. In the study, we have characterised the round cells, however, we do not know of their origin or their final fate. Although, through our genetic perturbation studies, it is possible to comment that they are the cells on the edge that change their shape prior to fusion. However, their fate is still not clear, after fusion has occurred.
2. The current study provides a characterisation of the otic vesicle closure. Although it has identified two potential transcriptional regulators of epithelial fusion, there are other interesting candidates from the DGE analysis that could either be at the same regulatory level or upstream/downstream targets of these genes. And these candidates also have to be tested to elucidate the chain of control in epithelial fusion.
3. While we had looked at the expression of F-actin during fusion, we did not include microtubules in the study, and they have been implicated in basement membrane breakdown during gastrulation in chick(Nakaya & Sheng, 2008, 2009).
4. We do not know if apoptosis is absolutely essential for fusion to occur. Bead experiments with apoptosis inhibitors were inconclusive as epithelial fusion occurred over the bead that was internalised by the surface ectoderm.
5. We do not know the source of ECM when the tissue is getting remodelled. A role for the mesenchymal cells in ECM remodelling is yet to be tested, and might prove insightful.

5.3 Future Directions

The partial EM phenotype is a relatively new field of research in development. There are fewer in vivo systems to study this phenomenon. Our system, the otic vesicle closure, is one of the ideal candidates to study this. As mentioned earlier, the relatively smaller size of the primordia and the short and well-defined time span makes it amenable for multiple techniques to study in the cell and tissue level.

As the next step to the study, we would recommend the following:

1. Characterise the mosaic knockdown mutants further, specifically the junctions, ECM and polarity proteins.
   Look at the cytoskeletal organisation of the cells with accumulated Cdh1 or cells that do not have Cdh1. This can also be a comparison with cells of the wild type.
2. Study the effects of mesenchymal cells on ECM remodelling by culturing the otic vesicle without the adjacent tissue.
3. Study the long-term effects of the mosaic knockdown of these genes in the chick.
4. Study the sequence of events in further detail using the mosaic knockdowns of other putative regulatory transcription factors.

References

1. Abbruzzese, G., Becker, S. F., Kashef, J., & Alfandari, D. (2016). ADAM13 cleavage of cadherin-11 promotes CNC migration independently of the homophilic binding site. *Developmental Biology*, *415*(2), 383–390. Retrieved from https://www.sciencedirect.com/science/article/pii/S0012160615300713
2. Aelst, L. V., & D'Souza-Schorey, C. (1997). Rho GTPases and signaling networks. *Genes & Development*, *11*(18), 2295–2322. Retrieved from http://genesdev.cshlp.org/content/11/18/2295
3. Aiello, N. M., Maddipati, R., Norgard, R. J., Balli, D., Li, J., Yuan, S., Yamazoe, T., et al. (2018). EMT Subtype Influences Epithelial Plasticity and Mode of Cell Migration. *Developmental Cell*, *45*(6), 681-695.e4.
4. Alberts, B. (1998). The Cell as a Collection of Protein Machines: Preparing the Next Generation of Molecular Biologists. *Cell*, *92*(3), 291–294.
5. Allagh, K. P., Shamanna, B. R., Murthy, G. V. S., Ness, A. R., Doyle, P., Neogi, S. B., & Pant, H. B. (2015). Birth Prevalence of Neural Tube Defects and Orofacial Clefts in India: A Systematic Review and Meta-Analysis. *PLoS ONE*, *10*(3), e0118961. Retrieved from https://www.ncbi.nlm.nih.gov/pmc/articles/PMC4358993/
6. Alvarez, I. S., & Navascués, J. (1990). Shaping, invagination, and closure of the chick embryo otic vesicle: scanning electron microscopic and quantitative study. *The Anatomical Record*, *228*(3), 315–326.
7. Ambrosini, A., Rayer, M., Monier, B., & Suzanne, M. (2019). Mechanical Function of the Nucleus in Force Generation during Epithelial Morphogenesis. *Developmental Cell*, *50*(2), 197-211.e5. Retrieved from https://linkinghub.elsevier.com/retrieve/pii/S1534580719304253
8. Andrade, D., & Rosenblatt, J. (2011). Apoptotic regulation of epithelial cellular extrusion. *Apoptosis*, *16*(5), 491–501. Retrieved from https://doi.org/10.1007/s10495-011-0587-z
9. Arnoux, V., Nassour, M., L'Helgoualc'h, A., Hipskind, R. A., & Savagner, P. (2008). Erk5 Controls Slug Expression and Keratinocyte Activation during Wound Healing. *Molecular Biology of the Cell*, *19*(11), 4738–4749. Retrieved from https://www.molbiolcell.org/doi/10.1091/mbc.e07-10-1078
10. Aue, A., Hinze, C., Walentin, K., Ruffert, J., Yurtdas, Y., Werth, M., Chen, W., et al. (2015). A Grainyhead-Like 2/Ovo-Like 2 Pathway Regulates Renal Epithelial Barrier Function and Lumen Expansion. *Journal of the American Society of Nephrology*, *26*(11), 2704. Retrieved from https://journals.lww.com/jasn/fulltext/2015/11000/a_grainyhead_like_2_ovo_like_2_pathway_regulates.16.aspx
11. Babb, S. G., & Marrs, J. A. (2004). E-cadherin regulates cell movements and tissue formation in early zebrafish embryos. *Developmental Dynamics*, *230*(2), 263–277. Retrieved from https://onlinelibrary.wiley.com/doi/abs/10.1002/dvdy.20057
12. Bahm, I., Barriga, E. H., Frolov, A., Theveneau, E., Frankel, P., & Mayor, R. (2017). PDGF controls contact inhibition of locomotion by regulating N-cadherin during neural crest migration. *Development*, *144*(13), 2456–2468. Retrieved from https://doi.org/10.1242/dev.147926

13. Bahri, S., Wang, S., Conder, R., Choy, J., Vlachos, S., Dong, K., Merino, C., et al. (2010). The leading edge during dorsal closure as a model for epithelial plasticity: Pak is required for recruitment of the Scribble complex and septate junction formation. *Development*, *137*(12), 2023–2032. Retrieved from https://doi.org/10.1242/dev.045088
14. Bancroft, M., & Bellairs, R. (1977). Placodes of the chick embryo studied by SEM. *Anatomy and Embryology*, *151*(1), 97–108.
15. Bang, A. G., Papalopulu, N., Kintner, C., & Goulding, M. D. (1997). Expression of Pax-3 is initiated in the early neural plate by posteriorizing signals produced by the organizer and by posterior non-axial mesoderm. *Development (Cambridge, England)*, *124*(10), 2075–2085.
16. Barald, K. F., & Kelley, M. W. (2004). From placode to polarization: new tunes in inner ear development. *Development*, *131*(17), 4119–4130. Retrieved from https://doi.org/10.1242/dev.01339
17. Basch, M. L., Bronner-Fraser, M., & García-Castro, M. I. (2006). Specification of the neural crest occurs during gastrulation and requires Pax7. *Nature*, *441*(7090), 218–222. Retrieved from https://www.nature.com/articles/nature04684
18. Batlle, E., Sancho, E., Francí, C., Domínguez, D., Monfar, M., Baulida, J., & Herreros, A. G. de. (2000). The transcription factor Snail is a repressor of E-cadherin gene expression in epithelial tumour cells. *Nature Cell Biology*, *2*(2), 84–89. Retrieved from https://www.nature.com/articles/ncb0200_84
19. Batut, B., Hiltemann, S., Bagnacani, A., Baker, D., Bhardwaj, V., Blank, C., Bretaudeau, A., et al. (2018). Community-Driven Data Analysis Training for Biology. *Cell Systems*, *6*(6), 752-758.e1. Retrieved from https://www.sciencedirect.com/science/article/pii/S2405471218302308
20. Begnaud, S., Chen, T., Delacour, D., Mège, R.-M., & Ladoux, B. (2016). Mechanics of epithelial tissues during gap closure. *Current Opinion in Cell Biology*, *42*, 52–62. Retrieved from https://linkinghub.elsevier.com/retrieve/pii/S0955067416300813
21. Belacortu, Y., & Paricio, N. (2011). Drosophila as a model of wound healing and tissue regeneration in vertebrates. *Developmental Dynamics: An Official Publication of the American Association of Anatomists*, *240*(11), 2379–2404.
22. Bement, W. M., Mandato, C. A., & Kirsch, M. N. (1999). Wound-induced assembly and closure of an actomyosin purse string in *Xenopus* oocytes. *Current Biology*, *9*(11), 579–587. Retrieved from https://www.sciencedirect.com/science/article/pii/S0960982299802619
23. Bénazéraf, B., Francois, P., Baker, R. E., Denans, N., Little, C. D., & Pourquié, O. (2010). A random cell motility gradient downstream of FGF controls elongation of an amniote embryo. *Nature*, *466*(7303), 248–252.
24. Bernstein, C. S., Anderson, M. T., Gohel, C., Slater, K., Gross, J. M., & Agarwala, S. (2018). The cellular bases of choroid fissure formation and closure. *Developmental Biology*, *440*(2), 137–151. Retrieved from https://www.sciencedirect.com/science/article/pii/S0012160618300113
25. Bolger, A. M., Lohse, M., & Usadel, B. (2014). Trimmomatic: a flexible trimmer for Illumina sequence data. *Bioinformatics*, *30*(15), 2114–2120. Retrieved from https://doi.org/10.1093/bioinformatics/btu170
26. Bolós, V., Peinado, H., Pérez-Moreno, M. A., Fraga, M. F., Esteller, M., & Cano, A. (2003). The transcription factor Slug represses E-cadherin expression

and induces epithelial to mesenchymal transitions: a comparison with Snail and E47 repressors. *Journal of Cell Science*, *116*(Pt 3), 499–511.
27. Boucaut, J. C., Clavilier, L., Darribère, T., Delarue, M., Riou, J. F., & Shi, D. L. (1996). What mechanisms drive cell migration and cell interactions in Pleurodeles? *The International Journal of Developmental Biology*, *40*(4), 675–683.
28. Braga, V. M. M. (2002). Cell–cell adhesion and signalling. *Current Opinion in Cell Biology*, *14*(5), 546–556. Retrieved from https://www.sciencedirect.com/science/article/pii/S0955067402003733
29. Brouns, M. R., Castro, S. C. P. D., Terwindt-Rouwenhorst, E. A., Massa, V., Hekking, J. W., Hirst, C. S., Savery, D., et al. (2011). Over-expression of Grhl2 causes spina bifida in the Axial defects mutant mouse. *Human Molecular Genetics*, *20*(8), 1536–1546. Retrieved from https://doi.org/10.1093/hmg/ddr031
30. Brown, T. L. (2003, May 5). UI Press | Theodore L. Brown | Making Truth. Retrieved February 2, 2025, from https://www.press.uillinois.edu/books/?id=p075827
31. Brückner, B. R., Pietuch, A., Nehls, S., Rother, J., & Janshoff, A. (2015). Ezrin is a Major Regulator of Membrane Tension in Epithelial Cells. *Scientific Reports*, *5*(1), 14700. Retrieved from https://www.nature.com/articles/srep14700
32. Bryan, C. D., Casey, M. A., Pfeiffer, R. L., Jones, B. W., & Kwan, K. M. (2020). Optic cup morphogenesis requires neural crest-mediated basement membrane assembly. *Development (Cambridge, England)*, *147*(4), dev181420.
33. Burk, U., Schubert, J., Wellner, U., Schmalhofer, O., Vincan, E., Spaderna, S., & Brabletz, T. (2008). A reciprocal repression between ZEB1 and members of the miR-200 family promotes EMT and invasion in cancer cells. *EMBO reports*, *9*(6), 582–589.
34. Cai, D., Dai, W., Prasad, M., Luo, J., Gov, N. S., & Montell, D. J. (2016). Modeling and analysis of collective cell migration in an in vivo three-dimensional environment. *Proceedings of the National Academy of Sciences*, *113*(15), E2134–E2141. Retrieved from https://www.pnas.org/doi/full/10.1073/pnas.1522656113
35. Cano, A., Pérez-Moreno, M. A., Rodrigo, I., Locascio, A., Blanco, M. J., Barrio, M. G. del, Portillo, F., et al. (2000). The transcription factor Snail controls epithelial–mesenchymal transitions by repressing E-cadherin expression. *Nature Cell Biology*, *2*(2), 76–83. Retrieved from https://www.nature.com/articles/ncb0200_76
36. Cao, M., Ouyang, J., Guo, J., Lin, S., & Chen, S. (2018). Metalloproteinase Adamts16 Is Required for Proper Closure of the Optic Fissure. *Investigative Ophthalmology & Visual Science*, *59*(3), 1167–1177.
37. Casey, M. A., Lusk, S., & Kwan, K. M. (2023). Eye Morphogenesis in Vertebrates. *Annual Review of Vision Science*, *9*(Volume 9, 2023), 221–243. Retrieved from https://www.annualreviews.org/content/journals/10.1146/annurev-vision-100720-111125
38. Castro, S. C. P. D., Hirst, C. S., Savery, D., Rolo, A., Lickert, H., Andersen, B., Copp, A. J., et al. (2018). Neural tube closure depends on expression of Grainyhead-like 3 in multiple tissues. *Developmental Biology*, *435*(2), 130–137.

Retrieved from https://www.sciencedirect.com/science/article/pii/S0012160617308060
39. Chapman, S. C., Collignon, J., Schoenwolf, G. C., & Lumsden, A. (2001). Improved method for chick whole-embryo culture using a filter paper carrier. *Developmental Dynamics*, *220*(3), 284–289. Retrieved from https://onlinelibrary.wiley.com/doi/abs/10.1002/1097-0177%2820010301%29220%3A3%3C284%3A%3AAID-DVDY1102%3E3.0.CO%3B2-5
40. Chauhan, B. K., Lou, M., Zheng, Y., & Lang, R. A. (2011). Balanced Rac1 and RhoA activities regulate cell shape and drive invagination morphogenesis in epithelia. *Proceedings of the National Academy of Sciences*, *108*(45), 18289–18294. Retrieved from https://www.pnas.org/doi/abs/10.1073/pnas.1108993108
41. Chen, X., Li, J., Xiang, A., Guan, H., Su, P., Zhang, L., Zhang, D., et al. (2024). BMP and activin receptor membrane bound inhibitor: BAMBI has multiple roles in gene expression and diseases (Review). *Experimental and Therapeutic Medicine*, *27*(1), 1–9. Retrieved from https://www.spandidos-publications.com/10.3892/etm.2023.12316
42. Cheung, K. J., Gabrielson, E., Werb, Z., & Ewald, A. J. (2013). Collective invasion in breast cancer requires a conserved basal epithelial program. *Cell*, *155*(7), 1639–1651.
43. Choo, D., Ward, J., Reece, A., Dou, H., Lin, Z., & Greinwald, J. (2006). Molecular mechanisms underlying inner ear patterning defects in kreisler mutants. *Developmental Biology*, *289*(2), 308–317.
44. Christophorou, N. A. D., Mende, M., Lleras-Forero, L., Grocott, T., & Streit, A. (2010). Pax2 coordinates epithelial morphogenesis and cell fate in the inner ear. *Developmental Biology*, *345*(2), 180–190. Retrieved from https://www.sciencedirect.com/science/article/pii/S0012160610009115
45. Chuai, M., & Weijer, C. J. (2009). Who moves whom during primitive streak formation in the chick embryo. *HFSP Journal*, *3*(2), 71–76. Retrieved from https://www.ncbi.nlm.nih.gov/pmc/articles/PMC2707795/
46. Chung, H. A., Medina-Ruiz, S., & Harland, R. M. (2014). Sp8 regulates inner ear development. *Proceedings of the National Academy of Sciences*, *111*(17), 6329–6334. Retrieved from https://www.pnas.org/doi/full/10.1073/pnas.1319301111
47. Cieply, B., Philip, I. R., Pifer, P. M., Widmeyer, J., Addison, J. B., Ivanov, A. V., Denvir, J., et al. (2012). Suppression of the Epithelial–Mesenchymal Transition by Grainyhead-like-2. *Cancer Research*, *72*(9), 2440–2453. Retrieved from https://doi.org/10.1158/0008-5472.CAN-11-4038
48. Colas, J. F., & Schoenwolf, G. C. (2001). Towards a cellular and molecular understanding of neurulation. *Developmental Dynamics: An Official Publication of the American Association of Anatomists*, *221*(2), 117–145.
49. Coles, E. G., Taneyhill, L. A., & Bronner-Fraser, M. (2007). A critical role for Cadherin6B in regulating avian neural crest emigration. *Developmental Biology*, *312*(2), 533–544. Retrieved from https://www.sciencedirect.com/science/article/pii/S0012160607014091
50. Copp, A. J., Adzick, N. S., Chitty, L. S., Fletcher, J. M., Holmbeck, G. N., & Shaw, G. M. (2015). Spina bifida. *Nature Reviews Disease Primers*, *1*(1), 1–18. Retrieved from https://www.nature.com/articles/nrdp20157

51. Copp, A. J., Greene, N. D. E., & Murdoch, J. N. (2003). The genetic basis of mammalian neurulation. *Nature Reviews Genetics*, *4*(10), 784–793. Retrieved from https://www.nature.com/articles/nrg1181
52. Cote, L. E., & Feldman, J. L. (2022). Won't You be My Neighbor: How Epithelial Cells Connect Together to Build Global Tissue Polarity. *Frontiers in Cell and Developmental Biology*, *10*, 887107.
53. Craene, B. D., & Berx, G. (2013). Regulatory networks defining EMT during cancer initiation and progression. *Nature Reviews Cancer*, *13*(2), 97–110. Retrieved from https://www.nature.com/articles/nrc3447
54. Dady, A., Blavet, C., & Duband, J.-L. (2012). Timing and kinetics of E- to N-cadherin switch during neurulation in the avian embryo. *Developmental Dynamics*, *241*(8), 1333–1349. Retrieved from https://onlinelibrary.wiley.com/doi/abs/10.1002/dvdy.23813
55. Dale, L., & Slack, J. M. W. (1987). Fate map for the 32-cell stage of Xenopus laevis. *Development*, *99*(4), 527–551. Retrieved from https://doi.org/10.1242/dev.99.4.527
56. Davidson, L. A., & Keller, R. E. (1999). Neural tube closure in Xenopus laevis involves medial migration, directed protrusive activity, cell intercalation and convergent extension. *Development*, *126*(20), 4547–4556. Retrieved from https://doi.org/10.1242/dev.126.20.4547
57. Davidson, Lance A., Keller, R., & DeSimone, D. W. (2004). Assembly and remodeling of the fibrillar fibronectin extracellular matrix during gastrulation and neurulation in Xenopus laevis. *Developmental Dynamics: An Official Publication of the American Association of Anatomists*, *231*(4), 888–895.
58. Davidson, Lance A., Marsden, M., Keller, R., & DeSimone, D. W. (2006). Integrin α5β1 and Fibronectin Regulate Polarized Cell Protrusions Required for *Xenopus* Convergence and Extension. *Current Biology*, *16*(9), 833–844. Retrieved from https://www.sciencedirect.com/science/article/pii/S0960982206013352
59. Doyle, M., Phipson, B., & Dashnow, H. (2018, September 23). 1: RNA-Seq reads to counts. *Galaxy Training Network*. text, . Retrieved from https://training.galaxyproject.org/training-material/topics/transcriptomics/tutorials/rna-seq-reads-to-counts/tutorial.html
60. Doyle, M., Phipson, B., Maksimovic, J., Trigos, A., Ritchie, M., Dashnow, H., Su, S., et al. (2018, December 31). 2: RNA-seq counts to genes. *Galaxy Training Network*. text, . Retrieved from https://training.galaxyproject.org/training-material/topics/transcriptomics/tutorials/rna-seq-counts-to-genes/tutorial.html
61. Duband, J. L., Monier, F., Delannet, M., & Newgreen, D. (1995). Epithelium-mesenchyme transition during neural crest development. *Acta Anatomica*, *154*(1), 63–78.
62. Dunn, N. R., Winnier, G. E., Hargett, L. K., Schrick, J. J., Fogo, A. B., & Hogan, B. L. (1997). Haploinsufficient phenotypes in Bmp4 heterozygous null mice and modification by mutations in Gli3 and Alx4. *Developmental Biology*, *188*(2), 235–247.
63. Eckert, P., Knickmeyer, M. D., Schütz, L., Wittbrodt, J., & Heermann, S. (2019). Morphogenesis and axis specification occur in parallel during optic cup and optic fissure formation, differentially modulated by BMP and Wnt. *Open Biology*, *9*(2), 180179. Retrieved from https://royalsocietypublishing.org/doi/abs/10.1098/rsob.180179

64. Eckhart, L., Ballaun, C., Hermann, M., VandeBerg, J. L., Sipos, W., Uthman, A., Fischer, H., et al. (2008). Identification of novel mammalian caspases reveals an important role of gene loss in shaping the human caspase repertoire. *Molecular Biology and Evolution*, *25*(5), 831–841.
65. Ellenrieder, V., Hendler, S. F., Boeck, W., Seufferlein, T., Menke, A., Ruhland, C., Adler, G., et al. (2001). Transforming growth factor beta1 treatment leads to an epithelial-mesenchymal transdifferentiation of pancreatic cancer cells requiring extracellular signal-regulated kinase 2 activation. *Cancer Research*, *61*(10), 4222–4228.
66. Eltsov, M., Dubé, N., Yu, Z., Pasakarnis, L., Haselmann-Weiss, U., Brunner, D., & Frangakis, A. S. (2015). Quantitative analysis of cytoskeletal reorganization during epithelial tissue sealing by large-volume electron tomography. *Nature Cell Biology*, *17*(5), 605–614. Retrieved from https://www.nature.com/articles/ncb3159
67. Essex, L. J., Mayor, R., & Sargent, M. G. (1993). Expression of Xenopus snail in mesoderm and prospective neural fold ectoderm. *Developmental Dynamics: An Official Publication of the American Association of Anatomists*, *198*(2), 108–122.
68. Fabregat, A., Sidiropoulos, K., Viteri, G., Marin-Garcia, P., Ping, P., Stein, L., D'Eustachio, P., et al. (2018). Reactome diagram viewer: data structures and strategies to boost performance. *Bioinformatics (Oxford, England)*, *34*(7), 1208–1214. Retrieved from https://doi.org/10.1093/bioinformatics/btx752
69. Fernández-Santos, B., Caro-Vega, J. M., Sola-Idígora, N., Lazarini-Suárez, C., Mañas-García, L., Duarte, P., Fuerte-Hortigón, A., et al. (2021). Molecular similarity between the mechanisms of epithelial fusion and fetal wound healing during the closure of the caudal neural tube in mouse embryos. *Developmental Dynamics*, *250*(7), 955–973. Retrieved from https://onlinelibrary.wiley.com/doi/abs/10.1002/dvdy.306
70. Ferrari, D., Harrington, A., Dealy, C. N., & Kosher, R. A. (1999). Dlx-5 in limb initiation in the chick embryo. *Developmental Dynamics: An Official Publication of the American Association of Anatomists*, *216*(1), 10–15.
71. Fish, J. L., Dehay, C., Kennedy, H., & Huttner, W. B. (2008). Making bigger brains-the evolution of neural-progenitor-cell division. *Journal of Cell Science*, *121*(Pt 17), 2783–2793.
72. Francou, A., & Anderson, K. V. (2020). The Epithelial-to-Mesenchymal Transition (EMT) in Development and Cancer. *Annual Review of Cancer Biology*, *4*(Volume 4, 2020), 197–220. Retrieved from https://www.annualreviews.org/content/journals/10.1146/annurev-cancerbio-030518-055425
73. Freter, S., Muta, Y., Mak, S.-S., Rinkwitz, S., & Ladher, R. K. (2008). Progressive restriction of otic fate: the role of FGF and Wnt in resolving inner ear potential. *Development*, *135*(20), 3415–3424.
74. Freter, S., Muta, Y., O'Neill, P., Vassilev, V. S., Kuraku, S., & Ladher, R. K. (2012). Pax2 modulates proliferation during specification of the otic and epibranchial placodes. *Developmental Dynamics*, *241*(11), 1716–1728. Retrieved from https://onlinelibrary.wiley.com/doi/abs/10.1002/dvdy.23856
75. Fuentes, P., Sesé, M., Guijarro, P. J., Emperador, M., Sánchez-Redondo, S., Peinado, H., Hümmer, S., et al. (2020). ITGB3-mediated uptake of small extracellular vesicles facilitates intercellular communication in breast cancer cells. *Nature Communications*, *11*(1), 4261.

76. Fukata, M., & Kaibuchi, K. (2001). Rho-family GTPases in cadherin-mediated cell — cell adhesion. *Nature Reviews Molecular Cell Biology*, *2*(12), 887–897. Retrieved from https://www.nature.com/articles/35103068
77. Furuse, M., Sasaki, H., Fujimoto, K., & Tsukita, S. (1998). A single gene product, claudin-1 or -2, reconstitutes tight junction strands and recruits occludin in fibroblasts. *The Journal of Cell Biology*, *143*(2), 391–401.
78. Furuse, Mikio, Fujita, K., Hiiragi, T., Fujimoto, K., & Tsukita, S. (1998). Claudin-1 and -2: Novel Integral Membrane Proteins Localizing at Tight Junctions with No Sequence Similarity to Occludin. *The Journal of Cell Biology*, *141*(7), 1539–1550. Retrieved from https://www.ncbi.nlm.nih.gov/pmc/articles/PMC2132999/
79. Futterman, M. A., García, A. J., & Zamir, E. A. (2011). Evidence for partial epithelial-to-mesenchymal transition (pEMT) and recruitment of motile blastoderm edge cells during avian epiboly. *Developmental Dynamics*, *240*(6), 1502–1511. Retrieved from https://onlinelibrary.wiley.com/doi/abs/10.1002/dvdy.22607
80. Gage, P. J., Rhoades, W., Prucka, S. K., & Hjalt, T. (2005). Fate maps of neural crest and mesoderm in the mammalian eye. *Investigative Ophthalmology & Visual Science*, *46*(11), 4200–4208.
81. Galea, G. L., Cho, Y.-J., Galea, G., Molè, M. A., Rolo, A., Savery, D., Moulding, D., et al. (2017). Biomechanical coupling facilitates spinal neural tube closure in mouse embryos. *Proceedings of the National Academy of Sciences of the United States of America*, *114*(26), E5177–E5186.
82. Gao, X., Vockley, C. M., Pauli, F., Newberry, K. M., Xue, Y., Randell, S. H., Reddy, T. E., et al. (2013). Evidence for multiple roles for grainyhead-like 2 in the establishment and maintenance of human mucociliary airway epithelium. *Proceedings of the National Academy of Sciences*, *110*(23), 9356–9361. Retrieved from https://www.pnas.org/doi/full/10.1073/pnas.1307589110
83. Garfield, E. (1986). The Metaphor-Science Connection. Retrieved from https://api.semanticscholar.org/CorpusID:17141741
84. Garnett, A. T., Square, T. A., & Medeiros, D. M. (2012). BMP, Wnt and FGF signals are integrated through evolutionarily conserved enhancers to achieve robust expression of Pax3 and Zic genes at the zebrafish neural plate border. *Development*, *139*(22), 4220–4231. Retrieved from https://doi.org/10.1242/dev.081497
85. Gautreau, A., Poullet, P., Louvard, D., & Arpin, M. (1999). Ezrin, a plasma membrane–microfilament linker, signals cell survival through the phosphatidylinositol 3-kinase/Akt pathway. *Proceedings of the National Academy of Sciences of the United States of America*, *96*(13), 7300–7305. Retrieved from https://www.ncbi.nlm.nih.gov/pmc/articles/PMC22080/
86. Geelen, J. A. G., & Langman, J. (1977). Closure of the neural tube in the cephalic region of the mouse embryo. *The Anatomical Record*, *189*(4), 625–639. Retrieved from https://onlinelibrary.wiley.com/doi/abs/10.1002/ar.1091890407
87. Geelen, J. A. G., & Langman, J. (1979). Ultrastructural observations on closure of the neural tube in the mouse. *Anatomy and Embryology*, *156*(1), 73–88. Retrieved from https://doi.org/10.1007/BF00315716
88. Geeraets, R. (1976). An electron microscopic study of the closure of the optic fissure in the golden hamster. *The American Journal of Anatomy*, *145*(4), 411–431.

89. Gestri, G., Bazin-Lopez, N., Scholes, C., & Wilson, S. W. (2018). Cell Behaviors during Closure of the Choroid Fissure in the Developing Eye. *Frontiers in Cellular Neuroscience*, *12*. Retrieved from https://www.frontiersin.org/journals/cellular-neuroscience/articles/10.3389/fncel.2018.00042/full
90. Gilbert, S. F. (2000). Early Drosophila Development. *Developmental Biology. 6th edition*. Sinauer Associates. Retrieved from https://www.ncbi.nlm.nih.gov/books/NBK10081/
91. Gorfinkiel, N., & Arias, A. M. (2007). Requirements for adherens junction components in the interaction between epithelial tissues during dorsal closure in *Drosophila*. *Journal of Cell Science*, *120*(18), 3289–3298. Retrieved from https://journals.biologists.com/jcs/article/120/18/3289/29778/Requirements-for-adherens-junction-components-in
92. Gorfinkiel, N., & Blanchard, G. B. (2011). Dynamics of actomyosin contractile activity during epithelial morphogenesis. *Current Opinion in Cell Biology*, *23*(5), 531–539. Retrieved from https://www.sciencedirect.com/science/article/pii/S0955067411000834
93. Gouignard, N., Andrieu, C., & Theveneau, E. (2018). Neural crest delamination and migration: Looking forward to the next 150 years. *genesis*, *56*(6–7), e23107. Retrieved from https://onlinelibrary.wiley.com/doi/abs/10.1002/dvg.23107
94. Goulding, M. D., Chalepakis, G., Deutsch, U., Erselius, J. R., & Gruss, P. (1991). Pax-3, a novel murine DNA binding protein expressed during early neurogenesis. *The EMBO journal*, *10*(5), 1135–1147.
95. Grande, M. T., Sánchez-Laorden, B., López-Blau, C., Frutos, C. A. D., Boutet, A., Arévalo, M., Rowe, R. G., et al. (2015). Snail1-induced partial epithelial-to-mesenchymal transition drives renal fibrosis in mice and can be targeted to reverse established disease. *Nature Medicine*, *21*(9), 989–997. Retrieved from https://www.nature.com/articles/nm.3901
96. Greenburg, G., & Hay, E. D. (1982). Epithelia suspended in collagen gels can lose polarity and express characteristics of migrating mesenchymal cells. *Journal of Cell Biology*, *95*(1), 333–339. Retrieved from https://doi.org/10.1083/jcb.95.1.333
97. Greene, R. M., & Pisano, M. M. (2010). Palate morphogenesis: Current understanding and future directions. *Birth Defects Research Part C: Embryo Today: Reviews*, *90*(2), 133–154. Retrieved from https://onlinelibrary.wiley.com/doi/abs/10.1002/bdrc.20180
98. Grigore, A. D., Jolly, M. K., Jia, D., Farach-Carson, M. C., & Levine, H. (2016). Tumor Budding: The Name is EMT. Partial EMT. *Journal of Clinical Medicine*, *5*(5), 51. Retrieved from https://www.mdpi.com/2077-0383/5/5/51
99. Grotewold, L., Plum, M., Dildrop, R., Peters, T., & Rüther, U. (2001). Bambi is coexpressed with Bmp-4 during mouse embryogenesis. *Mechanisms of Development*, *100*(2), 327–330. Retrieved from https://linkinghub.elsevier.com/retrieve/pii/S0925477300005244
100. Groves, A. K., & Fekete, D. M. (2012). Shaping sound in space: the regulation of inner ear patterning. *Development*, *139*(2), 245–257. Retrieved from https://doi.org/10.1242/dev.067074
101. Gumbiner, B. M. (2005). Regulation of cadherin-mediated adhesion in morphogenesis. *Nature Reviews Molecular Cell Biology*, *6*(8), 622–634. Retrieved from https://www.nature.com/articles/nrm1699

102. Hajra, K. M., Chen, D. Y.-S., & Fearon, E. R. (2002). The SLUG zinc-finger protein represses E-cadherin in breast cancer. *Cancer Research*, *62*(6), 1613–1618.
103. Halbleib, J. M., & Nelson, W. J. (2006). Cadherins in development: cell adhesion, sorting, and tissue morphogenesis. *Genes & Development*, *20*(23), 3199–3214.
104. Hall, A. (1998). Rho GTPases and the Actin Cytoskeleton. *Science*, *279*(5350), 509–514. Retrieved from https://www.science.org/doi/10.1126/science.279.5350.509
105. Hall, B. K. (2000). The neural crest as a fourth germ layer and vertebrates as quadroblastic not triploblastic. *Evolution & Development*, *2*(1), 3–5. Retrieved from https://onlinelibrary.wiley.com/doi/abs/10.1046/j.1525-142x.2000.00032.x
106. Hamada, S., Satoh, K., Hirota, M., Kimura, K., Kanno, A., Masamune, A., & Shimosegawa, T. (2007). Bone morphogenetic protein 4 induces epithelial-mesenchymal transition through MSX2 induction on pancreatic cancer cell line. *Journal of Cellular Physiology*, *213*(3), 768–774.
107. Hamburger, V., & Hamilton, H. L. (1951). A series of normal stages in the development of the chick embryo. *Journal of Morphology*, *88*(1), 49–92. Retrieved from https://onlinelibrary.wiley.com/doi/10.1002/jmor.1050880104
108. Hammerschmidt, M., & Nüsslein-Volhard, C. (1993). The expression of a zebrafish gene homologous to Drosophila snail suggests a conserved function in invertebrate and vertebrate gastrulation. *Development (Cambridge, England)*, *119*(4), 1107–1118.
109. Han, Y., Mu, Y., Li, X., Xu, P., Tong, J., Liu, Z., Ma, T., et al. (2011). Grhl2 deficiency impairs otic development and hearing ability in a zebrafish model of the progressive dominant hearing loss DFNA28. *Human Molecular Genetics*, *20*(16), 3213–3226. Retrieved from https://doi.org/10.1093/hmg/ddr234
110. Hardin, J., & Keller, R. (1988). The behaviour and function of bottle cells during gastrulation of Xenopus laevis. *Development*, *103*(1), 211–230. Retrieved from https://doi.org/10.1242/dev.103.1.211
111. Hardy, H., Prendergast, J. G., Patel, A., Dutta, S., Trejo-Reveles, V., Kroeger, H., Yung, A. R., et al. (2019). Detailed analysis of chick optic fissure closure reveals Netrin-1 as an essential mediator of epithelial fusion. (["Marianne E Bronner", "Jeremy Nathans", "Stephan Heermann", & "Teri Belecky-Adams"], Eds.)*eLife*, *8*, e43877. Retrieved from https://doi.org/10.7554/eLife.43877
112. Haro, E., Delgado, I., Junco, M., Yamada, Y., Mansouri, A., Oberg, K. C., & Ros, M. A. (2014). Sp6 and Sp8 Transcription Factors Control AER Formation and Dorsal-Ventral Patterning in Limb Development. *PLOS Genetics*, *10*(8), e1004468. Retrieved from https://journals.plos.org/plosgenetics/article?id=10.1371/journal.pgen.1004468
113. Harrisson, F., Callebaut, M., & Vakaet, L. (1991). Features of polyingression and primitive streak ingression through the basal lamina in the chicken blastoderm. *The Anatomical Record*, *229*(3), 369–383.
114. Hartsock, A., & Nelson, W. J. (2008). Adherens and Tight Junctions: Structure, Function and Connections to the Actin Cytoskeleton. *Biochimica et biophysica acta*, *1778*(3), 660–669. Retrieved from https://www.ncbi.nlm.nih.gov/pmc/articles/PMC2682436/

115. Hatch, E. P., Noyes, C. A., Wang, X., Wright, T. J., & Mansour, S. L. (2007). Fgf3 is required for dorsal patterning and morphogenesis of the inner ear epithelium. *Development (Cambridge, England)*, *134*(20), 3615–3625.
116. Hay, E. D. (2005). The mesenchymal cell, its role in the embryo, and the remarkable signaling mechanisms that create it. *Developmental Dynamics*, *233*(3), 706–720. Retrieved from https://onlinelibrary.wiley.com/doi/abs/10.1002/dvdy.20345
117. Hay, E. D., & Zuk, A. (1995). Transformations between epithelium and mesenchyme: Normal, pathological, and experimentally induced. *American Journal of Kidney Diseases*, *26*(4), 678–690.
118. Hayes, P., & Solon, J. (2017). Drosophila dorsal closure: An orchestra of forces to zip shut the embryo. *Mechanisms of Development*, *144*, 2–10. Retrieved from https://linkinghub.elsevier.com/retrieve/pii/S0925477316300983
119. Heasman, J., Kofron, M., & Wylie, C. (2000). βCatenin Signaling Activity Dissected in the Early Xenopus Embryo: A Novel Antisense Approach. *Developmental Biology*, *222*(1), 124–134. Retrieved from https://www.sciencedirect.com/science/article/pii/S0012160600997203
120. Heisenberg, C.-P., & Bellaïche, Y. (2013). Forces in Tissue Morphogenesis and Patterning. *Cell*, *153*(5), 948–962. Retrieved from https://www.sciencedirect.com/science/article/pii/S0092867413005734
121. Henrique, D., Adam, J., Myat, A., Chitnis, A., Lewis, J., & Ish-Horowicz, D. (1995). Expression of a Delta homologue in prospective neurons in the chick. *Nature*, *375*(6534), 787–790.
122. Hero, I. (1989). The optic fissure in the normal and microphthalmic mouse. *Experimental Eye Research*, *49*(2), 229–239.
123. Highstein, S. M. (2004). Anatomy and Physiology of the Central and Peripheral Vestibular System: Overview. In ["Stephen M. Highstein", "Richard R. Fay", & "Arthur N. Popper"] (Eds.), *The Vestibular System* (pp. 1–10). New York, NY: Springer New York. Retrieved from https://doi.org/10.1007/0-387-21567-0_1
124. Hiltemann, S., Rasche, H., Gladman, S., Hotz, H.-R., Larivière, D., Blankenberg, D., Jagtap, P. D., et al. (2023). Galaxy Training: A powerful framework for teaching! *PLOS Computational Biology*, *19*(1), e1010752. Retrieved from https://journals.plos.org/ploscompbiol/article?id=10.1371/journal.pcbi.1010752
125. Honda, A., Freeman, S. D., Sai, X., Ladher, R. K., & O'Neill, P. (2014). From placode to labyrinth: Culture of the chicken inner ear. *Methods*, *66*(3), 447–453. Retrieved from https://linkinghub.elsevier.com/retrieve/pii/S1046202313002120
126. Hopwood, N. (2022). 'Not birth, marriage or death, but gastrulation': the life of a quotation in biology. *The British Journal for the History of Science*, *55*(1), 1–26.
127. Huang, C., Kratzer, M.-C., Wedlich, D., & Kashef, J. (2016). E-cadherin is required for cranial neural crest migration in *Xenopus laevis*. *Developmental Biology*, *411*(2), 159–171. Retrieved from https://www.sciencedirect.com/science/article/pii/S0012160616300768
128. Huang, R. Y.-J., Guilford, P., & Thiery, J. P. (2012). Early events in cell adhesion and polarity during epithelial-mesenchymal transition. *Journal of Cell*

Science, *125*(19), 4417–4422. Retrieved from https://doi.org/10.1242/jcs.099697
129. Hutchins, E. J., & Bronner, M. E. (2018). Draxin acts as a molecular rheostat of canonical Wnt signaling to control cranial neural crest EMT. *Journal of Cell Biology*, *217*(10), 3683–3697. Retrieved from https://doi.org/10.1083/jcb.201709149
130. Hutchins, E. J., Piacentino, M. L., & Bronner, M. E. (2021). Transcriptomic Identification of Draxin-Responsive Targets During Cranial Neural Crest EMT. *Frontiers in Physiology*, *12*. Retrieved from https://www.frontiersin.org/journals/physiology/articles/10.3389/fphys.2021.624037/full
131. Hutson, M. S., Tokutake, Y., Chang, M.-S., Bloor, J. W., Venakides, S., Kiehart, D. P., & Edwards, G. S. (2003). Forces for Morphogenesis Investigated with Laser Microsurgery and Quantitative Modeling. *Science*, *300*(5616), 145–149. Retrieved from https://www.science.org/doi/10.1126/science.1079552
132. Iwata, J., Parada, C., & Chai, Y. (2011). The mechanism of TGF-β signaling during palate development. *Oral Diseases*, *17*(8), 733–744.
133. Jacinto, A., Wood, W., Balayo, T., Turmaine, M., Martinez-Arias, A., & Martin, P. (2000). Dynamic actin-based epithelial adhesion and cell matching during Drosophila dorsal closure. *Current Biology*, *10*(22), 1420–1426. Retrieved from https://linkinghub.elsevier.com/retrieve/pii/S096098220000796X
134. Jacinto, A., Woolner, S., & Martin, P. (2002). Dynamic Analysis of Dorsal Closure in Drosophila From Genetics to Cell Biology. *Developmental Cell*, *3*(1), 9–19.
135. James, A., Lee, C., Williams, A. M., Angileri, K., Lathrop, K. L., & Gross, J. M. (2016). The hyaloid vasculature facilitates basement membrane breakdown during choroid fissure closure in the zebrafish eye. *Developmental Biology*, *419*(2), 262–272.
136. Jena, N., Martín-Seisdedos, C., McCue, P., & Croce, C. M. (1997). BMP7 null mutation in mice: developmental defects in skeleton, kidney, and eye. *Experimental Cell Research*, *230*(1), 28–37.
137. Kane, D. A., McFarland, K. N., & Warga, R. M. (2005). Mutations in half baked/E-cadherin block cell behaviors that are necessary for teleost epiboly. *Development*, *132*(5), 1105–1116. Retrieved from https://doi.org/10.1242/dev.01668
138. Kee, Y., Hwang, B. J., Sternberg, P. W., & Bronner-Fraser, M. (2007). Evolutionary conservation of cell migration genes: from nematode neurons to vertebrate neural crest. *Genes & Development*, *21*(4), 391–396. Retrieved from https://www.ncbi.nlm.nih.gov/pmc/articles/PMC1804327/
139. Keller, R., Davidson, L. A., & Shook, D. R. (2003). How we are shaped: The biomechanics of gastrulation. *Differentiation*, *71*(3), 171–205. Retrieved from https://www.sciencedirect.com/science/article/pii/S0301468109602772
140. Keller, R. E. (1981). An experimental analysis of the role of bottle cells and the deep marginal zone in gastrulation of Xenopus laevis. *Journal of Experimental Zoology*, *216*(1), 81–101. Retrieved from https://onlinelibrary.wiley.com/doi/abs/10.1002/jez.1402160109
141. Keller, R., Jr, W. H. C., & Griffin, F. (2012). *Gastrulation: Movements, Patterns and Molecules*. Springer Science & Business Media.

142. Kida, Y., Maeda, Y., Shiraishi, T., Suzuki, T., & Ogura, T. (2004). Chick Dach1 interacts with the Smad complex and Sin3a to control AER formation and limb development along the proximodistal axis. *Development*, *131*(17), 4179–4187. Retrieved from https://doi.org/10.1242/dev.01252
143. Kiehart, D. P. (1999). Wound healing: The power of the purse string. *Current biology: CB*, *9*(16), R602-605.
144. Kiehart, Daniel P., Crawford, J. M., Aristotelous, A., Venakides, S., & Edwards, G. S. (2017). Cell Sheet Morphogenesis: Dorsal Closure in Drosophila melanogaster as a Model System. *Annual review of cell and developmental biology*, *33*, 169–202. Retrieved from https://www.ncbi.nlm.nih.gov/pmc/articles/PMC6524656/
145. Kim, Daehwan, Langmead, B., & Salzberg, S. L. (2015). HISAT: a fast spliced aligner with low memory requirements. *Nature Methods*, *12*(4), 357–360. Retrieved from https://www.nature.com/articles/nmeth.3317
146. Kim, Do, Xing, T., Yang, Z., Dudek, R., Lu, Q., & Chen, Y.-H. (2017). Epithelial Mesenchymal Transition in Embryonic Development, Tissue Repair and Cancer: A Comprehensive Overview. *Journal of Clinical Medicine*, *7*(1), 1. Retrieved from http://www.mdpi.com/2077-0383/7/1/1
147. Kim, Y.-K., Lee, H., Ismail, T., Kim, Y., & Lee, H.-S. (2020). Dach1 regulates neural crest migration during embryonic development. *Biochemical and Biophysical Research Communications*, *527*(4), 896–901. Retrieved from https://www.sciencedirect.com/science/article/pii/S0006291X20309141
148. Kirschner, M. W., & Mitchison, T. (1986). Microtubule dynamics. *Nature*, *324*(6098), 621–621. Retrieved from https://www.nature.com/articles/324621a0
149. Kluth, D., & Fiegel, H. (2003). The embryology of the foregut. *Seminars in Pediatric Surgery*, *12*(1), 3–9. Retrieved from https://www.sciencedirect.com/science/article/pii/S105585860370002X
150. Knickmeyer, M. D., Mateo, J. L., Eckert, P., Roussa, E., Rahhal, B., Zuniga, A., Krieglstein, K., et al. (2018). TGFβ-facilitated optic fissure fusion and the role of bone morphogenetic protein antagonism. *Open Biology*, *8*(3), 170134.
151. Kosodo, Y., Suetsugu, T., Suda, M., Mimori-Kiyosue, Y., Toida, K., Baba, S. A., Kimura, A., et al. (2011). Regulation of interkinetic nuclear migration by cell cycle-coupled active and passive mechanisms in the developing brain. *The EMBO Journal*, *30*(9), 1690–1704. Retrieved from https://www.embopress.org/doi/full/10.1038/emboj.2011.81
152. Kotini, M., Barriga, E. H., Leslie, J., Gentzel, M., Rauschenberger, V., Schambony, A., & Mayor, R. (2018). Gap junction protein Connexin-43 is a direct transcriptional regulator of N-cadherin in vivo. *Nature Communications*, *9*(1), 3846. Retrieved from https://www.nature.com/articles/s41467-018-06368-x
153. Krens, S. F. G., & Heisenberg, C.-P. (2011). Cell sorting in development. *Current topics in developmental biology*, *95*, 189–213. Retrieved from https://doi.org/10.1016/B978-0-12-385065-2.00006-2
154. LaBonne, C., & Bronner-Fraser, M. (1999). Molecular Mechanisms of Neural Crest Formation. *Annual Review of Cell and Developmental Biology*, *15*(1), 81–112. Retrieved from https://www.annualreviews.org/doi/10.1146/annurev.cellbio.15.1.81

155. Ladher, R. K. (2017). Changing shape and shaping change: Inducing the inner ear. *Seminars in Cell & Developmental Biology*, *65*, 39–46.
156. Ladher, R. K., O'Neill, P., & Begbie, J. (2010). From shared lineage to distinct functions: the development of the inner ear and epibranchial placodes. *Development*, *137*(11), 1777–1785.
157. Lakoff, G., & Johnson, M. (2003, April 5). Metaphors We Live By, Lakoff, Johnson. Retrieved February 2, 2025, from https://press.uchicago.edu/ucp/books/book/chicago/M/bo3637992.html
158. Lane, M. C., & Sheets, M. D. (2002). Rethinking axial patterning in amphibians. *Developmental Dynamics*, *225*(4), 434–447. Retrieved from https://onlinelibrary.wiley.com/doi/abs/10.1002/dvdy.10182
159. Latimer, A., & Jessen, J. R. (2010). Extracellular matrix assembly and organization during zebrafish gastrulation. *Matrix Biology: Journal of the International Society for Matrix Biology*, *29*(2), 89–96.
160. Law, C. W., Chen, Y., Shi, W., & Smyth, G. K. (2014). voom: precision weights unlock linear model analysis tools for RNA-seq read counts. *Genome Biology*, *15*(2), R29. Retrieved from https://doi.org/10.1186/gb-2014-15-2-r29
161. Leathers, T. A., & Rogers, C. D. (2022). Time to go: neural crest cell epithelial-to-mesenchymal transition. *Development*, *149*(15), dev200712. Retrieved from https://doi.org/10.1242/dev.200712
162. Lee, J. M., Dedhar, S., Kalluri, R., & Thompson, E. W. (2006). The epithelial–mesenchymal transition: new insights in signaling, development, and disease. *The Journal of Cell Biology*, *172*(7), 973–981.
163. Leptin, M. (1991). twist and snail as positive and negative regulators during Drosophila mesoderm development. *Genes & Development*, *5*(9), 1568–1576. Retrieved from http://genesdev.cshlp.org/content/5/9/1568
164. Leptin, Maria. (2005). Gastrulation Movements: the Logic and the Nuts and Bolts. *Developmental Cell*, *8*(3), 305–320. Retrieved from https://www.cell.com/developmental-cell/abstract/S1534-5807(05)00054-7
165. Levayer, R., & Lecuit, T. (2013). Oscillation and Polarity of E-Cadherin Asymmetries Control Actomyosin Flow Patterns during Morphogenesis. *Developmental Cell*, *26*(2), 162–175. Retrieved from https://www.sciencedirect.com/science/article/pii/S1534580713003833
166. Levayer, R., Pelissier-Monier, A., & Lecuit, T. (2011). Spatial regulation of Dia and Myosin-II by RhoGEF2 controls initiation of E-cadherin endocytosis during epithelial morphogenesis. *Nature Cell Biology*, *13*(5), 529–540.
167. Li, J., Perfetto, M., Neuner, R., Bahudhanapati, H., Christian, L., Mathavan, K., Bridges, L. C., et al. (2018). Xenopus ADAM19 regulates Wnt signaling and neural crest specification by stabilizing ADAM13. *Development*, *145*(7), dev158154. Retrieved from https://doi.org/10.1242/dev.158154
168. Liao, Y., Smyth, G. K., & Shi, W. (2014). featureCounts: an efficient general purpose program for assigning sequence reads to genomic features. *Bioinformatics*, *30*(7), 923–930. Retrieved from https://doi.org/10.1093/bioinformatics/btt656
169. Lillie, F. R. (1908). *The Development of the chick*. H. Holt and Company.
170. Lin, Z., Cantos, R., Patente, M., & Wu, D. K. (2005). Gbx2 is required for the morphogenesis of the mouse inner ear: a downstream candidate of hindbrain signaling. *Development (Cambridge, England)*, *132*(10), 2309–2318.

171. Liu, J.-P., & Jessell, T. M. (1998). A role for rhoB in the delamination of neural crest cells from the dorsal neural tube. *Development*, *125*(24), 5055–5067. Retrieved from https://doi.org/10.1242/dev.125.24.5055
172. Liu, R., Holik, A. Z., Su, S., Jansz, N., Chen, K., Leong, H. S., Blewitt, M. E., et al. (2015). Why weight? Modelling sample and observational level variability improves power in RNA-seq analyses. *Nucleic Acids Research*, *43*(15), e97. Retrieved from https://doi.org/10.1093/nar/gkv412
173. Lu, H., Sokolow, A., Kiehart, D. P., & Edwards, G. S. (2015). Remodeling Tissue Interfaces and the Thermodynamics of Zipping during Dorsal Closure in *Drosophila*. *Biophysical Journal*, *109*(11), 2406–2417. Retrieved from https://www.sciencedirect.com/science/article/pii/S0006349515010565
174. Lusk, S., & Kwan, K. M. (2022). Pax2a, but not pax2b, influences cell survival and periocular mesenchyme localization to facilitate zebrafish optic fissure closure. *Developmental Dynamics: An Official Publication of the American Association of Anatomists*, *251*(4), 625–644.
175. Maczkowiak, F., Matéos, S., Wang, E., Roche, D., Harland, R., & Monsoro-Burq, A. H. (2010). The Pax3 and Pax7 paralogs cooperate in neural and neural crest patterning using distinct molecular mechanisms, in *Xenopus laevis* embryos. *Developmental Biology*, *340*(2), 381–396. Retrieved from https://www.sciencedirect.com/science/article/pii/S0012160610000394
176. Maj, E., Künneke, L., Loresch, E., Grund, A., Melchert, J., Pieler, T., Aspelmeier, T., et al. (2016). Controlled levels of canonical Wnt signaling are required for neural crest migration. *Developmental Biology*, *417*(1), 77–90. Retrieved from https://www.sciencedirect.com/science/article/pii/S0012160615300920
177. Mak, L. L. (1978). Ultrastructural studies of amphibian neural fold fusion. *Developmental Biology*, *65*(2), 435–446. Retrieved from https://www.sciencedirect.com/science/article/pii/0012160678900398
178. Manohar, S., Camacho-Magallanes, A., Echeverria, C., & Rogers, C. D. (2020). Cadherin-11 Is Required for Neural Crest Specification and Survival. *Frontiers in Physiology*, *11*. Retrieved from https://www.frontiersin.org/journals/physiology/articles/10.3389/fphys.2020.563372/full
179. Martin, P., & Parkhurst, S. M. (2004). Parallels between tissue repair and embryo morphogenesis. *Development (Cambridge, England)*, *131*(13), 3021–3034.
180. Martin, P., & Wood, W. (2002). Epithelial fusions in the embryo. *Current Opinion in Cell Biology*, *14*(5), 569–574. Retrieved from https://www.sciencedirect.com/science/article/pii/S0955067402003691
181. Martínez-Morales, P. L., Corral, R. D. del, Olivera-Martínez, I., Quiroga, A. C., Das, R. M., Barbas, J. A., Storey, K. G., et al. (2011). FGF and retinoic acid activity gradients control the timing of neural crest cell emigration in the trunk. *Journal of Cell Biology*, *194*(3), 489–503. Retrieved from https://doi.org/10.1083/jcb.201011077
182. Masai, I., Lele, Z., Yamaguchi, M., Komori, A., Nakata, A., Nishiwaki, Y., Wada, H., et al. (2003). N-cadherin mediates retinal lamination, maintenance of forebrain compartments and patterning of retinal neurites. *Development (Cambridge, England)*, *130*(11), 2479–2494.

183. Mason, F. M., Tworoger, M., & Martin, A. C. (2013). Apical domain polarization localizes actin-myosin activity to drive ratchet-like apical constriction. *Nature cell biology*, *15*(8), 926–936. Retrieved from https://www.ncbi.nlm.nih.gov/pmc/articles/PMC3736338/
184. Massarwa, R., & Niswander, L. (2013). In toto live imaging of mouse morphogenesis and new insights into neural tube closure. *Development*, *140*(1), 226–236. Retrieved from https://doi.org/10.1242/dev.085001
185. Matamoro-Vidal, A., Cumming, T., Davidović, A., Levillayer, F., & Levayer, R. (2024). Patterned apoptosis has an instructive role for local growth and tissue shape regulation in a fast-growing epithelium. *Current Biology*, *34*(2), 376-388.e7. Retrieved from https://www.sciencedirect.com/science/article/pii/S0960982223016871
186. Mayor, R., Morgan, R., & Sargent, M. G. (1995). Induction of the prospective neural crest of Xenopus. *Development (Cambridge, England)*, *121*(3), 767–777.
187. McLarren, K. W., Litsiou, A., & Streit, A. (2003). DLX5 positions the neural crest and preplacode region at the border of the neural plate. *Developmental Biology*, *259*(1), 34–47. Retrieved from https://www.sciencedirect.com/science/article/pii/S0012160603001775
188. McMahon, A., Supatto, W., Fraser, S. E., & Stathopoulos, A. (2008). Dynamic analyses of Drosophila gastrulation provide insights into collective cell migration. *Science (New York, N.Y.)*, *322*(5907), 1546–1550.
189. Meier, S. (1978a). Development of the embryonic chick otic placode. I. Light microscopic analysis. *The Anatomical Record*, *191*(4), 447–458. Retrieved from https://onlinelibrary.wiley.com/doi/abs/10.1002/ar.1091910405
190. Meier, S. (1978b). Development of the embryonic chick otic placode. II. Electron microscopic analysis. *The Anatomical Record*, *191*(4), 459–477. Retrieved from https://onlinelibrary.wiley.com/doi/abs/10.1002/ar.1091910406
191. Millard, T. H., & Martin, P. (2008). Dynamic analysis of filopodial interactions during the zippering phase of *Drosophila* dorsal closure. *Development*, *135*(4), 621–626. Retrieved from https://journals.biologists.com/dev/article/135/4/621/64908/Dynamic-analysis-of-filopodial-interactions-during
192. Molè, M. A., Galea, G. L., Rolo, A., Weberling, A., Nychyk, O., Castro, S. C. D., Savery, D., et al. (2020). Integrin-Mediated Focal Anchorage Drives Epithelial Zippering during Mouse Neural Tube Closure. *Developmental Cell*, *52*(3), 321-334.e6. Retrieved from https://www.sciencedirect.com/science/article/pii/S1534580720300137
193. Monier, B., Gettings, M., Gay, G., Mangeat, T., Schott, S., Guarner, A., & Suzanne, M. (2015). Apico-basal forces exerted by apoptotic cells drive epithelium folding. *Nature*, *518*(7538), 245–248. Retrieved from https://www.nature.com/articles/nature14152
194. Monsonego-Ornan, E., Kosonovsky, J., Bar, A., Roth, L., Fraggi-Rankis, V., Simsa, S., Kohl, A., et al. (2012). Matrix metalloproteinase 9/gelatinase B is required for neural crest cell migration. *Developmental Biology*, *364*(2), 162–177. Retrieved from https://www.sciencedirect.com/science/article/pii/S0012160612000589
195. Monsoro-Burq, A.-H., Wang, E., & Harland, R. (2005). *Msx1* and *Pax3* Cooperate to Mediate FGF8 and WNT Signals during *Xenopus* Neural Crest

Induction. *Developmental Cell*, *8*(2), 167–178. Retrieved from https://www.sciencedirect.com/science/article/pii/S153458070500002X

196. Montero, J.-A., Carvalho, L., Wilsch-Bräuninger, M., Kilian, B., Mustafa, C., & Heisenberg, C.-P. (2005). Shield formation at the onset of zebrafish gastrulation. *Development*, *132*(6), 1187–1198. Retrieved from https://doi.org/10.1242/dev.01667

197. Nair, S., & Schilling, T. F. (2008). Chemokine signaling controls endodermal migration during zebrafish gastrulation. *Science (New York, N.Y.)*, *322*(5898), 89–92.

198. Nakajima, Y., Yamagishi, T., Hokari, S., & Nakamura, H. (2000). Mechanisms involved in valvuloseptal endocardial cushion formation in early cardiogenesis: Roles of transforming growth factor (TGF)-β and bone morphogenetic protein (BMP). *The Anatomical Record*, *258*(2), 119–127. Retrieved from https://onlinelibrary.wiley.com/doi/abs/10.1002/%28SICI%291097-0185%2820000201%29258%3A2%3C119%3A%3AAID-AR1%3E3.0.CO%3B2-U

199. Nakaya, Y., Kuroda, S., Katagiri, Y. T., Kaibuchi, K., & Takahashi, Y. (2004). Mesenchymal-Epithelial Transition during Somitic Segmentation Is Regulated by Differential Roles of Cdc42 and Rac1. *Developmental Cell*, *7*(3), 425–438. Retrieved from https://www.sciencedirect.com/science/article/pii/S1534580704002783

200. Nakaya, Y., & Sheng, G. (2008). Epithelial to mesenchymal transition during gastrulation: An embryological view. *Development, Growth & Differentiation*, *50*(9), 755–766. Retrieved from https://onlinelibrary.wiley.com/doi/abs/10.1111/j.1440-169X.2008.01070.x

201. Nakaya, Y., & Sheng, G. (2009). An amicable separation: Chick's way of doing EMT. *Cell Adhesion & Migration*, *3*(2), 160–163.

202. Narasimha, M., & Brown, N. H. (2004). Novel Functions for Integrins in Epithelial Morphogenesis. *Current Biology*, *14*(5), 381–385. Retrieved from https://www.sciencedirect.com/science/article/pii/S0960982204000880

203. Narita, T., Nishimatsu, S., Wada, N., & Nohno, T. (2007). A Wnt3a variant participates in chick apical ectodermal ridge formation: Distinct biological activities of Wnt3a splice variants in chick limb development. *Development, Growth & Differentiation*, *49*(6), 493–501. Retrieved from https://onlinelibrary.wiley.com/doi/abs/10.1111/j.1440-169X.2007.00938.x

204. Nelson, W. J. (2009). Remodeling Epithelial Cell Organization: Transitions Between Front–Rear and Apical–Basal Polarity. *Cold Spring Harbor Perspectives in Biology*, *1*(1), a000513. Retrieved from https://www.ncbi.nlm.nih.gov/pmc/articles/PMC2742086/

205. Newgreen, D. F., & Thompson, E. W. (2017). Return of EMT to the Land Downunder: TEMTIA-VII, Melbourne, 2015. *Cells Tissues Organs*, *203*(2), 69–70.

206. Niebert, K., & Gropengiesser, H. (2015). Understanding Starts in the Mesocosm: Conceptual metaphor as a framework for external representations in science teaching. *International Journal of Science Education*, *37*(5–6), 903–933.

207. Nieto, M. A., Sargent, M. G., Wilkinson, D. G., & Cooke, J. (1994). Control of cell behavior during vertebrate development by Slug, a zinc finger gene. *Science (New York, N.Y.)*, *264*(5160), 835–839.

208. Nieto, M. Angela. (2002). The snail superfamily of zinc-finger transcription factors. *Nature Reviews Molecular Cell Biology*, *3*(3), 155–166. Retrieved from https://www.nature.com/articles/nrm757
209. Nieto, M. Angela, Huang, R. Y.-J., Jackson, R. A., & Thiery, J. P. (2016). EMT: 2016. *Cell*, *166*(1), 21–45. Retrieved from https://www.sciencedirect.com/science/article/pii/S0092867416307966
210. Nikolopoulou, E., Galea, G. L., Rolo, A., Greene, N. D. E., & Copp, A. J. (2017). Neural tube closure: cellular, molecular and biomechanical mechanisms. *Development*, *144*(4), 552–566. Retrieved from https://doi.org/10.1242/dev.145904
211. Nikolopoulou, E., Hirst, C. S., Galea, G., Venturini, C., Moulding, D., Marshall, A. R., Rolo, A., et al. (2019). Spinal neural tube closure depends on regulation of surface ectoderm identity and biomechanics by Grhl2. *Nature Communications*, *10*(1), 2487. Retrieved from https://www.nature.com/articles/s41467-019-10164-6
212. Nishimura, T., Honda, H., & Takeichi, M. (2012). Planar cell polarity links axes of spatial dynamics in neural-tube closure. *Cell*, *149*(5), 1084–1097.
213. Nishioka, R., Itoh, S., Gui, T., Gai, Z., Oikawa, K., Kawai, M., Tani, M., et al. (2010). SNAIL induces epithelial-to-mesenchymal transition in a human pancreatic cancer cell line (BxPC3) and promotes distant metastasis and invasiveness in vivo. *Experimental and Molecular Pathology*, *89*(2), 149–157.
214. Ocaña, O. H., Córcoles, R., Fabra, A., Moreno-Bueno, G., Acloque, H., Vega, S., Barrallo-Gimeno, A., et al. (2012). Metastatic colonization requires the repression of the epithelial-mesenchymal transition inducer Prrx1. *Cancer Cell*, *22*(6), 709–724.
215. Oda, H., Tsukita, S., & Takeichi, M. (1998). Dynamic Behavior of the Cadherin-Based Cell–Cell Adhesion System during*Drosophila*Gastrulation. *Developmental Biology*, *203*(2), 435–450. Retrieved from https://www.sciencedirect.com/science/article/pii/S0012160698990479
216. Pai, Y.-J., Abdullah, N. L., Mohd.-Zin, S. W., Mohammed, R. S., Rolo, A., Greene, N. D. E., Abdul-Aziz, N. M., et al. (2012). Epithelial fusion during neural tube morphogenesis. *Birth defects research. Part A, Clinical and molecular teratology*, *94*(10), 817–823. Retrieved from https://www.ncbi.nlm.nih.gov/pmc/articles/PMC3629791/
217. Patel, A., & Sowden, J. C. (2019). Genes and pathways in optic fissure closure. *Seminars in Cell & Developmental Biology*, *91*, 55–65. Retrieved from https://www.sciencedirect.com/science/article/pii/S1084952117301490
218. Peralta, X. G., Toyama, Y., Hutson, M. S., Montague, R., Venakides, S., Kiehart, D. P., & Edwards, G. S. (2007). Upregulation of Forces and Morphogenic Asymmetries in Dorsal Closure during Drosophila Development. *Biophysical Journal*, *92*(7), 2583–2596. Retrieved from https://www.ncbi.nlm.nih.gov/pmc/articles/PMC1864829/
219. Perez-Moreno, M., & Fuchs, E. (2006). Catenins: Keeping Cells from Getting Their Signals Crossed. *Developmental cell*, *11*(5), 601–612. Retrieved from https://www.ncbi.nlm.nih.gov/pmc/articles/PMC2405914/
220. Pézeron, G., Mourrain, P., Courty, S., Ghislain, J., Becker, T. S., Rosa, F. M., & David, N. B. (2008). Live analysis of endodermal layer formation identifies random walk as a novel gastrulation movement. *Current biology: CB*, *18*(4), 276–281.

221. Piacentino, M. L., Hutchins, E. J., & Bronner, M. E. (2021). Essential function and targets of BMP signaling during midbrain neural crest delamination. *Developmental Biology*, *477*, 251–261. Retrieved from https://www.sciencedirect.com/science/article/pii/S0012160621001457
222. Piloto, S., & Schilling, T. F. (2010). Ovo1 links Wnt signaling with N-cadherin localization during neural crest migration. *Development*, *137*(12), 1981–1990. Retrieved from https://doi.org/10.1242/dev.048439
223. Pocha, S. M., & Montell, D. J. (2014). Cellular and molecular mechanisms of single and collective cell migrations in Drosophila: themes and variations. *Annual Review of Genetics*, *48*, 295–318.
224. Powell, D. R., Williams, J. S., Hernandez-Lagunas, L., Salcedo, E., O'Brien, J. H., & Artinger, K. B. (2015). Cdon promotes neural crest migration by regulating N-cadherin localization. *Developmental Biology*, *407*(2), 289–299. Retrieved from https://www.sciencedirect.com/science/article/pii/S001216061530097X
225. Pyrgaki, C., Liu, A., & Niswander, L. (2011). Grainyhead-like 2 regulates neural tube closure and adhesion molecule expression during neural fold fusion. *Developmental Biology*, *353*(1), 38–49. Retrieved from https://www.sciencedirect.com/science/article/pii/S0012160611001448
226. Pyrgaki, C., Trainor, P., Hadjantonakis, A.-K., & Niswander, L. (2010a). Dynamic imaging of mammalian neural tube closure. *Developmental Biology*, *344*(2), 941–947. Retrieved from https://linkinghub.elsevier.com/retrieve/pii/S0012160610008304
227. Pyrgaki, C., Trainor, P., Hadjantonakis, A.-K., & Niswander, L. (2010b). Dynamic imaging of mammalian neural tube closure. *Developmental Biology*, *344*(2), 941–947.
228. Ray, H. J., & Niswander, L. (2012). Mechanisms of tissue fusion during development. *Development*, *139*(10), 1701–1711. Retrieved from https://doi.org/10.1242/dev.068338
229. Rekler, D., & Kalcheim, C. (2022). Completion of neural crest cell production and emigration is regulated by retinoic-acid-dependent inhibition of BMP signaling. (["Carole LaBonne", "Didier YR Stainier", & "Laura Kerosuo"], Eds.)*eLife*, *11*, e72723. Retrieved from https://doi.org/10.7554/eLife.72723
230. Reynolds, A. S. (2018, June 3). The Third Lens: Metaphor and the Creation of Modern Cell Biology, Reynolds. Retrieved February 2, 2025, from https://press.uchicago.edu/ucp/books/book/chicago/T/bo28301818.html
231. Reynolds, A. S. (2022, December 12). Master your metaphors. *Master your metaphors*. Feature, . Retrieved January 25, 2025, from https://www.rsb.org.uk/biologist-features/master-your-metaphors
232. Rifat, Y., Parekh, V., Wilanowski, T., Hislop, N. R., Auden, A., Ting, S. B., Cunningham, J. M., et al. (2010). Regional neural tube closure defined by the *Grainy head*-like transcription factors. *Developmental Biology*, *345*(2), 237–245. Retrieved from https://www.sciencedirect.com/science/article/pii/S0012160610009486
233. Robertis, E. M. D., Larraín, J., Oelgeschläger, M., & Wessely, O. (2000). THE ESTABLISHMENT OF SPEMANN'S ORGANIZER AND PATTERNING OF THE VERTEBRATE EMBRYO. *Nature reviews. Genetics*, *1*(3), 171–181. Retrieved from https://www.ncbi.nlm.nih.gov/pmc/articles/PMC2291143/

234. Robledo, R. F., & Lufkin, T. (2006). Dlx5 and Dlx6 homeobox genes are required for specification of the mammalian vestibular apparatus. *Genesis (New York, N.Y.: 2000)*, *44*(9), 425–437. Retrieved from https://onlinelibrary.wiley.com/doi/abs/10.1002/dvg.20233
235. Rodriguez-Diaz, A., Toyama, Y., Abravanel, D. L., Wiemann, J. M., Wells, A. R., Tulu, U. S., Edwards, G. S., et al. (2008). Actomyosin purse strings: renewable resources that make morphogenesis robust and resilient. *HFSP Journal*, *2*(4), 220–237. Retrieved from https://www.ncbi.nlm.nih.gov/pmc/articles/PMC2639939/
236. Roellig, D., Tan-Cabugao, J., Esaian, S., & Bronner, M. E. (2017). Dynamic transcriptional signature and cell fate analysis reveals plasticity of individual neural plate border cells. (["Alejandro Sánchez Alvarado"], Ed.)*eLife*, *6*, e21620. Retrieved from https://doi.org/10.7554/eLife.21620
237. Roellig, D., Theis, S., Proag, A., Allio, G., Bénazéraf, B., Gros, J., & Suzanne, M. (2022). Force-generating apoptotic cells orchestrate avian neural tube bending. *Developmental Cell*, *57*(6), 707-718.e6. Retrieved from https://www.sciencedirect.com/science/article/pii/S1534580722001228
238. Roeth, J. F., Sawyer, J. K., Wilner, D. A., & Peifer, M. (2009). Rab11 Helps Maintain Apical Crumbs and Adherens Junctions in the Drosophila Embryonic Ectoderm. (["Andreas Bergmann"], Ed.)*PLoS ONE*, *4*(10), e7634. Retrieved from https://dx.plos.org/10.1371/journal.pone.0007634
239. Rogers, C. D., Sorrells, L. K., & Bronner, M. E. (2018). A catenin-dependent balance between N-cadherin and E-cadherin controls neuroectodermal cell fate choices. *Mechanisms of Development*, *152*, 44–56. Retrieved from https://www.sciencedirect.com/science/article/pii/S0925477318300819
240. Rolo, A., Savery, D., Escuin, S., Castro, S. C. de, Armer, H. E., Munro, P. M., Molè, M. A., et al. (2016). Regulation of cell protrusions by small GTPases during fusion of the neural folds. (["Marianne E Bronner"], Ed.)*eLife*, *5*, e13273. Retrieved from https://doi.org/10.7554/eLife.13273
241. Röper, K. (2015). Integration of cell-cell adhesion and contractile actomyosin activity during morphogenesis. *Current topics in developmental biology*, *112*, 103–127. Retrieved from https://doi.org/10.1016/bs.ctdb.2014.11.017
242. Rosenblatt, J., Raff, M. C., & Cramer, L. P. (2001). An epithelial cell destined for apoptosis signals its neighbors to extrude it by an actin- and myosin-dependent mechanism. *Current Biology*, *11*(23), 1847–1857. Retrieved from https://www.sciencedirect.com/science/article/pii/S0960982201005875
243. Runyan, R. B., & Markwald, R. R. (1983). Invasion of mesenchyme into three-dimensional collagen gels: A regional and temporal analysis of interaction in embryonic heart tissue. *Developmental Biology*, *95*(1), 108–114. Retrieved from https://www.sciencedirect.com/science/article/pii/0012160683900106
244. Sai, XiaoRei, & Ladher, R. K. (2008). FGF signaling regulates cytoskeletal remodeling during epithelial morphogenesis. *Current biology: CB*, *18*(13), 976–981.
245. Sai, Xiaorei, & Ladher, R. K. (2015a). Early steps in inner ear development: induction and morphogenesis of the otic placode. *Frontiers in Pharmacology*, *6*, 19.
246. Sai, Xiaorei, & Ladher, R. K. (2015b). Early steps in inner ear development: induction and morphogenesis of the otic placode. *Frontiers in*

Pharmacology, *6*, 19. Retrieved from https://www.frontiersin.org/journals/pharmacology/articles/10.3389/fphar.2015.00019/full

247. Sai, Xiaorei, Yonemura, S., & Ladher, R. K. (2014). Junctionally restricted RhoA activity is necessary for apical constriction during phase 2 inner ear placode invagination. *Developmental Biology*, *394*(2), 206–216. Retrieved from https://www.sciencedirect.com/science/article/pii/S0012160614004138

248. Saias, L., Swoger, J., D'Angelo, A., Hayes, P., Colombelli, J., Sharpe, J., Salbreux, G., et al. (2015). Decrease in Cell Volume Generates Contractile Forces Driving Dorsal Closure. *Developmental Cell*, *33*(5), 611–621. Retrieved from https://linkinghub.elsevier.com/retrieve/pii/S1534580715002129

249. Sauer, F. C. (1936). The interkinetic migration of embryonic epithelial nuclei. *Journal of Morphology*, *60*(1), 1–11. Retrieved from https://onlinelibrary.wiley.com/doi/abs/10.1002/jmor.1050600102

250. Scarpa, E., Szabó, A., Bibonne, A., Theveneau, E., Parsons, M., & Mayor, R. (2015). Cadherin Switch during EMT in Neural Crest Cells Leads to Contact Inhibition of Locomotion via Repolarization of Forces. *Developmental Cell*, *34*(4), 421–434. Retrieved from https://www.sciencedirect.com/science/article/pii/S1534580715004013

251. Schmidt, C., Christ, B., Maden, M., Brand-Saberi, B., & Patel, K. (2001). Regulation of Epha4 expression in paraxial and lateral plate mesoderm by ectoderm-derived signals. *Developmental Dynamics: An Official Publication of the American Association of Anatomists*, *220*(4), 377–386. Retrieved from https://onlinelibrary.wiley.com/doi/abs/10.1002/dvdy.1117

252. Schneeberger, E. E., & Lynch, R. D. (2004). The tight junction: a multifunctional complex. *American Journal of Physiology. Cell Physiology*, *286*(6), C1213-1228.

253. Schöck, F., & Perrimon, N. (2002). Molecular Mechanisms of Epithelial Morphogenesis. *Annual Review of Cell and Developmental Biology*, *18*(Volume 18, 2002), 463–493. Retrieved from https://www.annualreviews.org/content/journals/10.1146/annurev.cellbio.18.022602.131838

254. Schoenwolf, G. C., & Sheard, P. (1990). Fate mapping the avian epiblast with focal injections of a fluorescent-histochemical marker: ectodermal derivatives. *The Journal of Experimental Zoology*, *255*(3), 323–339.

255. Schoenwolf, Gary C. (1979). Observations on closure of the neuropores in the chick embryo. *American Journal of Anatomy*, *155*(4), 445–465. Retrieved from https://onlinelibrary.wiley.com/doi/abs/10.1002/aja.1001550404

256. Schoenwolf, Gary C. (1991). Cell movements driving neurulation in avian embryos. *Development*, *113*(Supplement_2), 157–168. Retrieved from https://doi.org/10.1242/dev.113.Supplement_2.157

257. Seal, S., & Monsoro-Burq, A. H. (2020). Insights Into the Early Gene Regulatory Network Controlling Neural Crest and Placode Fate Choices at the Neural Border. *Frontiers in Physiology*, *11*. Retrieved from https://www.frontiersin.org/journals/physiology/articles/10.3389/fphys.2020.608812/full

258. See, A. W.-M., & Clagett-Dame, M. (2009). The temporal requirement for vitamin A in the developing eye: mechanism of action in optic fissure closure and new roles for the vitamin in regulating cell proliferation and adhesion in the embryonic retina. *Developmental Biology*, *325*(1), 94–105.

259. Selleck, M. A., & Bronner-Fraser, M. (1995). Origins of the avian neural crest: the role of neural plate-epidermal interactions. *Development (Cambridge, England)*, *121*(2), 525–538.
260. Senga, K., Mostov, K. E., Mitaka, T., Miyajima, A., & Tanimizu, N. (2012). Grainyhead-like 2 regulates epithelial morphogenesis by establishing functional tight junctions through the organization of a molecular network among claudin3, claudin4, and Rab25. *Molecular Biology of the Cell*, *23*(15), 2845–2855. Retrieved from https://www.molbiolcell.org/doi/10.1091/mbc.e12-02-0097
261. Seo, H.-C., Sætre, B. O., Håvik, B., Ellingsen, S., & Fjose, A. (1998). The zebrafish *Pax3* and *Pax7* homologues are highly conserved, encode multiple isoforms and show dynamic segment-like expression in the developing brain. *Mechanisms of Development*, *70*(1), 49–63. Retrieved from https://www.sciencedirect.com/science/article/pii/S0925477397001755
262. Shamir, E. R., Pappalardo, E., Jorgens, D. M., Coutinho, K., Tsai, W.-T., Aziz, K., Auer, M., et al. (2014). Twist1-induced dissemination preserves epithelial identity and requires E-cadherin. *The Journal of Cell Biology*, *204*(5), 839–856.
263. Shaw, T. J., & Martin, P. (2016). Wound repair: a showcase for cell plasticity and migration. *Current Opinion in Cell Biology*, *42*, 29–37. Retrieved from https://www.sciencedirect.com/science/article/pii/S095506741630076X
264. Shih, J., & Keller, R. (1994). Gastrulation in *Xenopus laevis*: involution—a current view. *Seminars in Developmental Biology*, *5*(2), 85–90. Retrieved from https://www.sciencedirect.com/science/article/pii/S1044578184710127
265. Shimizu, T., Yabe, T., Muraoka, O., Yonemura, S., Aramaki, S., Hatta, K., Bae, Y.-K., et al. (2005). E-cadherin is required for gastrulation cell movements in zebrafish. *Mechanisms of Development*, *122*(6), 747–763.
266. Shook, D., & Keller, R. (2003). Mechanisms, mechanics and function of epithelial–mesenchymal transitions in early development. *Mechanisms of Development*, *120*(11), 1351–1383. Retrieved from https://www.sciencedirect.com/science/article/pii/S0925477303002090
267. Slepecky, N. B. (1996). Structure of the Mammalian Cochlea. In ["Peter Dallos", "Arthur N. Popper", & "Richard R. Fay"] (Eds.), *The Cochlea* (pp. 44–129). New York, NY: Springer New York. Retrieved from https://doi.org/10.1007/978-1-4612-0757-3_2
268. Solnica-Krezel, L., & Sepich, D. S. (2012). Gastrulation: making and shaping germ layers. *Annual Review of Cell and Developmental Biology*, *28*, 687–717.
269. Steinberg, M. S. (2007). Differential adhesion in morphogenesis: a modern view. *Current Opinion in Genetics & Development*, *17*(4), 281–286.
270. Stoker, M., & Perryman, M. (1985). An epithelial scatter factor released by embryo fibroblasts. *Journal of Cell Science*, *77*(1), 209–223. Retrieved from https://doi.org/10.1242/jcs.77.1.209
271. Streit, A., & Stern, C. D. (1999). Establishment and maintenance of the border of the neural plate in the chick: involvement of FGF and BMP activity. *Mechanisms of Development*, *82*(1), 51–66. Retrieved from https://www.sciencedirect.com/science/article/pii/S0925477399000131
272. Stundl, J., Bertucci, P. Y., Lauri, A., Arendt, D., & Bronner, M. E. (2021). Evolution of new cell types at the lateral neural border. In ["Scott F.

Gilbert"] (Ed.), *Current Topics in Developmental Biology*, Current Topics in Developmental Biology (Vol. 141, pp. 173–205). Academic Press. Retrieved from https://www.sciencedirect.com/science/article/pii/S0070215320301277

273. Sweeton, D., Parks, S., Costa, M., & Wieschaus, E. (1991). Gastrulation in Drosophila: the formation of the ventral furrow and posterior midgut invaginations. *Development (Cambridge, England)*, *112*(3), 775–789.

274. Takeichi, M. (2014). Dynamic contacts: rearranging adherens junctions to drive epithelial remodelling. *Nature Reviews Molecular Cell Biology*, *15*(6), 397–410. Retrieved from https://www.nature.com/articles/nrm3802

275. Tam, P. P. L., & Behringer, R. R. (1997). Mouse gastrulation: the formation of a mammalian body plan. *Mechanisms of Development*, *68*(1), 3–25. Retrieved from https://www.sciencedirect.com/science/article/pii/S0925477397001238

276. Tam, P. P., Williams, E. A., & Chan, W. Y. (1993). Gastrulation in the mouse embryo: ultrastructural and molecular aspects of germ layer morphogenesis. *Microscopy Research and Technique*, *26*(4), 301–328.

277. Tam, W. L., & Weinberg, R. A. (2013). The epigenetics of epithelial-mesenchymal plasticity in cancer. *Nature Medicine*, *19*(11), 1438–1449. Retrieved from https://www.nature.com/articles/nm.3336

278. Tamilkumar, V. N. (2023). Andrew S. Reynolds, The third lens: metaphor and the creation of modern cell biology, Chicago: the Chicago University Press, 2018. *History and Philosophy of the Life Sciences*, *45*(4), 38.

279. Taneyhill, L. A., Coles, E. G., & Bronner-Fraser, M. (2007). Snail2 directly represses cadherin6B during epithelial-to-mesenchymal transitions of the neural crest. *Development*, *134*(8), 1481–1490. Retrieved from https://doi.org/10.1242/dev.02834

280. Taylor, C., & Dewsbury, B. M. (2018). On the Problem and Promise of Metaphor Use in Science and Science Communication. *Journal of Microbiology & Biology Education*, *19*(1), 10.1128/jmbe.v19i1.1538.

281. Thiery, J. P. (2002). Epithelial–mesenchymal transitions in tumour progression. *Nature Reviews Cancer*, *2*(6), 442–454. Retrieved from https://www.nature.com/articles/nrc822

282. Thiery, J. P., Acloque, H., Huang, R. Y. J., & Nieto, M. A. (2009). Epithelial-Mesenchymal Transitions in Development and Disease. *Cell*, *139*(5), 871–890. Retrieved from https://www.sciencedirect.com/science/article/pii/S0092867409014196

283. Thiery, J. P., & Huang, R. (2005). Linking Epithelial-Mesenchymal Transition to the Well-Known Polarity Protein Par6. *Developmental Cell*, *8*(4), 456–458.

284. Thisse, C., Thisse, B., & Postlethwait, J. H. (1995). Expression of snail2, a second member of the zebrafish snail family, in cephalic mesendoderm and presumptive neural crest of wild-type and spadetail mutant embryos. *Developmental Biology*, *172*(1), 86–99.

285. Thisse, C., Thisse, B., Schilling, T. F., & Postlethwait, J. H. (1993). Structure of the zebrafish snail1 gene and its expression in wild-type, spadetail and no tail mutant embryos. *Development (Cambridge, England)*, *119*(4), 1203–1215.

286. Townes, P. L., & Holtfreter, J. (1955). Directed movements and selective adhesion of embryonic amphibian cells. *Journal of Experimental*

Zoology, *128*(1), 53–120. Retrieved from https://onlinelibrary.wiley.com/doi/abs/10.1002/jez.1401280105

287. Trelstad, R. L., Hay, E. D., & Revel, J.-P. (1967). Cell contact during early morphogenesis in the chick embryo. *Developmental Biology*, *16*(1), 78–106. Retrieved from https://www.sciencedirect.com/science/article/pii/0012160667900188

288. Trelstad, R. L., Revel, J.-P., & Hay, E. D. (1966). TIGHT JUNCTIONS BETWEEN CELLS IN THE EARLY CHICK EMBRYO AS VISUALIZED WITH THE ELECTRON MICROSCOPE. *The Journal of Cell Biology*, *31*(1), C6–C10. Retrieved from https://www.ncbi.nlm.nih.gov/pmc/articles/PMC2107036/

289. Tríbulo, C., Aybar, M. J., Sánchez, S. S., & Mayor, R. (2004). A balance between the anti-apoptotic activity of *Slug* and the apoptotic activity of *msx1* is required for the proper development of the neural crest. *Developmental Biology*, *275*(2), 325–342. Retrieved from https://www.sciencedirect.com/science/article/pii/S0012160604005482

290. Tsai, J. H., Donaher, J. L., Murphy, D. A., Chau, S., & Yang, J. (2012). Spatiotemporal regulation of epithelial-mesenchymal transition is essential for squamous cell carcinoma metastasis. *Cancer Cell*, *22*(6), 725–736.

291. Ulrich, F., & Heisenberg, C.-P. (2008). Probing E-cadherin endocytosis by morpholino-mediated Rab5 knockdown in zebrafish. *Methods in Molecular Biology (Clifton, N.J.)*, *440*, 371–387.

292. Villars, A., & Levayer, R. (2022). Collective effects in epithelial cell death and cell extrusion. *Current Opinion in Genetics & Development*, *72*, 8–14. Retrieved from https://www.sciencedirect.com/science/article/pii/S0959437X21001106

293. Vollmer, G. (1984). Concepts and Approaches in Evolutionary Epistemology, Towards an Evolutionary Theory of Knowledge, 69–121.

294. Wada, A., Kato, K., Uwo, M. F., Yonemura, S., & Hayashi, S. (2007). Specialized extraembryonic cells connect embryonic and extraembryonic epidermis in response to Dpp during dorsal closure in *Drosophila*. *Developmental Biology*, *301*(2), 340–349. Retrieved from https://www.sciencedirect.com/science/article/pii/S0012160606012218

295. Wang, M.-H., & Baskin, L. S. (2008). Endocrine Disruptors, Genital Development, and Hypospadias. *Journal of Andrology*, *29*(5), 499–505. Retrieved from https://onlinelibrary.wiley.com/doi/abs/10.2164/jandrol.108.004945

296. Washausen, S., & Knabe, W. (2019). Chicken embryos share mammalian patterns of apoptosis in the posterior placodal area. *Journal of Anatomy*, *234*(4), 551–563. Retrieved from https://www.ncbi.nlm.nih.gov/pmc/articles/PMC6422804/

297. Waterman, R. E. (1976). Topographical changes along the neural fold associated with neurulation in the hamster and mouse. *American Journal of Anatomy*, *146*(2), 151–171. Retrieved from https://onlinelibrary.wiley.com/doi/abs/10.1002/aja.1001460204

298. Weaver, M. L., Piedade, W. P., Meshram, N. N., & Famulski, J. K. (2020). Hyaloid vasculature and mmp2 activity play a role during optic fissure fusion in zebrafish. *Scientific Reports*, *10*(1), 10136. Retrieved from https://doi.org/10.1038/s41598-020-66451-6

299. Werner, S., Frey, S., Riethdorf, S., Schulze, C., Alawi, M., Kling, L., Vafaizadeh, V., et al. (2013). Dual Roles of the Transcription Factor Grainyhead-like 2 (GRHL2) in Breast Cancer*. *Journal of Biological Chemistry*, *288*(32), 22993–23008. Retrieved from https://www.sciencedirect.com/science/article/pii/S002192582045327X
300. Werth, M., Walentin, K., Aue, A., Schönheit, J., Wuebken, A., Pode-Shakked, N., Vilianovitch, L., et al. (2010a). The transcription factor grainyhead-like 2 regulates the molecular composition of the epithelial apical junctional complex. *Development*, *137*(22), 3835–3845.
301. Werth, M., Walentin, K., Aue, A., Schönheit, J., Wuebken, A., Pode-Shakked, N., Vilianovitch, L., et al. (2010b). The transcription factor grainyhead-like 2 regulates the molecular composition of the epithelial apical junctional complex. *Development*, *137*(22), 3835–3845. Retrieved from https://doi.org/10.1242/dev.055483
302. Winklbauer, R. (2009). Cell adhesion in amphibian gastrulation. *International Review of Cell and Molecular Biology*, *278*, 215–275.
303. Winklbauer, R., & Nagel, M. (1991). Directional mesoderm cell migration in the *Xenopus* gastrula. *Developmental Biology*, *148*(2), 573–589. Retrieved from https://www.sciencedirect.com/science/article/pii/0012160691902758
304. Winklbauer, R., & Schürfeld, M. (1999). Vegetal rotation, a new gastrulation movement involved in the internalization of the mesoderm and endoderm in Xenopus. *Development*, *126*(16), 3703–3713. Retrieved from https://doi.org/10.1242/dev.126.16.3703
305. Wu, C.-Y., & Taneyhill, L. A. (2019). Cadherin-7 mediates proper neural crest cell–placodal neuron interactions during trigeminal ganglion assembly. *genesis*, *57*(1), e23264. Retrieved from https://onlinelibrary.wiley.com/doi/abs/10.1002/dvg.23264
306. Wu, S.-Y., Ferkowicz, M., & McClay, D. R. (2007). Ingression of primary mesenchyme cells of the sea urchin embryo: A precisely timed epithelial mesenchymal transition. *Birth Defects Research Part C: Embryo Today: Reviews*, *81*(4), 241–252. Retrieved from https://onlinelibrary.wiley.com/doi/abs/10.1002/bdrc.20113
307. Yang, A. D., Camp, E. R., Fan, F., Shen, L., Gray, M. J., Liu, W., Somcio, R., et al. (2006). Vascular endothelial growth factor receptor-1 activation mediates epithelial to mesenchymal transition in human pancreatic carcinoma cells. *Cancer Research*, *66*(1), 46–51.
308. Yang, J., Antin, P., Berx, G., Blanpain, C., Brabletz, T., Bronner, M., Campbell, K., et al. (2020). Guidelines and definitions for research on epithelial–mesenchymal transition. *Nature Reviews Molecular Cell Biology*, *21*(6), 341–352. Retrieved from https://doi.org/10.1038/s41580-020-0237-9
309. Yang, J., Mani, S. A., Donaher, J. L., Ramaswamy, S., Itzykson, R. A., Come, C., Savagner, P., et al. (2004). Twist, a master regulator of morphogenesis, plays an essential role in tumor metastasis. *Cell*, *117*(7), 927–939.
310. Yang, X., Dormann, D., Münsterberg, A. E., & Weijer, C. J. (2002). Cell Movement Patterns during Gastrulation in the Chick Are Controlled by Positive and Negative Chemotaxis Mediated by FGF4 and FGF8. *Developmental Cell*, *3*(3), 425–437. Retrieved from https://www.sciencedirect.com/science/article/pii/S1534580702002563

311. Ybot-Gonzalez, P., Gaston-Massuet, C., Girdler, G., Klingensmith, J., Arkell, R., Greene, N. D. E., & Copp, A. J. (2007). Neural plate morphogenesis during mouse neurulation is regulated by antagonism of Bmp signalling. *Development*, *134*(17), 3203–3211. Retrieved from https://doi.org/10.1242/dev.008177
312. Yu, M., Bardia, A., Wittner, B. S., Stott, S. L., Smas, M. E., Ting, D. T., Isakoff, S. J., et al. (2013). Circulating Breast Tumor Cells Exhibit Dynamic Changes in Epithelial and Mesenchymal Composition. *Science*, *339*(6119), 580–584. Retrieved from https://www.science.org/doi/10.1126/science.1228522
313. Yue, Q., Wagstaff, L., Yang, X., Weijer, C., & Münsterberg, A. (2008). Wnt3a-mediated chemorepulsion controls movement patterns of cardiac progenitors and requires RhoA function. *Development*, *135*(6), 1029–1037. Retrieved from https://doi.org/10.1242/dev.015321
314. Zamir, E. A., Rongish, B. J., & Little, C. D. (2008). The ECM Moves during Primitive Streak Formation—Computation of ECM Versus Cellular Motion. *PLOS Biology*, *6*(10), e247. Retrieved from https://journals.plos.org/plosbiology/article?id=10.1371/journal.pbio.0060247
315. Zhou, C. J., Ji, Y., Reynolds, K., McMahon, M., Garland, M. A., Zhang, S., Sun, B., et al. (2020). Non-neural surface ectodermal rosette formation and F-actin dynamics drive mammalian neural tube closure. *Biochemical and Biophysical Research Communications*, *526*(3), 647–653. Retrieved from https://www.sciencedirect.com/science/article/pii/S0006291X20306355
316. Zhu, C., Kong, Z., Wang, B., Cheng, W., Wu, A., & Meng, X. (2019). ITGB3/CD61: a hub modulator and target in the tumor microenvironment. *American Journal of Translational Research*, *11*(12), 7195–7208.
317. Zulueta-Coarasa, T., & Fernandez-Gonzalez, R. (2017). Tension (re)builds: Biophysical mechanisms of embryonic wound repair. *Mechanisms of Development*, *144*, 43–52. Retrieved from https://www.sciencedirect.com/science/article/pii/S0925477316300636

APPENDIX

A. EMT, a metaphorical journey.

Philosophy is a battle against the bewitchment of our intelligence by means of our language.

-Ludwig Wittgenstein, *Philosophical Investigations,* p.47

A.1 Metaphors and Similes

The words metaphors and similes remind us of poetic devices commonly used in literary articles. Their significance in science communication is often overlooked; we have been using these metaphors in science, without consciously acknowledging their existence. They have been used since Robert Hooke first observed cork slices under his primitive microscope and used the word “cell” to describe the miniscule compartments in the section. He used the term “cell” to refer to the small rooms occupied by monks in monasteries. These small rooms were referred to as cells owing to their similarity to the honey comb structure of bee hives. The journey of this humble metaphor, the cell, has now come to an end, and the term now is a dead metaphor. A dead metaphor refers to those metaphors whose original meaning had been replaced by its metaphorical meaning due to the continued usage. For instance, the word cell neither reminds us of the rooms in monasteries nor the combs in bee hives, and hence is a dead metaphor(Reynolds, 2022)

The term metaphor originates from the Greek word metaphora, meta meaning over and pherein meaning to carry(Garfield, 1986; Taylor & Dewsbury, 2018). It is employed as a heuristic device to help us understand and connect abstract or unknown concepts with familiar ones. Aristotle, in his De Poetics, has claimed that, “the greatest thing by far is to be a master of metaphor; it is the one thing that cannot be learnt from

others; and it is also a sign of genius, since a good metaphor implies an intuitive perception of the similarity in the dissimilar. Another poetic device commonly used is the simile. While the use of a simile emphasizes how similar two disparate entities can be, the use of a metaphor provides the reader with an opportunity to interpret how the two entities can be similar in more than one way. An instance that Andrew Reynolds mentions is the ribosome and its function. A simile is, 'the ribosome is like a machine for manufacturing proteins' and a metaphor is, 'the ribosome is a machine for manufacturing proteins'(Reynolds, 2022). In the case of a simile, we see the ribosome as a machine that manufactures proteins but with the use of a metaphor, the reader now has the scope of attributing other properties of a machine to the ribosome. While employing metaphors help us envision and push the limits of existing ideas, they can often mislead or even restrict our perspectives(Alberts, 1998) .

A.2 The journey of metaphors in science.

Metaphors have had a long and tedious journey along with scientific and technological advancements. Through the ages, there have been different schools of thought on whether to accept and continue the use of metaphors in the communication of discoveries or not. The promise of a metaphor can be explained by considering why they were chosen in the first place(Taylor & Dewsbury, 2018) .

According to Lakoff and Johnson's theory, human knowledge is a result of our physical and social experiences. Metaphors is how the human cognition perceives new ideas. They are not mere linguistic aggrandizements, rather they help in the mapping of knowledge from a familiar domain to an unfamiliar one. This is important when we try to understand intangible or abstract concepts by drawing similarities from our embodied experiences(Lakoff & Johnson, 2003). Science, often employs the use of models based on these experiences, as we do so in our everyday interactions (Brown, 2003). According to Gerhard Vollmer, scientific reasoning lies within the range of what we cope up in the real world, the mesocosm (Vollmer, 1984). Based on these theories, authors Niebert and Gropengieber put forth their argument on how the human cognition is not inherently equipped to relate to macro and micro cosmic concepts, thus mandating the use of mesocosm based metaphors for communicating new ideas. "Consider the following constructs where scientists make use of everyday experience

to explain their theories. Robert Hooke was the first to denote the cell using the term ‘cell’ when an image of a piece of cork under his microscope reminded him of the small rooms, or cells, occupied by monks in monasteries. Kepler developed his concept of planetary motion by comparison with a clock. Huygens used water waves to theorise that light is wavelike. Arrhenius described the greenhouse effect by referring to his experience with hot pots. In ever new variations, scientists employ experiences from everyday life to understand scientific phenomena” (p.2) (Niebert & Gropengiesser, 2015). Despite the criticism surrounding the use of metaphors, specifically about their potential to be ambiguous, inaccurate and generative, they have proved their worth as agents of scientific advancements and theories (Taylor & Dewsbury, 2018).

A.3 Metaphors in cell biology: A book review(Tamilkumar, 2023)

Andrew S. Reynolds, *The Third Lens: Metaphor and the Creation of Modern Cell Biology,* Chicago: The Chicago University Press, 2018 (Reynolds, 2018) **.**

The Third Lens is a manual of, and testimony to, the use of metaphors in science. Metaphors are extensions of our thoughts. The dictionary defines a metaphor as a literary device in which a word or a phrase denoting one kind of object or idea is used in place of another to suggest a likeness between them. Andrew Reynolds, a philosopher of science, justifies the use of a metaphor over a simile in science by pointing out that “metaphors encourage us to think of two things not just as similar in some nonessential properties, but as identical in some important essential sense” (p.14).

Indeed, as he shows us in this detailed history of the journey of metaphors in cell biology, this very field may be said to have been born out of metaphor. In his 1665 book Micrographia, Robert Hooke described the porous nature of sections of dead cork plant, noting how the perforations and pores resembled a slightly irregular honeycomb. He eventually called these perforations ‘cells’, the term we now use to represent the basic structural and functional unit of life. The cell of a honeycomb was itself a metaphor drawn from the small rooms of monks. Thus, as Reynolds points out, today’s biological ‘cell’ is a “twice borrowed metaphor” (p. 15).

The often-misleading nature of a metaphor has led some writers to question their utility beyond a heuristic function in the initial phases of scientific discovery. However, Reynolds argues that metaphors "can and do play important roles". When scientists say that "genes are the units of hereditary 'information' transmitted from one generation of organisms to the next", they don't simply mean DNA is similar to information; they mean that "DNA is in some essential sense a form of information". Reynolds illustrates through multiple examples in Chaps. 1 to 4 how influential metaphors have been throughout the history of cell theory and cell biology.

The book's title, The Third Lens, is itself a metaphor for the role that Reynolds argues metaphors have played in the history of cell biology. In this field, metaphors have helped us understand and visualize cells just as much as the ocular and objective lenses of a microscope. The first four chapters of the book focus on particular phases in the of development of cell biology.

The first chapter begins with a brief history of the origins of the term 'cell' in the mid seventeenth century. Reynolds then moves on to show how this metaphor helped frame cell theory in the mid-nineteenth century. Reynolds also discusses the challenges faced by the term 'cell', and how the metaphor was eventually accepted. In the second chapter, Reynolds sheds light on the cell as a chemical laboratory, as a machine, and as an industrial factory. These metaphors encouraged scientists to explore and monetize on the utility of cells for industrial production. This chapter emphasizes how metaphors can also be a form of "experimental technology" (p. 72).Pathologist Rudolf Virchow remarked in 1858 how starch was transformed into sugar in both animal and plant, just as in a factory (p. 63). This is one of the many instances pointed out by Reynolds where cells were deemed similar to human artefacts in the sense that they could be rewired for human benefit.

The development of cell culture techniques in the twentieth century furthered scientific curiosity about cell behaviour. As Reynolds explains in Chap. 3, cells were considered not as autonomous individuals but as complicated social beings capable of organizing themselves as a community (p. 91). The surgeon Alexis Carrel emphasized in 1931 that considering cells as structural elements deprives them of their ability to organize and constitute living wholes. Within an organism they are associated according to certain laws, resulting in what we can refer to as 'cell sociology' (p. 88). The embryologist Rosine Chandebois insisted that embryonic development is not a process consisting of autonomous cells, but rather a social cellular phenomenon

comparable to the history of a developing civilization (p. 97).The ways in which cells form communities, which implies the presence of short and long-range forms of communication and networking, is the theme of the fourth chapter.

Endocrinologist Oscar Hechter, a close associate of the founder of cybernetics, Norbert Wiener, used cybernetics and information theory to explain the effect of hormones on cells. This idea was taken up by biochemist Martin Rodbell, who popularized the idea of signal transduction (p. 119). Reynolds also examines the adoption of techno-morphic metaphors, such as circuits, switches, and signal amplification, in the emerging field of synthetic biology (p. 140).In the last two chapters, Reynolds analyses the philosophical significance of metaphors and their true utility in scientists' quest for knowledge. He argues that metaphors have played an active role in the development of technology. For instance, opening the black box of the cell nucleus with molecular genetics led to the use of terms like 'DNA instructions' and 'blueprints' that later opened up in turn possibilities for 'reprogramming' the genome (p. 87).

Besides showing the reader how metaphors have influenced cell biology, *The Third Lens* is full of examples of how society has shaped which metaphors were used and when. For instance, during the rise of industrial systems of production in Europe, cells came to be seen as chemical laboratories or factories that could be regulated and manipulated for production of a particular compound. Historian Theodore Merz had remarked that physiology and economics joined hands during the Victorian period. The eminent physiologist Claude Bernard described the structure and function of animal organs as factories in an advanced society that provide the various members of the society with means of clothing, heating, feeding, and lighting themselves (p.63). Similarly, when cells were considered as active members of a social community, terms from electrical and computer engineering such as 'signal transduction' and gene regulatory 'networks' were borrowed by cell biologists.

Throughout the book, Reynolds constantly reminds us of the reciprocal influence of society on metaphors in cell biology. Some have become so familiar that they are now considered to be 'dead metaphors', suggesting that grasping their original meaning is no longer necessary to understand them (for example, when we speak of a colony of cells). Overall, Reynolds accomplishes what he sets out to do in The Third Lens, as he is able to show convincingly the indispensability of metaphors in cell biology. Philosophically, he urges scientists to not get caught up in the pursuit of one

objective description of the natural world. As he points out, the quest for one "uniquely correct account" seems to rely on a "dubious theological-metaphysical thesis that the world was designed and created by a language-speaking agent, to whose privileged 'way' the uniquely correct (True) account of science must correspond" (p. 207). Reynolds insists that a true account of the world should be achieved by more than one means, while making use of objective methodologies. For instance, both mechanical and agential descriptions of cell signalling were in their own way necessary for scientists to fully elucidate this phenomenon (p. 145).

While Reynolds champions the cause of metaphor in science, he also warns the reader about the perils of their misuse. For example, the reduction of gene regulatory networks to circuits is a misleading metaphor, for 'cross-talks' in cells have far more significant consequences than a simple circuit cross-talk. As Colin Turbayne noted in 1970, "[a] good metaphor is also a beguiling thing. Once it is understood and accepted, one sees the thing illustrated through new spectacles that, when worn fora while, are hard to discard". One example is how cell theory led researchers to see cells with defined boundaries even in the absence of one, as in the case of syncytia(p. 156).

In conclusion, Reynolds has shown in this book how the use of metaphors has often been employed in the explanation and advancement of complex concepts in biology, and he has offered a careful and interesting review of the main historical developments in cell biology. Training in science seldom incorporates a historical and philosophical perspective, despite its necessity to truly appreciate the nature and purpose of science. The Third Lens serves as an ideal example of how to bridge the gap between the two cultures.

A.4 Metaphors in the field of Epithelial to Mesenchymal Transition (EMT).

EMT was first observed by late Professer Elizabeth Hay and Gary Greenburg, a graduate student in 1982. They isolated chicken epithelial tissues and cultured them in collagen droplets and observed their transformation into mesenchymal stem cells (Greenburg & Hay, 1982). Since then, the distinguishing features of epithelial cells, mesenchymal cells and EMT have been redefined. In 1995, the term transition was adopted instead of transformation to differentiate the process from neoplastic

transformation used in cancer biology(Hay & Zuk, 1995; J. Yang et al., 2020) . The briefings of The EMT International Association (TEMTIA) meetings that have been conducted since its inception in 2003 have been a vital source of information on the history of this field. To better understand the use of some metaphors in the field, I have included the following excerpts from some of the proceedings.

"This ability of cells to express attributes of both epithelial and mesenchymal phenotypes was referred to by Savagner as a "metastable phenotype" … These markers may allow further investigation into the role of metastability in cancer. Metastability indicates the existence of cells with features of both epithelial and mesenchymal cells. This concept is consistent with the sequential steps of junctional dissolution that were described by Thiery (Thiery & Huang, 2005) and is gaining momentum through the accumulation of evidence in favor of such hybrid states" (Lee, Dedhar, Kalluri, & Thompson, 2006). In this excerpt the terms 'metastable' and 'hybrid' are employed to define the 'state' of the cells. The metaphors 'metastable' and 'state' create a thermodynamic profile for the cells undergoing EMT. 'Hybrid' helps us envision the cell as an entity carrying properties of two different entities.

"Importantly, however, although it is now recognized that the EMT programs do not operate as binary switches that shunt cells from fully epithelial to fully mesenchymal extremes, it remains unclear whether discrete phenotypic states are arrayed along the epithelial to mesenchymal (E to M) phenotypic spectrum or, alternatively, a continuum of such states exist that lack distinct, definable boundaries"(J. Yang et al., 2020). In this excerpt, the term 'binary switches' for the process of EMT was replaced by 'a phenotypic spectrum' or 'a continuum'. With new discoveries in the field, we see the inclusion of new and pertinent metaphors to replace obsolete ideas, thus enabling the advancement of theories and models to better define the system.

"In addition, over the period of TEMTIA's existence the EMT field has exploded, and has therefore been confronted by the difficulties that arise from success: of "big data" and complex systems biology. The recent TEMTIA meetings have identified these emerging trends, including the positive impact that new methods of systems analysis can have in identifying novel regulators of EMT and the utility of mathematical models in identifying potential impacts of EMT on the emergent behavior of tissues and in discriminating between stochastic and deterministic processes"

(Newgreen & Thompson, 2017). This excerpt provides an example of the use of metaphors to apply inter-disciplinary ideas to further our understanding; conceptualizing EMT, a biological process as a mathematical model.

"TEMTIA proposes the following guidelines to define the EMT programme, its phenotypic plasticity and the resulting multiple intermediate epithelial–mesenchymal states. By building such a consensus on EMT related concepts, we aim to eliminate semantic problems in the EMT debate and facilitate genuine cross-disciplinary discussion of the roles of EMT in both normal development and pathological conditions" (J. Yang et al., 2020). Finally, in this last excerpt, we see a requirement for contextual definitions of concepts and ideas to avoid miscommunication. This provides a solution to overcome one of the biggest challenges in the use of metaphors in science communication. Even though metaphors help us grasp new ideas, they are also capable of creating ambiguity. Defining the scope of the metaphors, thus becomes essential for fully exploring their potential.

A.5 Conclusion

EMT is a new field to explore for philosophers of science history interested in metaphors. Since its discovery in 1982, the technological advancements have enabled scientists to further their research and conceptual understanding of the process. Additionally, the role of EMT in multiple contexts during both development and pathogenesis has garnered the interests of scientists from multiple disciplines to understand this evasive process that aids the malignant cells in evading cancer treatments. We also saw that the use of metaphors can mislead us into wrong interpretations and hence warrants a complete and proper description of the scope of the metaphorical devices employed. As we saw in Reynolds' book on the metaphors in cell biology, history is repetitive. Most metaphors are lost during the course of scientific progress while others face scrutiny and persist, like the humble cell.